A STUDY OF THE BEHAVIOUR OF POST-TENSIONED BRICKWORK BEAMS

Remo Francesco Pedreschi, B.Sc.

A thesis submitted for the Degree
of Doctor of Philosophy

Department of Civil Engineering and Building Science,
The University of Edinburgh,

September, 1983.

DECLARATION

This thesis is the result of research work for the degree of Doctor of Philosophy undertaken in the Department of Civil Engineering and Building Science, University of Edinburgh.

It is declared that all the work and results in this thesis have been carried out and achieved by the author himself and the thesis has been composed by him under the supervision of Dr. B.P. Sinha, unless otherwise stated.

Edinburgh, September 1983

Remo F. Pedreschi.

ACKNOWLEDGEMENTS

I am deeply indebted to Dr. B.P. Sinha, who by initiating this project, stimulated my interest in brickwork and for his enthusiasm, encouragement and guidance throughout.

Thanks are due to the Science and Engineering Research Council, Structural Clay Products Ltd., The Building Research Establishment and Armitage Bricks Ltd. for their financial and material support of this work. And also to Miss Gillian Erskine for typing the manuscript.

Finally, to my wife, Theresa, for her great patience and to my mother and the rest of the family for their support during the last three years.

PUBLISHED PAPERS

In collaboration with Dr. B.P. Sinha, the author has published a number of papers dealing with aspects of the work herein. The papers are as follows:

1. 'The Development and Ultimate Behaviour of Post-Tensioned Brickwork Beams', International Seminar/Workshop for Load Bearing Brickwork in the Developing Countries, New Delhi, 1981.

2. 'The Stress/Strain Relationship of Brickwork', 6th International Brick Masonry Conference, ed. Laterconsult, Rome, 1982, pp.321-334.

3. 'Development and Investigation of the Ultimate Load Behaviour of Post-Tensioned Brickwork Beams', The Structural Engineer, Vol.60B, No.3, September, 1982, pp.63-67.

4. 'Compressive Strength and Some Elastic Properties of Brickwork', Int. Journal of Masonry Construction, Vol.3, No.1, 1983, pp.19-25.

5. 'The Behaviour of Post-Tensioned Brickwork Beams', C.I.B. International Council for Building Research Studies and Documentation, Stockholm, 1983.

ABSTRACT

This thesis presents the results of a study into the behaviour of post-tensioned brickwork beams. A total of 51 full-scale beams were tested. The following variables were considered:

(i) brick strength,

(ii) mortar grade,

(iii) steel area and prestress force,

(iv) shear span/effective depth ratio.

The effect of these variables on the deflection, cracking and ultimate load were studied. A comprehensive series of small specimen tests were also undertaken to determine the material properties of the brickwork. A computer programme was developed to predict the flexural behaviour of the beams, using the non-linear stress/strain relationship of brickwork obtained from the small specimen tests and taking tension-stiffening into account. The theoretical method was then compared with the experimental results. An expression for predicting the average crack width in the beams was also developed.

A limited investigation into the shear strength of post-tensioned brickwork beams was carried out, the variables studied being the shear span/effective depth ratio, % of steel and the influence of shear reinforcement. It is shown that the plastic method for predicting the shear strength of prestressed concrete beams can be applied to prestressed brickwork beams.

CONTENTS

NOTATION

a	shear span
a_o	sum of perimeters of reinforcement
A	cross-sectional area of beam
A_e	effective area in tension
A_{ps}	area of prestressed reinforcement
A_s	area of non-stressed tension reinforcement
A_s'	area of compression reinforcement
b	breadth of beam
b_j	distance between vertical cross-joints
c	cover to reinforcement
C	compressive force in section
C_o, C_1, C_2	factors used in tension stiffening
d	effective depth of prestressing strand
d'	effective depth of compression reinforcement
d_1	effective depth of non-stressed reinforcement
e	eccentricity of prestress force

E	elastic modulus of brickwork
E'	initial elastic modulus of brickwork
E_s	elastic modulus of steel
f	compressive stress in brickwork
f_c	cylinder strength of concrete
f_{ct}	fictious tensile stress in concrete
f_k	characteristic compressive strength of brickwork
f_m	compressive strength of brickwork
f_{mt}	mean tensile stress in brickwork
f_r	modulus of rupture of brickwork
f_s	stress in steel at crack
f_s'	stress in steel after cracking away from crack
f_{sc}	stress in compression reinforcement
f_{scr}	stress in steel at crack at cracking moment
f_{st}	stress in non-tensioned reinforcement
f_{su}	stress in prestressing strand at ultimate
f_{sy}	proof stress of prestressing strand
F_{ns} (ε_{sc} or ε_{st})	stress/strain relationship of non-tensioned reinforcement

$F_m(\varepsilon)$	stress/strain relationship of brickwork
$F_s(\varepsilon_s)$	stress/strain relationship of prestressing strand
F_y	yield force of prestressing strand
h	total depth of section
h_{cr}	initial height of cracks
I	moment of inertia
I_{cr}	moment of inertia of cracked section
I_e	effective moment of inertia
I_g	gross moment of inertia
J_1, J_2, J_3	lever arm factors
k	tension stiffening factor
k_1	coefficient for cracking of concrete beams
ℓ	distance between nodes
l_a	lever arm
m_r	modular ratio
M	bending moment
M_{cr}	cracking moment

M_u	ultimate moment
n	neutral axis depth
n_r	centroid of uncracked transformed section
N_j	number of joints
P	prestressing force
P_u	ultimate load of prestressing strand
r	n/d
r_t	$\varepsilon_1'/\varepsilon_2'$
R	degree of reinforcement
S_m	average crack spacing
S_o	minimum crack spacing
T_m	tensile force in masonry
T_s	tensile force in steel
v	relative displacement rate
V	shear force at failure
w	crack width
w_{ave}	average crack width
w_{max}	maximum crack width

W_E	external work done
W_I	internal work done
x_w	effective depth of Whitney stress block
X_1-X_4	coefficients of stress/strain relationship of brickwork
Y	depth of beam in hydrastatic compression
Z	section modulus
α	angle of displacement to yield line
β	angle of yield line to axis of beam
β_1, β_2	bond factors
ε_1, ε_2	strains in top and bottom fibres of beams
ε_{a2}, ε_{a1}	applied strains in top and bottom fibres of beams
ε	strain in brickwork
ε_e	strain in brickwork at level of steel due to prestressing
ε_m	ultimate compressive strain in brickwork
ε_{ms}	strain in masonry at level of steel due to applied load
ε_{ps}	strain in prestressing strand due to prestress

ε_{p1}, ε_{p2} — prestress strains

ε_r — ultimate tensile stain of brickwork

ε_s — total strain in prestressing strand

ε_{sa} — strain in strand caused by applied loads

ε_{sam} — average additional strain in strain after cracking

ε_{smb} — average strain after cracking at any level of beam

ε_{sc}, ε_{st} — strains in non-tensioned reinforcement

ε_1', ε_2' — initial strains in top and bottom fibres of beam due to prestress

ε_{sy} — strain in prestressing strand at proof stress

λ_1, λ_2, λ_3 — stress block factors

ϕ — curvature of beam

ϕ_p — curvature of beam due to prestress

ϕ_{cr} — curvature of beam at cracked section

ϕ_{ave} — average curvature of beam

τ_b — bond stress

τ shear stress, V/bh

σ_1, σ_2 stresses in top and bottom fibres at beam due to prestress

σ stress in compression strut

θ angle of inclination of compressive strut

ν effectiveness factor

ρ A_{ps}/bd

CHAPTER 1 : INTRODUCTION

1.1 Historical Background

1.1.1 Plain Masonry

Masonry is the oldest of man's building materials and it's use has been traced back to the very beginnings of mankind. Perhaps the most dramatic example of this still in existence today is the mammoth structure of Stonehenge in the south of England.

The first recognised civilisation to use masonry extensively were the Ancient Egyptians[2] who were responsible for many large structures of stone masonry, e.g. the Pharos lighthouse in Alexandria, which was 169 metres high and whose light could be seen from a distance of 35 miles. The lighthouse stood for 1500 years before it was destroyed by an earthquake in the 13th century, this was a tremendous achievement by any standard. The use of brick masonry originated with sun-baked clay bricks made by the Summerians[21] as long ago as 5500 years ago. From this time onwards it was then possible to produce large quantities of bricks of readily handled dimensions. Throughout the following period traditional structural forms developed that utilised the tremendous compressive strength of the brickwork, such as arches, columns and vaulted roofs.

In traditional multi-storey masonry construction the lateral stability required by the structure to resist the effects of lateral loads such as wind pressure was provided by means of the massive self weight of the building. A very good example of this 'traditional'

approach to design is the Monadonack building in Chicago[2], which was one of the last buildings to be constructed in this manner. Completed in 1891, it was, at that time considered the acme of masonry construction. It has 16 storeys and to provide adequate lateral stability by means of self weight the walls at the base of the building were 1.6 metres thick. By todays cost-conscious standards this represents a grossly uneconomic and wasteful use of both materials and space. Its not surprising to find that designers were soon to realise the potential savings offered by framed construction using the relatively new materials of steel and reinforced concrete.

In the earlier parts of this century brickwork was then rather neglected as a structural medium and its use was restricted to mainly low-rise buildings or in-fill material in framed construction.

In the last thirty or so years a more scientific approach in testing and design, based on structural engineering principles has brought about a renaissance of brickwork as a structural material. Lateral stability may be provided by using the in-plane stiffness of brickwork panels as shear walls. Thus walls that were formally used merely as partitioning or in-fill in framed construction may now be used to carry the structure, eliminating the need for the frame.

Designers, engineers and researchers, spurred on by this new awareness, are beginning to think of brickwork as a structural material comparable to steel and concrete. This is reflected in the adoption of the limit state code of practice[1] for unreinforced masonry, which in turn has fuelled further areas of interest in reinforced brickwork.

1.1.2 Reinforced Brickwork

The first recorded[22] application of reinforced brickwork was by Marc Brunel in 1825. During the construction of two large vertical shafts, as part of the Thames river tunnel project, Brunel used wrought iron bolts and hoops to strengthen the shaft both vertically and circumferentially. The shafts were sunk into the ground by excavating the earth from the interior. In spite of considerable differential settlement no cracks developed in the brickwork.

As a consequence of Brunel's work interest in reinforced masonry began to develop among other engineers. In 1837 Colonel Pasley[2,22] of the corps of Royal engineers, tested beams with and without reinforcement and proved that reinforcement signficantly increased the flexural strength of brickwork.

From Pasley's work the research continued but the true beginning of modern reinforced brickwork is generally said to have started in 1923. At this time Brebner[2], of the public works department, of the Government of India, published a research report in which an extensive number or reinforced brickwork beams, columns and slabs were tested. The report also included a rational theory for the design of such elements. Engineers in countries like India, Japan and the U.S.A. were quick to grasp the significance of this work and they found that the combination of steel and brickwork provided a material that offered excellent resistance to the seismic forces so prevalent in these countries.

Today, in these countries, reinforced brickwork is more common than in Britain. However, reinforced brickwork is gaining

popularity as it has a number of advantages over its main rival, reinforced concrete:

1. The construction of reinforced brickwork does not generally require shuttering, which may be costly in both labour and material.

2. The greatest proportion of the total volume of a reinforced brickwork element is composed of brick and therefore the quantity of cement is greatly reduced.

3. Brickwork is a low energy input material that does not normally require large items of equipment such as batching plants and concrete pumps which are expensive to run and maintain, especially in view of upward spiralling fuel costs.

4. The finished appearance of brickwork is much more appealing than concrete, given the wide range of textures and colours of modern facing bricks. Brickwork weathers better and staining that often occurs in older concrete structures does not happen in brickwork.

A cost study by Haseltine and Tutt[3] in which they compared a number of reinforced brickwork and reinforced concrete retaining walls showed that reinforced brickwork was considerably cheaper.

Although in recent years, the use of reinforced brickwork[23] has increased in Britain, it suffers certain disadvantages. Reinforced brickwork flexural members crack very early and to keep these cracks within acceptable limits the stress in the steel

must be kept low - an inefficient use. Further, the failure of reinforced brickwork is usually due to shear, hence the full compressive strength of brickwork is not utilised to its optimum. These disadvantages may be overcome by prestressing.

1.2 Advantages of Prestressing

The technique of prestressing is almost as old as stone masonry and has been applied in a much broader sense than soley the enhancement of the behaviour of concrete beams. Consider the bow and arrow, by inducing flexural stresses into the bow the archer takes advantage of the rapid recoil to propel the arrow. Numerous other applications exist. The iron rim round a wooden cartwheel which is heated, causing it to expand. The rim is then placed onto the wheel and as it cools it contracts inducing compressive stresses in the wheel.

The iron hoops round a wooden barrel are forced down the increasing diameter of the barrel. The hoops tighten round the barrel causing a compression in the wooden staves, which prevents leakage.

Prestressing was first applied to concrete by W. Dohring[24,25] in 1888 who used tensioned wires in concrete to produce small slabs and beams.

Most of the earlier attempts to prestress concrete were rather unsuccessful, mainly due to the use of mild steel, and it was not until 1928 when Fressyinet[24,25], who had been studying creep in concrete, realised that most of the prestress force was lost because the strain in the concrete due to creep was of the same magnitude

as the initial prestrain in the steel. He therefore advocated that high tensile steel should be used which allowed greater elongations and would reduce the losses caused by creep to a tolerable level.

Prestressed concrete has now established itself as a major structural material being used in such diverse applications as medium span bridges, railway sleepers and the nuclear power industry. In buildings prestressed concrete is used in the manufacture of precast frames, floors and lintols.

The principle of prestressing, as applied to concrete is also applicable to brickwork, but so far no serious attempt has been made to prestress masonry so that it may be used as flexural members. By inducing a system of stresses that will counteract the stresses due to external loads then the net deformation of the beam will be decreased.

In materials such as concrete and brickwork in which the tensile strength is considerably less than the compressive strength cracking will occur at comparatively low loads in flexure. By applying a compressive force, taking advantage of the greater compressive strength of the material, the externally applied load necessary to cause cracking is increased. Hence, by comparison, with an ordinary reinforced beam, an uncracked section is obtained under working loads.

Along with the advantages mentioned in section 1.1.2 prestressing has a number of other benefits.

The strength of steel normally used for prestressing is some 2 to 3 times that of the high yield steel used in reinforced brick-

work. This means that for a given section the area of steel will be 2 to 3 times less than that of high yield steel to produce the same moment. Hence, due to the elastic modulii of both types of steel being approximately equal then the reduced area of steel in the prestressed beams will exhibit greater ductility in post-cracking stages of behaviour. The greater ductility is desirable as it allows the beam to deform more noticeably before failure, giving warning of impending failure.

By applying the techniques of prestressing developed for reinforced concrete to brickwork, a structural material that has the benefits of reinforced brickwork but without some of the disadvantages is obtained.

1.3 Scope of the Present Investigation

As there is complete lack of data on the behaviour of full-scale prestressed brickwork a comprehensive investigation was undertaken. The principal aim of this experimental investigation was to study the effects of the following variables:

(i) brick strength,
(ii) mortar strength,
(iii) prestressing force,
(iv) percentage steel area,

on the ultimate moment, deflection and cracking of post-tensioned brickwork beams. A limited number of tests were carried out to study the influence of the shear span/effective depth (a/d) ratio

and % of steel area on the shear strength of post-tensioned brickwork beams.

A total of 51 beams varying from 1.75 to 6.2 metres in span were tested to complete the test programme.

In conjunction with this work a comprehensive series of tests on small scale specimens was undertaken to determine the strength and mechanical properties of all the materials used in the construction of the beams. This was necessary for brickwork due to the lack of data and also for the theoretical analysis.

A computer programme was developed to predict the moment-curvature relationship and load-deflection response up to the ultimate moment, taking into account the nonlinear material behaviour and effect of tension stiffening of brickwork after cracking. No attempt has been previously made to predict the flexural behaviour of structural brickwork from the stress/strain relationship obtained from small prism tests.

From these prism tests an attempt has been made to predict the shear strength of prestressed brickwork beams using the plastic theory earlier developed[26] for concrete beams.

CHAPTER 2 : REVIEW OF LITERATURE

2.1 Introduction

Up to the present there has been very little research carried out into the behaviour of prestressed brickwork beams. This literature survey describes all the known previous experimental studies on prestressed brickwork to date.

In advance of some of the experimental work a number of prestressed brickwork structures have been constructed and these are dealt with briefly in section 2.3.

2.2 Previous Experimental Work

2.2.1 Work of K. Thomas[4]

In 1963, as part of a study into the feasibility of the construction of a suspended floor system using prestressed brickwork beams, Thomas[4] tested 2 prestressed brickwork beams. The first of these was built from three hole bricks laid as soldiers (Figure 2.2.1(a)). Six, 7 mm diameter high tensile steel rods were threaded through the bottom hole and a prestressing force of 67 kN was applied, inducing a maximum compressive stress of 7.2 N/mm^2. The wires were unbonded and the beam was tested under central point loading over a span of 2515 mm. The beam was loaded to 18.3 kN and then unloaded; the prestress force was increased to 107 kN (maximum compressive stress, 11.6 N/mm^2). Failure of the beam occurred at a load of 17.17 kN which was less than the maximum load in the previous cycle. Failure of the beam was attributed to

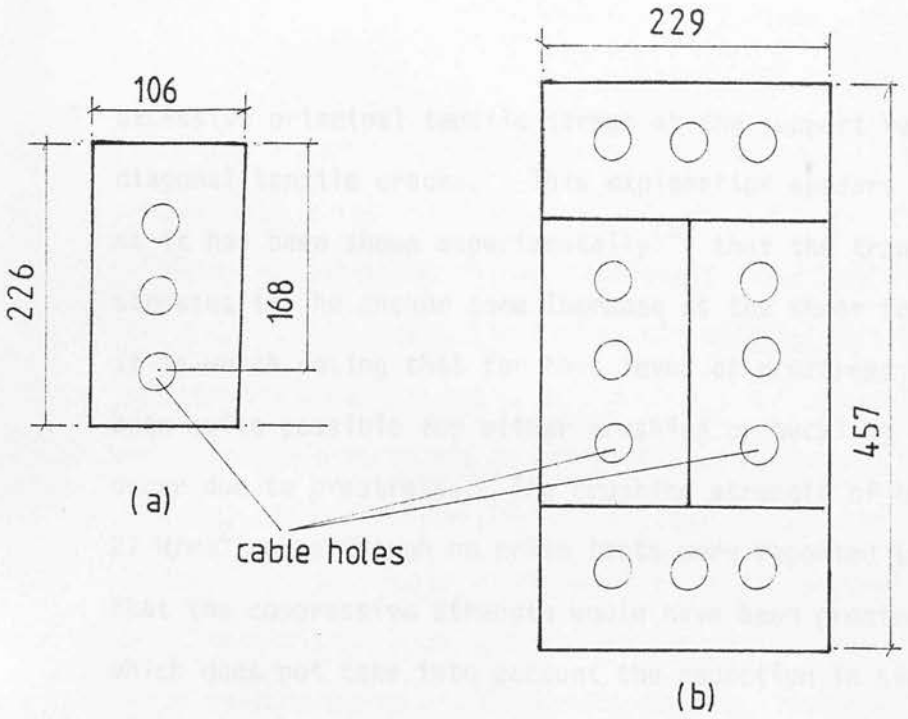

fig. 2.2.1 Beams of K.Thomas[1]

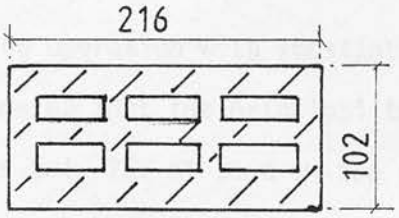

all dimensions in mm.

fig. 2.2.2 Beam of L.S Ng[1]

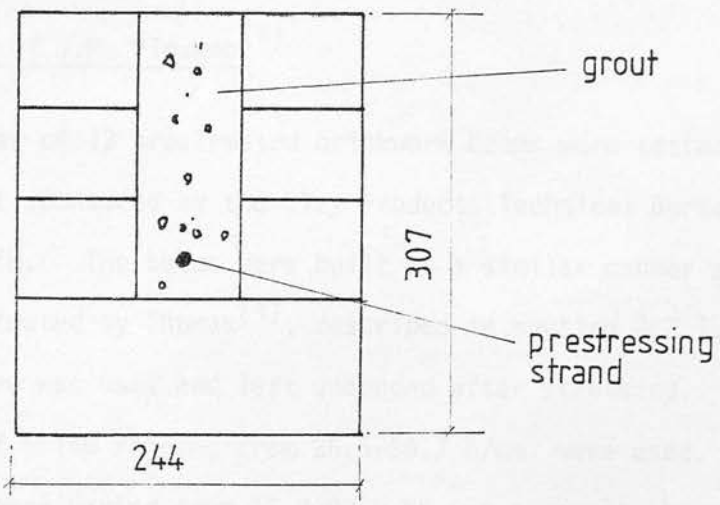

fig. 2.2.3 Typical beam (Mehta & Fincher[7])

excessive principal tensile stress at the support resulting in diagonal tensile cracks. This explanation appears satisfactory as it has been shown experimentally[5] that the transverse tensile stresses in the anchor zone increase as the shear force increases. It is worth noting that for this level of prestress it might have been quite possible for either crushing or buckling of the beam to occur due to prestress. The crushing strength of the bricks was 27 N/mm^2 and although no prism tests were reported it is very unlikely that the compressive strength would have been greater than 14 N/mm^2 [32], which does not take into account the reduction in strength due to slenderness or eccentricity.

A second beam, using the same bricks but of the section shown in Figure 2.2.1(b) was built. Failure of this beam occurred during the stressing operation with substantial cracking behind the anchorage. Thomas estimated that the principal tensile stress in this beam, at failure, was only 75% of that in the first beam. This is not surprising as the tensile strength in this case is governed by the strength of the brick/mortar interface and not the tensile strength of the brick unit as in the first beam.

2.2.2 Work of J.M. Plowman[4]

A series of 13 prestressed brickwork beams were tested as part of a project sponsored by the Clay Products Technical Bureau of Great Britain. The beams were built in a similar manner as the first beam tested by Thomas[4], described in section 2.2.1. 7 mm diameter wire was used and left unbonded after stressing. Four strengths of brick ranging from 26.5-54.7 N/mm^2 were used. The prestress force varied from 17.8-93.9 kN, as a result the maximum

compressive stress varied from 1.48-7.73 N/mm^2. The beams were tested over a span of 3048 mm under central point loading. The majority of the beams failed in flexure resulting in crushing of the compression zone. No comparison between flexural strength and compressive strength was made and it was not possible to do so here as information relating to the steel areas in each beam was not given. The analysis of the results was limited to the consideration of the factor of safety against failure taking the working load as that to cause decompression of the prestress force at the soffit. As the wires were unbonded, then, during loading, the wire will move relative to the beam causing a reduction in eccentricity of the prestress force and reducing the load to cause decompression. The factor of safety was calculated taking into account both the maximum and minimum eccentricity.

The lowest value for any beam was 2.1. Of the two beams that did not fail by crushing of the compression zone; one failed due to fracture of the prestressing strand and the other failed due to excessive deflections without further increase in load. Plowman concluded that flexural failure caused by steel failure was sudden and complete. This is obviously based on the former beam, however the result of the latter beam suggests that the large deflections were in fact caused by yielding of the steel.

2.2.3 Work of L.S. Ng[4]

In 1966 L.S. Ng tested three prestressed beams made from extruded clay units, Figure 2.2.2, with a view to the possible development of a ceramic flooring system. In an effort to avoid

tensile splitting during prestress the traditional mortar joints were replaced with thin epoxy resin joints. Two, 5 mm diameter high tensile steel wires were fed through the perforations in the ceramic units. The beams were stressed to either 34 or 43 kN (maximum compressive stress of 5.4 N/mm^2). After prestressing the beams were grouted with a 1:1 cement/sand mix. The beams were then tested under third point loading, over a span of 3050 mm. Failure of the beams was by crushing of the compression zone. In one of the beams it was noticed that the wires had moved up to the top of the cavity and this was due to the grout not being sufficiently cured. Based on the load to cause decompression a factor of safety of 3.5 was obtained. As a result of this work a patent was taken out on a prestressed ceramic floor system.

2.2.4 Work of Mehta and Fincer[7]

Mehta and Fincer, in 1970, carried out tests on six pretensioned brickwork beams. Each beam was built in a different coursing pattern, five of these having the same basic dimensions, Figure 2.2.3. The beams were of grouted cavity construction and were prestressed with three, 10 mm diameter, seven wire strands. The strand was tensioned in the cavity which was then grouted. The prestress force varied from 94-187 kN. The beams were tested under central point loading over a span of 1829 mm. All the beams failed in shear with diagonal cracks running from load point to support. The shear strength was calculated using a modified expression from the American Building Codes[7]. Although there were a number of simplifying assumptions, namely ignoring self weight, prestress losses and that the masonry

and grout had the same elastic properties, the predicted values were within 20% of the experimental results. The ultimate flexural capacities of the beams were calculated again, using American Building Code requirements and in three of the results the experimental moments were greater than the predicted ones. The deflections were measured and compared with theoretical deflections up to the decompression load using simple beam theory. The measured deflections were between 1.46 and 2.36 times greater than the predicted deflections.

No explanation for these differences was put forward. However the elastic modulus of brickwork was obtained from an empirical relationship in terms of the compressive strength of masonry normal to the bedjoint. This assumes that the modulus of elasticity of brickwork is the same in all directions and again that the grout has the same elastic properties as the brickwork, which is not strictly correct.

2.2.5 Work of Williams and Phipps[8]

Williams and Phipps reported the results of tests on six masonry box beams of span 4.8 m. These beams, although tested horizontally were built to represent the behaviour of masonry diaphragm walls. The prestressing force was applied via a single, 40 mm diameter MaCalloy bar, threaded through the cavity, along the central axis of the beam, Figure 2.2.4. Because of the large cavity, during bending the tendon will move toward the compression face of the beam. In order to prevent this cross ribs were incorporated in three of the beams, Figure 2.2.4(b). The pre-stressing force varied from 132-330 kN, resulting in compressive

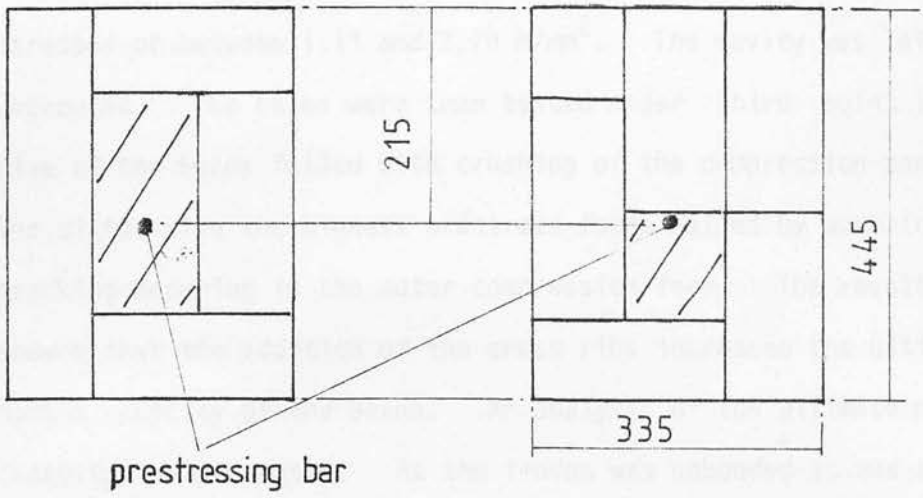

fig. 2.2.4 Beams of Williams & Phipps [8]

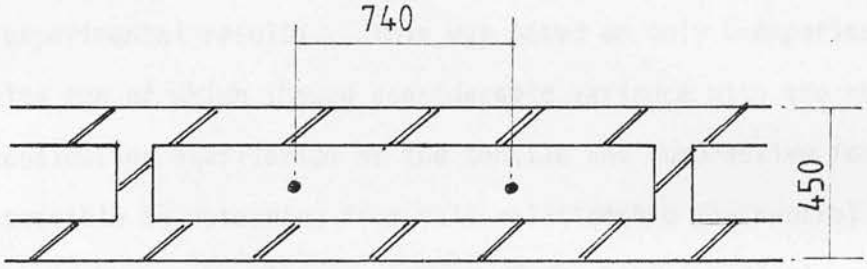

fig. 2.2.5 Diaphragm wall section [9]

all dimensions in mm

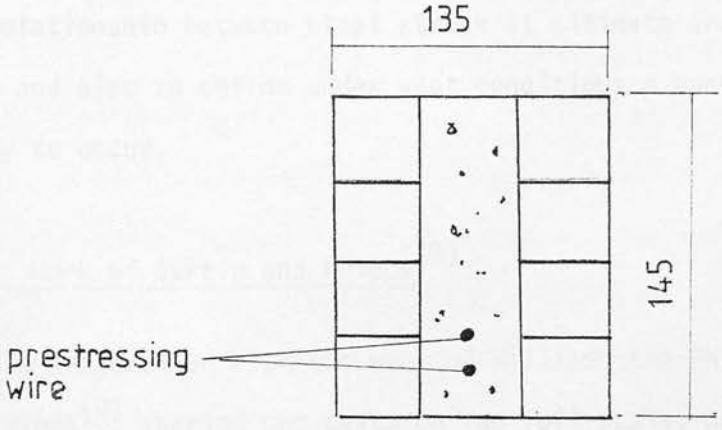

fig. 2.2.6 Model section [10,11]

stresses of between 1.11 amd 2.79 N/mm^2. The cavity was left ungrouted. The beams were then tested under third point loading. Five of the beams failed with crushing of the compression zone. The sixth, with the highest prestress force failed by buckling with cracking occuring in the outer compression face. The results showed that the addition of the cross ribs increased the ultimate moment capacity of the beams. An analysis of the ultimate moment capacity was presented. As the tendon was unbonded it was assumed that the distribution of strain in the tendon, along the span was the same as the bending moment diagram, although this was not verified experimentally. An empirical relationship between the steel stress and the neutral axis depth at failure was obtained from the experimental results. This was based on only 6 experimental results two of which showed considerable variance with the relationship. By considering equilibrium of the tensile and compressive forces it was possible to determine from this relationship the neutral axis depth and hence the ultimate moment of the beams. Fairly good agreement with the experimental results was obtained. However, before this method could be applied in a more general case further work should be carried out to establish more clearly the nature of the relationship between steel stress at ultimate and neutral axis depth and also to define under what conditions a buckling failure is likely to occur.

2.2.6 Work of Curtin and Phipps[9]

In conjunction with the work of Williams and Phipps[8], Curtin and Phipps[9] carried out tests on two full-scale, post-tensioned

brickwork diaphragm walls. The walls were 7.26 m high and built side by side. Prestressing was by 40 mm diameter MaCalloy bars, cast into the foundation of the walls (Figure 2.2.5). The walls were 'tied' together at the top and lateral pressure, to simulate wind loading, was applied by means of an air bag sandwiched between the walls. The walls were then assumed to behave as propped cantilevers under uniform loading. The main aim of the tests was to determine the effect of varying levels of axial precompression on the formation of tensile cracks in flexure, which may define the limit of serviceability of the walls. The degree of precompression varied from 0-1.38 N/mm^2. They found that the load at which cracks developed increased as the prestress force increased. Using simple elastic theory they predicted the cracking loads reasonably accurately. This analysis hinged on the assumption that the walls behaved as propped cantilevers. It might have been worthwhile, given the scale of the tests to verify this assumption by measuring the force in the tie and rotation of the base.

2.2.7 Model Tests

Some work[10,11] has been carried out on prestressed brickwork beams built from half scale bricks, at the University of Edinburgh. The beams were of grouted cavity construction as shown in Figure 2.2.6. A duct was formed in the grout by means of a metal rod which was removed after grouting. The beams were stressed up to 42 kN using two, 7 mm diameter wires. The wires were left unbonded in the duct. Two series of beams were tested with a/d ratios varying from 2-5. In the first[10] of these a grade 1 mortar

(1:¼:3, cement:lime:sand), was used, in the latter a grade 2 mortar (1:½:4½, cement:lime:sand), everything else being kept the same. For both series of beams failure occurred by crushing of the compression zone, the beam's behaviour was similar to a tied arch. Comparing the results of the two series of beams, the mortar grade did not appear to significantly influence the flexural strength.

2.2.8 Work of Robson et al[12]

Very recently, after some of the results of this work had been published[13], Robson et al[12] reported the results of a series of tests on unbonded prestressed brickwork beams. The beams were all built of the same section as shown in Figure 2.2.7. Two series of beams with a/d ratios varying from 2-5 were tested. The prestress force in the first series of beams was 169 kN and in the second, 261 kN. Failure of the beams occurred by crushing of the compression zone with yielding of steel. The material properties of the brickwork namely the compressive strength and elastic modulus were taken from the recommendations of the draft code of practice for reinforced masonry[14] and used to predict the ultimate strength of the beams. The predicted failure moments tended to underestimate the experimental results by between 9 and 48%. Using elastic theory they compared the elastic modulii from the experimental results with the elastic modulus from the code of practice recommendations and found that in all cases the elastic modulus was greater experimentally, by as much as 250%. The basis of using a draft code of practice to determine the material properties of the brickwork is rather dubious

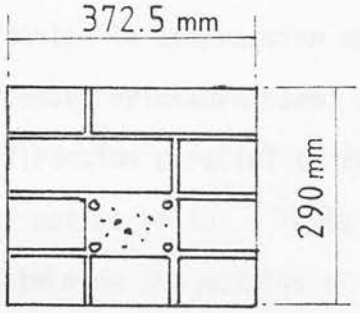

fig. 2.2.7 Beam of Robson et al.[12]

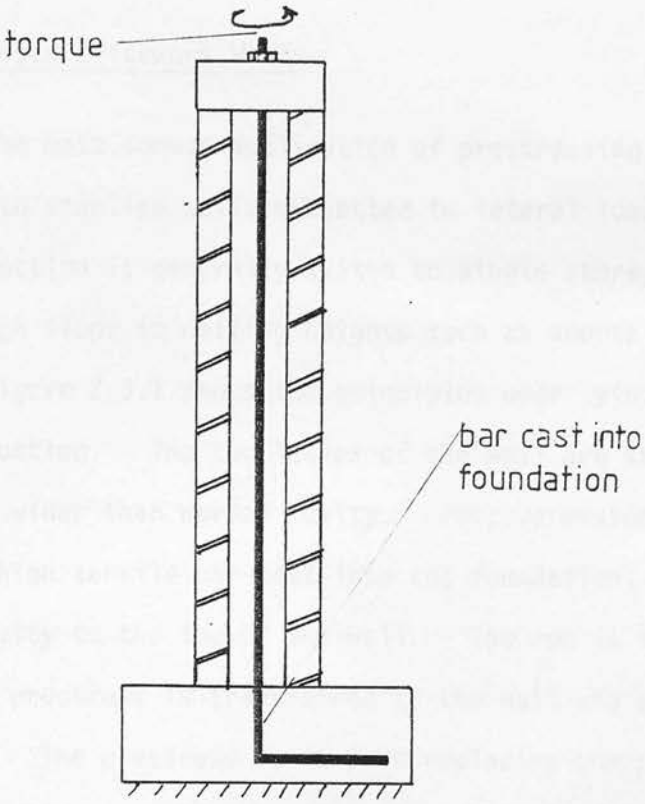

fig. 2.3.1 Typical post-tensioned
brickwork walls.

as the recommendations are based on empirical relationships obtained from brickwork tested in compression normal to the bedjoint. In the prestressed brickwork beam test the compressive forces developed in the direction parallel to the bedjoint and hence these recommendations may not be valid. Tests on small scale brickwork specimens to determine the modulus of elasticity and compressive strength were not reported although this would probably have given better results than the values taken from the draft code of practice.

2.3 Prestressed Brickwork Structures

2.3.1 Prestressed Brickwork Walls

To date the most common application of prestressing of brickwork has been to stablise walls subjected to lateral loads. This form of construction is generally suited to single storey structures with fairly high floor to ceiling heights such as sports halls and workshops. Figure 2.3.1 shows the principles underlying this type of construction. The two leaves of the wall are separated by a generally wider than normal cavity. Precompression is applied by means of a high tensile bar cast into the foundation, passing through the cavity to the top of the wall. The rod is threaded at the top and prestress is transferred to the wall via a nut and torque wrench. The prestress is in fact replacing the precompression that would normally be applied by the self weight of additional storeys above.

A number of structures have been constructed using these principles, a few of which are considered in the following.

In 1966 Neil[15] employed this method to stabilise the walls of a factory in Darlington. The walls were 7 m high and the prestressing rods passed through the bottom flange of a steel fascia beam at the top of the wall. A prestress of 0.7 N/mm^2 was applied axially to the wall through the flange of the beams. Once prestressing was completed the fascia beams were welded to steel columns which were designed to carry all the vertical loads. By adopting this form of construction the need for buttressing that would normally be required, was eliminated and the thickness of the wall was kept to 275 mm.

Curtin et al[16] described the construction of an assembly hall with 8.5 m high walls. At the top of the walls clerestorey windows were required by the architect. This meant that the wall would have to be designed as a free cantilever. A 665 mm thick diaphragm wall was chosen. Prestress was applied via 32 mm diameter MaCalloy bars which induced an axial precompression of 0.5 N/mm^2.

Bradshaw et al[17] reported the design of a steel framed farm building which incorporated a prestressed brickwork wall. The wall was 2.5 m high designed as a cantilever, to retain grain with a 20% surcharge. In the two previous cases the walls were prestressed through their central axis because of the possibility of load reversal. However, because the load was due to retained material the direction of load was constant and the prestressing bar was placed eccentrically in a duct built into the web of the wall. The maximum compressive stress induced in the wall was 0.3 N/mm^2.

2.3.2 Other Applications of Prestressed Brickwork

As a solution to the problem of providing an on site water

supply as part of the fire fighting system for a brick factory, Foster[18], the architect opted for the imaginative solution of a prestressed brickwork water tank. The tank was cylindrical in plan, 12 m in diameter and 5 m high. The tank was prestressed both in the horizontal and vertical direction. A 225 mm thick wall in Flemish bond was chosen as this enabled the vertical tendons to be placed at 180 mm centres in a continuous vertical cavity in the wall. The applied vertical prestress was 1.0 N/mm^2. The hoop stresses in the wall were resisted by circumferential prestressing using 7 mm high tensile wires inducing a maximum compressive stress of 2.0 N/mm^2. After the circumferential steel had been stressed a protective skin of decorative bricks was built round the wall. Due to the relatively high head of water, at the base of the tank an internal water-proof render was applied, to date the tank is still performing its function satisfactorily.

Some patent flooring systems, such as Stahlton flooring[19] utilise masonry in prestressing. In this particular system pre-stressed masonry planks are formed by laying clay tiles in line, with prestressing wires running between. The wires are stressed and then grouted forming a prestressed, composite section. These planks are then used to provide tensile resistance, working in conjunction with an insitu concrete topping, hence the greatest stresses that the masonry undergoes will be that due to initial precompression.

During tests[20] on storey height box beams of composite brick/concrete construction, concrete slabs forming both flanges and reinforced brickwork forming the webs, it was found that applying

vertical prestressing to the webs vastly improved the resistance of the web to diagonal cracking.

2.4 Summary and Discussion

To date the previous experimental work on prestressed beams has been rather fragmented. The majority of the work reported by the researchers has dealt with only a small number of tests however certain trends appear. The largest number of tests has dealt with beams in which the tendon remained unbonded and generally the failure of these beams was in flexure with crushing of the compression zone. This is different from the work on bonded beams by Mehta and Fincer[7] in which shear failure predominated. In the unbonded beams the behaviour is rather like a shallow tied arch and so shear failure was unlikely anyway. The reason for the tendency towards unbonded construction was probably due to practical difficulties in grouting the tendon as opposed to it being a more preferable structural element.

Excluding, perhaps reference 8, there has been little or no attempts on the part of researchers to develop methods for predicting the behaviour of the beams, based on the actual behaviour of the brickwork itself.

With the only exception of the water-tank, section 2.3 it is clear that prestressing of brickwork in practise has been done in very limited cases to enhance the ability of a wall to resist lateral loads[16,17] or to increase the shear resistance of walls[20]. It would not be out of place to mention here that the prestressing in these cases were merely an alternative and convenient way of

'increasing' the dead weight of the structure and as such does not represent a tremendous departure from more accepted forms of construction in which the masonry is largely used as compression elements.

To the author's knowledge, prestressed brickwork in practise has not been employed as a structural member, carrying load primarily in bending. This is understandable and is due mainly to the lack of research experience and design guidance, in the form of a code of practice. Before designers will start to consider prestressed brickwork as a viable alternative to reinforced or prestressed concrete there has to be more research carried out to define the behaviour more thoroughly and to prove that it can be used as efficiently and economically as other structural materials.

CHAPTER 3 : MATERIAL PROPERTIES

3.1 Introduction

This chapter summarises briefly the results of tests to determine the properties of materials used in this investigation.

Brickwork in its application as a structural material has been most commonly used as walls or piers, to resist compressive loads. In this method of construction the compressive stresses develop normal to the bedjoint. Not surprisingly, the majority of the research into the material properties of brickwork has considered the behaviour normal to the bedjoint which led to the standard practice of testing bricks flat[29].

Brickwork is an anisotropic material both in terms of strength and stiffness. In flexural members such as reinforced or pre-stressed brickwork beams the compressive stresses may develop parallel to the bedjoint. Very little work[27,28] has previously been done to fully define the behaviour of brickwork in this direction. Although the part of anisotropic nature may be explained by the presence of mortar joints the strength of the brickwork in a particular direction will also be dependent on the strength of the brick in that direction. Since, in this work, the compressive stresses developed in the brick, in the two directions other than on the bed it was felt proper to determine the compressive strength of the brick in all three orthogonal directions, i.e. on bed, edge and on end. The results of these tests are given in Table 3.2.1.

A systematic investigation into the compressive strength of the

brickwork was also carried out by testing brickwork prisms. Two types of test prisms were used, Figure 3.4.1, representing the compressive zone of a prestressed brickwork beam and the compressive strength of each type was compared.

The stress/strain relationship of brickwork, parallel to the bedjoint was obtained from strain measurements taken during the prism tests and the deformation characteristics of both prism types were compared.

The load that a prestressed brickwork beam can sustain between decompression and cracking is determined by the flexural tensile strength of the brickwork most often referred to as the modulus of rupture. This property may have a significant influence on the moment-curvature relationship and hence the load/deflection response; a number of specimens were therefore tested to determine the modulus of rupture.

A number of samples of the prestressing strand were tested from which the stress/strain relationship and strength was obtained.

The ultimate strengths and deformations of the prestressed brickwork beams were predicted using the results of the tests on the strands and prisms. For this purpose the stress/strain relationship of the brickwork was mathematically idealised in the form of a polynomial and the strand was represented by a tri-linear stress/strain relationship.

3.2 Properties of Brick

Four kinds of brick were used in the construction of the beams. The first three of these were extruded, three hole bricks of high,

medium and low strength, as shown in Figure 3.2.1(a). The average % area of perforations was 13.4, 16.7 and 15.8%, for the high, medium and low strength bricks respectively. The fourth brick was a single, deep frogged, pressed common brick, Figure 3.2.1(b).

3.2.1 Compressive Strength and Water Absorption

A random sample of ten bricks was tested, for each brick type, in each of the three possible directions of load, Figure 3.2.2. The tests were carried out in accordance with the relevant British standard[29]. In the case of the common brick the frog was filled with mortar to provide a level testing surface. The results are presented in Table 3.2.1.

From this table it may be seen that the compressive strength of the brick in the bedjoint direction is greater than that in the two other directions. Table 3.2.2 compares the compressive strength in each direction, in terms of the ratio of the bedjoint strength. The strength of the bricks was always lowest when tested on end, though the difference between this and the strength on edge was much less than the difference between the strength on edge and on bed. The medium and low strength bricks exhibited the greatest reduction in strength in the two directions other than the bedjoint. Indeed referring to Table 3.2.1, although the compressive strength of the low strength brick on bed was 50% greater than that of the common brick, the compressive strength of the low strength brick in the two other directions was some 30% less than the common brick.

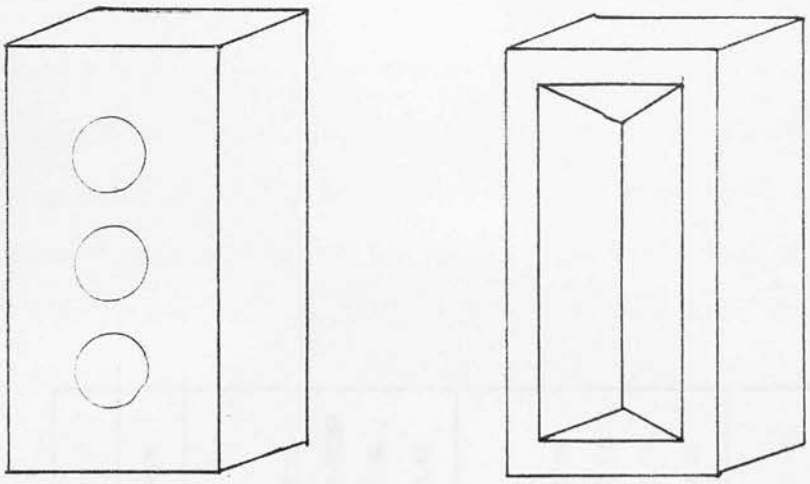

fig.3.2.1 Brick types

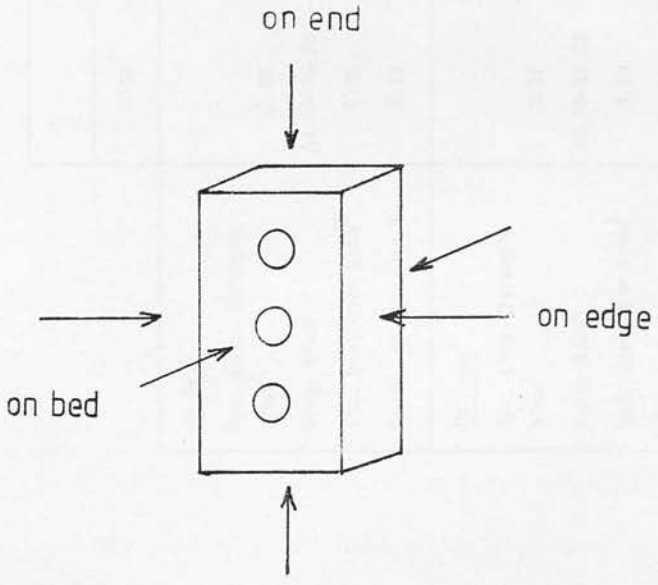

fig.3.2.2 Direction of compressive tests

Table 3.2.1 Compressive Strength and Absorption of Bricks

	Brick Type			
	High	Medium	Low	Common
On Bed				
Ave. Comp. Strength N/mm^2	82.03	67.58	34.18	22.72
Range N/mm^2	64.80-96.70	44.16-91.08	30.70-40.88	15.47-28.84
Std. Deviation N/mm^2	5.85	12.20	2.79	3.36
Coeff. of Variance %	7.13	18.06	8.16	14.81
On Edge				
Ave. Comp. Strength N/mm^2	53.17	26.36	11.48	16.95
Range N/mm^2	33.54-68.03	19.32-39.36	7.51-20.21	12.52-20.21
Std. Deviation N/mm^2	9.43	5.71	3.54	2.24
Coeff. of Variance %	17.73	21.66	30.84	13.20
On End				
Ave. Comp. Strength N/mm^2	40.23	23.23	10.67	15.81
Range N/mm^2	30.00-50.76	10.79-33.80	7.54-18.76	12.62-4.54
Std. Deviation N/mm^2	6.94	5.90	3.24	2.23
Coeff. of Variance %	17.25	25.40	30.37	14.71
24 Absorption % by wt.	4.17	5.71	7.20	23.85
Range % by wt.	3.21-4.71	4.62-8.07	6.82-7.74	23.41-24.19
Std. Deviation % by wt.	0.461	0.900	0.303	0.244
Coeff. of Variance	11.06	15.80	4.21	1.02

The effects of platen friction were liable to have a significant influence on the differences between bedjoint strength and the strength in the two other directions. However, from Table 3.2.2 the brick that showed the smallest reduction in strength was the common brick, the only brick type without perforations. Hence the effect of the reduction in cross-sectional area due to the perforations, in the three other bricks may have influenced the results. In Tables 3.2.1 and 3.2.2 the compressive strength was calculated based on the gross cross-sectional area, neglecting the effects of the perforations. Table 3.2.3 shows the compressive strength in each direction, for the three perforated bricks based on the net cross-sectional area.

By using the net cross-sectional area there is a marked increase in the compressive strength in all three directions, compared with the results of Table 3.2.1. There is also a substantial increase in the ratio of the strength on end and on edge to the strength on bed, indicating that the area of perforations has a significant effect on the strength in the two directions other than the bed. However, with the exception of the high strength brick, tested on edge the compressive strength in these two directions is still considerably lower than the bed strength, again with the strength on end being the lowest. These differences may be attributed to orthogonal strength characteristics and platen friction effects. It is of interest to note that bricks tested on end had the highest aspect ratio (height to least lateral dimension) and so the effects of platen restraint will be lowest in this case.

Table 3.2.2 Comparison of Brick Strength in Three Directions

	Brick Type			
Ratio to Bedjoint Strength	High	Medium	Low	Common
On Bed	1.0	1.0	1.0	1.0
On Edge	0.648	0.390	0.336	0.746
On End	0.49	0.312	0.312	0.696

Table 3.2.3 Compressive Strength of Perforated Bricks Based on Net Cross-Sectional Area

	Brick Type		
	High	Medium	Low
Compressive Strength			
On Bed N/mm^2	94.7	81.1	40.6
On Edge N/mm^2	103.8	57.8	24.4
On End N/mm^2	61.9	38.1	17.2
Ratio to Strength on Bed (i.e. strength on bed equal to 1.0)			
On Edge	1.096	0.712	0.601
On End	0.653	0.470	0.423

Lenczner and Foster[28] carried out tests on bricks in three different directions. Their results showed a similar trend in that the lowest strengths were obtained on end followed by that on edge. One of the bricks they tested was a three hole brick with an average compressive strength on bed of 58 N/mm^2. The ratio of strengths on edge and on end to the bed were 0.36 and 0.25 respectively which were similar to the corresponding ratios for the medium strength brick, Table 3.2.2.

3.3 Mortar and Grout

3.3.1 Mortar

Two grades of mortar were used a 1:¼:3 (cement;lime;sand by volume) grade I and a 1:½:4½ grade II. The mixes were proportioned using gauging boxes and the water content adjusted by the bricklayer to achieve a workable mix. 100 mm control cubes were taken during construction and tested at 28 days. The mortar strengths, thus obtained are given in Table 5.3.1 for each beam. The average compressive strength of the mortar for the brickwork prisms was 19.1 N/mm^2 for grade I and 6.2 N/mm^2 for grade II.

3.3.2 Cement and Lime

Ordinary portland cement conforming to B.S.12 'Portland Cement (Ordinary and Rapid Hardening)' and lime in accordance with B.S.890 'Building Limes' were used throughout.

3.3.3 Sand

There was some difficulty in finding a building sand which conformed to the grading limits of B.S.1200[30] for reinforced brickwork, however suitable sand was obtained from a pit in Edzell, Fife. The sieve analysis of the sand is given in Table 3.3.1.

3.3.4 Grout

The same sand and cement as used in the manufacture of the mortar was used for the grout. A number of mixes were tried initially. In the first series of beams, 1-7, a neat cement mix and a 1:1 sand/cement mix was used. The former mix although readily pumped proved very expensive in terms of cement usage and the latter mix was very difficult to pump with frequent blockages occurring. As described in Chapter 4 the construction sequence was then changed and a 1:2½ cement/sand mix was used. For all mixes a chemical additive 'conbex' was used, always in the same proportion to the cement content. This was a plasticiser which helped reduce the shrinkage of the grout. 100 mm cubes were cast during each grouting operation and then tested at seven days. Compressive strengths of over 40 N/mm^2 were attained for the first two mixes, whereas for the third mix the compressive strength was between 14-20 N/mm^2 at seven days.

3.4 Properties of Brickwork

In order to determine the strength and deformation properties

Table 3.3.1 Sieve Analysis of Sand

Test Sieve	% by Weight Passing Through Sieve	
	Test Result	B.S.1200 limit (Table 2)
5.0 mm	100	100
2.36 mm	100	90-100
1.18 mm	98	70-100
600 μm	67	40-80
300 μm	22	5-40
150 μm	5	0-10

of the brickwork it was necessary to adopt a suitable test specimen. The construction of the beams was such that the compressive forces developed in the direction parallel to the bedjoint.

Two types of prism, both built to represent the compression zone in a prestressed brickwork beam were chosen. The first prism, Figure 3.4.1(a) represented the upper three courses of the brickwork beam and was of the same form as recommended in design guides[31]. During the initial stages of the project splitting of the top bedjoint, in the constant moment zone of the beams was observed, prior to failure and it became apparent that the uppermost course of the beam was carrying most of the compressive forces in the section. It was then decided to test a prism, consisting of a single course of brickwork, to represent the top course of the prestressed brickwork beams, Figure 3.4.1(b).

Strain measurements were taken on the prisms using a 'demec' gauge with a gauge length of 150 mm. The strains were measured at six points on the three course prisms and four points on the single course prisms (Figure 3.4.1). The prisms were capped and levelled using either a rich mortar mix or dental plaster. 6 mm thick plywood sheets were placed between the prisms and the platens of the testing machine to help distribute the load more evenly.

At the beginning of the test, axial loading was ensured by comparing the strain measurements on opposite faces of the prism. Compressive loading was then applied in small equal increments. Normally, at between 60 and 70% of the ultimate load the load increment was halved. At each increment the load was held constant

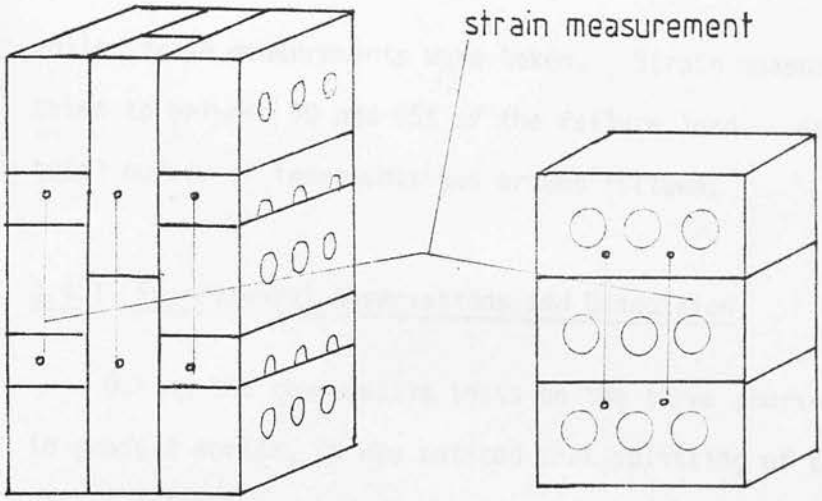

three course prisms

(a)

single course prisms

(b)

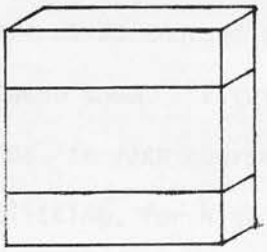

prism with frog removed

(c)

fig. 3.4.1 Prism types

while strain measurements were taken. Strain measurements were taken to between 90 and 95% of the failure load. Generally the total number of increments was around fifteen.

3.4.1 Experimental Observations and Discussion

During the compressive tests on the three course prisms, made in grade I mortar, it was noticed that splitting of the vertical mortar joints occurred at loads considerably lower than the failure loads. This splitting occurred at approximately 60% of the ultimate load in the case of the high strength bricks, 80% for medium strength, 90% for low strength and 59% for the common brick. For the medium strength brick in grade II, mortar splitting occurred at 90% of the failure load.

After splitting the prism behaved like three separate prisms, corresponding to each of the three courses and the compressive load was redistributed between them. Figure 3.4.2(a) shows typical average strain distributions, in each course of the three course prisms before and after splitting, for high strength brick. Prior to splitting the strains in each course were uniform but after splitting there was a dramatic change in the strain distribution with considerable variations from course to course. Once splitting had taken place it was impossible to adjust the loading to return to conditions of axial strain. The variations in compressive strain may be attributed to differences in the elastic properties of each course and movement of the upper platen. In order to check the strain distribution in the single course prisms, one or two prisms were tested with demecs at 6 points, three on either face.

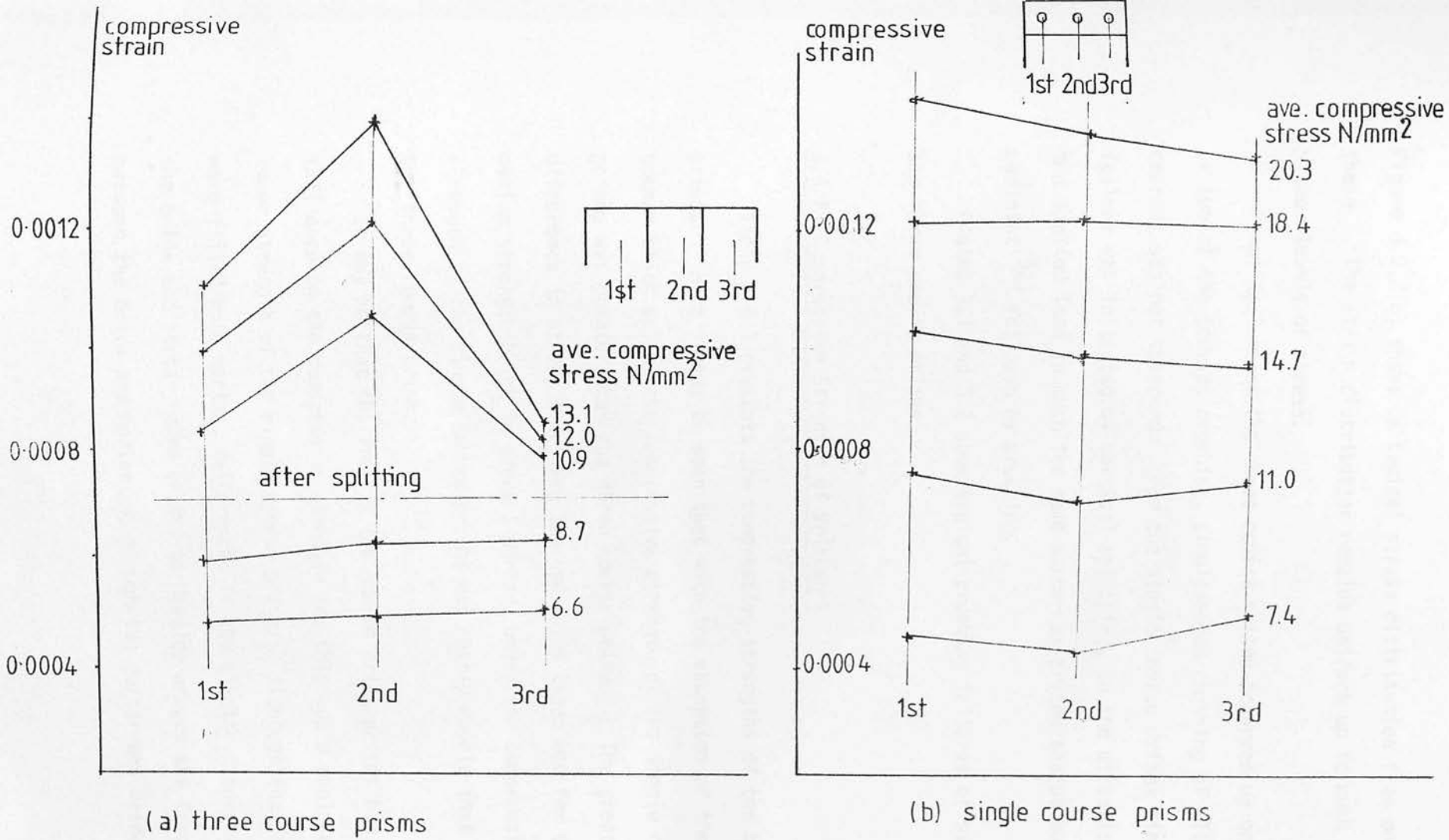

fig. 3.4.2 Typical distribution of strain for high strength brick prisms

Figure 3.2.2(b) shows a typical strain distribution from one of these. The strain distribution remains uniform up to much higher levels of stress.

Final failure of the three course prisms occurred by one or two of the courses crushing, simultaneous crushing of all three courses was not observed. For the single course prisms final failure was initiated by vertical splitting, in the direction of the applied load in much the same manner as prisms tested on the bedjoint[32] followed by crushing.

Plates 3.1 and 3.2 show typical crushing failures of single and three course prisms.

3.4.2 Compressive Strength of Brickwork

Table 3.4.1 presents the compressive strengths of the brickwork prisms. Here it may be seen that with the exception of the common brick prisms the compressive strength of the single course prisms was greater than the three course prisms. The greatest difference in strength between the two prism types was for the medium strength brick in grade I mortar, where the compressive strength of the single course prisms was nearly double that of the three course prism.

It may be that the frog in the common brick prisms had some influence on the compressive strength and this would explain the lower strength of the single course prism. Although the frogs were filled with mortar, differences in the elastic properties of the brick and mortar cause cracks to develop around the frog, between the brick and mortar, as though the mortar was being

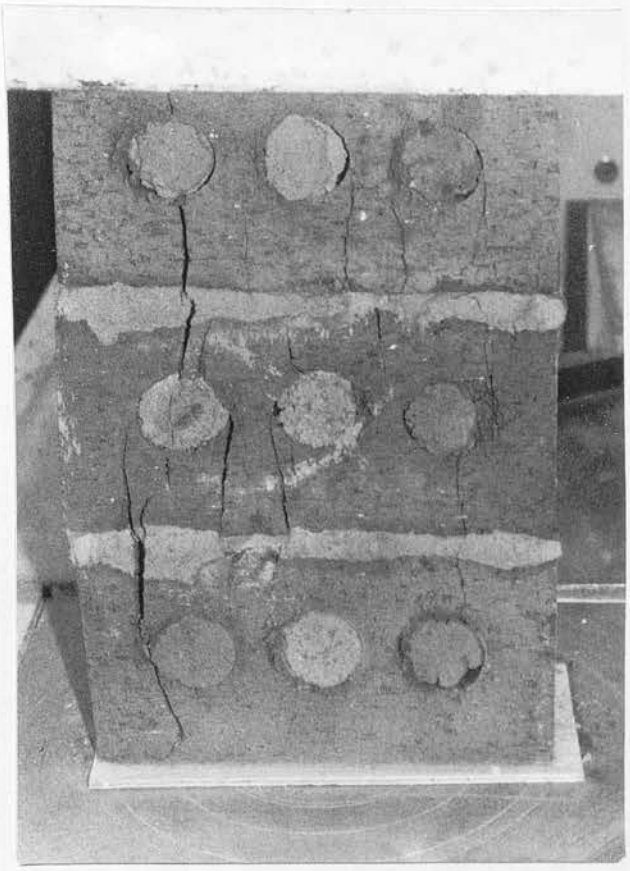

Plate 3.1 Typical failure of single course prism.

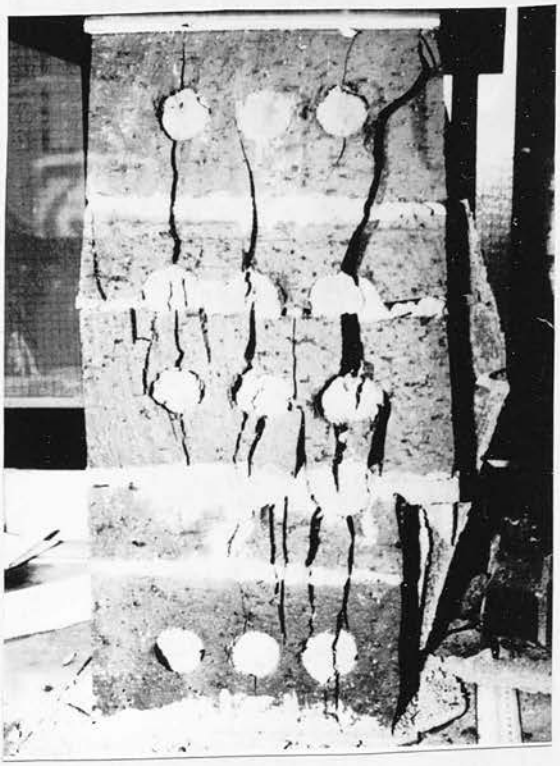

Plate 3.2 Typical failure of three course prisms.

Table 3.4.1 Compressive Strength of Brickwork Prisms

Brick Type	High Strength		Medium Strength		Low Strength		Common Brick		Medium Strength	
Mortar Type	1:¼:3		1:¼:3		1:¼:3		1:¼:3		1:½:4½	
Prism Type	Three Course	Single Course	Three Course	Single Course	Three Course	Single Course	Three Course	Single Course	Three Course	Single Course
Compressive Strength N/mm^2										
	22.15	33.17	9.82	19.85	10.05	9.53	8.98	5.56	13.29	21.13
	19.44	29.30	14.40	18.86	9.26	10.73	8.25	5.82	15.21	14.38
	18.17	47.63	10.20	29.30	9.75	8.94	9.23	8.07	10.35	16.61
	22.21	29.70	12.17	28.20	8.25	8.59	14.15	7.87	14.44	18.78
	20.30	25.92	14.40	25.09	9.23	8.23	13.20	5.80	9.63	14.45
	20.60	29.58	12.94	21.10	9.64	10.20	12.11	8.35	17.72	16.25
Average N/mm^2	20.48	32.56	12.36	23.70	9.36	9.37	10.99	6.92	13.48	16.93
Std. Deviation N/mm^2	1.43	7.06	1.82	4.05	0.57	0.88	2.26	1.20	2.99	2.63
Coeff. of Variance %	6.97	21.69	14.70	17.10	6.06	9.40	20.61	17.30	22.18	15.50

squeezed out of the frog. This must reduce the area of prism effectively carrying the load and at the same time inducing an eccentricity into the loading. Consequently the failure load was reduced and the compressive strength based on the gross cross-sectional area was reduced. To study the effect of the frog on the compressive strength of the common brick, a further three prisms were built. These were built in the same format as the single course prisms as shown in Figure 3.4.1(c), however the bricks had their frogs removed by cutting the brick in two, along the plane parallel to the bedjoint. This resulted in the prism having half the thickness of the single course prism. In order to reduce slenderness effects the top and bottom bricks in each prism were halved again, to reduce the overall height. The average compressive strength of these prisms was 16.05 N/mm^2. This is 2.3 times greater than the compressive strength of the single course prism which indicates that the presence of the frog weakens the single course prism considerably. The strength of these prisms was also 46% greater than the three course prisms.

Returning to the prisms built from the extruded bricks, it has generally been shown[32] that bonded prisms, i.e. prisms with a continuous mortar joint in the same direction of the compressive force have lower strength than prisms of the same brickwork without the continuous joint. Work by Hodgkinson and Davies[27] and Lenczner and Foster[28] on prisms similar to the three course prisms showed a reduction in strength when compared to the strength on the bed.

It is apparent, considering the previous work[27,28,32], that

the compressive strength of brickwork prisms is reduced by having continuous joints in the direction of load or by testing in directions other than the bedjoint. However the previous work has normally considered this to be due to the different strength properties of the bricks in the three orthogonal directions and while this may indeed have some influence, the single course prisms in which the bricks are laid on edge showed considerably higher strengths than the three course prisms, although the bricks were tested in the same directions for both prism types. The lower strength of the three course prisms is then most likely due to the splitting of the continuous mortar joint and the consequent redistribution of load. The prism is then divided into three separate courses, each carrying a different proportion of the total applied load. Failure of all three courses is very unlikely to occur simultaneously and hence the average compressive strength of the prism will be less than that of the individual course.

In considering the merits of the single and three course prisms as a means of providing an estimate of the strength of a brickwork flexural member, it is necessary to consider the behaviour of the beam in relation to the behaviour of the prism. In the three course prisms it has been shown that the strain distribution after splitting is very irregular as shown in Figure 3.4.2. In a flexural situation the strain distribution is very well defined up to failure with the maximum compressive strains occurring in the outer fibres. Splitting of the mortar joints parallel to the direction of the compressive forces may increase the strains near the outer fibres but will not result in

a redistribution of the load away from this region. In other words when a beam fails in flexure then crushing will occur in the outer fibres at the crushing strength of the brickwork. The average compressive strength of the three course prisms will therefore be less than the crushing strength of the compression zone in a brickwork beam.

Following this argument then the single course prism is more likely to produce a closer estimate of the flexural compressive strength of the brickwork as the strain distribution is uniform up to greater levels of stress and hence the average compressive strength of the prism will be much closer to the crushing strength of the brickwork.

3.4.3 Stress/Strain Relationship of Brickwork and Elastic Modulus

The stress/strain relationship for each prism was obtained on the basis of the average compressive stress and average of the measured strains.

The stress/strain relationships thus obtained are presented in Figures 3.4.3-7. In each figure the stress/strain relationship of both prism types are compared for each type of brickwork.

Previous work on the stress/strain relationship of brickwork prisms tested normal to the bedjoint[33,34] produced a relationship which showed a falling branch past the peak compressive stress, i.e. decreasing compressive stress with increasing strain.

It was not possible to measure strain past the maximum compressive stress with the method used to test the prisms and therefore not possible to detect the presence of a falling branch.

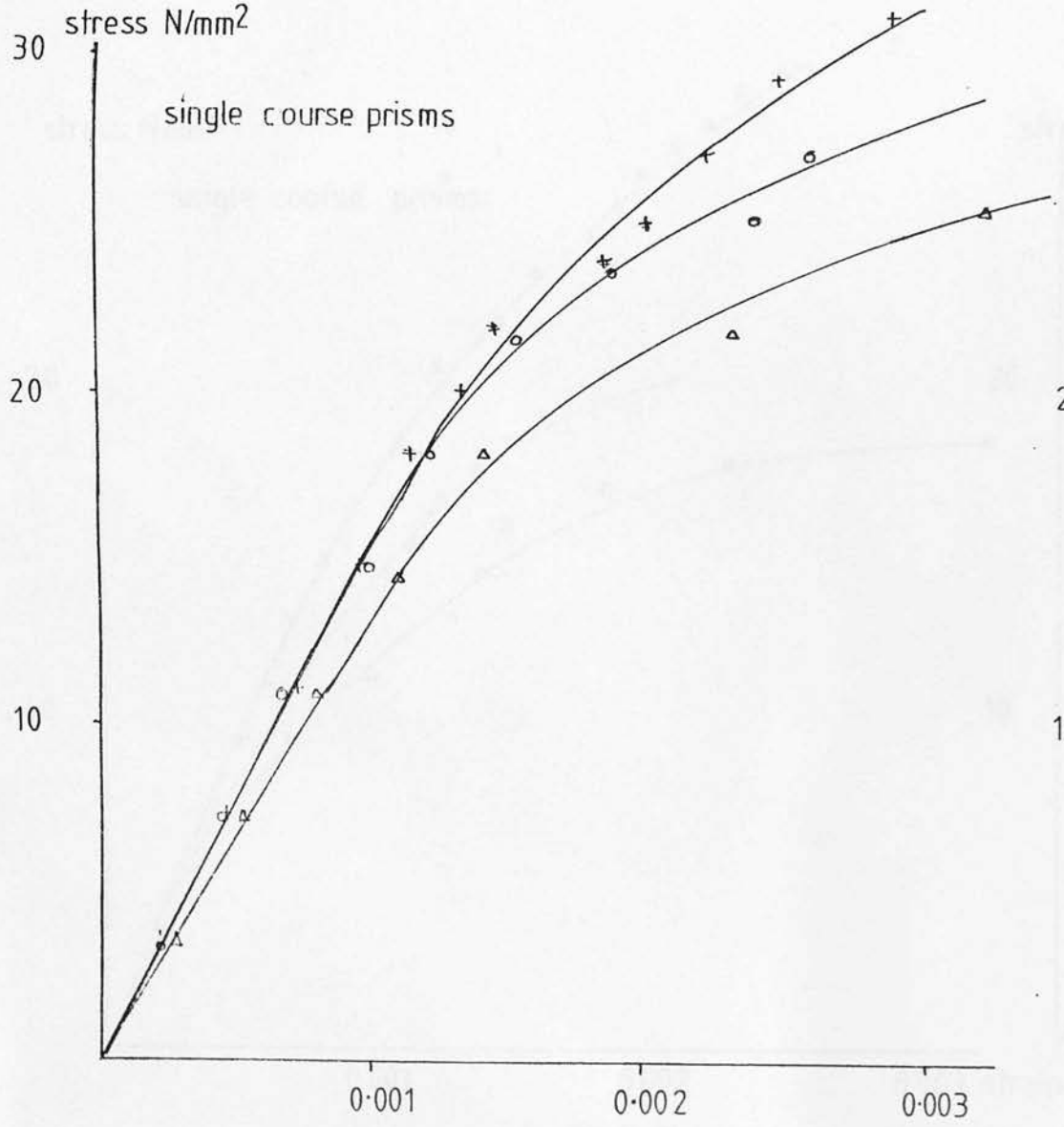

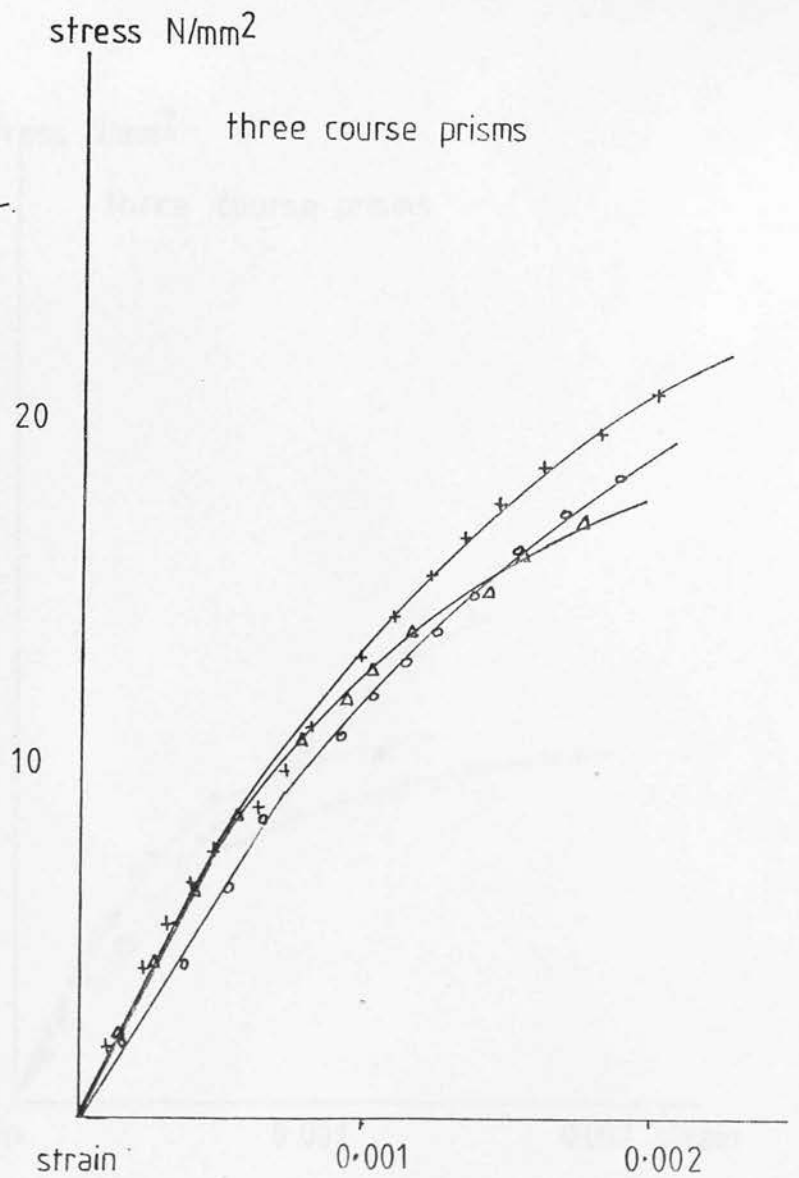

fig. 3.4.3 Stress/strain relationships for high strength brickwork

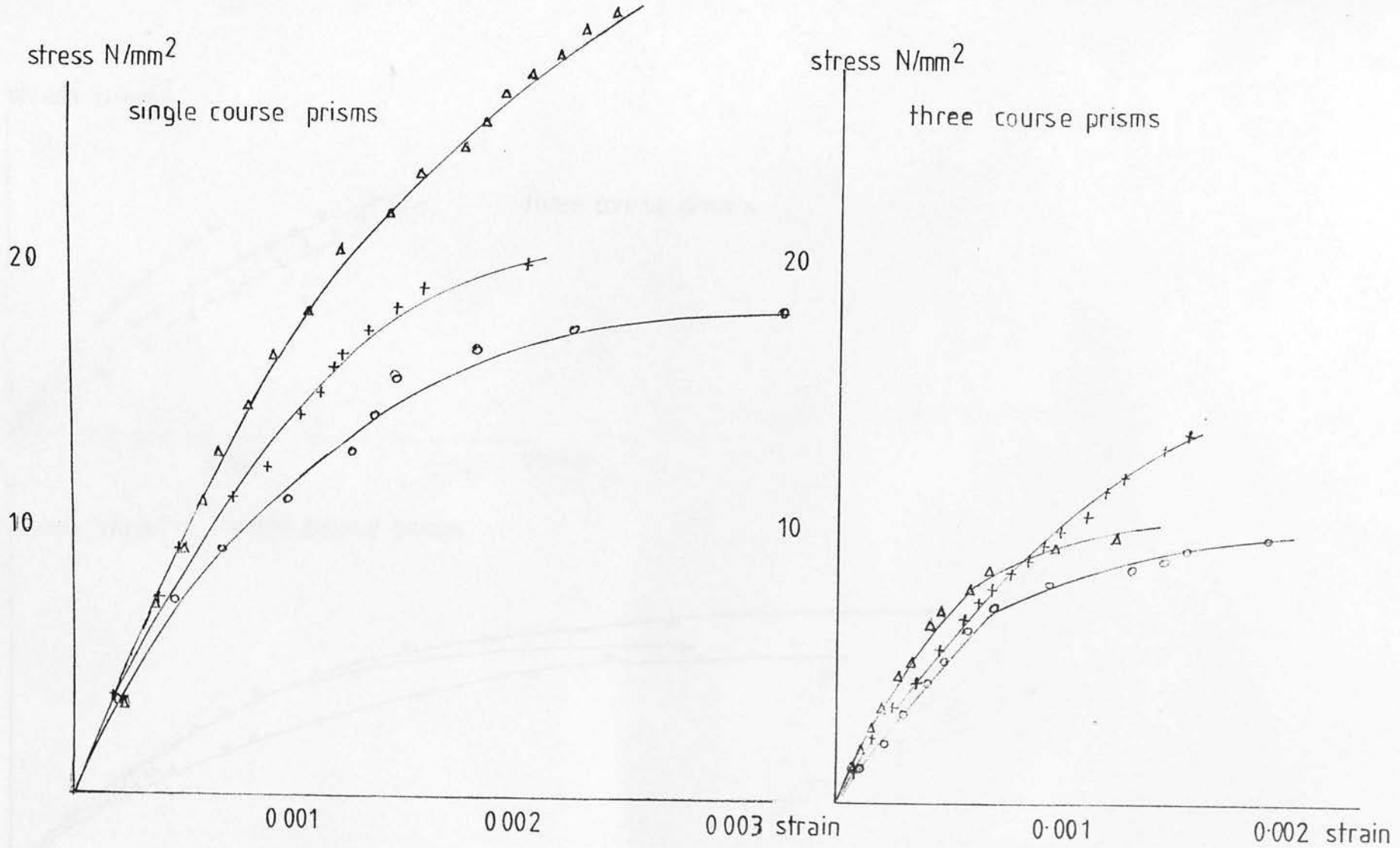

fig. 3.4.4 Stress/strain relationships for medium strength brickwork in grade I mortar

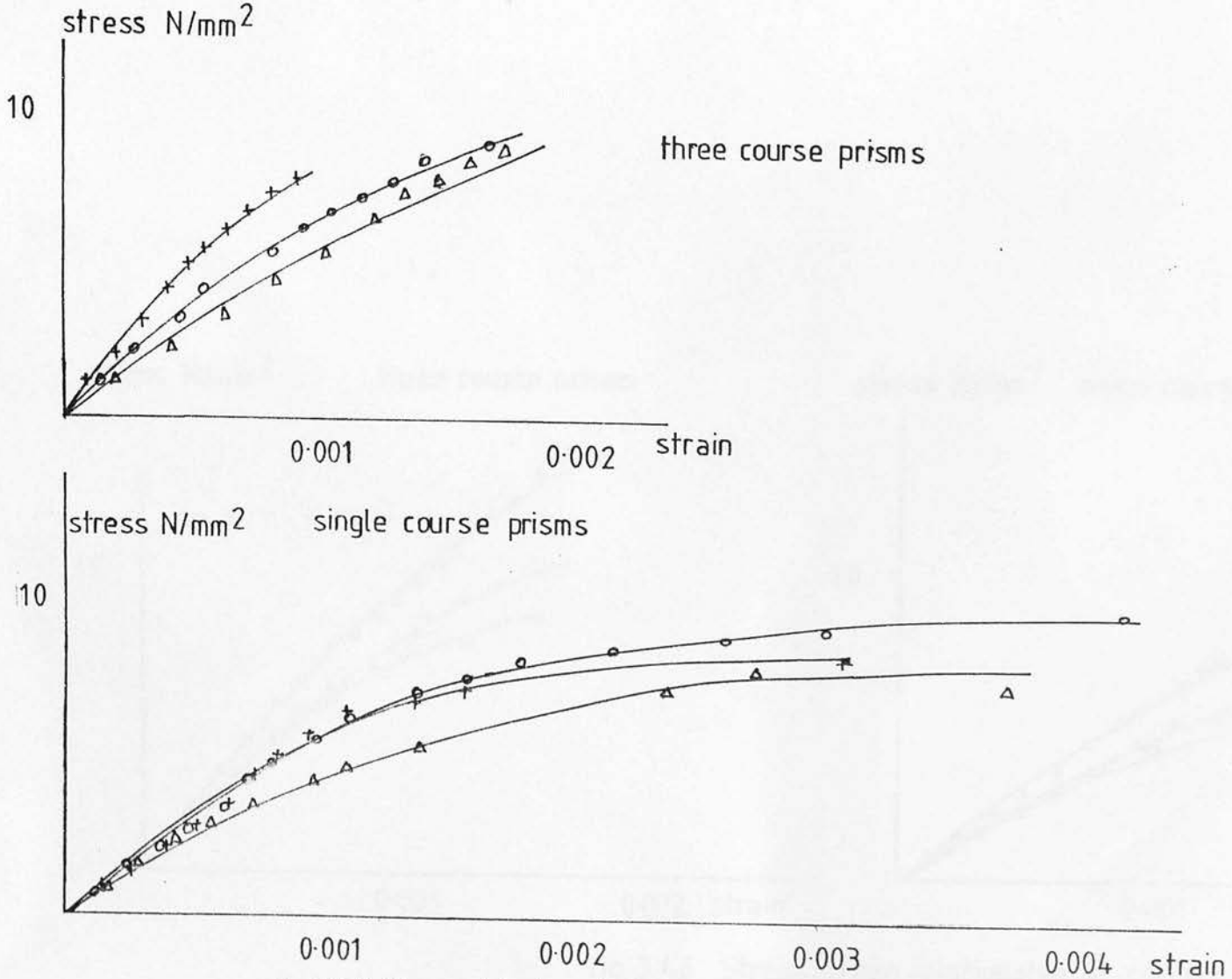

fig. 3.45 Stress/strain relationships for low strength brickwork

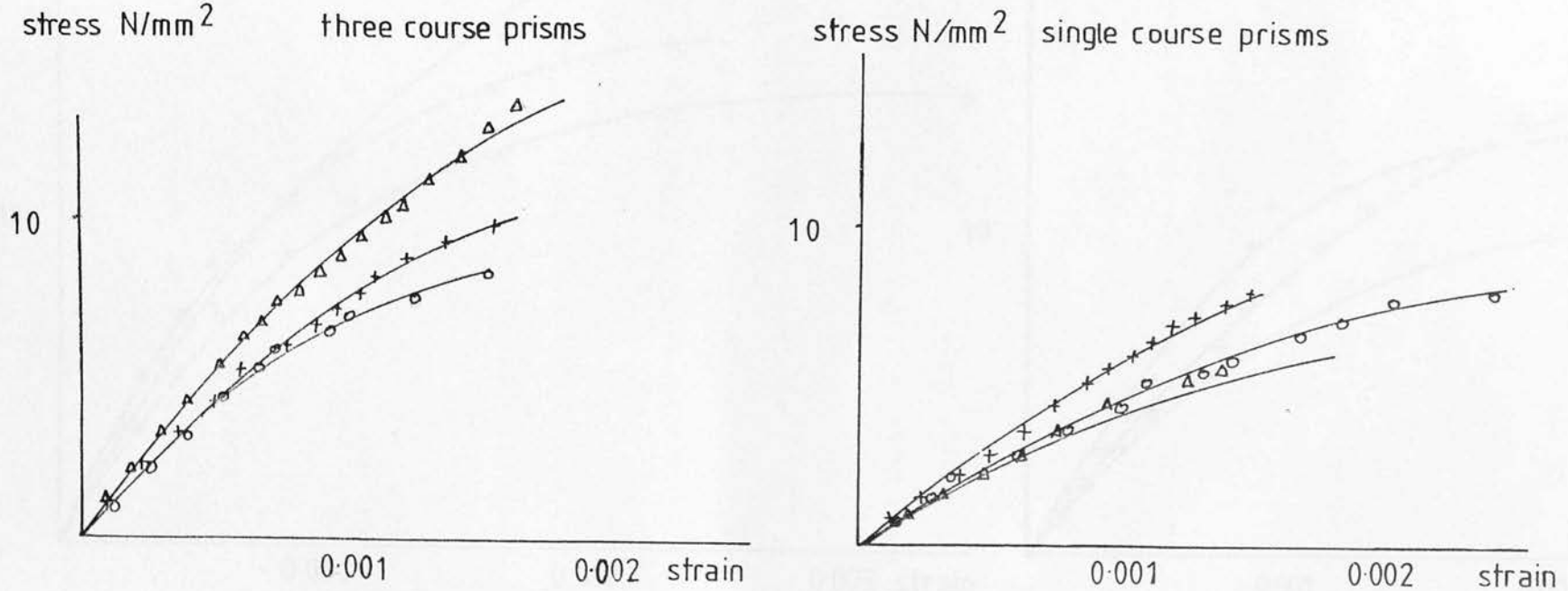

fig. 3.4.6 Stress/strain relationship of common brickwork

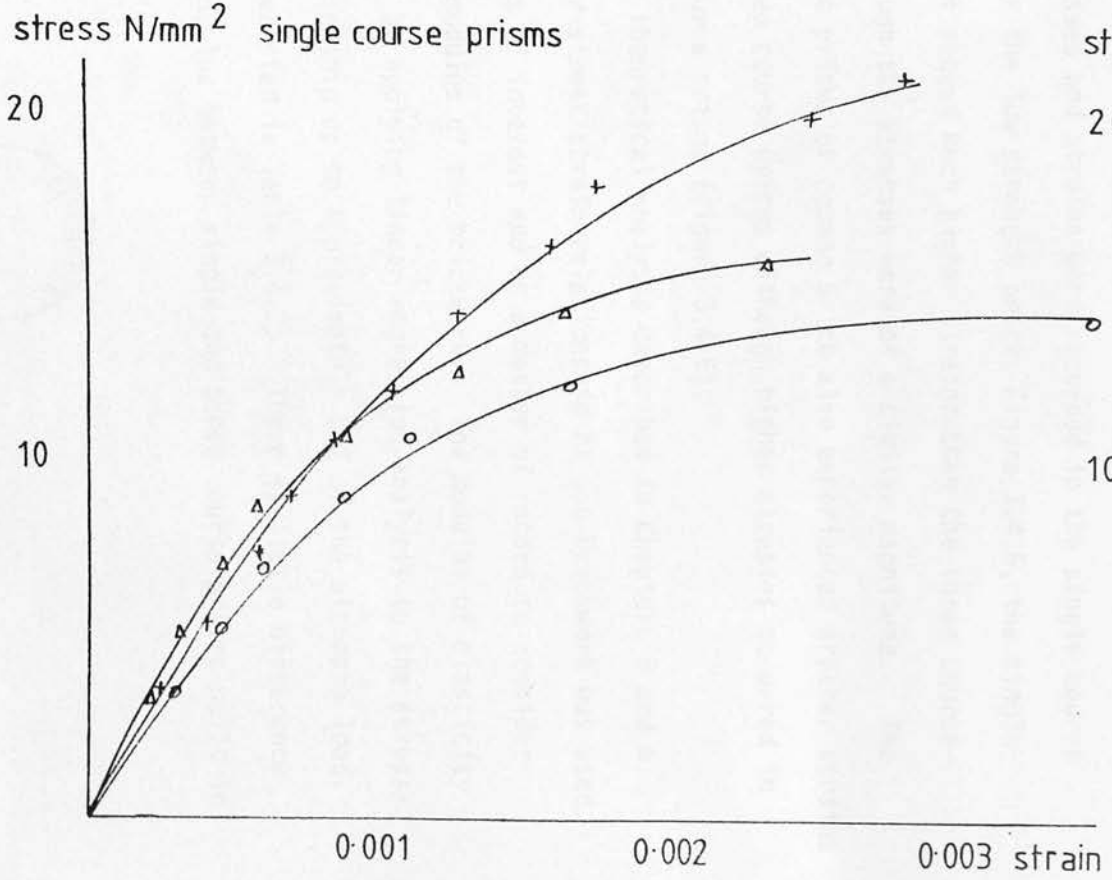

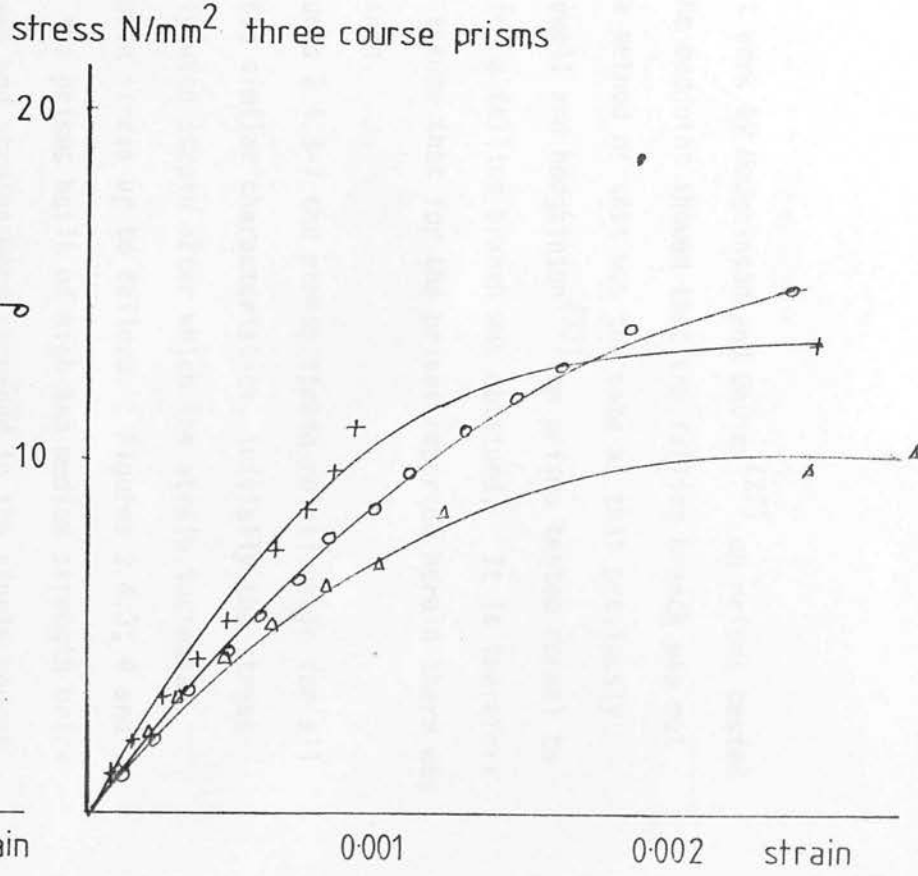

fig. 3.4.7 Stress / strain relationship of medium strength brickwork in grade II mortar

However recent work by Hodgkinson and Davies[27] on prisms tested parallel to the bedjoint showed that the falling branch was not present. The method of test was the same as that previously employed by Powell and Hodgkinson[33] on prisms tested normal to the bed in which a falling branch was obtained. It is therefore reasonable to assume that for the prisms reported herein there was no falling branch.

From Figures 3.4.3-7 the stress/strain relationship for all prisms exhibited similar characteristics, initially the stress varies linearly with strain after which the strain increases more rapidly with stress up to failure. Figures 3.4.3, 4 and 7 show that for the prisms built of high and medium strength brick greater stresses and strains were recorded in the single course prisms. For the low strength brick, Figure 3.4.5, the single course prisms showed much higher strains than the three course prisms although the stresses were of a similar magnitude. The single course prisms of common brick also experienced greater strains than the three course prisms although higher stresses occurred in the three course prisms (figure 3.4.6).

For the theoretical analysis described in Chapters 5 and 6 the nonlinear stress/strain relationship of the brickwork was used. However it is of interest and as a matter of record to consider the elastic modulus of the brickwork. The modulus of elasticity was obtained by applying linear regression analysis to the stress/strain relationship up to approximately 35% of the ultimate load. These are presented in Table 3.4.2. There is little difference in elastic modulus between single and three course prisms built in

Table 3.4.2 Summary of Stress/Strain Characteristics

Brick Type	Prism Type	Compressive Strength N/mm^2	Ultimate Strain	(Ave.)	Elastic Modulus	kN/mm^2 (Ave.)
High (82 N/mm^2) Strength	Single	33.17	0.00307		15.7	
		29.30	0.00318	(0.00326)	14.6	14.6
		25.92	0.00353		13.4	
High (82 N/mm^2) Strength	Three	22.12	0.00224		12.9	
		19.44	0.00201	(0.00205)	13.3	14.2
		18.17	0.00190		16.5	
Medium (67 N/mm^2) Strength 1:¼:3 Mortar	Single	19.85	0.00230		12.8	
		18.86	0.00306	(0.00263)	11.3	
		29.3	0.00253		19.7	14.6
Medium (67 N/mm^2) Strength 1:¼:3 Mortar	Three	14.4	0.00165		11.5	
		9.82	0.00203	(0.00171)	11.3	13.3
		10.2	0.00147		17.0	
Medium (67 N/mm^2) Strength 1:¼:4½	Single	21.13	0.00286		11.85	
		14.58	0.00351	(0.0030)	12.6	12.9
		16.61	0.00267		14.4	
Medium (67 N/mm^2) Strength 1:¼:4½	Three	15.21	0.00240		8.74	
		10.35	0.00310	(0.00261)	8.26	9.2
		13.25	0.00250		10.63	
Low (34 N/mm^2) Strength	Single	9.53	0.00402		5.6	
		10.73	0.00450	(0.00433)	5.7	5.4
		8.95	0.00448		4.8	
Low (34 N/mm^2) Strength	Three	8.26	0.00108		10.9	
		9.24	0.00154	(0.00152)	8.1	8.1
		9.64	0.00193		5.2	
Common (22 N/mm^2) Strength	Single	8.07	0.00174		5.6	
		7.87	0.00258	(0.00202)	4.2	4.9
		5.80	0.00175		4.9	
Common (22 N/mm^2) Strength	Three	10.67	0.00171		8.14	
		14.15	0.00201	(0.00177)	9.6	8.8
		8.33	0.00161		8.8	

high and medium strength brick. This is not the case for the low strength and common brick in which the single course prisms appear to have considerably lower values for the elastic modulus than the three course prisms. From Table 3.2.2 it can also be seen that the elastic modulus appears to increase with the compressive strength.

Previous work[35] in which the results of Table 3.4.2 were combined with a large number of tests on other brickwork prisms, tested parallel to the bedjoint, developed the following empirical expression for elastic modulus in terms of the compressive strength of brickwork:

$$E = 1180 \cdot f_m^{0.83} \qquad (3.4.1)$$

This expression is derived from quite a wide scatter of experimental results and can of course only give an approximate estimate of the elastic modulus.

3.4.4 Ultimate Compressive Strain of Brickwork

As previously mentioned it was not possible to measure strains at the point of failure, however the strains were measured very close to the failure for most of the prisms. By using regression analysis the stress/strain relationship was mathematically extrapolated to find the strain at the ultimate compressive stress for each prism. The ultimate strains thus obtained are given in Table 3.4.2. For all the different brickwork and prism types the

average ultimate strain varies from 0.00152 to 0.00433. It is interesting to note that these lower and upper limits correspond to the three and the single course prisms built from the low strength brick. In all cases the average ultimate strain of the single course prisms was greater than that of the three course prisms. The average ultimate strain of the single course prisms for all types of brickwork was 0.00304 and for the three course prisms was 0.00194. The former value of ultimate compressive strain from the single course prisms is very similar to the previously assumed value of 0.003 for brickwork in flexural compression[36] and also for brickwork under axial compression normal to the bedjoint[32].

3.4.5 Non-Dimensional Stress/Strain Relationship for Brickwork

In order to use the experimental stress/strain relationship for the brickwork prisms to calculate the deformations and ultimate strength of prestressed brickwork beams it was necessary to have the relationship expressed in some mathematical form.

From Figures 3.4.3-7 it can be seen that there is some variation between individual stress/strain relationships for a particular brickwork and prism type. In order to obtain a more general picture of the stress/strain relationship and at the same time eliminate some of the variations the stress/strain relationship was expressed in non-dimensional form, Figure 3.4.8.

Once the experimental test results were presented in this form it was then possible to combine the results of each prism for a particular grouping of brickwork and prism type and then

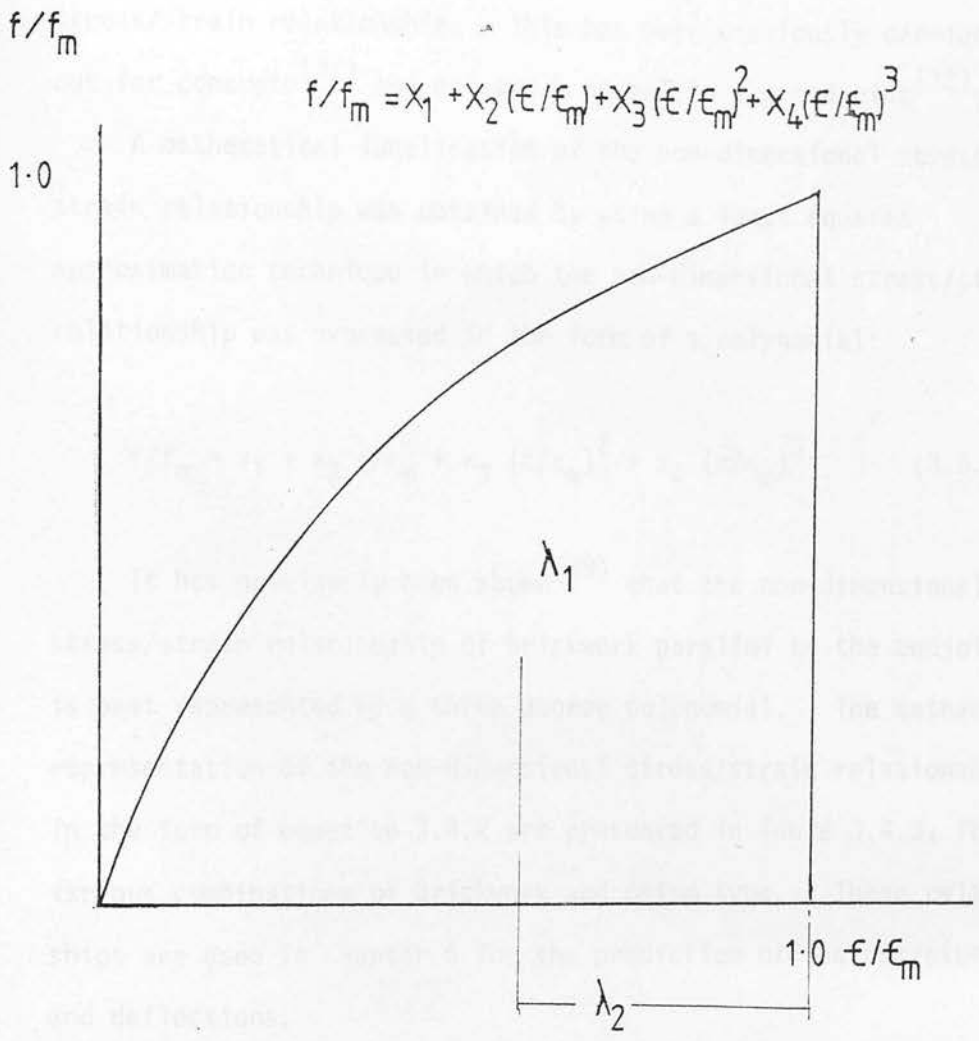

fig. 3.4.8 Non dimensional stress/strain relationship

obtain a mathematical representation of the non-dimensional stress/strain relationship. This has been previously carried out for concrete[37] and brickwork normal to the bedjoint[32].

A mathematical idealisation of the non-dimensional stress/strain relationship was obtained by using a least squares approximation technique in which the non-dimensional stress/strain relationship was expressed in the form of a polynomial:

$$f/f_m = x_1 + x_2\ \varepsilon/\varepsilon_m + x_3\ (\varepsilon/\varepsilon_m)^2 + x_4\ (\varepsilon/\varepsilon_m)^3 \qquad (3.4.2)$$

It has previously been shown[38] that the non-dimensional stress/strain relationship of brickwork parallel to the bedjoint is best represented by a three degree polynomial. The mathematical representation of the non-dimensional stress/strain relationships, in the form of equation 3.4.2 are presented in Table 3.4.3, for the various combinations of brickwork and prism type. These relationships are used in Chapter 6 for the prediction of the curvatures and deflections.

In the prediction of the ultimate flexural strength of reinforced or prestressed brickwork there are two very useful properties of the non-dimensional stress/strain curve which are used to describe the distribution of compressive forces in the compressive zone of the beams. These are geometric properties of the non-dimensional stress/strain relationship and are often called stress block factors. These are discussed in greater detail in Chapter 5. The first of the stress block factors, λ_1 is equal to the area under the non-dimensional stress/strain curve and is related to the average compressive stress in the compression zone

Table 3.4.3 Non-Dimensional Stress/Strain Characteristics

Brick Type	Mortar	Prism	f_m N/mm^2	Ultimate Strain	X_1	X_2	X_3	X_4	Correlation Coefficient	λ_1	λ_2
High	1:¼:3	Single	32.56	0.00326	-0.05	2.373	-2.095	0.776	0.985	0.652	0.390
High	1:¼:3	Three	20.48	0.00205	0.011	1.740	-1.004	0.254	0.991	0.610	0.368
Medium	1:¼:3	Single	23.70	0.00263	0.017	2.064	-1.245	0.150	0.980	0.672	0.382
Medium	1:¼:3	Three	12.36	0.00172	-0.054	3.104	-4.067	2.034	0.912	0.651	0.389
Medium	1:½:4½	Single	16.93	0.00302	-0.002	2.769	-2.999	1.231	0.962	0.691	0.394
Medium	1:½:4½	Three	13.48	0.00270	-0.004	2.822	-3.314	1.505	0.932	0.679	0.394
Low	1:¼:3	Single	9.37	0.00433	-0.070	3.393	-4.719	2.194	0.991	0.702	0.399
Low	1:¼:3	Three	9.36	0.00160	-0.035	1.623	-0.678	0.074	0.985	0.569	0.352
Common	1:¼:3	Single	6.91	0.0025	-0.014	1.709	-0.729	0.044	0.990	0.609	0.36
Common	1:¼:3	Three	10.99	0.00178	-0.045	1.985	-1.978	1.015	0.820	0.542	0.359

of a prestressed brickwork beam. λ_1 is therefore:

$$\lambda_1 = \int_0^{1.0} (x_1 + x_2\ (\varepsilon/\varepsilon_m) + x_3\ (\varepsilon/\varepsilon_m)^2 + x_4\ (\varepsilon/\varepsilon_m)^3) d\ \varepsilon/\varepsilon_m \quad (3.4.3)$$

The second stress block factor, λ_2 is the centroid of the area under the non-dimensional stress/strain curve, taken from $\varepsilon/\varepsilon_m = 1.0$ and indicates the position of the resultant thrust of the compressive forces in the compression zone, λ_2 is:

$$\lambda_2 = 1.0 - \frac{\int_0^{1.0} \varepsilon/\varepsilon_m\ (x_1 + x_2(\varepsilon/\varepsilon_m) + x_3\ (\varepsilon/\varepsilon_m)^2 + x_4\ (\varepsilon/\varepsilon_m)^3)\ d\ \varepsilon/\varepsilon_m}{\lambda_1} \quad (3.4.4)$$

From Table 3.4.3 it can be seen that there is always a small value assigned to x_1, the first term in the non-dimensional stress/strain relationship. This is not quite correct as it implies that the stress/strain relationship does not pass through the origin. This is caused by the statistical nature of the analysis and the variations between the individual stress/strain relationships. However the value of x_1 is really very small and does not significantly influence the stress/strain relationship and is consequently ignored.

The correlation coefficients listed in Table 3.4.3 are a measure of the correlation between the mathematically idealised relationship and the experimental data, such that with perfect correlation the coefficient is 1.0. With the exception of the common brick, three course prisms the correlation coefficients are all greater than 0.9. It can also be seen that there is little variation between the stress block factor λ_1 for the range of prisms tested, the upper and lower limits being 0.702 and 0.542. There is even less variation in λ_2,

the maximum and minimum values being 0.399 and 0.352 respectively. This suggests that although the actual stress/strain relationship of brickwork is greatly affected by the brick, mortar and prism type, these factors do not have the same influence on the non-dimensional stress/strain relationship.

As with the treatment of the elastic modulus in section 3.4.3 the non-dimensional stress/strain data described in this chapter was combined with the results from[35] a large number of other prisms tested parallel to the bedjoint. A non-dimensional stress/strain relationship which is based on a wide range of bricks, mortar and prism types was obtained, as follows:

$$f/f_m = -0.006 + 2.264\ \varepsilon/\varepsilon_m - 2.092\ (\varepsilon/\varepsilon_m)^2 + 0.834\ (\varepsilon/\varepsilon_m)^3 \quad (3.4.5)$$

This relationship is based on over 1200 measurements taken from over eighty prism tests and is shown graphically in Figure 3.4.9.

Table 3.4.2 provides all the necessary information to describe the stress/strain relationship for each type of brickwork for use in predicting the strength and deformations of prestressed brickwork beams in Chapters 5 and 6.

3.4.6 Modulus of Rupture

The tensile strength of brick masonry is extremely low compared to the compressive strength and in design the tensile strength is generally ignored. A more detailed analysis will however require some knowledge of the tensile strength. The tensile strength of individual bricks and mortar is normally greater than that of the

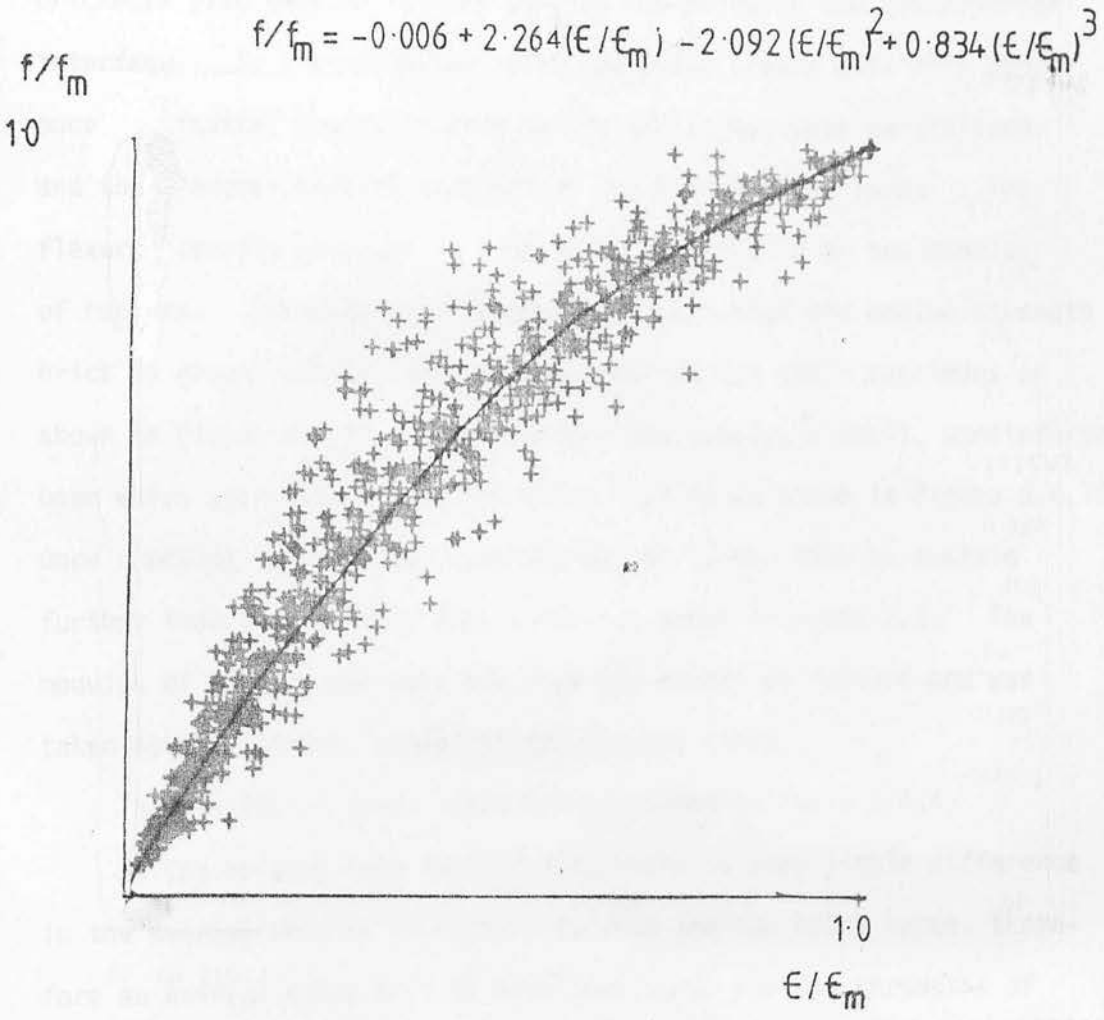

fig. 3.4.9 Nondimensional stress/strain relationship of brickwork.

brickwork with tensile failure usually occurring in the brick/mortar interface. In a prestressed brickwork beam, cracks will only occur once the initial precompression at the soffit has been neutralised and the flexural tensile strength of the brickwork exceeded. The flexural tensile strength is most often referred to as the modulus of rupture. The modulus of rupture for both high and medium strength brick in grade I mortar was found by testing the small specimens as shown in Figure 3.4.10. The specimen was simply, a small, unreinforced beam which was tested under two point loading as shown in Figure 3.4.10(b). Once cracking occurred the specimen was no longer able to sustain further load and collapse took place, as shown in plate 3.3. The modulus of rupture was obtained from the moment at failure and was taken as the flexural stress at the extreme fibre.

The results of these tests are presented in Table 3.4.4.

As can be seen from Table 3.4.4, there is very little difference in the average modulus of rupture between the two brick types, therefore an average value of 1.49 N/mm^2 was taken for all strengths of brickwork in grade I mortar. It has been recognised[1] that the tensile strength of brickwork is influenced by the mortar grade and it would appear that the tensile strength of brickwork in 1:½:4½ mortar (grade II) is approximately 0.7 times the strength of grade I. Hence the modulus of rupture of the beams in grade II mortar is taken as 0.7 times 1.49, i.e. 1.13 N/mm^2.

3.5 Properties of Prestressing Strand

Seven wire stabilised prestressing strand was used throughout. The nominal diameter was 10.9 mm and cross-sectional area 72 mm^2.

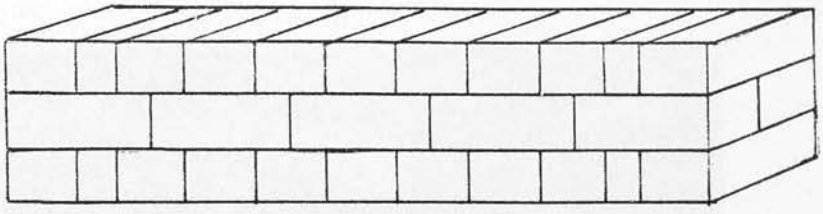

(a) modulus of rupture specimen

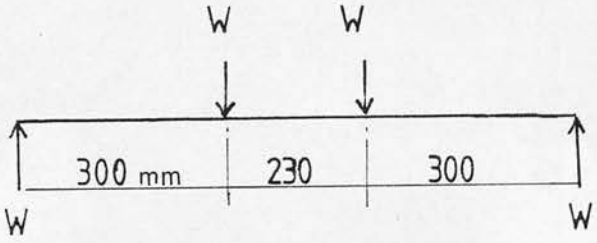

(b) loading arrangement

fig. 3.4.10 Modulus of rupture test

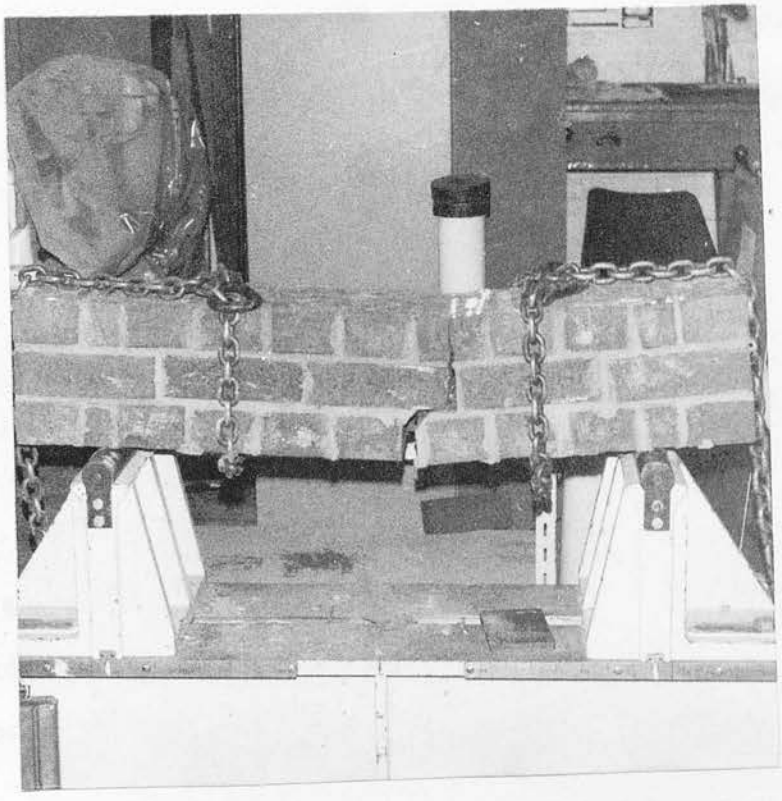

Plate 3.3 Modulus of rupture test.

Table 3.4.4 Modulus of Rupture Tests

Specimen No.	Modulus of Rupture N/mm^2	
	High Strength Brick	Medium Strength Brick
1	1.27	1.36
2	1.78	1.33
3	1.60	1.72
4	1.44	1.72
5	1.09	1.62
6	1.62	1.32
Average N/mm^2	1.47	1.51
Std. Deviation N/mm^2	0.251	0.196
Coeff. of Variation %	17.17	12.95

Table 3.5.1 Summary of Tests on Strand

Specimen No.	Elastic Modulus kN/mm^2	Ultimate Strength N/mm^2	0.2% Proof Stress N/mm^2
1	211	1736	1600
2	219	1653	1620
3	217	1708	1670
4	216	1736	1680
Average	216	1708	1642

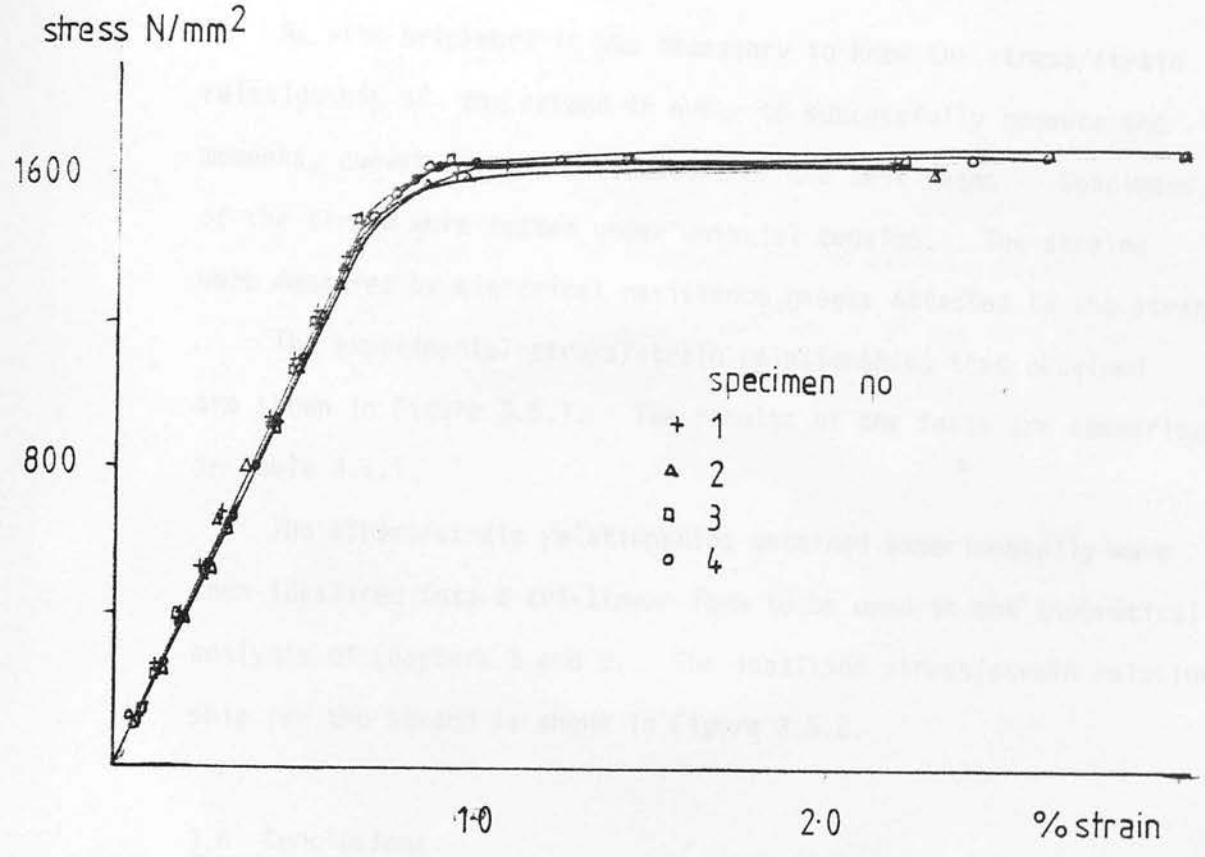

fig.3.5.1 Stress/strain relationships for strand

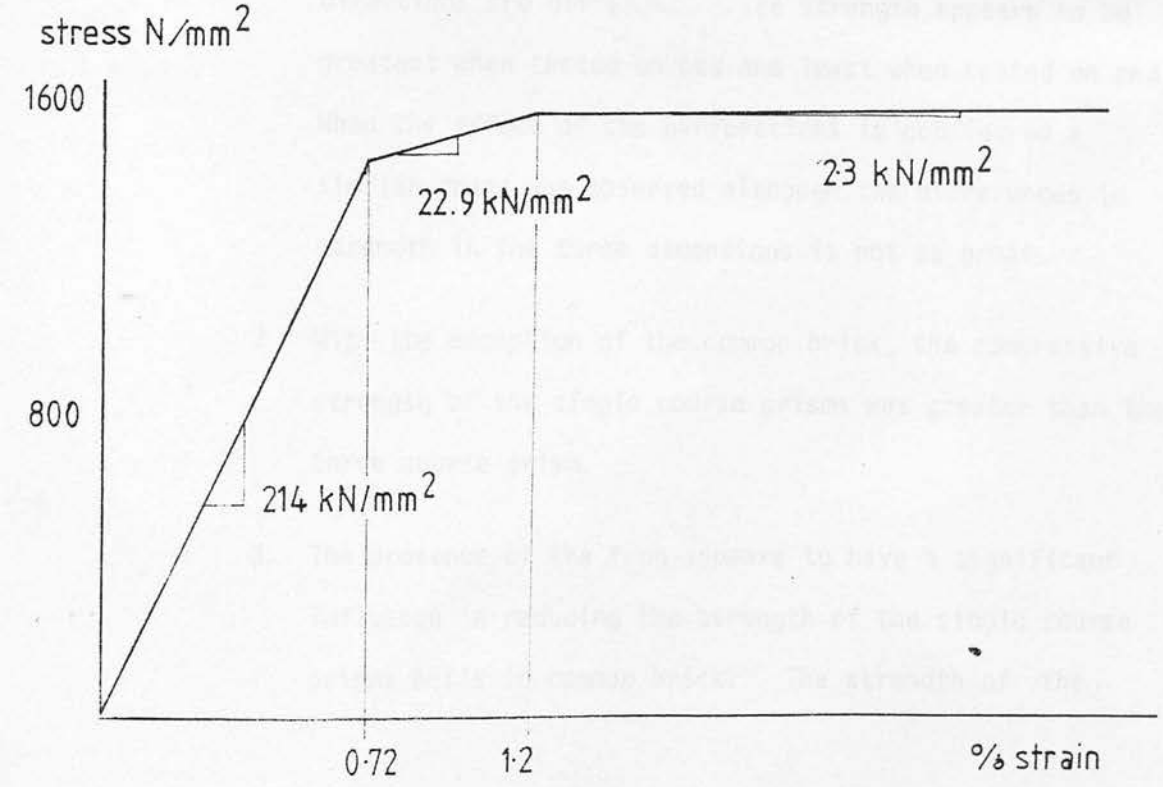

fig.3.5.2 Idealised stress/strain relationship for strand

As with brickwork it was necessary to know the stress/strain relationship of the strand in order to successfully compute the moments, curvatures and deflections of the test beams. Specimens of the strand were tested under uniaxial tension. The strains were measured by electrical resistance gauges attached to the strand.

The experimental stress/strain relationships thus obtained are shown in Figure 3.5.1. The results of the tests are summarised in Table 3.5.1.

The stress/strain relationships obtained experimentally were then idealised into a tri-linear form to be used in the theoretical analysis of Chapters 5 and 6. The idealised stress/strain relationship for the strand is shown in Figure 3.5.2.

3.6 Conclusions

1. The compressive strengths of bricks in three orthogonal directions are different. The strength appears to be greatest when tested on bed and least when tested on end. When the effect of the perforations is considered a similar trend was observed although the differences in strength in the three dimensions is not as great.

2. With the exception of the common brick, the compressive strength of the single course prisms was greater than the three course prism.

3. The presence of the frog appears to have a significant influence in reducing the strength of the single course prisms built in common brick. The strength of the

single course prisms built with bricks after the removal of the frogs increases significantly.

4. The ultimate compressive strain of brickwork prisms tested parallel to the bedjoint is influenced by the type of prism. The single course prisms appear to fail at higher ultimate strains when compared with the three course prisms.

5. The characteristics of the non-dimensional stress/strain relationship of brickwork parallel to the bedjoint is not significantly affected by brick, mortar or prism type.

CHAPTER 4 : EXPERIMENTAL PROCEDURE AND TEST BEAMS

4.1 Introduction

This chapter deals with the development of the sections for the prestressed brickwork beams, their construction and testing. Details of the materials used in the construction were considered in Chapter 3.

4.2 Test Beams

4.2.1 Development of Beam Section

In reinforced brickwork flexural members the reinforcement is either laid in the bedjoint during construction or it is placed in a preformed cavity after construction which is then grouted with a concrete mix to form a monolithic construction.

The former method is only suited for lightly loaded members as the maximum diameter of the reinforcement is restricted by the thickness of the mortar joints. It would be possible to construct a prestressed brickwork beam in this type of section, however, it is obvious that only small diameter wires could be used and that these would need to be pretensioned with the beam constructed round them. This would make the construction of the beams rather unsafe and unnecessarily complicated.

Considering the grouted cavity type of construction the type of section most often adopted is one which consists of two outer leaves of brickwork and a cavity the full depth of the beam into which the reinforcement is placed at the correct depth and then

filled with concrete. In this form of construction the cavity may occupy as much as 35% of the total cross section, hence the concrete must carry a considerable proportion of the load. It was decided then from the outset that neither of these section types would be used.

In selecting a suitable section for the prestressed brickwork beams the following criteria were adopted:

(i) effective utilisation of as much ceramics as possible;

(ii) ease in grouting of tendons;

(iii) ease of construction;

(iv) similar bonding pattern as used in brick wall, hence no special skill is required of bricklayer;

(v) provision of cavity so that tendons may be placed at required depth.

In addition to these requirements, which could be applicable to any prestressed brickwork beam, it was decided that the position of the resultant thrust on the section should not be greater than h/6 from the centroid, where h is the overall depth, thereby avoiding tensile stresses due to prestress. At one stage a section was considered in which the bricks in one course were laid on edge in such a manner as to provide a duct, through the perforations, running the total length of the beam, into which the prestressing strand would be placed. It was then realised that it would be very difficult for the bricklayer to align the holes and keep them

clear of mortar for large span beams. It was also likely that grouting would prove difficult and that the range of possible tendon eccentricities was very limited.

Two basic section types were eventually chosen as shown in Figure 4.2.1. The first section, type A, was built in normal English bond, except for the second course. In this course the bricks were laid on edge, with the perforations pointing outwards from the face of the beam. This left a gap between the bricks, forming a cavity for the tendon. All the perforations were filled with mortar with the exception of 3 or 4 which were used for grouting. The second section, type B, Figure 4.2.1, was also built in normal English bond. In this section the cavity was formed by cutting the bricks in the 2nd course lengthwise and placing the halves flush with the face of the beam. The area of the cavity for both these sections is only approximately 10% of the total cross-sectional area.

4.2.2 Constructional Details

The beams were built on the floor of the testing laboratory by an experienced bricklayer, Plate 4.1. In order to resist the transverse tensile forces that develop in the 'lead in length' of the beams due to anchor zone stresses, some reinforcement was provided in these zones (Figure 4.2.1). In beams of section type A the reinforcement consisted of four, 6 mm diameter mild steel rods placed along the centre line of the beam at a pitch of approximately 100 mm. These rods were installed after construction by drilling a hole in the brickwork, placing the rod in the hole and then firmly

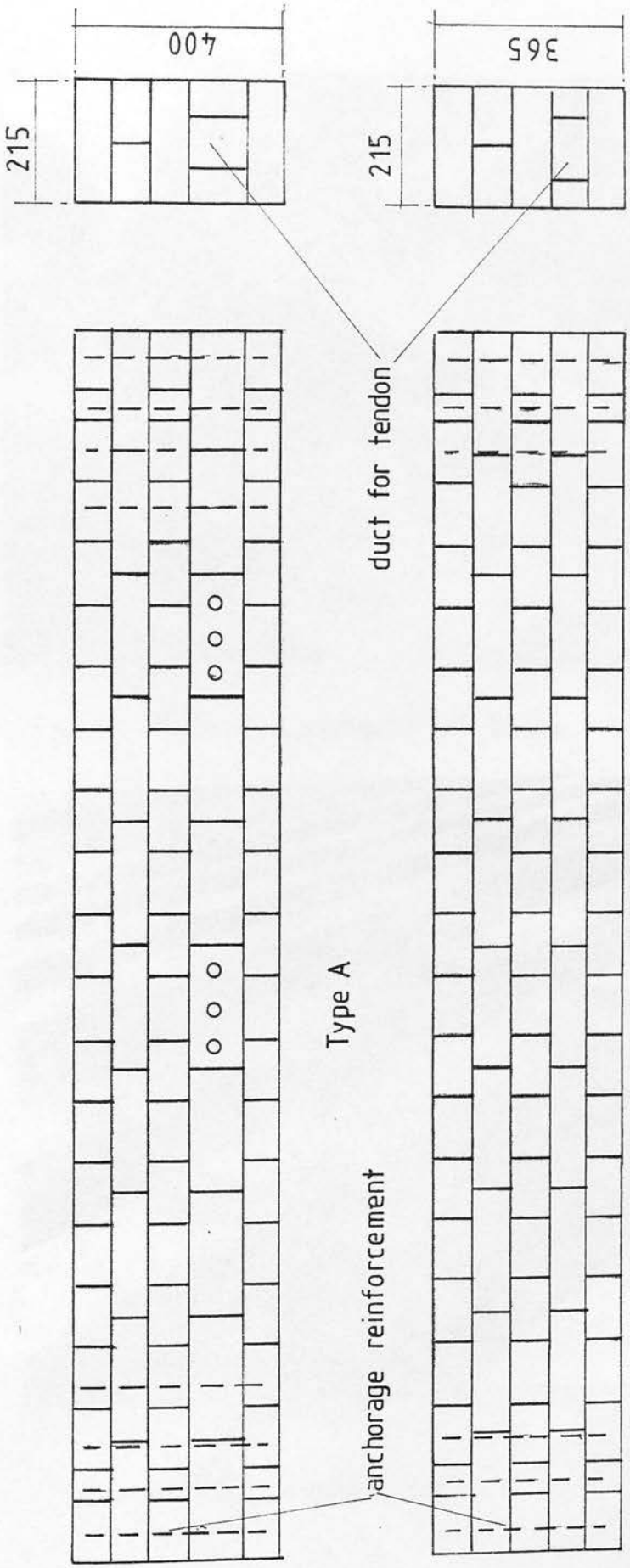

fig. 4.2.1 Bonding patterns and beam types

Plate 4.1 Construction of beams.

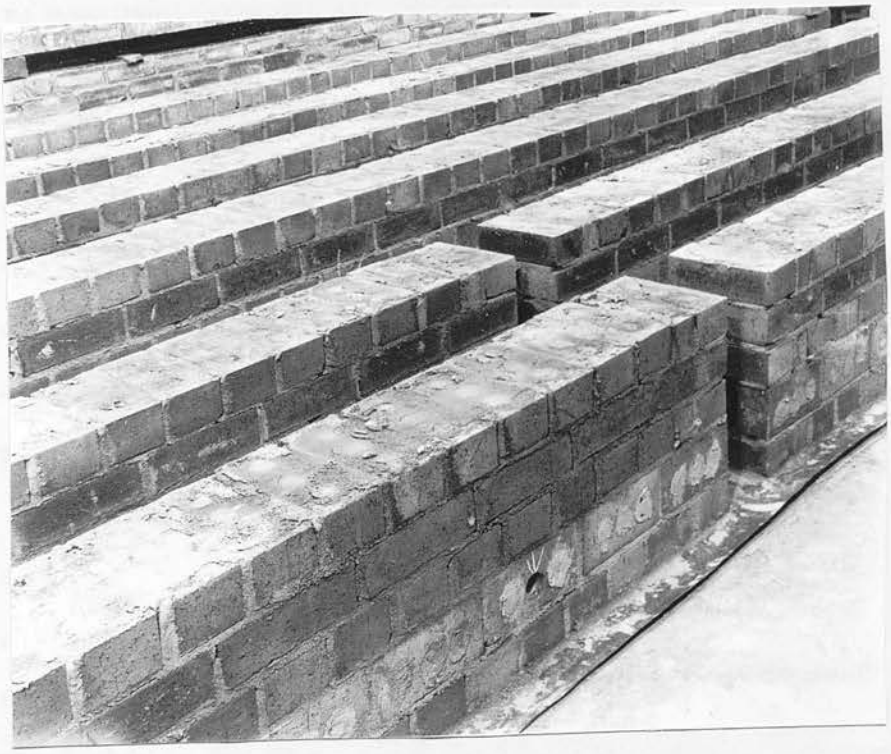

Plate 4.2 Finished beams.

packing the hole with mortar. In beams of section type B three pairs of 6 mm diameter mild steel rods were built in during construction of the beams. The rods were placed either side of the cavity and passing through the perforations in the bricks for the full depth of the beam. In the beams that were subjected to higher prestressing forces the strands were placed in the beams with the anchor plates attached, holding the strand in the correct position. A plastic sleeve of approximately 400 mm length had been fitted over the strand, at each end of the beam. The ends of the beam were then filled with mortar up to a length of 350 mm, thereby increasing the cross-sectional area carrying the prestress forces. The function of the plastic sleeve was to prevent the mortar from bonding to the strand allowing the strand to move during stressing.

The beams of section type A were built 'right side up', corresponding to the way in which they would be tested. The beams of section type B, were,on the other hand built upside down. By doing this the cavity carrying the tendon was then the second course from the top. This made grouting of the beams much easier as the grout could be poured manually into the cavity through the perforations in the top course.

Section type B proved to be the most suitable method of construction and was used for the majority of the beams. However, some modifications were made in specific instances. The single frogged common brick has no perforations and therefore placing the steel rods in the anchor zone and grouting would be impossible. These problems were overcome by building the anchor zones, at the

end of the beams, in high strength brick. Grouting was made possible by replacing every fifth brick in the bottom course, (top course as built), with three hole high strength brick, as shown in Figure 4.2.2(a).

Four beams were built in high strength brick with shear reinforcement. Pairs of 6 mm diameter mild steel rods were placed at 200 mm centres for the whole length of the span, Figure 4.2.2.

Although only two basic sections were used for the prestressed brickwork beams because the area of steel was not constant the effective depths were changed accordingly. Figure 4.2.3 gives the precise details of the sections for each group of beams. Further details relating to span, brick strength, mortar grade, prestress force and steel area are given in Table 5.3.1.

4.2.3 Prestressing

The beams were cured for a minimum of 21 days before pre-stressing. Mild steel anchor plates (Plate 4.3) were bedded onto the ends of the beams using either a rich mortar mix or dental plaster. These plates were removed after testing the beam, for future re-use. In one or two of the beams a specially designed, concrete anchor block was used in place of the steel plate (Plate 4.4).

The prestressing was carried out using a C.C.L. 'stressomatic system' employing a series I stressomatic pump with a type 300 manual control stressing head capable of delivering prestress forces up to 300 kN. The stressing head is fitted with a load cell which is connected to a battery operated measuring meter that records the

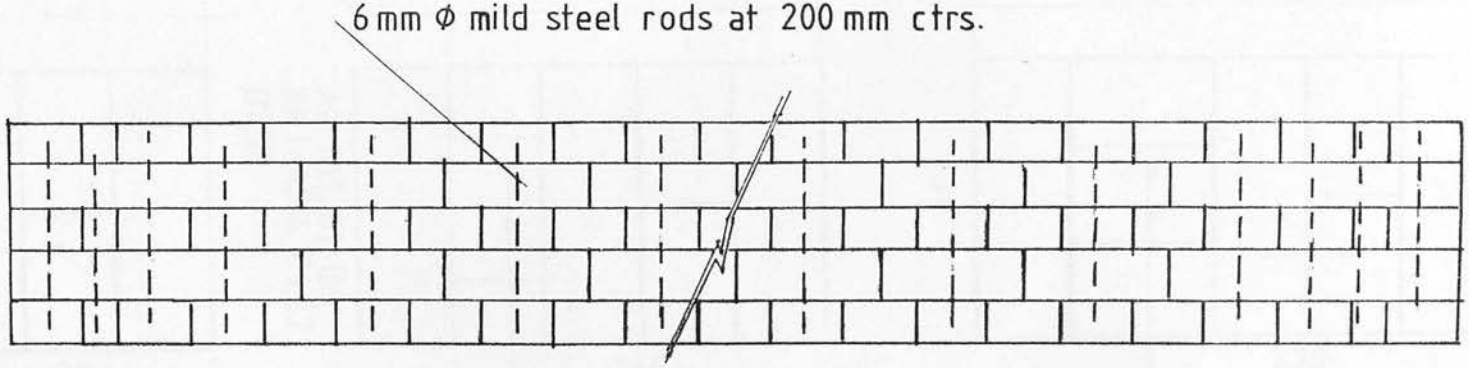

fig. 4.2.2(b) Shear reinforced beam

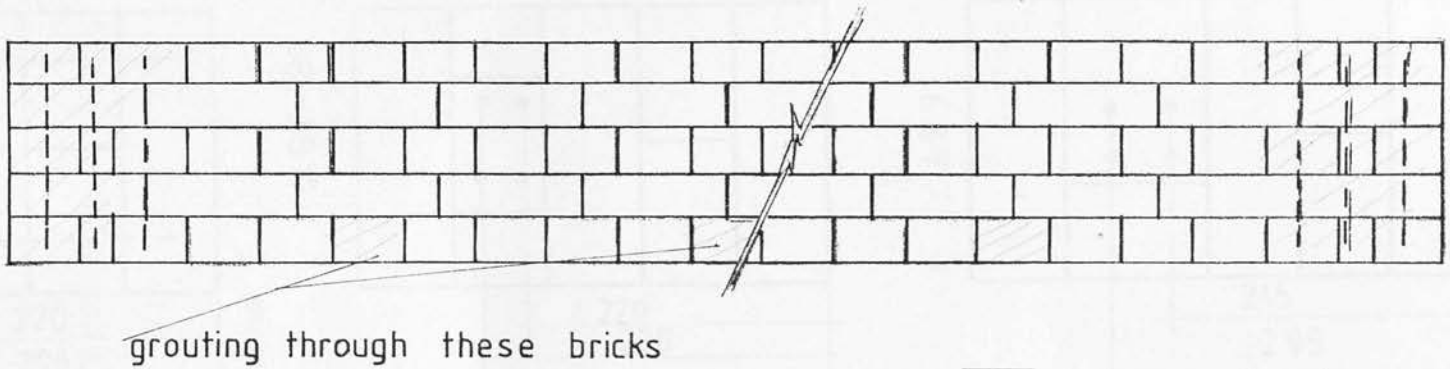

fig. 4.2.2(a) Common brick beams

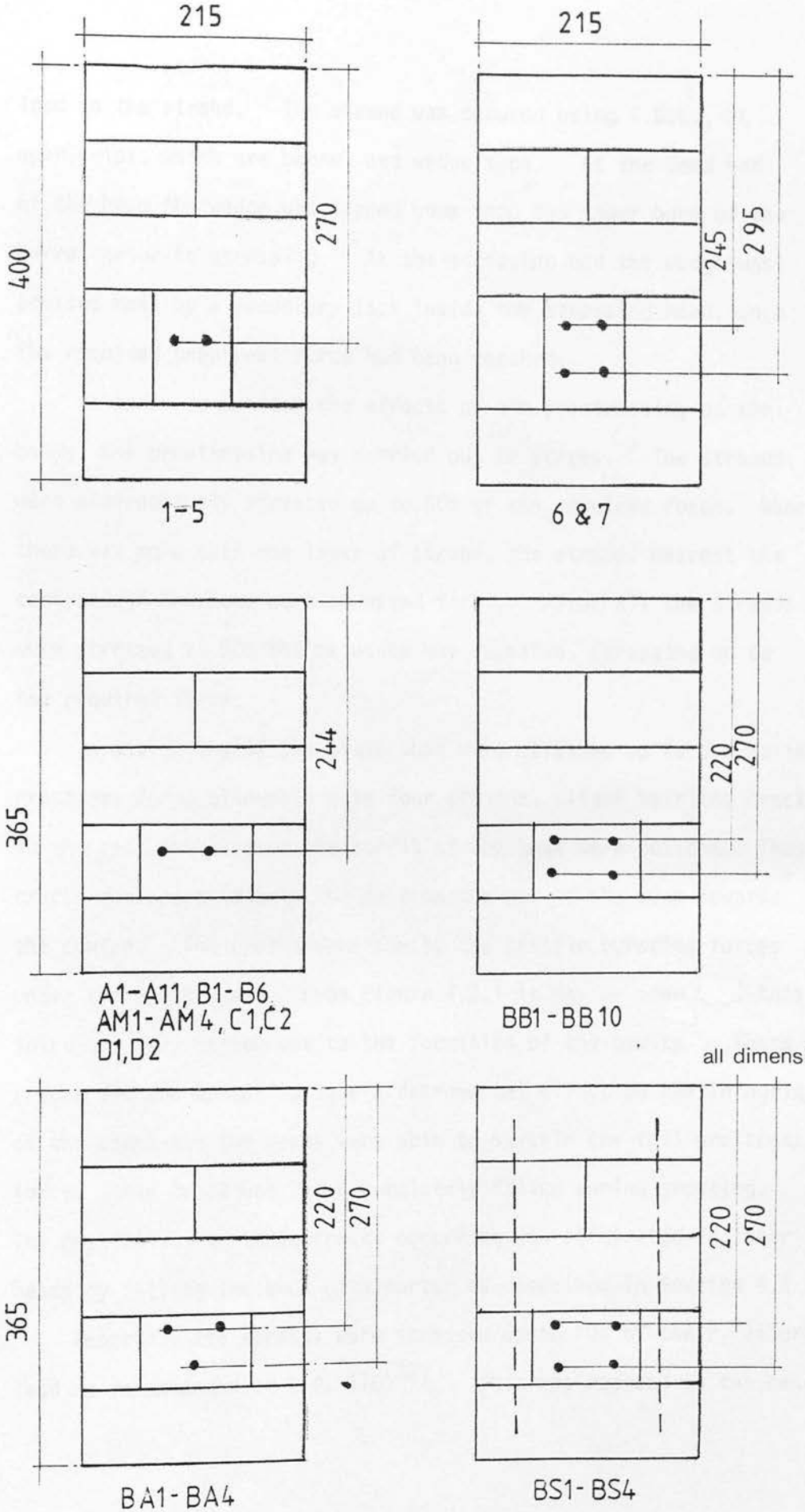

fig. 4.2.3 Beam sections

load in the strand. The strand was secured using C.C.L., XL open grips, which are barrel and wedge type. At the dead end of the beam the wedge was tapped home into the taper bore of the barrel prior to stressing. At the stressing end the wedge was pressed home by a secondary jack inside the stressing head, once the required prestress force had been reached.

In order to monitor the effects of the prestressing on the beams, the prestressing was carried out in stages. The strands were alternatively stressed up to 50% of the required force. Where there was more than one layer of strand, the strands nearest the centroid of the beam were stressed first. After all the strands were stressed to 50% the sequence was repeated, stressing up to the required force.

In one or two of the beams that were stressed up to the maximum prestress force allowable with four strands, slight hairline cracks in the bedjoint nearest the soffit of the beam were noticed. These cracks ran approximately 700 mm from the end of the beam towards the centre. The cracks were due to the tensile bursting forces under the anchorages. From Figure 4.2.1 it may be seen that this joint was very narrow due to the formation of the cavity. These cracks did not appear to have a detremental effect on the integrity of the beams and the beams were able to sustain the full prestress force. The crack was later completely filled during grouting. The possibility of these cracks occurring was eliminated in later beams by filling the ends with mortar as described in Section 4.2.2.

Generally the strands were stressed up to 70% of their failure load as recommended in C.P. 110[39]. This was reduced in two cases.

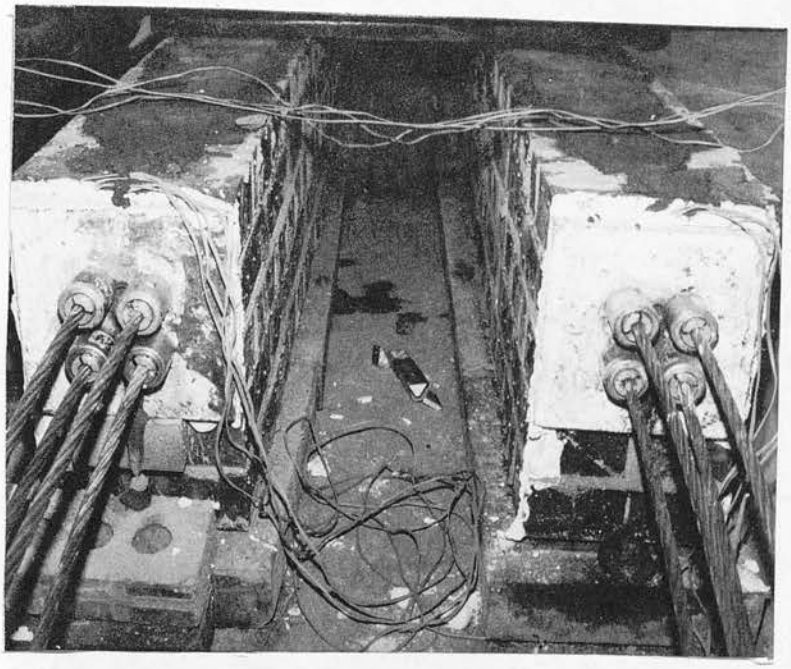

Plate 4.3 Steel anchor plates.

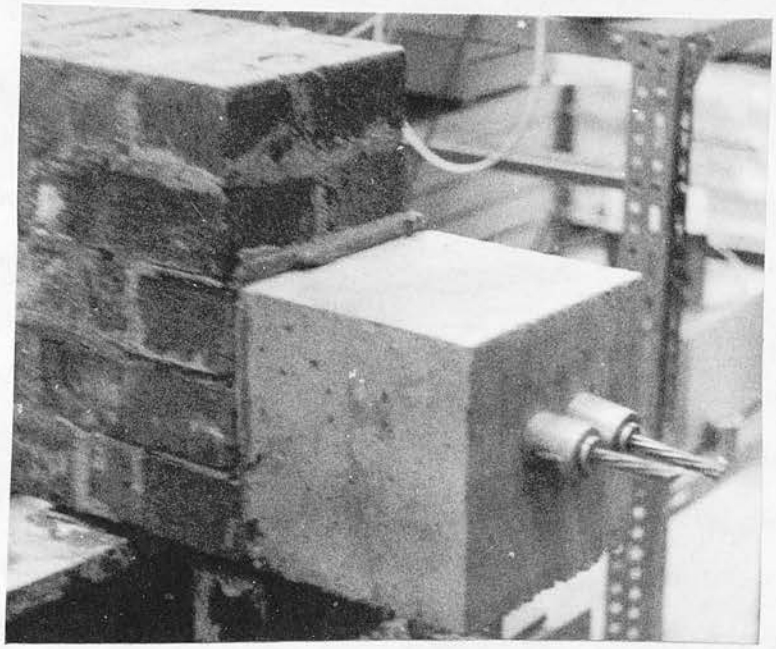

Plate 4.4 Concrete end blocks.

The first of these were the low strength and common brick beams. During the prestressing operation the beam is in fact a slender, eccentrically loaded column, therefore in order to avoid the possibility of buckling the area of steel was kept the same as in the higher strength brick beams but the prestress force was reduced by 50%. One of the low strength brick beams was successfully stressed to the full prestress but it was later felt imprudent to risk stressing the remaining beams to this level. The other case in which the strand was only stressed to 35% of its ultimate strength was the high strength brick beams with four strands. In order to compare the effect of prestress on the behaviour of the beams a number of these beams had the prestress force in two of the strands reduced to 35% of the ultimate capacity. These two strands were those furthest from the centroid of the section, at the greatest eccentricity.

The prestressing force was measured using the meter and checked with the electrical strain gauges placed on the strand. The meter was able to measure the amount of load applied to the strand, but was not able to measure the load once lock off has taken place. During lock off, losses occurred due to slip of the strand between the wedge. These losses were measured with the strain gauges. The average lock off losses varied from 11.8% for longer span beams to as much as 25% for the shortest beams. The amount of slip at the wedge for a given type of anchorage will be more or less constant, irrespective of the length of beam and will therefore result in the greatest loss of prestress in shorter beams.

Losses caused by elastic shortening and creep of brickwork

between stressing and testing were on average a further 10%. The effective prestress force, after losses is given in Table 5.3.1 for each beam.

4.2.4 Grouting

Although it is not unusual for the tendon to remain unbonded, it was decided that the tendon should be bonded for the beams in this work. Grouting of the tendon was therefore essential in the post-tensioned brickwork beams in order to ensure adequate bond.

For the beams built in section type A, Figure 4.2.1, grouting was carried out using a manually operated, positive displacement, diaphragm pump attached to a drum mixer. The grout was pumped through one of the open holes in the side of the beam. Initially a neat cement mix was used. This was very expensive requiring between 3 and 4 bags of cement for a 6.0 m long beam. The mix was then changed to a 1:1 sand/cement mix but there was some difficulty in pumping this mix, with frequent blockages occurring. With the construction of the beams of type B section the grouting operation was considerably simplified. The mix was changed to a 1:2½ cement/sand mix and was poured through the perforations in the upper most course, by the bricklayer. The grout was mixed in an ordinary cement mixer and transported to the beam by wheel barrow. The bricklayer was able to pour grout through the perforations along the whole length of the beam. The grout was tamped with a metal rod to ensure proper filling. This method proved much more effective than the previous one. In the previous

method the grout had to travel along a considerable length of the beam and there was a tendency for the brick to draw water from the grout, making it stiffer and more difficult for it to flow. In the second method the grout only had to move vertically through the perforations in the brick.

The beams were allowed to cure for a minimum of seven days, after grouting and prior to testing.

4.3 Instrumentation

4.3.1 Strain Measurement

Strains were measured on the faces of the prestressed brickwork beams using demountable 'Demec' gauges, with gauge lengths of 100 and 150 mm. Measurements were taken in the constant moment zone of the beams at various depths using 150 mm gauge length as shown in Figure 4.3.1(a). The strains were measured on both faces at a particular depth thereby obtaining the average strain across the section. For a number of beams, the strains were measured at six vertical sections in the constant moment zone to examine the variation of neutral axis depth and compressive strain across and between the cracks, Figure 4.3.1(b), using a 100 mm gauge length.

Strains were measured on the prestressing strand using 3 mm electrical resistance strain gauges. This small size of gauge was necessary as it had to be attached to an individual wire of the strand. The surface of the strand was abraided and cleaned of grease and dirt using acetone. The gauge was then bonded to the

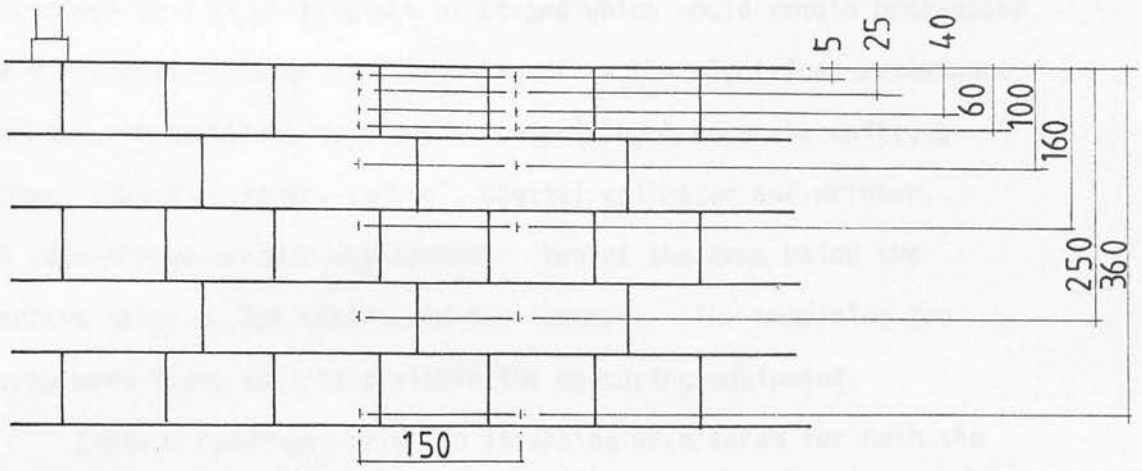

(a)

all dimensions in mm

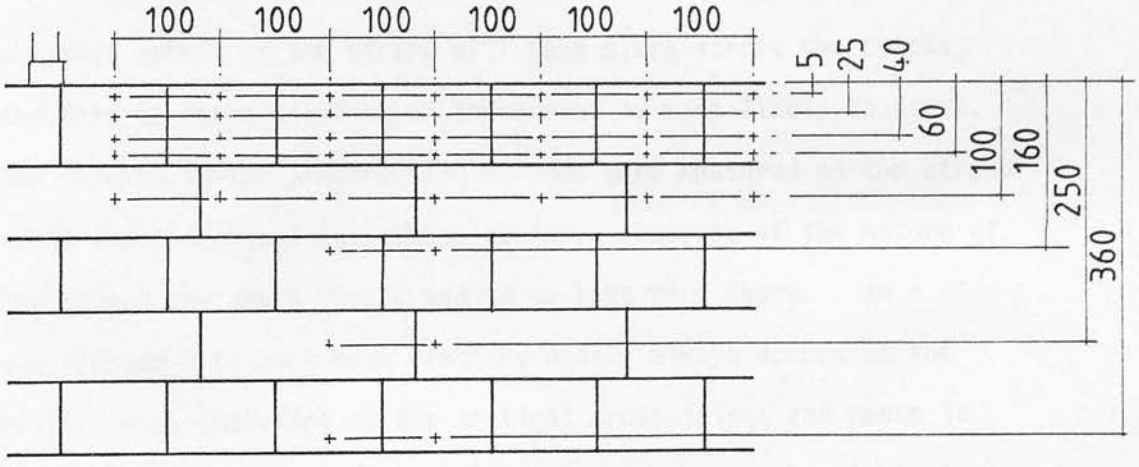

(b)

fig.4.3.1 Position of strain gauges on brickwork in constant moment zone

strand using cyanoacrylate adhesive. Foil gauges were also attached to a separate piece of strand which would remain unstressed and acted as a 'dummy'. The output from the electrical resistance gauges was monitored by a system comprising 5 separate units, a power supply, scanner, control, digital voltmeter and printer. A half-bridge circuit was formed. Two of the arms being the active gauge on the strand and the 'dummy'. The remaining two arms were fixed resistors within the measuring equipment.

Initial readings, prior to stressing were taken for both the demountable gauges and the electrical resistance gauges. The actual strain for a given load was then obtained by subtracting this initial reading.

In a prestressed brickwork beam, once cracking occurs the greatest strain in the strand will take place across the cracks, and this is where yielding of the strand is most likely to start. The strains in the prestressing strands were measured on the strand using the electrical resistance gauges. Because of the nature of the strand the gauge length had to be kept very short. In a prestressed brickwork beam cracking nearly always occurs at the brick/mortar interface in the vertical cross-joints and hence it is possible to have a reasonable idea where the cracks might start. The strand could have been placed in the beam such a way that the gauge length of the gauge was measuring across the interface at a joint. However as soon as stressing takes place the strand will move relative to the beam and it would only take a movement of 2 mm to move the gauge from the interface. Although in some cases the electrical strain gauges measured strains of up to 1.3% suggesting

that these particular strain gauges were in fact measuring across cracks, in most cases, then gauges were measuring strains between cracks and were used to determine tension-stiffening effect of the brickwork between the cracks, as described in Chapter 6. The additional strains in the strand across the cracks were obtained from the demountable strain gauges on the brickwork assuming a linear distribution of strain and full bond between strandand brick-work.

4.3.2 Deflections and Crackwidths

The deflections of the beams were measured using mechanical dial gauges. In all beams the deflections were measured at midspan and in a number of beams the deflections at various points in the shear span were also measured.

Dial gauges reading to 0.01 mm were used for these measurements. Support settlements were also measured using gauges reading to 0.002 mm.

The test rig itself was self-straining and not bolted to the floor of the laboratory, because of this the deflections of the rig, at all points where the beam deflections were being taken, were also measured. The actual deflections of the beams were obtained by calculating the deflections of the beams relative to the floor and then adjusting the deflections to take account of any support settlements. In some cases the support settlements and deflections were measured directly from the floor of the laboratory using a supporting rig, eliminating the need for the rig deflections to be measured at these points.

In longer span beams the dial gauge at midspan often reached the end of its travel as the beam approached failure at this point the deflections would be around 70-80 mm. The dial gauge was removed, to avoid the possibility of damage and the deflections were measured with a ruler graded in 1 mm intervals.

Crack widths were measured using an 'Ultra-lomara' microscope. This microscope is supplied with its own light source and a graded scale capable of measuring crack widths down to 0.02 mm.

4.3.3 Load Measurement

The applied load to the beam was measured at jacking point using either 200 or 100 kN load cells. The power supply to the load cells was from a 10 volt power supply. The output from the load cells was monitored by a digital voltmeter and a penchart recorder which plotted the loading history of each jack and from which the failure load could be determined.

Prior to use, each load cell was calibrated in a compression testing machine using the same voltmeter and power supply as in the beam tests.

4.4 Testing of Beams

4.4.1 Test Rig

All the beams were tested under two point loading in a self-straining rig, specially designed for beam testing, Figure 4.4.1. The rig was able to test beams of up to 6.2 m long. The test beam was placed on the supports of the beam, previously placed at

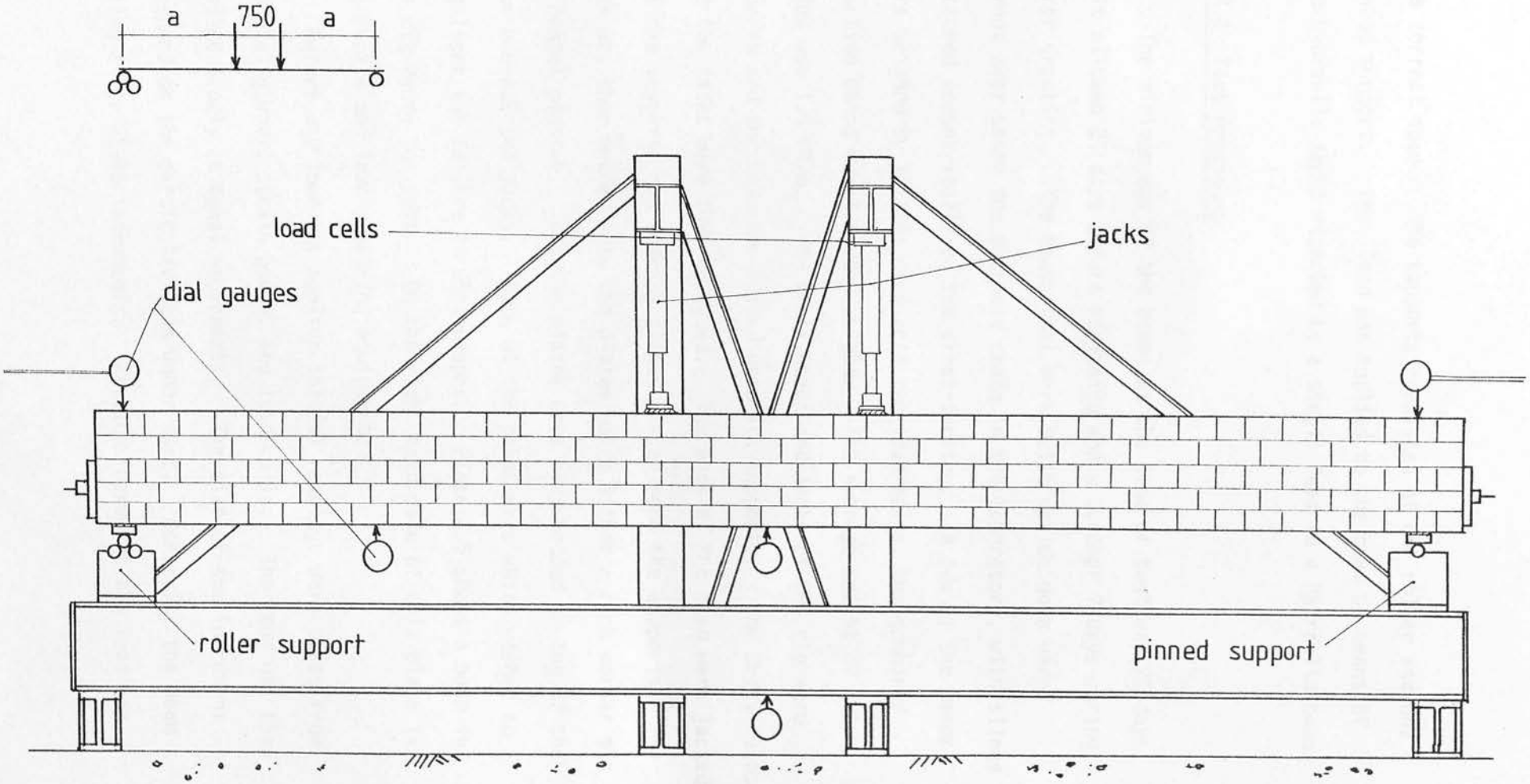

fig 4.4.1 Layout of test rig.

the correct span. The supports consisted of one roller and one pinned support. The load was applied to the beam by means of two hydraulic jacks attached by a single feed to a hydraulic pump.

4.4.2 Test Procedure

The minimum age of the beams at the time of test was 28 days, this allowed 21 days before stressing and a further 7 days curing after grouting. The beams that were built upside down were turned over using the overhead crane in the laboratory, with slings attached eccentrically to the cross-section. A few of the beams were weighed by lifting them onto two load cells, the combined reaction being equal to the weight. The average weight of the beams was 1.5 kN/m. The cross heads and jacks of the rig were removed and the beam was lifted onto its supports. The cross heads and the jacks were then replaced. The ends of the beam were jacked off the supports and bearing plates placed onto the supports. The beam was then bedded onto the plates using either a rich mortar mix or dental plaster. Bearing plates were also bedded on top of the beam beneath the jacks. Some of the beams were white washed to highlight the failure in photographs. Plate 4.5 shows a beam in the rig ready for test. On the right hand side of this plate is the strain and load measuring equipment.

Before any load was applied initial readings were taken from the dial gauges, strain gauges and load cells. The load was then applied slowly in equal increments. The size of the increment depended on the particular beam under test. Generally the beam failed after 12-15 increments. At each increment the load was

Plate 4.5 Beam in rig, ready for test.

held constant and strains and deflections were measured. Once cracking started the crack pattern was marked on the beam, tracing the development of the cracks through the section and along the span. Crack widths were measured in the constant moment zone near the soffit of the beam. As the beam approached failure the loading increment was reduced and strain and deflection measurements were taken as close as possible to the ultimate load.

CHAPTER 5 : ULTIMATE MOMENT OF PRESTRESSED BRICKWORK BEAMS

5.1 Introduction

In the past the design of reinforced concrete[40] and masonry[41] was carried out on the basis of an elastic analysis. The section was designed for the actual applied loads and the stresses in both the steel and masonry were obtained assuming linear elastic behaviour. The section was deemed satisfactory if these stresses were below prescribed maximum permissible stresses. The permissible stresses were chosen to provide an adquate factor of safety against failure of the particular material. However, in this method of design the overall factors of safety on the finished structure tend to vary from structure to structure. Codes of practice[14,39] are now adopting the 'limit state' approach to the design of reinforced masonry and concrete.

These codes recognise that it is impossible to ensure that a structure will never collapse in its design life, but the probability of this happening must be kept to within an acceptable limit[42]. Partial safety factors are applied to the loads and to the strengths of the constituent materials and these allow for the possibility of the actual load exceeding the design load, workmanship, variations in quality of materials etc. In limit state design, the design of reinforced concrete or masonry beams is generally governed by conditions at the ultimate or failure state.

The design of prestressed brickwork or concrete beams, necessarily has to be different. The section is designed to suit the actual

working load in order to determine the magnitude and position of the prestressing forces. The ultimate strength of the beam then has to be calculated to check if there is an adequate factor of safety against collapse.

When dealing with the flexural behaviour of prestressed or reinforced brickwork beams the mode of failure may have a considerable influence on design, for two reasons:

(i) If failure occurs with the crushing of brickwork, while the stresses in the steel are comparatively low then this material has not been utilised to its fullest extent which is uneconomic.

(ii) The type of failure in (i) does not generally give a great deal of advance warning, due to the comparatively small deformations before failure.

The accurate prediction of the flexural strength and failure mode is, therefore, very important.

The ultimate flexural strength of bonded, prestressed brickwork beams may be influenced by the following variables:

(i) brick strength (low, medium, high);

(ii) mortar grade, 1:¼:3 or 1:½:4½ (cement, lime, sand);

(iii) % of steel and degree of prestress;

(iv) shear span/effective depth ratio.

The last factor (iv) will only influence the ultimate moment if the failure is in shear and consequently the full flexural capacity of the beam is not reached.

This chapter describes a series of experiments designed to investigate the effect of the above variables on the flexural strength of prestressed brickwork beams.

The effect of brick strength (i) was investigated by testing a series of beams with constant mortar grade and steel areas with varying brick strengths.

The brick type, steel area and prestress force was kept constant while investigating the effect of the mortar grade.

A number of beams built from the same brick types and mortar grades were tested to study the influence of steel area and prestress force.

A series of beams of varying spans but constant steel area brick type and prestress force were tested to determine the influence of shear span/effective depth ratio.

The experimental results are compared with the theoretical predicted flexural strengths. The theoretical moments were calculated using the stress/strain relationships and compressive strengths of brickwork obtained from the two different prism types as described in Chapter 3. The results are also compared with the provisions of the draft code of practice for reinforced and prestressed masonry, B.S.5628 part 2[14].

5.2 The Prediction of the Flexural Strength of Prestressed Brickwork Beams

5.2.1 Flexural Theory

A flexural failure occurs in a reinforced or prestressed brickwork beam when either the brickwork or reinforcement or both are no

longer able to withstand the internal forces caused by the applied loads. Normally, the failure is such that crushing of the brickwork will occur regardless of whether the steel yields or not.

The following assumptions are made:

(a) The masonry crushes at a known value of ultimate compressive strain. As crushing occurs irrespective of the mode of flexural failure this implies that a fully developed compression zone exists irrespective of an under or over-reinforced section.

(b) Plane sections remain plane, i.e. there is a linear distribution of strain through the depth of the beam. This assumption has been verified by the experimental work described in this chapter, Figure 5.3.23.

(c) The tensile strength of the masonry is ignored. The tensile strength of brick masonry is very low in relation to its compressive strength, because of this the tensile stress distribution in the masonry below the neutral axis depth in a cracked beam has a small lever arm. The combination of small lever arm and low strength results in a very small contribution to the flexural strength.

(d) The stress distribution in the compression zone may be determined from the stress/strain relationship of brickwork tested in uniaxial compression. This assumption enables the magnitude and resultant thrust of the forces in the compression zone to be found.

(e) The stress/strain relationship of the steel is known.

(f) The magnitudes of any initial strains in the reinforcement are known. In prestressed brickwork beams the initial strains in the reinforcement must be known in order to determine the total strain and hence the tensile force from assumption (e).

In the general case a section may have reinforcement in both the tension and compression zones and it may be stressed or unstressed.

The stress/strain relationship for the non-stressed reinforcement is:

$$f_{sc} \text{ or } f_{st} = F_{ns} (\varepsilon_{sc} \text{ or } \varepsilon_{st}) \qquad (5.2.1)$$

where subscripts c and t denote compression and tension. The stress/strain relationship for the prestressed reinforcement is:

$$f_s = F_s (\varepsilon_{ps} + \varepsilon_{sa}) \qquad (5.2.2)$$

where f_s is the stress in the reinforcement, ε_{ps} is the strain due to prestressing and ε_{sa} is the strain in the steel due to the applied loading. ε_{sa} is a combination of the effects of the strains in the masonry at the level of the steel due to prestressing and dead load, ε_e, and the strains in the masonry at the level of steel due to applied loads, ε_{ms}, thus ε_{sa} is:

$$\varepsilon_{sa} = \beta_1 \varepsilon_e + \beta_2 \varepsilon_{ms} \qquad (5.2.3)$$

β_1 and β_2 are bond factors which represent the ratio of strains in the concrete or masonry at the level of the reinforcement to the actual strain in the reinforcement due to the applied loads. For fully bonded beams such as reinforced, pretensioned or grouted post-tensioned beams, β_1 and β_2 are both equal to 1.0. Typical values[43] associated with concrete are β_1 = 0.5 and β_2 between 0.1 and 0.25.

The stress/strain relationship for masonry in compression may be expressed as:

$$f = F_m(\varepsilon) \qquad (5.2.4)$$

Figure 5.2.1 shows the conditions at failure for a section in which there is compression reinforcement A_s' at depth, d', tension reinforcement, A_s at d_1 and prestressed reinforcement, A_{ps} at depth d.

For assumption (a) the maximum compressive strain in the masonry at failure is ε_m.

The strain in the compressive reinforcement is:

$$\varepsilon_{sc} = \varepsilon_m (1 - d'/n) \qquad (5.2.5)$$

where n is the neutral axis depth. The strain in the tension reinforcement is:

$$\varepsilon_{st} = \varepsilon_m (d_1/n - 1) \qquad (5.2.6)$$

The strain in the brickwork at the level of the prestressed rein-

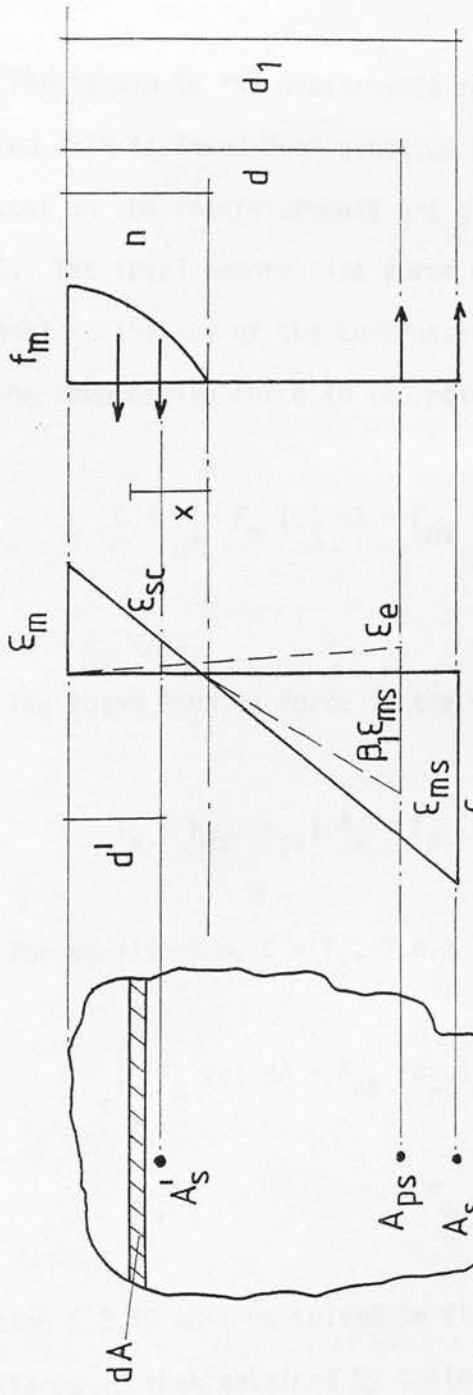

fig. 5.2.1 Conditions at failure in a prestressed brickwork beam

forcement is:

$$\varepsilon_{ms} = \varepsilon_m \, (d/n - 1) \qquad (5.2.7)$$

The strain in the prestressed reinforcement due to the applied load is found from equation 5.2.3. The corresponding stresses in the reinforcements are given by equations 5.2.1 and 5.2.2. The total compressive force developed in the section, C is equal to the sum of the compressive stresses in the brickwork and the compressive force in the reinforcement.

$$C = \int_0^n F_m \, (\varepsilon) \, dA + F_{ns} \, (\varepsilon_{sc}) \, A_s' \qquad (5.2.8)$$

where $\varepsilon = \varepsilon_m \, x/n$.

The total tensile force in the section, T_s is:

$$T_s = F_{ns} \, (\varepsilon_{st}) \, A_s + F_s \, (\varepsilon_{ps} + \varepsilon_{sa}) \, A_{ps} \qquad (5.2.9)$$

Then for equilibrium, $C = T_s$, i.e.:

$$\int_0^n F_m \, (\varepsilon) \, dA + F_{ns} \, (\varepsilon_{sc}) \, A_s' = F_{ns} \, (\varepsilon_{st}) \, A_s + F_s \, (\varepsilon_{ps} + \varepsilon_{sa}) \, A_{ps} \qquad (5.2.10)$$

Equation 5.2.10 must be solved to find n. The ultimate moment of resistance is then obtained by taking moments about n, the neutral axis depth.

$$M_u = \int_0^n F_m (\varepsilon) \times dA + F_{ns} (\varepsilon_{sc}) A_s' (n - d') + F_{ns} (\varepsilon_{st})$$

$$A_s (n - d_1) + F_s (\varepsilon_{ps} + \varepsilon_{sa}) A_{ps} (n - d) \qquad (5.2.11)$$

5.2.2 Rectangular Prestressed Brickwork Beams

The beams tested in this work were all rectangular, with only prestressed reinforcement. The theory described in section 5.2.1 can therefore be simplified. The assumptions of section 5.2.1 still hold, but it is more convenient to describe the stress distribution in the compression zone by stress block factors. The compressive stress distribution is described by three factors, which relate to the magnitude and position of the resultant thrust of the compressive forces, Figure 5.2.2.

λ_1 is the ratio of the stress distribution to the enclosing rectangle. When multiplied by the stress in the extreme fibre, λ_1 produces the average stress in the compression zone.

λ_2 is the ratio of the centroid of the stress distribution to the neutral axis depth, as measured from the extreme fibre.

λ_3 represents the ratio of the ultimate compressive stress at failure to the compressive strength obtained from uniaxial tests.

Using these 3 factors, equation 5.2.8 becomes:

$$C = \lambda_3 \cdot \lambda_1 f_m b \cdot n \qquad (5.2.12)$$

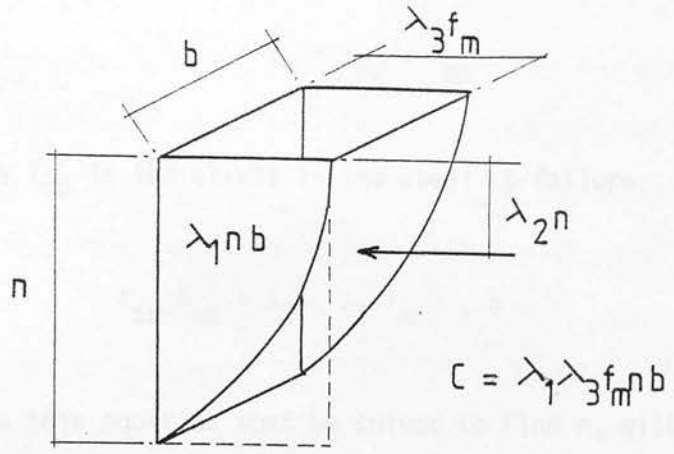

fig. 5.2.2 Stress block characteristics.

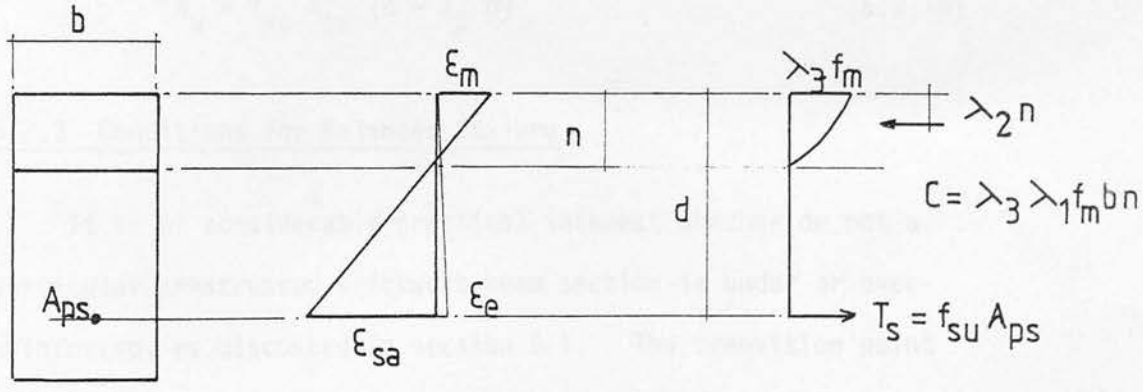

fig 5.2.3 Failure conditions in a rectangular prestressed brickwork beam.

and the tensile forces in equation 5.2.9 may be expressed as:

$$T_s = f_{su} \cdot A_{ps} \qquad (5.2.13)$$

where f_{su} is the stress in the steel at failure. For equilibrium,

$$f_{su} A_{ps} = \lambda_3 \cdot \lambda_1 f_m b \cdot n \qquad (5.2.14)$$

Again this equation must be solved to find n, with the strains and stresses in the steel obtained from equations 5.2.7 and 5.2.2. It is assumed that full bond between steel and grout exists, therefore β_1 and β_2 are equal to 1.0 in equation 5.2.7.

The ultimate moment is then given as:

$$M_u = f_{su} A_{ps} (d - \lambda_2 n) \qquad (5.2.15)$$

5.2.3 Conditions for Balanced Failure

It is of considerable practical interest whether or not a particular prestressed brickwork beam section is under or over-reinforced, as discussed in section 5.1. The transition point between these two phases represents the most efficient use of both the steel and the masonry. This is often defined as the balanced section, in which both materials reach their respective yield points simultaneously. In a reinforced brickwork beam the calculation of the area of steel for balanced failure is straight forward. The strain distribution is determined by the yield strain in the reinforcement and the ultimate strain in the masonry. From

this the neutral axis depth and the compressive forces at failure may be found. The balanced steel area is that area of steel required to satisfy equilibrium conditions for both materials to yield simultaneously. The situation is somewhat more complicated for prestressed brickwork beams, due to the presence of the pre-stress strain, the magnitude of which influences the ultimate strain in the reinforcement. The strain at the yield stress, f_{sy}, is defined as ε_{sy}. Referring to Figure 5.2.3, replacing ε_{sa} and f_{su} with ε_{sy} and f_{sy} respectively. The tensile force of failure is:

$$T_s = f_{sy} \cdot A_{ps} \qquad (5.2.16)$$

From the distribution of strains,

$$\frac{n}{d-n} = \frac{\varepsilon_m}{\varepsilon_{sy} - (\varepsilon_e + \varepsilon_{ps})} \qquad (5.2.17)$$

Let $n/d = r$ and $\rho = A_{ps}/bd$ then:

$$r = \frac{f_{sy}\,\rho}{\lambda_1\,\lambda_3\,f_m} \qquad (5.2.18)$$

r may also be expressed as:

$$r = \frac{\varepsilon_m}{\varepsilon_m + \varepsilon_{sy} - (\varepsilon_e + \varepsilon_{ps})} \qquad (5.2.19)$$

Thus by combining 5.2.18 and 5.2.19 the steel area corresponding to balanced conditions ρ_{bal} is found,

$$\rho_{bal} = \frac{\varepsilon_m}{\varepsilon_m + \varepsilon_{sy} - (\varepsilon_e + \varepsilon_{ps})} \cdot \frac{\lambda_1 \lambda_3 f_m}{f_{sy}} \qquad (5.2.20)$$

Here it can be seen that ρ_{bal} depends on the level of prestress.

5.2.4 Characteristics of Stress Blocks

The three coefficients of the stress blocks that are used to describe the compressive stress distribution at failure were mentioned briefly in sections 5.2.2 and 5.2.3. This approach has been used extensively for the analysis of concrete elements. A considerable number of different stress blocks have been developed. The more popular formulations have been reviewed elsewhere[43,44].

Some of the stress blocks for concrete have also been applied to brickwork[45]. Figure 5.2.4 shows typical stress blocks that have been used to analyse reinforced brickwork members.

Figure 5.2.4(a) shows the Whitney[46] stress block. Whitney proposed that the stress block based on a parabolic stress/strain relationship could be replaced by one of an equivalent rectangular shape. The average stress in this block is equal to 0.85 f_c where f_c is the cylinder strength, in the case of concrete. For the brickwork, the average stress is assumed to be equal to the compressive strength from prism tests. The depth of the stress block, x_w is less than the actual depth. If the section was over-reinforced then the value of x_w was limited to 0.536 d based on experimental results.

The stress block in the code of practice for concrete C.P.110[39] has previously been applied to brickwork[45], Figure 5.2.4(b) and (c). In C.P.110 two stress blocks are proposed. The first is based on

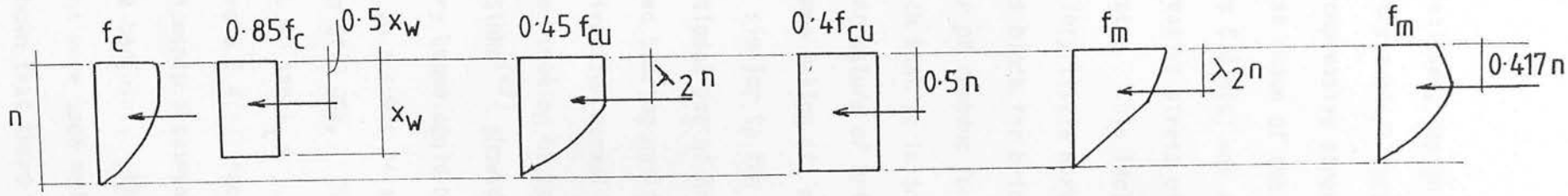

fig.5.2.4 Typical stress blocks

an idealised, design stress/strain curve for concrete in compression. The stress block factors obtained from this curve will vary with the compressive strength of the concrete, as this determines the precise shape of the curve. A second, simplified stress block, Figure 5.2.4(c) was adopted, rectangular in shape with an average compressive stress of 0.4 times the cube compressive strength of concrete. This includes a partial safety factor of 1.5.

Very little work has been carried out into the nature of the stress block for brickwork flexural members. There may be a number of reasons for this, notably, the nature of the brickwork is such that it is inherently more variable than concrete. The modular nature of bricks restrict the shape of brickwork test specimen making it more difficult to adopt a standard test piece similar to the concrete cube or cylinder. Also the more traditional use of brick masonry as a structural material has been as load bearing walls, in which the compressive forces develop in the direction normal to the bedjoint and this has been reflected in the testing of masonry specimens and prisms.

Sinha[47] showed that the flexural strength of reinforced masonry beams could be reliably predicted using a stress block based on a cubic parabolic stress/strain relationship and a failure strain of 0.003. The stress block factors were then $\lambda_1 = 0.75$, $\lambda_2 = 0.40$ and $\lambda_3 = 1.0$. He later[36] proposed a stress block (Figure 5.2.4(d)) based on an idealised curvelinear stress/strain relationship obtained from axial compression tests on prisms parallel to the bedjoint. The actual compressive stresses and ultimate strains were used and compared with his previous method[47]. It was shown that there was little variation in the predicted ultimate moments.

Beard[48] proposed a stress block for reinforced brickwork in bending based on a parabolic stress/strain relationship of the form:

$$f/f_m = 2\ \varepsilon/\varepsilon_m - (\varepsilon/\varepsilon_m)^2 \qquad (5.2.21)$$

This was obtained[33] from prisms tested normal to the bedjoint. The relationship exhibited a falling branch past $\varepsilon/\varepsilon_m = 1.0$. By expressing the forces in the compressive zone in terms of this relationship and differentiating to find the maximum value of compressive force, Beard showed, for a rectangular section, that the maximum force occurs when $\varepsilon/\varepsilon_m = 1.5$. That is, the failure strain is 50% greater than the strain at maximum stress. The coefficients of this stress block where $\lambda_1 = 0.75$, $\lambda_2 = 0.417$ and $\lambda_3 = 1.0$ (Figure 5.2.4(e)). This stress block is very similar to the parabolic block of Sinha[47] however the ultimate strains have increased.

More recent work[35] based on a large number of test results has shown that the stress block factor λ_1 is slightly less than 0.75, around 0.64.

There is some thought among researchers[49] that the presence of a strain gradient, as occurs in flexural members, causes higher strains at failure than axially loaded specimens.

Cavanagh and Edgell[49] reviewed the work of a number of researchers on brickwork under eccentric loading. They concluded that although there was a wide range of ultimate strains for different types of brickwork the effect of the strain gradient

would produce higher strains than if tested under axial conditions.

B.S.5628 part 2[14], the draft code of practice for reinforced and prestressed masonry, has adopted a rectangular stress block similar to C.P.110[39]. The characteristic compressive strength of masonry, f_k, may be obtained from either tests or from a table provided, for various combinations of brick and mortar type. The ultimate compressive strain is taken as 0.0035. The main difference between this approach and that of C.P.110 is that the compressive stress at failure is taken as the characteristic strength, whereas in C.P.110[39] this is equal to 0.6 times the cube strength, indicating that λ_3 = 1.0 in the masonry code[14].

In Chapter 3 the stress block factors for each prism and brickwork type were presented. The average stress block factors λ_1 and λ_2, for each brick/mortar combination were obtained from the non-dimensional stress/strain relationship and are given in Table 3.4.3. Also given in this table is the average compressive strength and ultimate strain. For the purposes of comparing the predicted ultimate moments from both prism types λ_3 is taken as 1.0.

5.3 Experimental Results and Discussion

5.3.1 General

The experimental results, ultimate moments and shear stresses at failure for all beams tested are summarised in Table 5.3.1. Where failure was in flexure as opposed to shear the general behaviour was similar. Once decompression of the prestress force occurred tensile stresses developed and flexural cracking took place.

Table 5.3.1 Summary of Experimental Results

Beam	Brick Strength N/mm^2	Mortar Strength N/mm^2	Grout Strength N/mm^2	Span m	a/d Ratio	% Steel	Effective Prestress kN	Ultimate Moment kNm	Shear Stress N/mm^2	Failure Mode
1	67	22.2	32.8	6.0	9.7	.255	152	61.4	0.453	tension
2	"	21.7	32.8	2.0	2.3	"	141	49.5	0.370	"
7	"	20.7	21.9	2.0	2.3	.510	287	67.8	2.08	compressio
3	"	21.5	20.1	4.43	6.82	.255	124	49.4	0.485	shear
4	"	21.5	20.1	4.43	6.82	"	154	57.0	0.556	tension
5	"	21.2	48.0	3.2	4.61	"	140	56.0	0.790	"
6	"	20.8	14.6	3.2	4.61	.510	303	77.9	2.186	compressio
A1	"	21.6	17.5	2.0	2.56	.274	124	47.9	1.470	tension
A2	"	18.1	13.0	2.0	2.56	"	135	45.3	1.396	shear
A3	"	21.6	17.5	3.2	5.02	"	124	46.0	0.705	tension
A4	"	21.6	17.5	3.2	5.02	"	149	46.1	0.714	tension
A5	"	18.1	13.0	4.43	7.57	"	139	48.8	0.517	shear
A6	"	18.1	13.0	4.43	7.57	"	122	40.6	0.430	shear
A7	"	18.3	16.3	6.0	10.80	"	134	53.4	0.437	tension
A8	"	18.3	16.3	6.0	10.80	"	142	51.8	0.424	"
A9	"	21.6	15.9	6.2	11.21	"	134	54.1	0.440	"
A10	"	21.6	21.6	"	"	"	152	51.7	0.401	"
A11	"	16.6	16.6	"	"	"	129	56.3	0.431	"
AM1	"	5.3	10.0	"	"	"	132	48.6	0.401	compressio
AM2	"	5.3	"	"	"	"	127	45.8	0.431	"
AM3	"	8.2	"	"	"	"	144	43.1	0.383	shear
AM4	"	8.2	"	"	"	"	142	48.6	0.366	compressio
B1	88	15.8	17.8	"	"	"	133	52.9	0.440	tension
B2	"	"	17.8	"	"	"	115	56.4	0.428	shear
B3	"	"	6.2	"	"	"	133	61.5	0.476	tension
B4	"	20.8	"	"	"	"	144	58.4	0.448	"
B5	"	20.8	"	"	"	"	133	59.2	0.454	"
B6	"	16.6	13.4	"	"	"	152	58.8	0.451	"
BA1	"	33.2	13.3	"	"	.441	221	72.6	0.546	shear
BA2	"	27.3	13.3	"	"	"	221	79.9	0.598	"
BA3	"	26.8	"	"	"	"	216	74.8	0.561	tension
BA4	"	22.2	"	"	"	"	196	74.5	0.539	shear

Table 5.3.1 (continued/...)

Table 5.3.1 (continued)

Beam	Brick Strength N/mm²	Mortar Strength N/mm²	Grout Strength N/mm²	Span m	a/d Ratio	% Steel	Effective Prestress kN	Ultimate Moment kNm	Shear Stress N/mm²	Failure Mode
BB1	88	15.2	13.6	6.2	11.21	.548	275	87.2	0.657	shear
BB2	"	"	"	"	"	"	213	72.5	0.547	"
BB3	"	18.6	11.3	"	"	"	212	71.5	0.549	"
BB4	"	"	"	"	"	"	199	75.2	0.572	"
BB5	"	19.5	14.0	2.75	4.0	"	180	69.3	1.330	"
BB6	"	"	"	2.75	4.0	"	194	65.7	1.271	"
BB7	"	"	"	1.75	2.0	"	180	59.1	2.15	"
BB8	"	16.4	"	1.75	2.0	"	176	71.6	2.710	"
BB9	"	"	15.0	4.50	7.0	"	190	73.8	0.751	"
BB10	"	"	"	4.50	7.0	"	191	68.9	0.700	"
BS1	"	21.0	12.8	6.2	11.21	"	194	87.2	0.652	compression
BS2	"	21.0	12.8	"	"	"	202	92.6	0.690	"
BS3	"	23.0	11.7	"	"	"	309	103.0	0.763	shear
BS4	"	23.0	"	"	"	"	280	92.9	0.703	"
C1	34	16.0	15.5	"	"	.274	75	45.9	0.359	compression
C2	"	"	"	"	"	"	61	42.5	0.333	"
C3	"	15.5	"	"	"	"	119	54.1	0.412	"
D1	22	"	15.0	"	"	"	61	35.5	0.276	"
D2	"	16.0	"	"	"	"	72	25.8	0.208	"

Note: The shear stress in the 2nd last column of this table has been calculated as V/bd at point of failure irrespective of failure mode.

The cracks progressed up through the section to a depth dependent on the type of brickwork and area of steel. At high levels of load, near failure, horizontal splitting of the top bedjoints in the constant moment zone was observed. In some of the beams with higher steel areas splitting in the upper two bedjoints occurred prior to failure. Crushing of the compression zone then followed. This type of behaviour, splitting of the joints parallel to the direction of the compressive forces followed by crushing was similar to that observed during the three course prisms, described in Chapter 3, with the difference that in the case of the beams the strain distribution is much more well defined up to failure.

There are three possible modes of failure for prestressed brickwork beams, each mode is characterised by failure of one or other of the two materials, namely the brickwork or steel, as follows:

(i) fracture of steel: the nature of prestressing strand is such that for fracture to occur under normal conditions enormous strains must develop, the magnitude of which may only occur in a grossly under-reinforced beam;

(ii) excessive elongation: the stresses in the reinforcement exceed the proof stress and further increases in load result in very large increases of strain causing the neutral axis depth to rise and resulting in crushing of the compression zone;

(iii) compression failure: the strain in the brickwork reaches its ultimate before the proof stress in the steel has been reached and crushing of the brickwork takes place.

Barring flaws in the strand, it was very unlikely that failure by mode (i) will happen for the beams tested in this work. Flexural failure is then, therefore, caused by either mode (ii) or (iii). The important distinction between these two modes is the level of stress in the steel at failure. Failure by mode (ii) is associated with more ductile beams and crushing of the compression zone occurs as a secondary failure. Plates 5.1 and 5.2 show a typical flexural failure of prestressed brickwork beams. From strain measurements it was possible to determine whether or not the strain in the steel exceeded the strain corresponding to the proof stress and hence the failure mode. The maximum compressive strain at failure was also measured.

5.3.2 Additional Strain in Steel Across Cracks

Recent work[50] on reinforced concrete specimens tested in axial tension has shown that the strain in the reinforcement was profoundly influenced by the presence of cracks, with the greatest strains occurring across the cracks. Therefore yielding of the steel is most liable to occur across cracks. Using the strain measurements on the surface of the beams, where cracks formed within the gauge length, the additional strain in the strand due to the applied loading was obtained. The additional strains in the reinforcement after cracking are shown in Figures 5.3.1-5.3.11 for the various parameters considered. Also shown in these figures is the additional strain required to take the total strain, including prestress strain, in the steel up to the yield point. As cracks did not form within the gauge length in some beams it was not

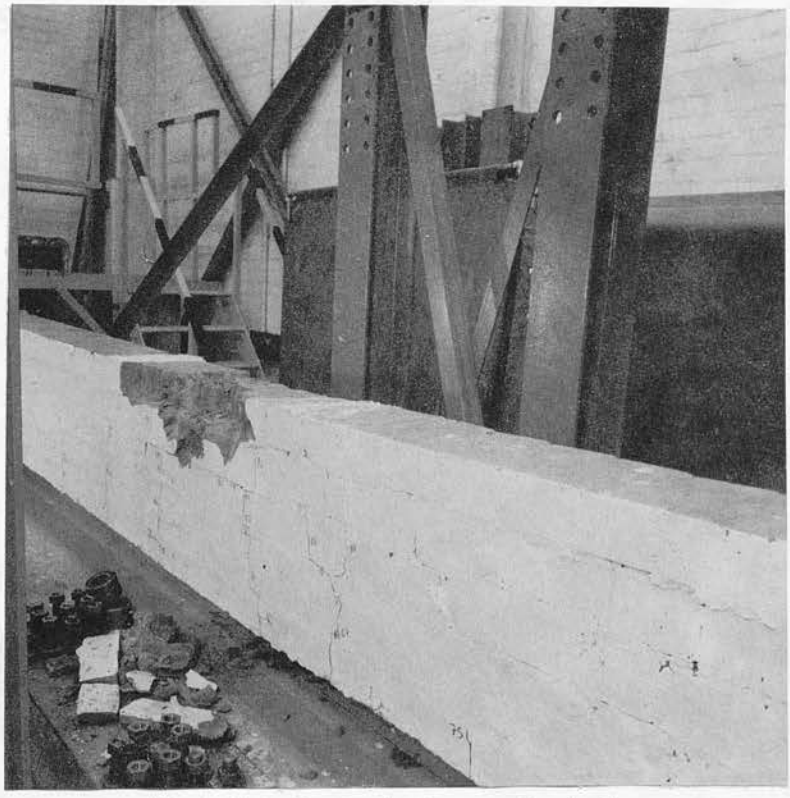

Plate 5.1 Typical flexural failure.

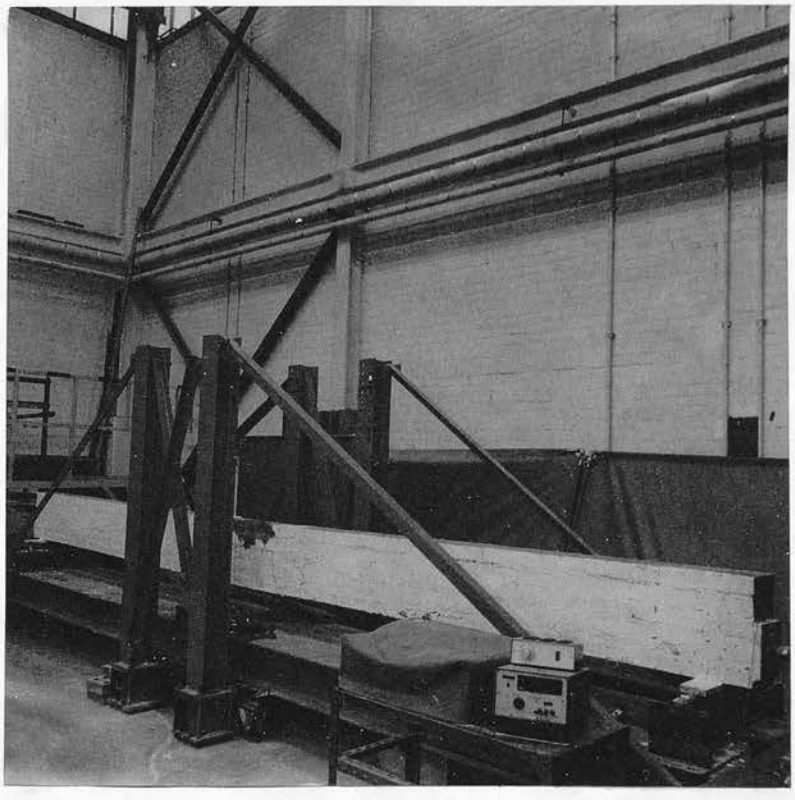

Plate 5.2 Typical flexural failure.

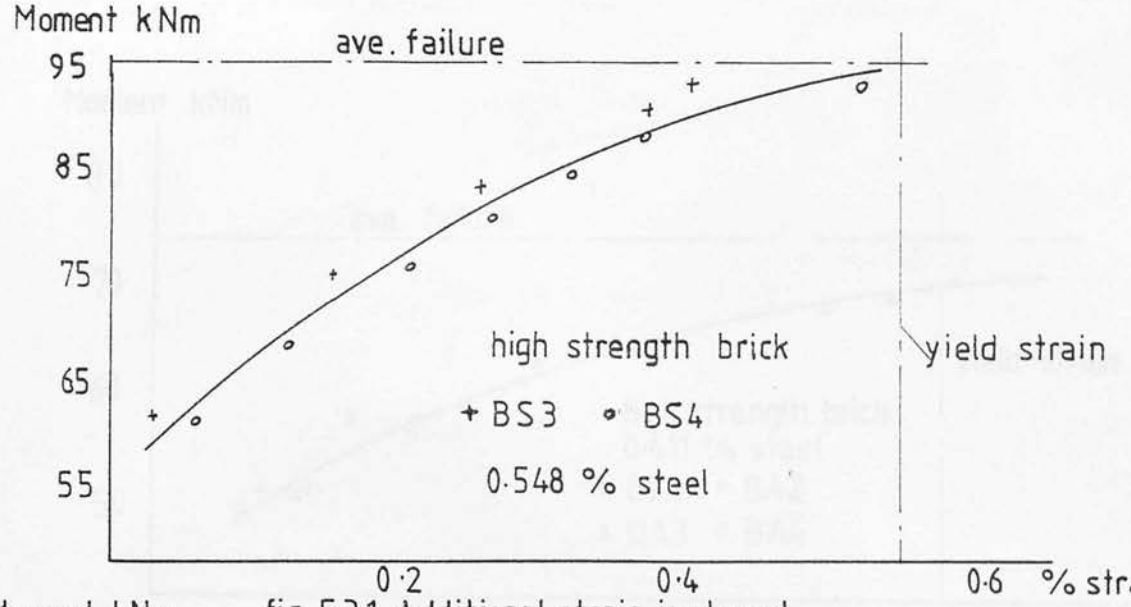

fig. 5.3.1 Additional strain in strand

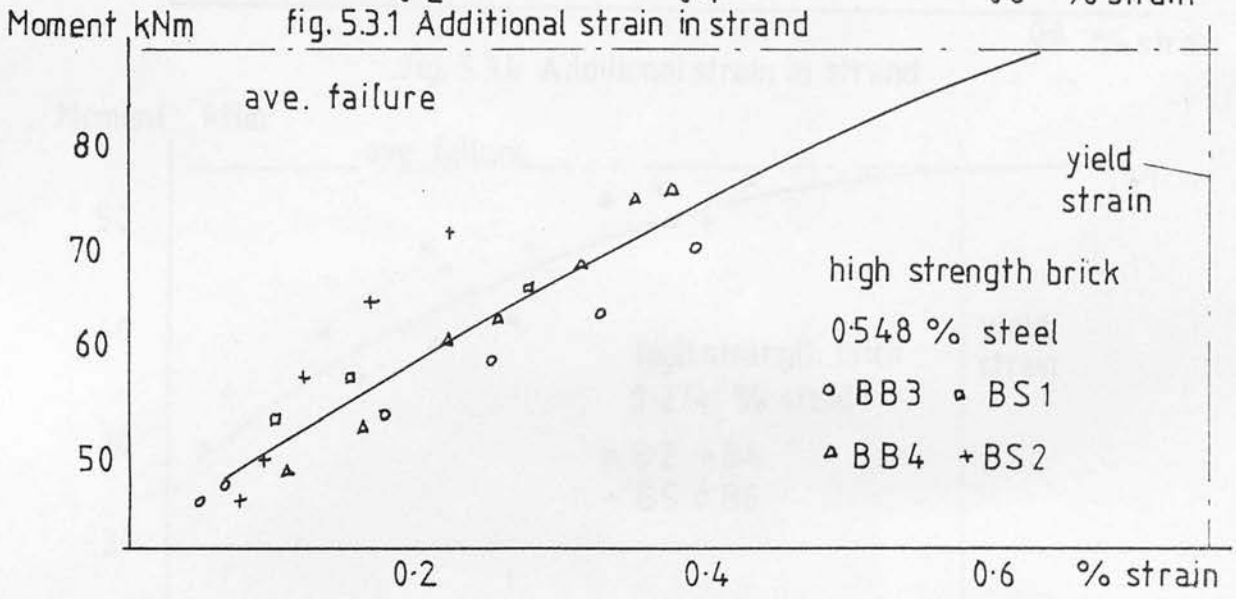

fig. 5.3.2 Additional strain in strand

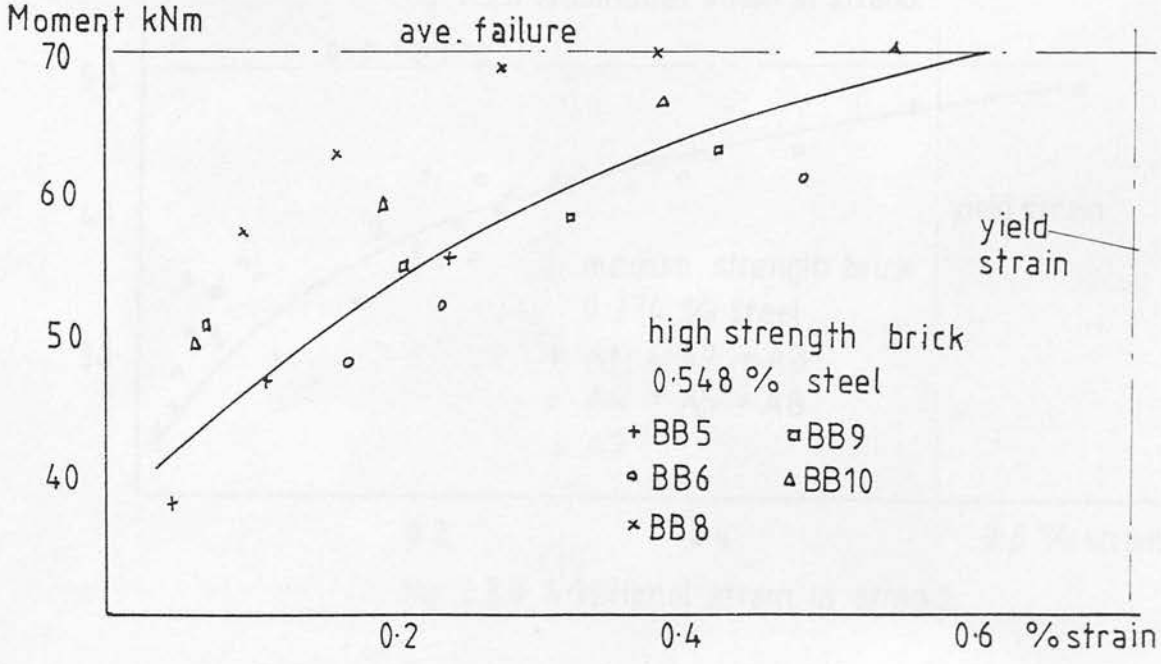

fig. 5.3.3 Additional strain in strand

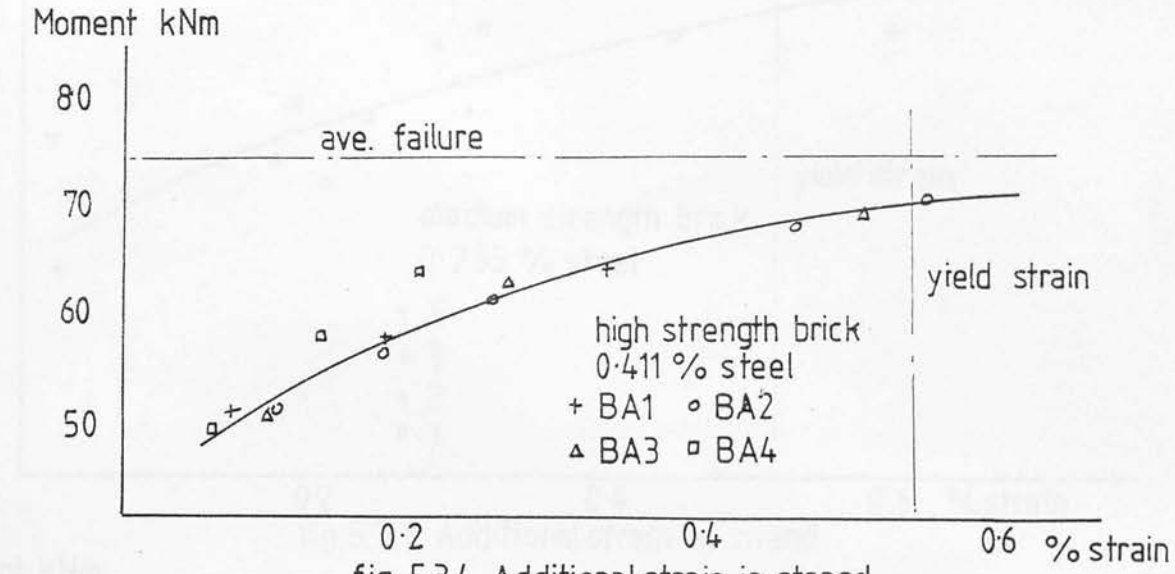

fig. 5.3.4 Additional strain in strand

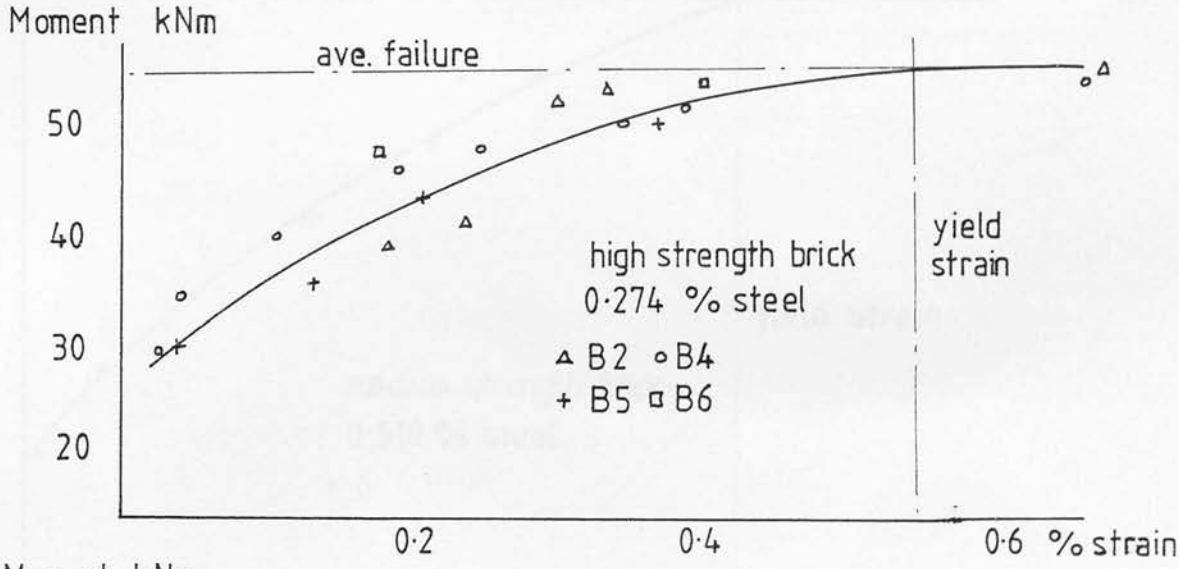

fig. 5.3.5 Additional strain in strand

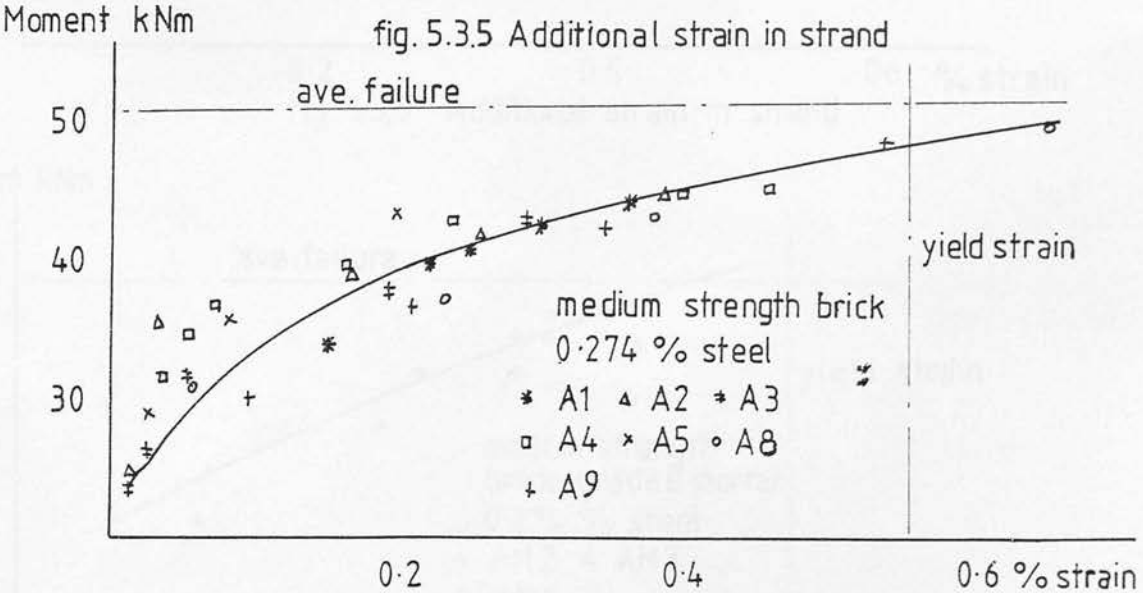

fig. 5.3.6 Additional strain in strand

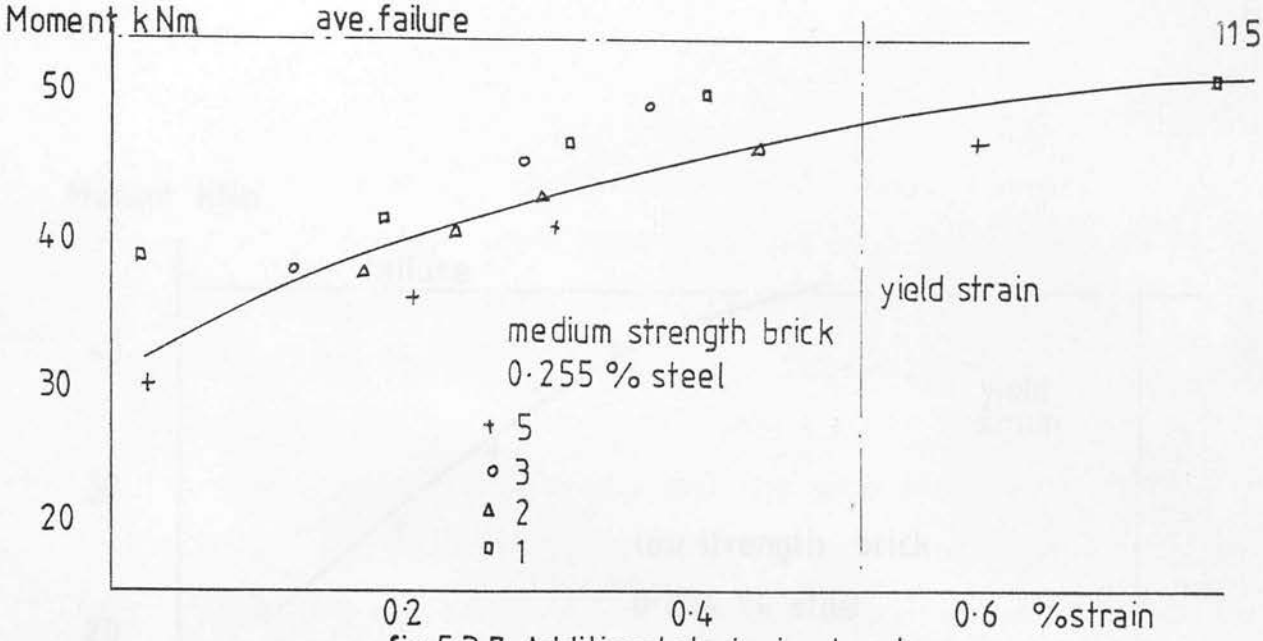

fig. 5.3.7 Additional strain in strand

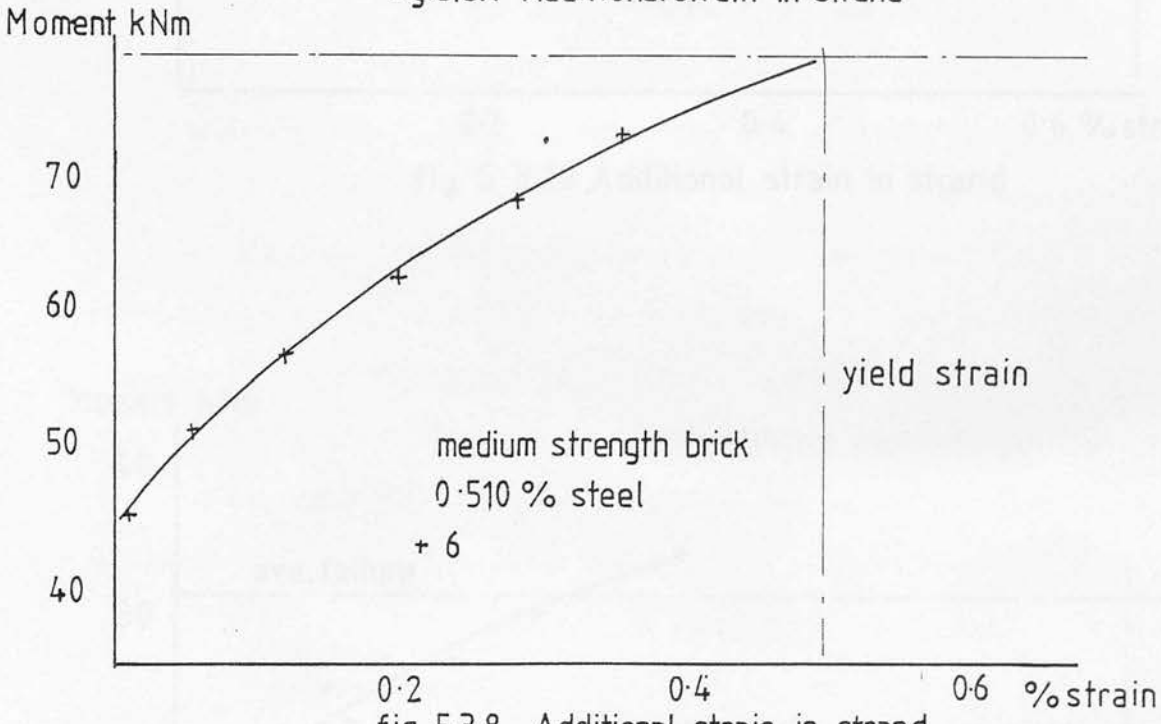

fig. 5.3.8 Additional strain in strand

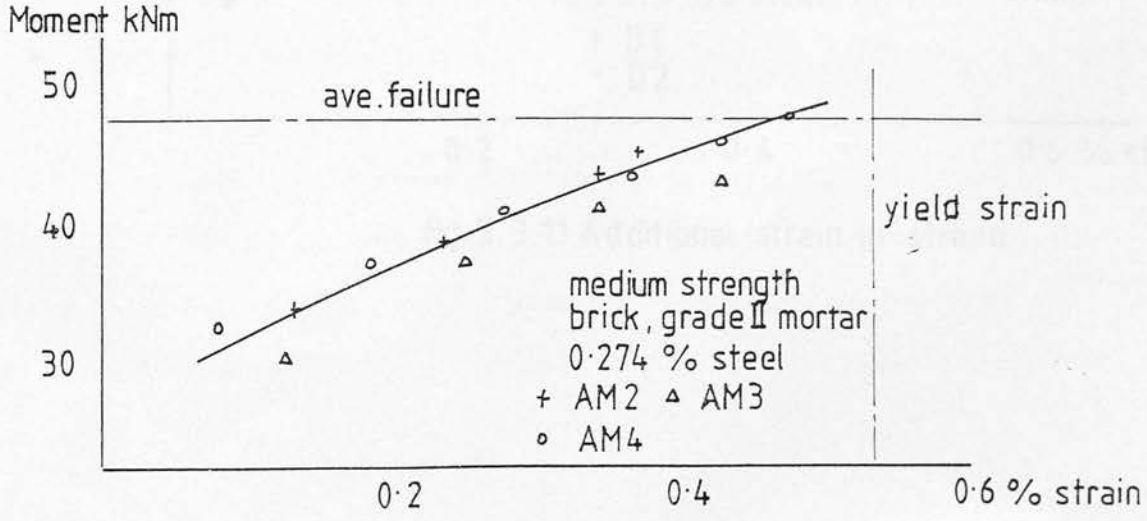

fig. 5.3.9 Additional strain in strand

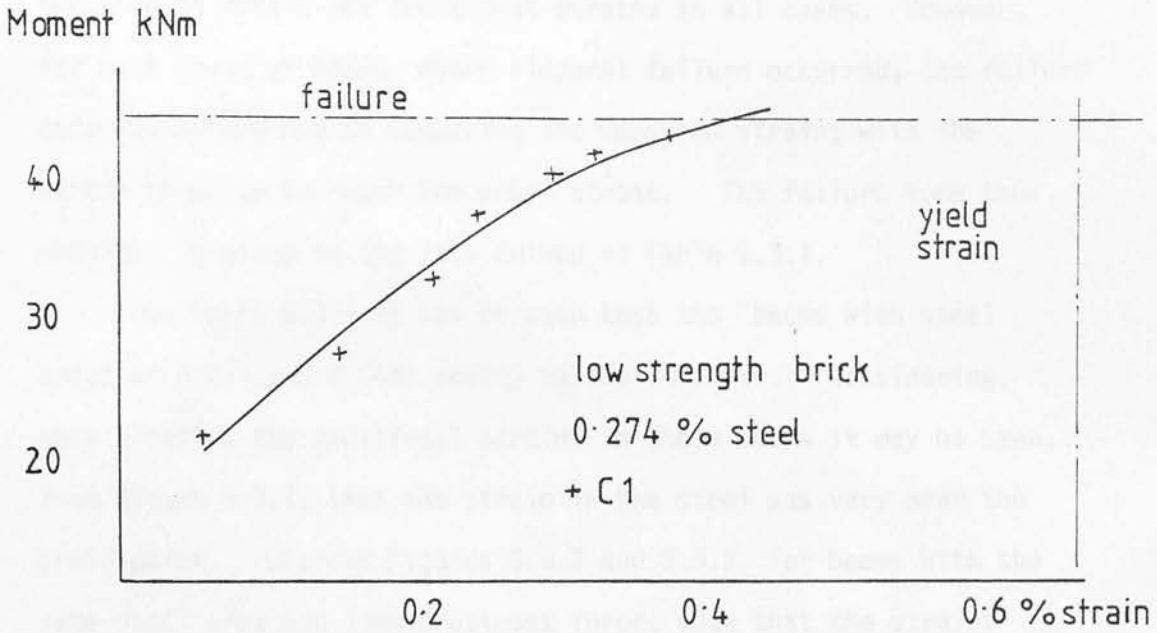

fig. 5.3.10 Additional strain in strand

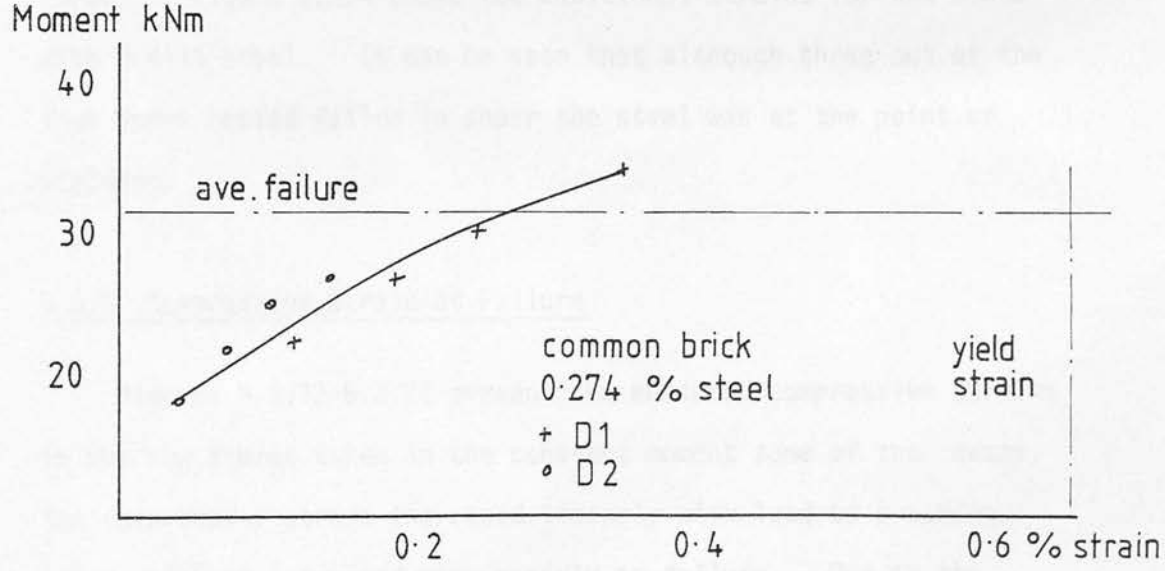

fig. 5.3.11 Additional strain in strand

possible to obtain the additional strains in all cases. However, for each group of beams, where flexural failure occurred, the failure mode was determined by comparing the measured strains with the strain required to reach the proof stress. The failure mode thus obtained is given in the last column of Table 5.3.1.

From Table 5.3.1 it can be seen that the beams with steel areas of 0.411 and 0.548% mostly failed in shear. Considering, very briefly, the additional strains in these beams it may be seen, from Figure 5.3.1, that the strain in the steel was very near the yield point. Whereas Figures 5.3.2 and 5.3.3, for beams with the same steel area but lower prestress force, show that the strains are well below the yield point. This is due to the different initial strains caused by the differences prestress forces, with greater additional strains required for the beams with the lower prestress forces. Figure 5.3.4 shows the additional strains for the beams with 0.411% steel. It can be seen that although three out of the four beams tested failed in shear the steel was at the point of yielding.

5.3.3 Compressive Strain at Failure

Figures 5.3.12-5.3.22 present the measured compressive strains in the top fibres taken in the constant moment zone of the beams. The compressive strain increased linearly with load up cracking after which it increased more rapidly to failure. Due to the explosive nature of a compressive failure, it would be dangerous to attempt to measure the strains up to failure, nevertheless the strains were measured very close to this point, as can be seen from

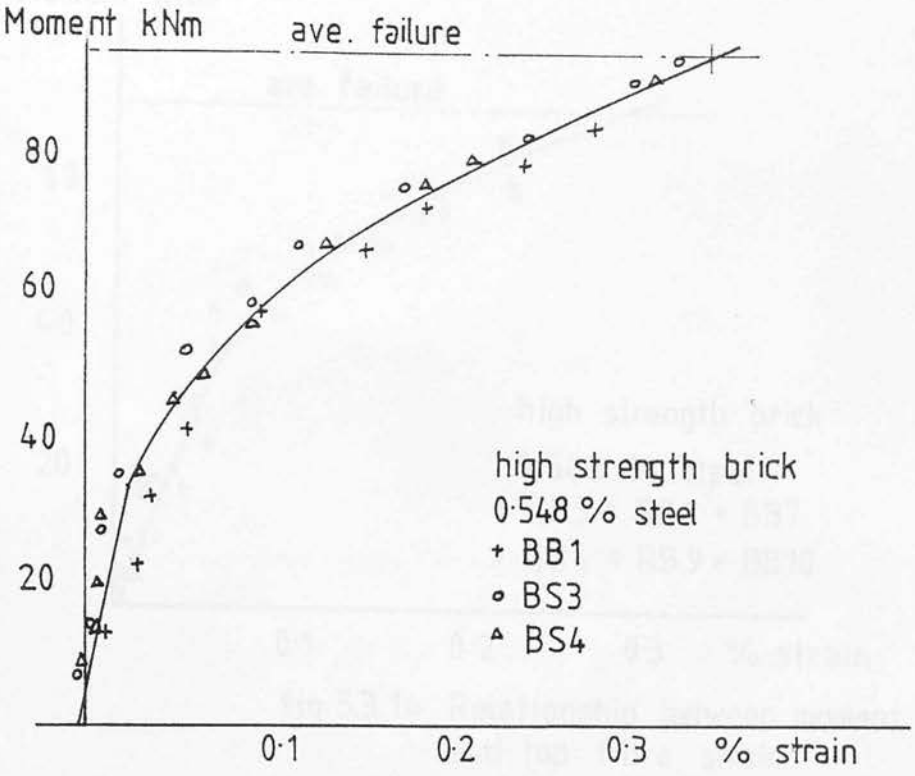

fig. 5.3.12 Relationship between moment and top fibre strain.

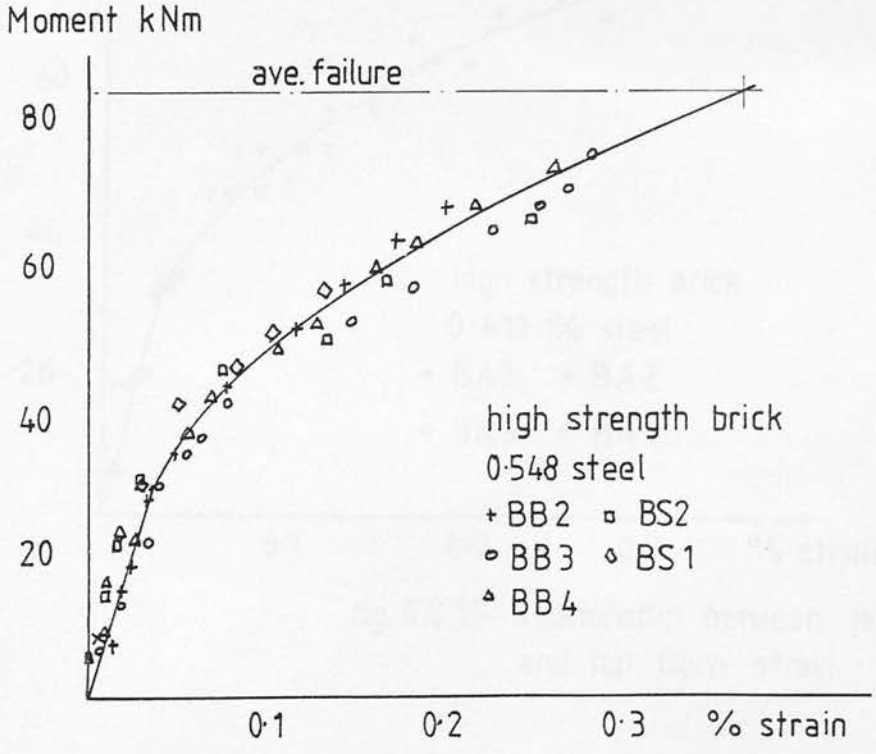

fig. 5.3.13 Relationship between moment and top fibre strain

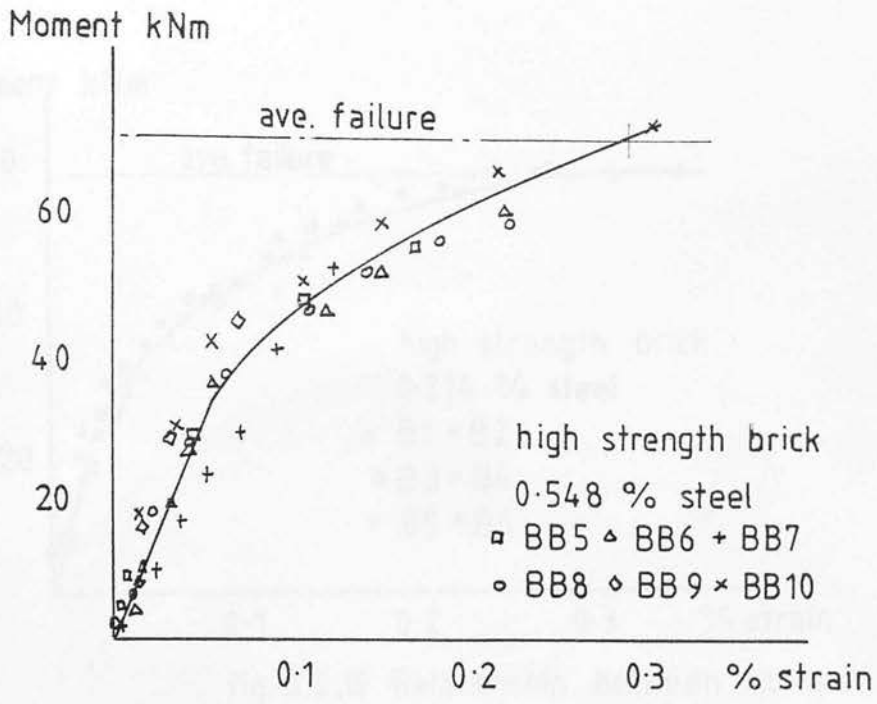

fig.5.3.14 Relationship between moment and top fibre strain

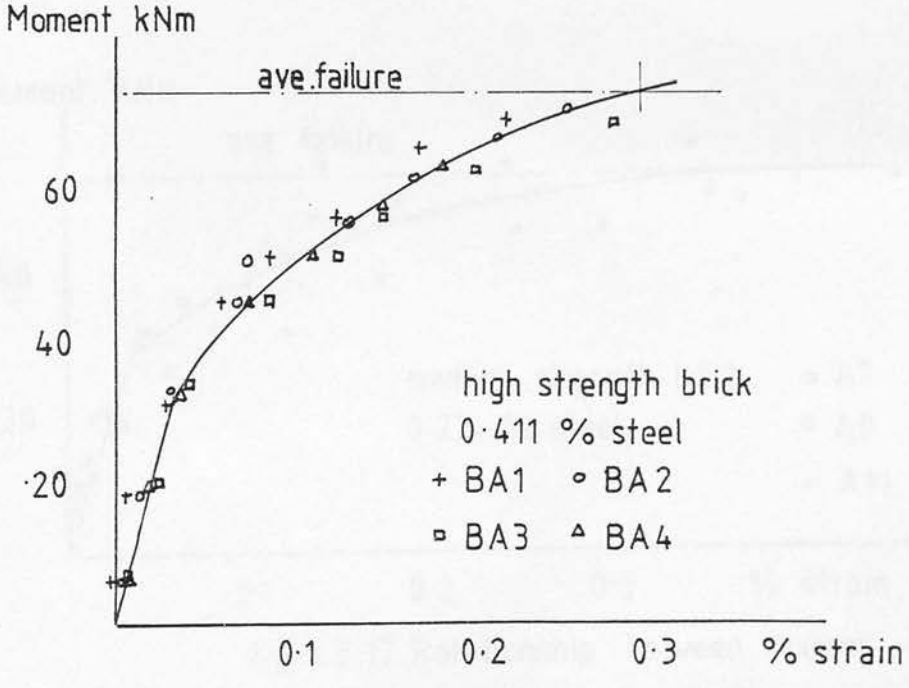

fig. 5.3.15 Relationship between moment and top fibre strain

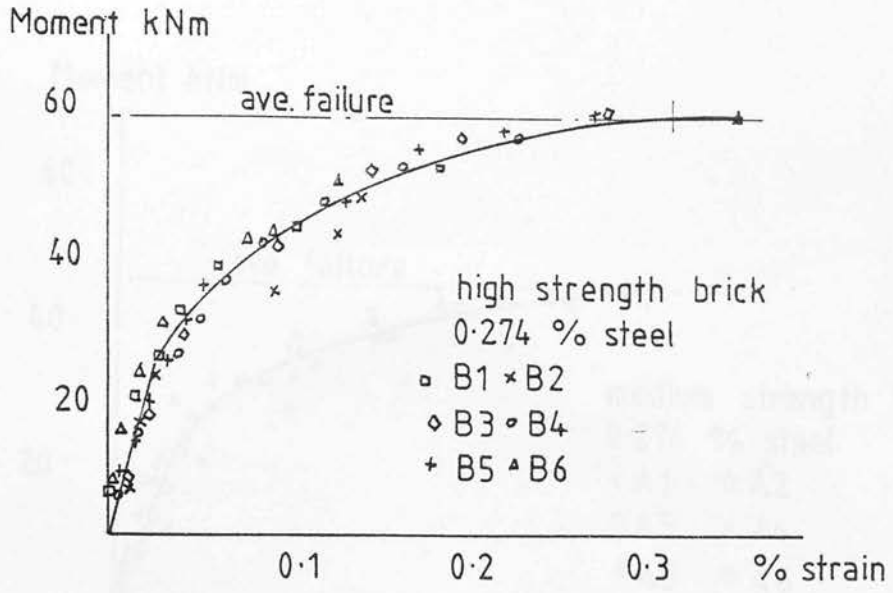

fig. 5.3.16 Relationship between moment and top fibre strain

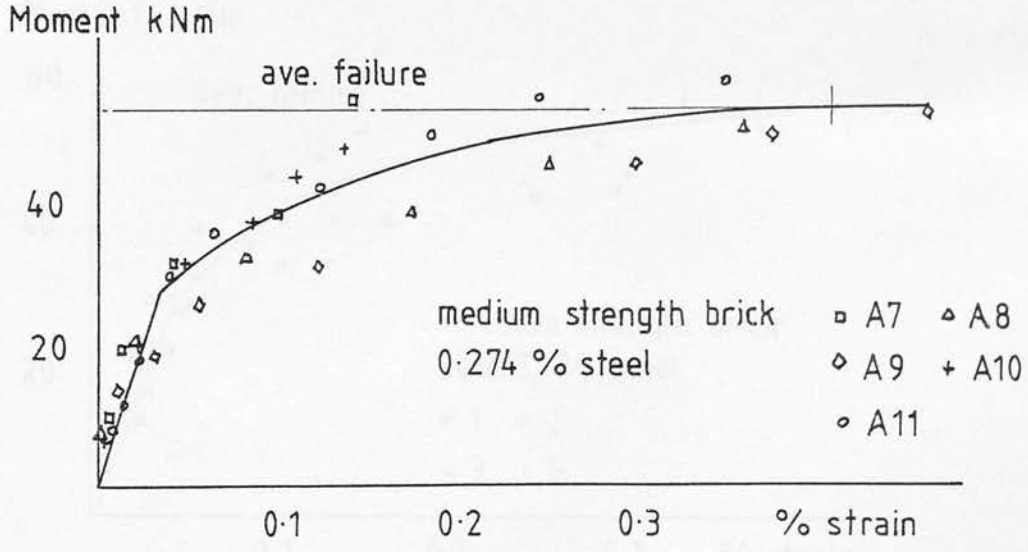

fig. 5.3.17 Relationship between moment and top fibre strain

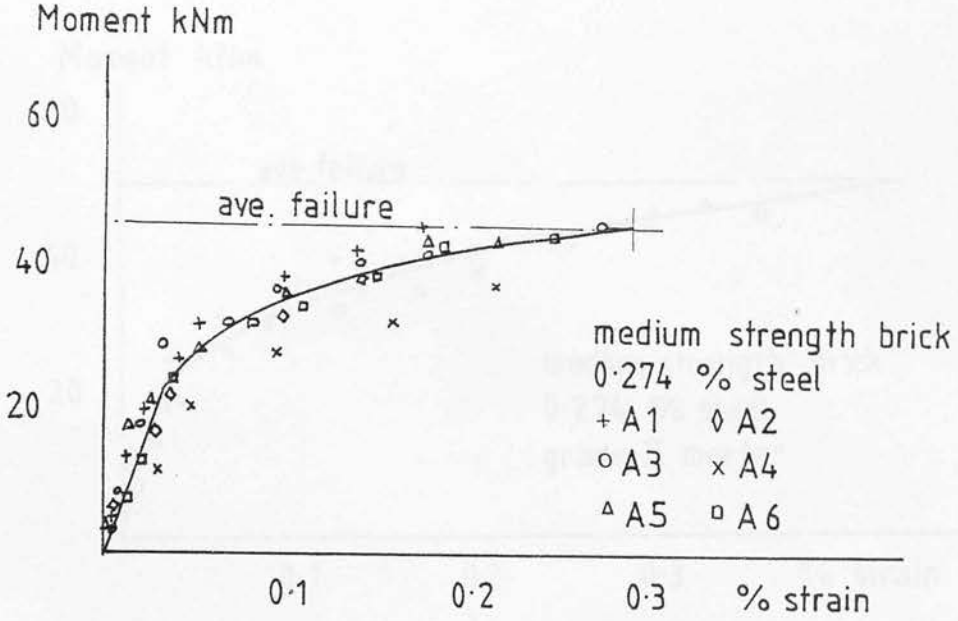

fig. 5.3.18 Relationship between moment and strain in top fibre

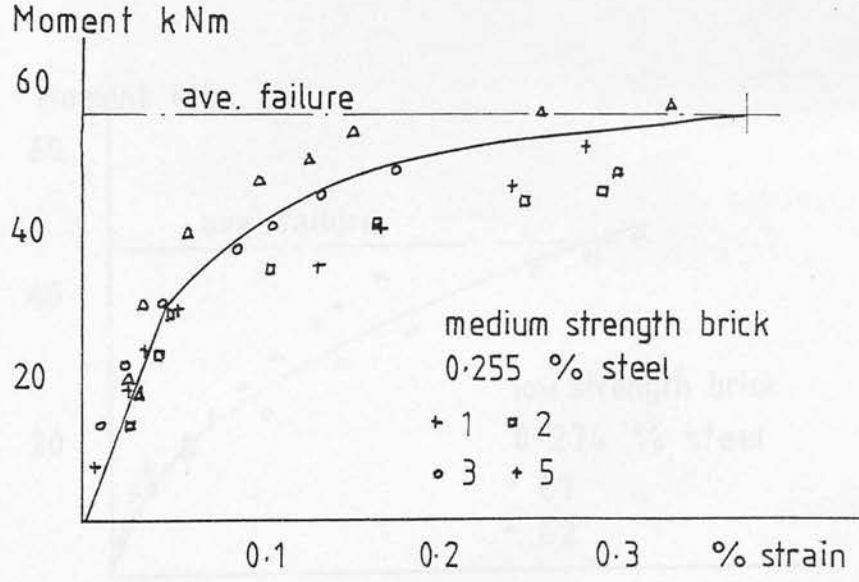

fig. 5.3.19 Relationship between moment and top fibre strain

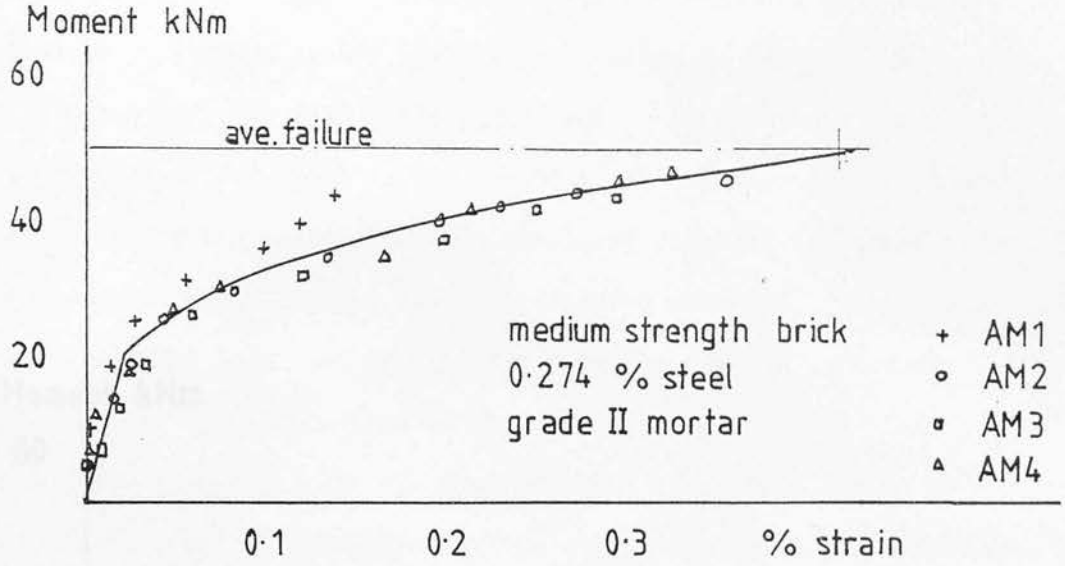

fig. 5.3.20 Relationship between moment and top fibre strain.

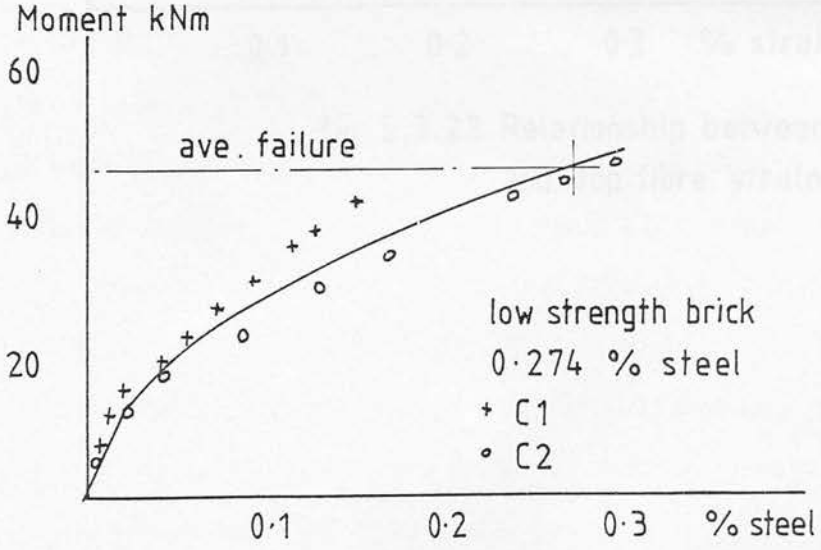

fig. 5.3.21 Relationship between moment and top fibre strain.

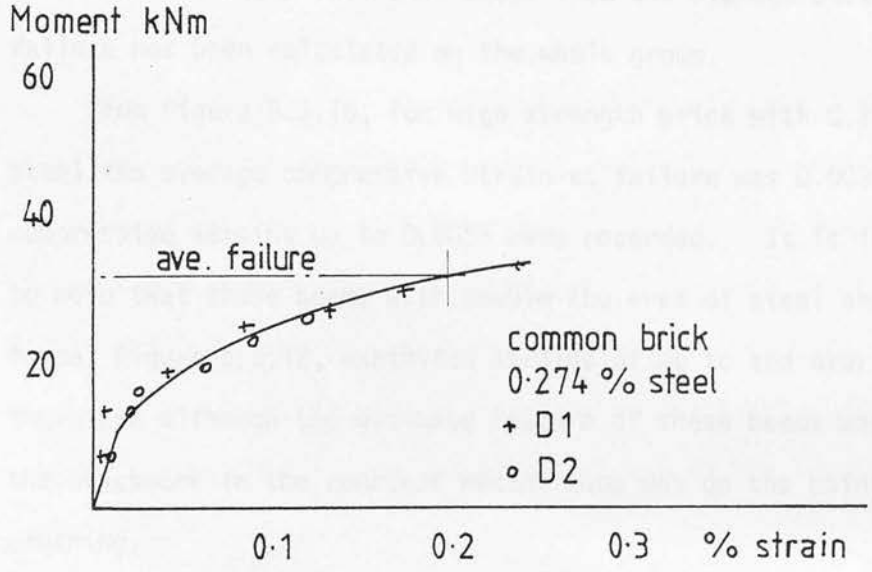

fig. 5.3.22 Relationship between moment and top fibre strain.

the figures where the average strain reaches the average failure moment. The average curve of compressive strain has been extrapolated or stopped at the level corresponding to the average failure moment for that particular group. In groups of beams where some of the beams failed in shear, the average failure moment was taken as the average of the remaining flexural failures, as these were the only beams in which crushing occurred. In groups where all the beams failed in shear then the average strain at failure has been calculated on the whole group.

From Figure 5.3.16, for high strength brick with 0.274% of steel the average compressive strain at failure was 0.0031 although compressive strains up to 0.0035 were recorded. It is interesting to note that those beams with double the area of steel and prestress force, Figure 5.3.12, exhibited strains of up to and over 0.0031, therefore although the ultimate failure of these beams was in shear the brickwork in the constant moment zone was on the point of crushing.

Figures 5.3.17-19 present the measured strains for the medium strength brick in 1:$\frac{1}{4}$:3 mortar. Each figure suggests average ultimate strains of 0.0042, 0.0030 and 0.0037 respectively. Taking an average for all the results in the three figures, the ultimate strain for medium strength brick in 1:$\frac{1}{4}$:3 mortar is 0.0037.

For the medium strength brick in 1:$\frac{1}{2}$:4$\frac{1}{2}$ mortar, Figure 5.3.20, strains of up to 0.0036 were measured and the average ultimate strain extrapolated at failure was 0.0042.

The average ultimate strain for the low strength brick beams, Figure 5.3.21, show an average ultimate strain of 0.00275.

An average ultimate strain of 0.0021 was obtained for the common brick, Figure 5.3.22.

The significance and influence of the ultimate compressive strains in relation to the predicted moments using the information obtained from small specimen tests will be dealt with further on in this chapter.

5.3.4 Strain Distribution and Neutral Axis Depth

Figure 5.3.23 shows typical variations of strain with distance from top fibre of beam for two beams, built in high strength brick. It can be seen that the distribution of strain with depth was essentially linear, throughout the full loading range of the beams. After prestressing the compressive strains in the bottom fibres were greatest, due to the eccentricity of prestress. As the load increased the compressive strains decreased in the lower sections of the beam and increased in the upper sections. At this point the neutral axis lay outside the section. On further loading the gradient of the strain distribution, i.e. curvature, changed direction and the neutral axis depth then moved to some point below the soffit of the beam. As tension developed the neutral axis depth moves upward into the section. Once cracking occurs, the compressive strains above the neutral axis depth increased rapidly with load and the neutral axis depth rose further. Typical variations of neutral axis with load, after cracking are shown in Figure 5.3.24. The neutral axis depth rose quickly on cracking and then levelled off. Beam BB3, which had twice the area of steel as B3 and a greater prestress force, levelled off at a greater neutral axis

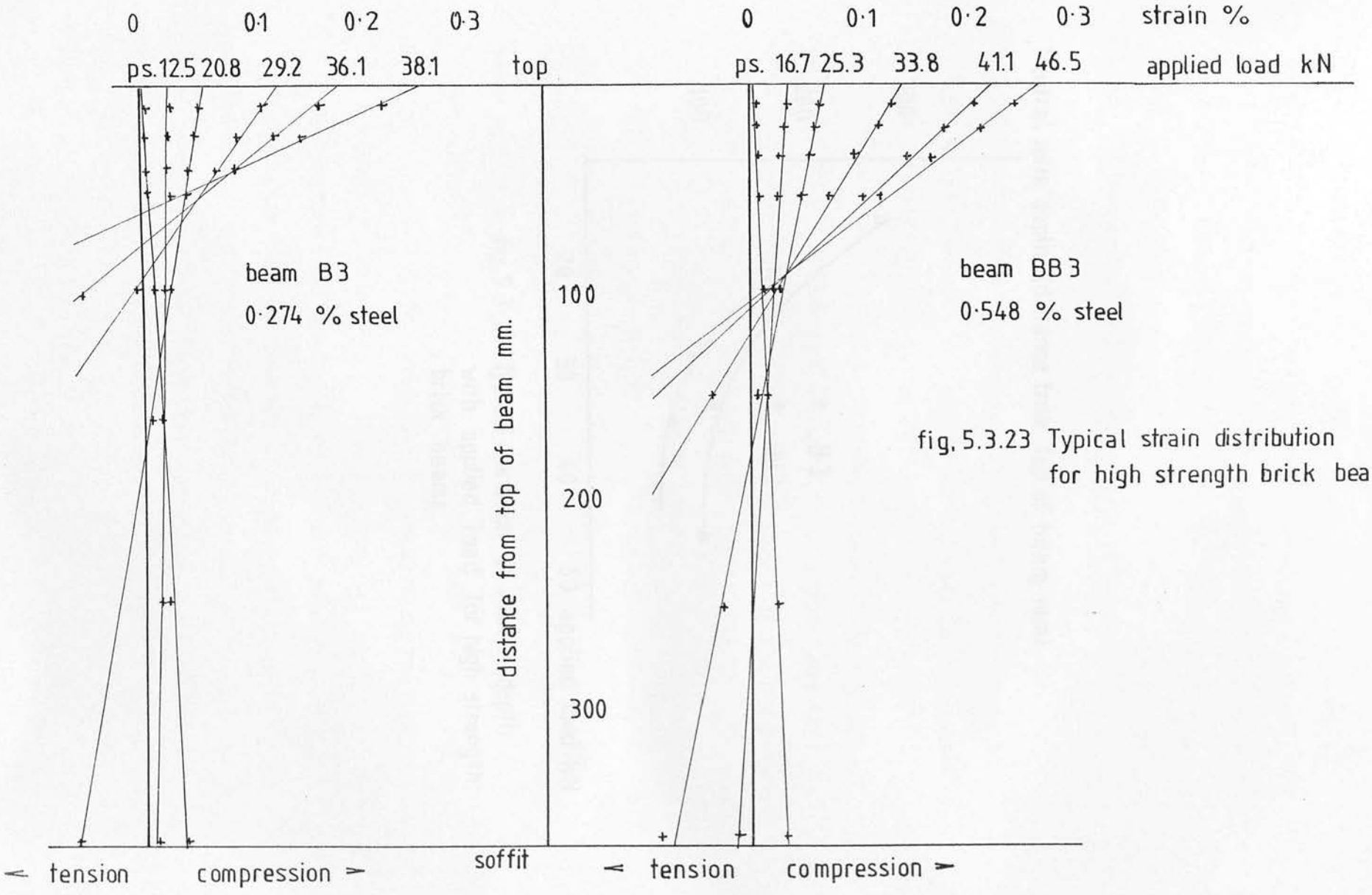

fig. 5.3.23 Typical strain distribution for high strength brick beams

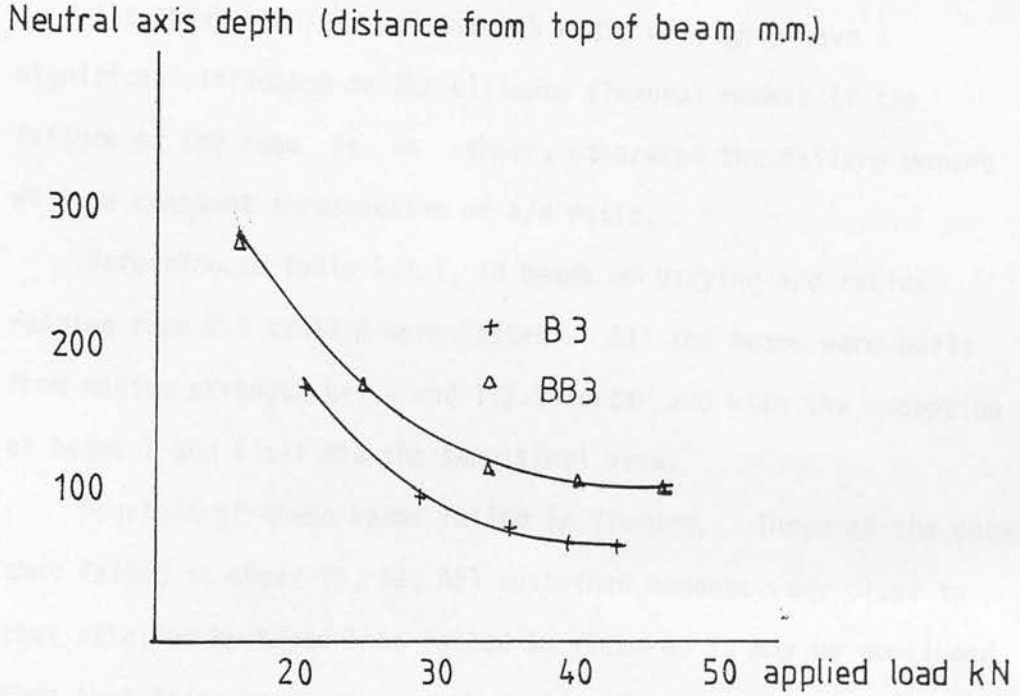

fig. 5.3.24 Typical variation of neutral depth with applied load for high strength brick beams.

depth. This was due to the greater steel area which allows larger tensile forces to develop, thereby requiring a greater neutral axis depth in order to develop compressive forces of a similar magnitude.

5.3.5 Influence of Shear Span/Effective Depth Ratio

The shear span/effective depth ratio will only have a significant influence on the ultimate flexural moment if the failure of the beam is in shear, otherwise the failure moment will be constant irrespective of a/d ratio.

Referring to Table 5.3.1, 18 beams of varying a/d ratios ranging from 2.3 to 11.2 were tested. All the beams were built from medium strength brick and 1:¼:3 mortar and with the exception of beams 7 and 6 all had the same steel area.

Fourteen of these beams failed in flexure. Three of the beams that failed in shear (3, A2, A5) sustained moments very close to that attained by those that failed in flexure, it may be concluded then that these beams were on the point of flexural failure. The beams built from high, low and common brick with 0.274% steel also failed in flexure. Hence, beams with 0.255-0.274% steel tended to fail in flexure and the a/d ratio had no influence on the strength of these beams.

From Figures 5.3.6 and 5.3.7, the average additional strain required for the steel to yield was exceeded and this has initiated the failure of the medium strength brick beams. Figure 5.3.8 shows the additional strain for the medium strength brick with 0.51% steel. The steel was very close to yielding and this suggests that with this %

of steel, fully prestressed, the medium strength brick beams are on the point of balanced failure.

From Table 5.3.1 it can be seen that a second series of beams with varying a/d ratios which all failed in shear were tested. These are dealt with in more detail in Chapter 7.

5.3.6 Influence of Brick Strength

Six beams, B1-B6 were built with high strength brick and had 0.274% steel. Out of this group all but one failed in flexure. Figure 5.3.5 shows that the strain in the steel had exceeded the yield point and were, consequently, under-reinforced, as with the beams built with medium strength brick and equal steel areas, section 5.3.5. The average failure moment of the five high strength brick beams was 58.2 kNm, Table 5.3.2. The average flexural failure moment for the medium strength brick beams was 50.91 kNm. There was a 16% increase in ultimate moment corresponding to a 31% increase in brick strength.

Comparing the average ultimate moment of the low strength brick beams with the common brick beams. The average failure moments are 44.2 and 30.7 kNm, respectively, Table 5.3.2. An increase in brick strength from 22.7 to 34.18 N/mm^2 (51%) results in a 44% increase in flexural strength. Figures 5.3.10 and 5.3.11 shows that the low strength and common brick beams were over-reinforced, the steel did not yield. The prestress force in these beams was approximately half that of the high and medium strength brick beams to avoid overstressing. This makes comparisons between the high and medium and the low and common brick beams difficult.

Table 5.3.2 Influence of Brick Strength on Flexural Strength of Prestressed Brickwork Beams

Beams	Brick Strength N/mm^2	Failure Moment kNm	Ave. Failure Moment kNm
B1	88	52.9	
B3	"	61.5	58.2
B4	"	58.4	
B5	"	59.2	
B6	"	58.8	
A1	67	47.9	
A3	"	46.0	
A4	"	46.1	
A7	"	53.4	50.9
A8	"	51.8	
A9	"	54.1	
A10	"	51.7	
A11	"	56.3	
C1	34	45.9	
C2	"	42.5	44.2
D1	22	35.5	
D2	"	25.8	30.7

Table 5.3.3 Influence of Mortar Grade

Beams	Mortar Grade/Strength N/mm^2		Ave. Mortar Strength N/mm^2	Failure Moment kNm	Ave. Failure Moment kNm
A1-A11	I	-	20.4	-	50.9
AM1	II	5.3		48.6	
AM2	"	5.3	6.8	45.8	47.7
AM3	"	8.2		48.6	

If the brick or brickwork strength is lower, then in order for equilibrium to be maintained the depth to the neutral axis depth must increase to cause the steel to yield. The lower the neutral axis depth, the lower the additional strain in the steel for a given ultimate brickwork strain. The lowercompressive strengths and prestress force in the low strength and common brick result in beams in which insufficient compressive forces can develop to allow the proof stress of the steel to be reached.

From these results it may be concluded that when the compressive strength of the brickwork is strong enough to result in steel yielding the internal forces of beam are governed by the total force that may be developed in the steel. The compressive strength in this case has only a secondary effect on the ultimate moment, influencing the position of the neutral axis depth. If the compressive strength of the brickwork is such that yielding of the steel will not occur, i.e. over-reinforced, then the compressive strength has a much more significant influence on the final stress in the steel. Small increases in the compressive strength will result in comparatively large increases in steel stress and hence ultimate strength.

5.3.7 Influence of Mortar Grade

Four beams, AM1-AM4, were built with medium strength brick and 1:$\frac{1}{2}$:4$\frac{1}{2}$ mortar (grade II), Table 5.3.3. Of these, three failed flexure with an average ultimate moment of 47.7 kNm. Figure 5.3.9 shows that the steel has not yielded.

Comparing the average ultimate moment with that of the medium

strength brick beams built in 1:¼:3 mortar (grade I) there is a reduction in flexural strength of 6.3%. The average compressive strengths of the mortars were 6.8 N/mm^2 and 20.4 N/mm^2 for grade II and grade I mortars, respectively, a reduction in strength of 67%. It has long been recognised[32] that the compressive strength of mortar has only a nominal influence on the compressive strength of brickwork. This may be seen by referring to Table 3.4.1. The compressive strength from the three course prisms was slightly greater for those built in grade II mortar and for the single course prisms the compressive strength of the prisms in grade II mortar is 28% less than those of grade I.

5.3.8 Influence of Prestress Force and Steel Area

The group of beams B1-B6 had 0.274% area of steel, the majority of these failed in flexure. When the area of steel and prestress force increased the failure load also increased. However the greater proportion of these beams, with 0.411% steel (BA1-BA4) and 0.548% steel (BB1-BB4, BS1-BS4) failed in shear. Beam BS1 and BS2 had shear reinforcement and failed in flexure at an average ultimate moment of 89.9 kNm. These beams had an approximately 50% increase in prestress and a 100% increase in stress area over beams B1-B6. The increase in ultimate moment was 52%.

One of the beams in group BA1-BA4, BA3, failed in flexure. Again, there was an increase of 50% in prestress but only a 50% increase in steel area over beams B1-B6. The increase in ultimate moment was 27%, which is almost exactly half the increase obtained with the beams with 0.548% steel. As the levels of prestress were

the same for both these groups the increase in ultimate moment was due entirely to the increase in steel area.

The effect that the prestress force has on the ultimate moment may be seen by comparing the average ultimate moment of beams BS1 and BS2 with BS3 and BS4. All the beams had the same steel area but the prestress force in the latter two beams was 33% greater. Table 5.3.1 shows that there is a 9% increase in average failure moment for the beams with the higher prestress, even though final failure of these beams was in shear.

Comparing Figures 5.3.1 and 5.3.2 it may be seen that the strain in the steel for the beams with the greater prestress force, Figure 5.3.1, was much closer to the yield point than the beams with the reduced prestress. The effect of the prestress is to determine the position on the stress/strain relationship of the reinforcement when cracking occurs. The higher the prestress the further along the stress/strain relationship and the lower the additional strain necessary to reach the yield point.

An increase in prestress force with steel area constant will increase the ultimate moment, especially if the section is over-reinforced and the steel will not yield.

5.3.9 Comparison Between Variations in Flexural Strength, Brick and Brickwork Strength

It was stated in section 5.3.6 that the brickwork strength only has a moderate influence on the flexural strength if the section is under-reinforced. This was in relation to bricks of differing average compressive strengths. Here the effect of variations in

brick strength for a given brick type are considered.

Eight beams failed in flexure in series A1-A11. It is therefore possible to calculate the variance of the ultimate strength. As previously stated the average ultimate moment was 50.9 kNm. The standard deviation was 3.82 kNm with a coefficient of variance of 7.5%. The average compressive strength of the brick on edge was 26.36 N/mm^2, standard deviation was 5.71 N/mm^2 and coefficient of variance 21.66% (Table 3.2.1). Hence the variance of the brick strength is 2.9 times that of the flexural strength. This difference may be explained, in part, by considering the variance in brickwork strength. Again from Table 3.4.1 the variance in brickwork strength was either 14.7 or 17.1% depending on prism type. The brickwork strength varies less than the brick strength.

It is possible to study the effect of the variations in brickwork strength on the ultimate flexural strength. The ultimate moment of an under-reinforced masonry beam may be expressed as:

$$M_u = f_{sy} A_{ps} \left(1 - \frac{\lambda_2 f_{sy} A_{ps}}{\lambda_1 f_m b \cdot n}\right) \qquad (5.3.1)$$

where, for the purposes of this discussion only λ_1 and λ_2 are taken as 0.75 and 0.4[13]. Substituting the relevant data for beams A1-A11 into equation 5.3.1, the ultimate moment may then be determined from:

$$M_u = 55.5 \times 10^6 \left(1 - 2.33/f_m\right) \qquad (5.3.2)$$

Assuming a normal distribution for the brickwork strength then

for a confidence interval of 95%, the upper and lower limits of the compressive strength[43] will be:

$$f_m = 23.7 \pm (1.64 \times 4.05) \qquad (5.3.3)$$

Using equation 5.3.3 the maximum and minimum values of f_m are 30.3 and 17.06 N/mm^2. Substituting these values in equation 5.3.2, the range of ultimate moments is 47.9-51.2 kNm, compared to the ultimate moment based on the average compressive strength of brickwork, 50.04 kNm.

Comparing the range of ultimate moments predicted using equation 5.3.3, with the range of the experimental results it can be seen that the maximum and minimum predicted moment are well within $\pm$ one standard deviation of the average experimental results.

Where the section is under-reinforced, the compressive forces that may be developed are dictated by the steel area. The high degree of quality control during manufacture of the steel ensures that the properties of the steel do not vary greatly. Thus the compressive forces in an under-reinforced beam will also not be subject to large variations.

Hence although the brick strength may be prone to considerable variation the flexural strength of under-reinforced prestressed brickwork beams will not undergo the same degree of variation.

It should be noted that although the brick strength itself may not have a great influence on the variability of the flexural strength, it has a contributory effect that must be added to variations caused by construction tolerances and prestress losses.

5.4 Comparison Between Experimental and Predicted Ultimate Moments

Using the theory described in section 5.2, the ultimate moments of the beams were predicted. The relevant stress block factors compressive strengths and ultimate strains were given in Table 3.4.3. The idealised stress/strain relationship for the reinforcement was given in Figure 3.5.2. The predicted ultimate moments for those beams that failed in flexure are shown in Table 5.4.1. The pre-stress forces were taken from Table 5.3.1, which include the effects of any losses due to creep, elastic shortening and lock off, up to the start of the test.

The experimental ultimate moments are compared with the predicted moments using the stress block characteristics from both the single and three course prisms. The ultimate moments obtained from the recommendations of the draft code of practice[14] are also given for comparison.

5.4.1 Ultimate Moment Based on Single and Three Course Prisms

Comparing the ultimate moments predicted from the single and the three course prisms for high and medium strength in 1:¼:3 mortar, the single course prisms predict moments on average within 7.4% of the experimental results, whereas the ultimate moments based on the three course prisms generally underestimate the experimental results by 28% on average, in the case of the high strength brick and 24% for the medium strength brick.

Considering those beams with the highest steel area, that failed in flexure, BS1 and BS2, then the three course prisms under-

Table 5.4.1 Predicted Ultimate Moments

Beam	Experimental kNm	Theoretical Ultimate Moments: Single Course kNm	Single Course Exp/Theo	Three Course kNm	Three Course Exp/Theo	B.S.5628, Part II kNm	B.S.5628, Part II Exp/Theo
B1	56.94	54.32	1.05	49.40	1.15	53.78	1.06
B3	61.5	54.34	1.13	49.26	1.25	53.78	1.14
B4	58.40	54.39	1.07	49.74	1.21	53.78	1.09
B5	59.20	54.36	1.09	49.32	1.20	53.78	1.10
B6	58.8	54.37	1.08	49.46	1.19	53.78	1.09
BA3	74.81	72.5	1.03	58.11	1.29	70.06	1.07
BS1	87.18	94.75	0.92	62.14	1.40	86.70	1.02
BS2	92.16	94.97	0.98	67.30	1.38	86.28	1.07
A1	47.95	52.23	0.92	38.17	1.26	52.80	0.901
A3	46.02	52.23	0.88	38.56	1.19	52.86	0.87
A4	46.11	52.38	0.88	41.06	1.12	52.81	0.87
A7	53.40	52.34	1.02	39.57	1.35	52.83	1.01
A8	51.77	52.45	0.99	41.80	1.24	52.82	1.01
A9	54.14	52.34	1.03	39.57	1.37	52.83	1.02
A10	54.72	52.38	0.99	40.98	1.26	52.82	0.97
A11	56.26	52.35	1.07	38.68	1.45	52.83	1.06
1	61.39	58.65	1.05	44.45	1.38	59.31	1.04
2	49.50	58.65	0.84	44.45	1.11	59.32	0.83
3	49.38	58.73	0.84	44.51	1.11	59.33	0.83
4	56.98	58.80	0.97	47.90	1.19	59.31	0.96
5	56.02	58.77	0.95	46.14	1.21	59.32	0.94
6	77.07	90.9	0.84	62.05	1.25	94.7	0.82
7	67.80	90.1	0.75	61.5	1.10	94.21	0.719
AM1	48.60	49.0	0.99	44.54	1.10	49.0	0.99
AM2	45.80	47.83	0.96	42.15	1.09	48.8	0.94
AM4	48.66	49.05	0.99	44.54	1.09	49.37	0.99
C1	46.70	36.11	1.29	26.69	1.75	42.14	1.11
C2	42.50	37.20	1.14	28.4	1.50	41.84	1.02
C3	54.06	40.25	1.34	33.39	1.62	43.55	1.23
D1	35.50	24.05	1.48	27.75	1.28	35.83	0.99
D2	25.79	24.76	1.04	28.69	0.90	36.20	0.71

estimate the ultimate moments by as much as 59%.

The predicted strengths of the medium strength brick beams in 1:½:4½ mortar, AM1-AM4 are within 5.7% of the experimental, based on the single course prisms and 7.3% based on the three course prisms.

For the low strength brick the three course prisms give a very low estimate of the ultimate strength and although the single course gives a closer prediction, the ultimate moments are still underestimated by an average of 25%.

The single course prisms, then for high, medium and low strength predict higher moments than the three course prisms, which are also in better agreement with the experimental results. This is not the case for the two common brick beams. Experimentally, there was quite a difference between the two results, however lower moments were predicted using the single course prisms.

Referring to Table 3.4.3 it can be seen that the stress block factors λ_1 and λ_2 are not greatly influenced by the prism type. There is a considerable variation in compressive strength between prism types of high and medium strength brick. For the high strength brick the single course exhibited compressive strengths 60% greater than the three course prisms and the compressive strength of the medium strength brick single course prisms was almost twice that of the single course prisms.

Comparing also the average ultimate strains for high and medium strength brick, the ultimate strains in the single course prisms were greater than the three course prisms, by 60% and 53% for the high and medium strength brick respectively. These

higher ultimate strains show much more favourable agreement with the measured ultimate strains, Figures 5.3.16-19. From section 5.3.3 the average ultimate strain was 0.0031 for high strength brick, while the ultimate strain from the single course prisms was 0.0032. The ultimate strain of the medium strength brick was 0.0037 while the ultimate strain from the single course prisms was 0.0026.

The compressive strength for the low strength brick was almost identical for both prism types but the ultimate strains were considerably higher in the single course prisms. The ultimate strain obtained experimentally appears to fall between the ultimate strains from the two different prism types, Figure 5.3.21.

The compressive strengths and ultimate strains of the medium strength brick in grade II mortar were also greater for the single course prisms, although the differences between the two prisms were not as wide as the medium strength brick in grade I mortar. Figure 5.3.20 shows that the ultimate strains measured on the beams were greater than ultimate strains from both the prism types.

Although the compressive strength of the common brick was greater in the three course prisms the ultimate strains from the single course prisms were larger and closer to the experimental results, Figure 5.3.22.

Figures 5.4.1(a)-5.4.10(a) show the relationship between ultimate moment and steel area for varying degrees of prestress based on both prism types, for each brick/mortar combination. The average experimental results are plotted on these figures. Also shown is the balanced section obtained from 5.2.20. Figures 5.4.1(b)-5.4.10(b) show the variation of neutral axis depth with steel area and prestress force.

From Figures 5.4.1(b) and 5.4.2(b), for high strength brick, the neutral axis depths predicted from the single course prisms are closer to the experimental results, with the three course prisms predicting greater depths. This trend is also apparent for the medium strength in both mortar grades, (Figures 5.4.3(b)-6(b)) and the low strength brick (Figures 5.4.9(b)-10(b)).

Based on the foregoing, with the exception of the common brick it is apparent that the ultimate compressive strains and neutral axis at failure are more closely modelled using the stress block characteristics obtained from the axial compression tests on single course prisms. As a result it leads to a more accurate prediction of the ultimate strength.

Referring to Figures 5.4.1(a)-10(a), it is possible to examine further the influence of prism type on the ultimate moment for a wide range of steel areas. The same characteristics may be observed in the relationship between ultimate moment and steel area, irrespective of prism type. Initially there is an almost linear increase in moment with steel area. Once the steel area reaches a certain value, dependent on the brick and prism type, the influence of the prestressing force becomes more noticeable, as the area of steel exceeds the balanced steel area. At this stage the higher prestress force results in greater moments although further increases in steel area do not cause the ultimate moment to rise as rapidly.

It can be seen that, again with the exception of the common brick, the steel area at which the balanced section occurs is higher for the moments predicted using the single course prisms than the three course prisms.

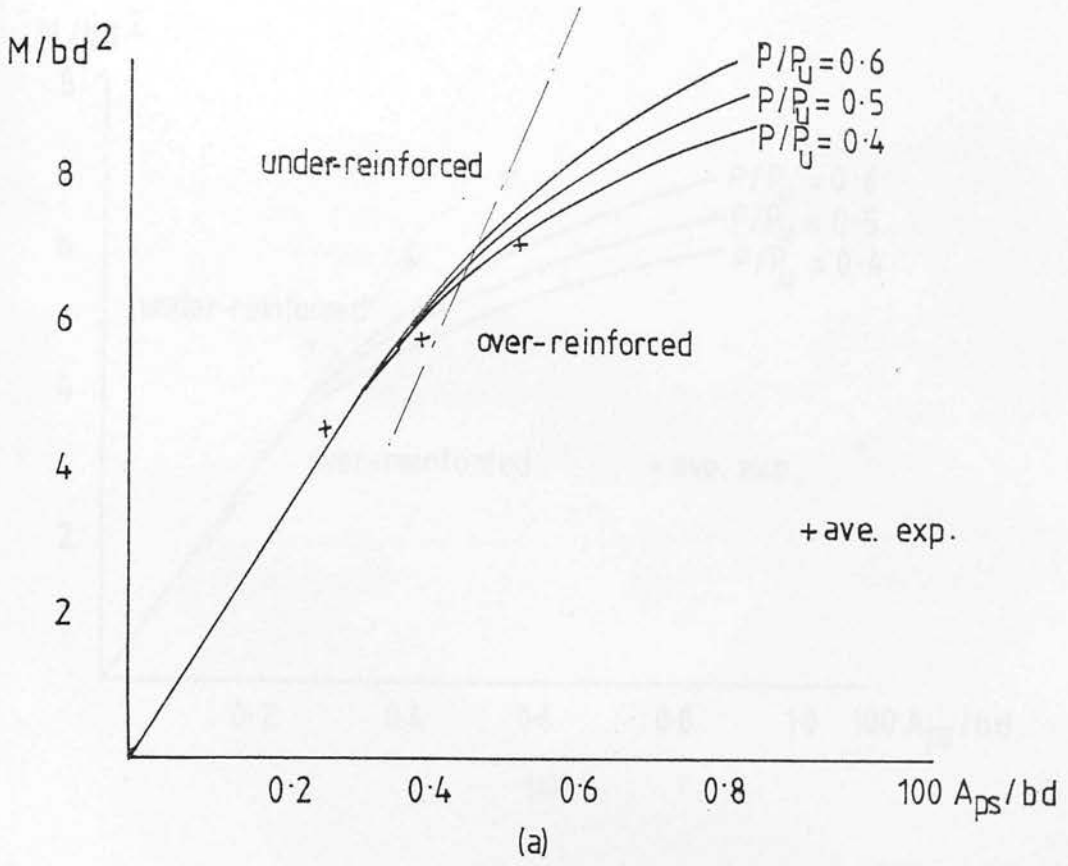

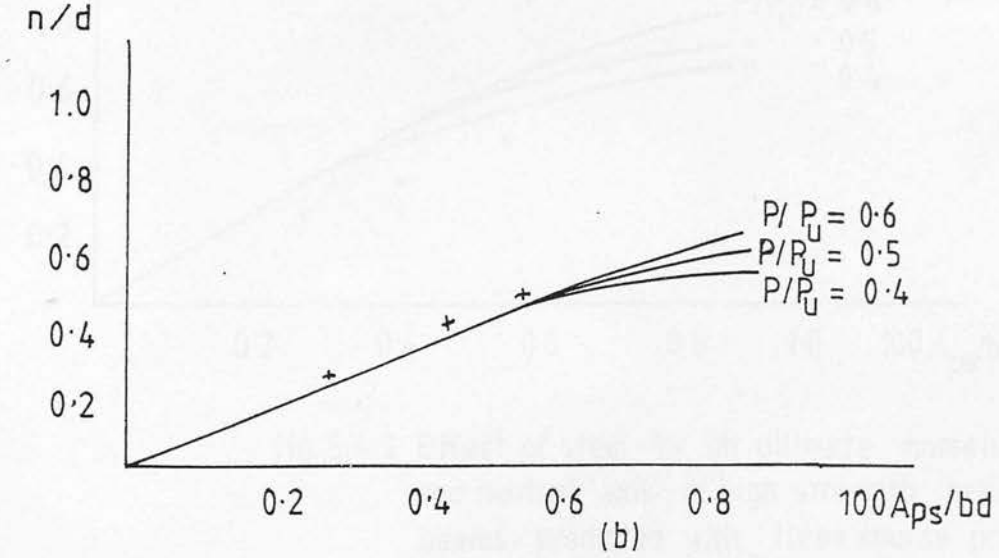

fig. 5.4.1 Effect of steel % on ultimate moment and neutral axis of high strength brick beams predicted with single course prisms.

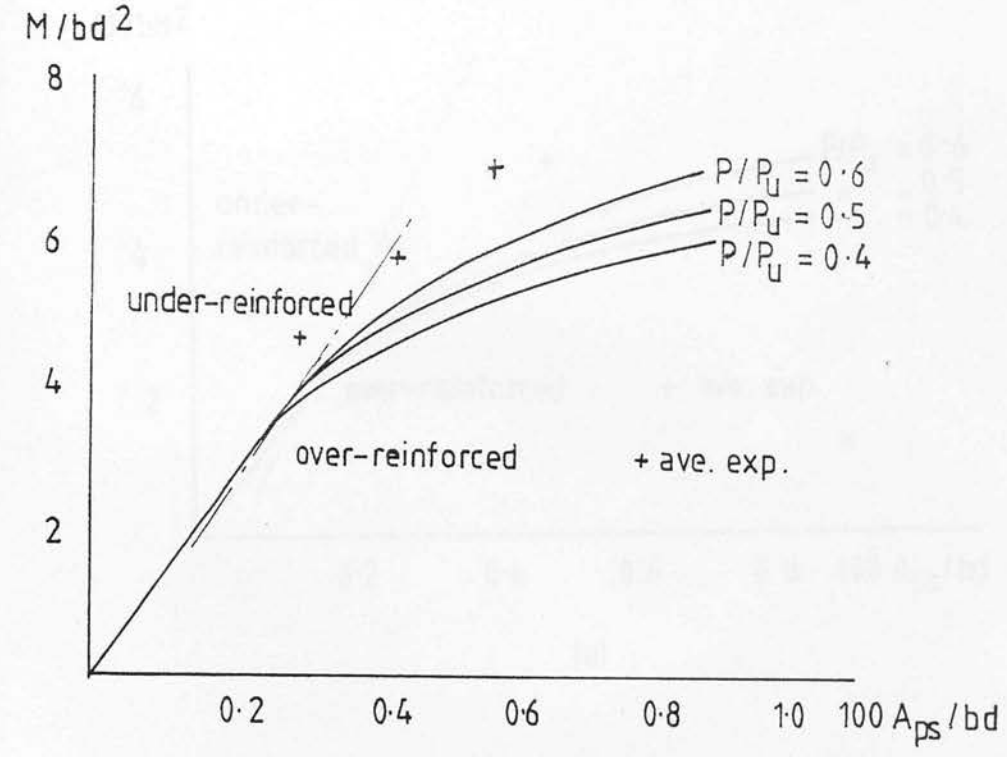

(a)

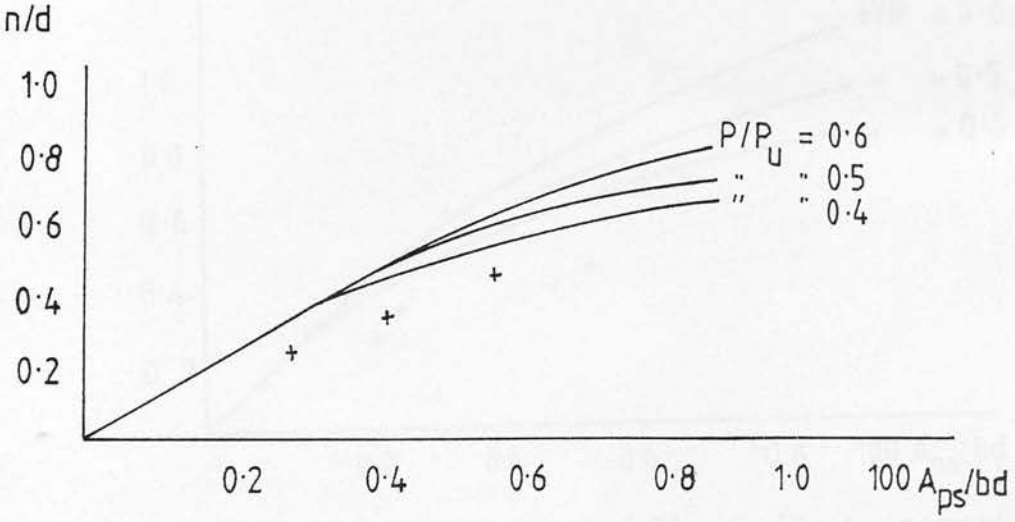

fig. 5.4.2 Effect of steel % on ultimate moment and neutral axis of high strength brick beams predicted with three course prisms.

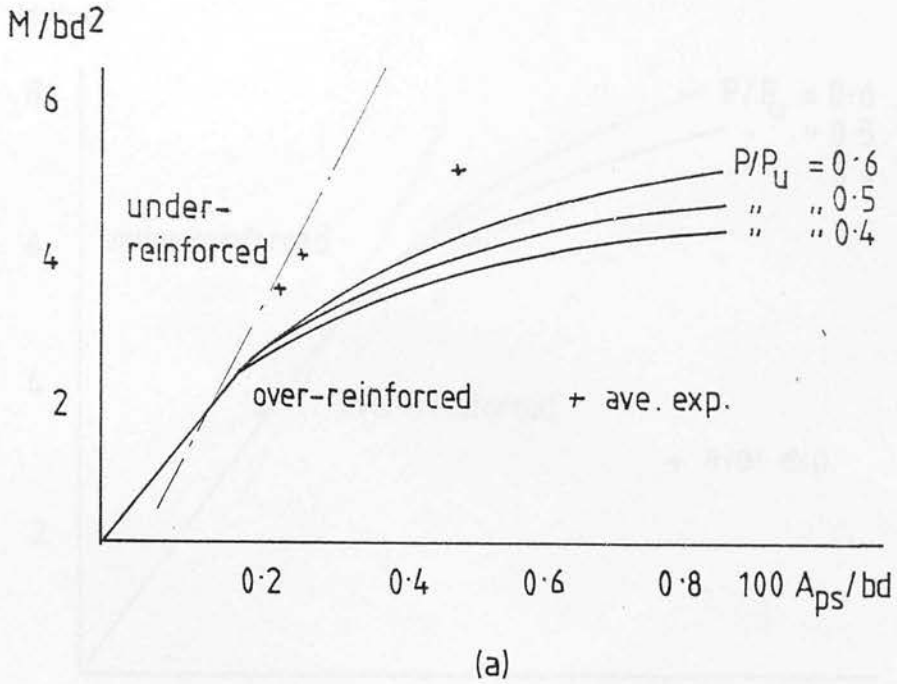

(a)

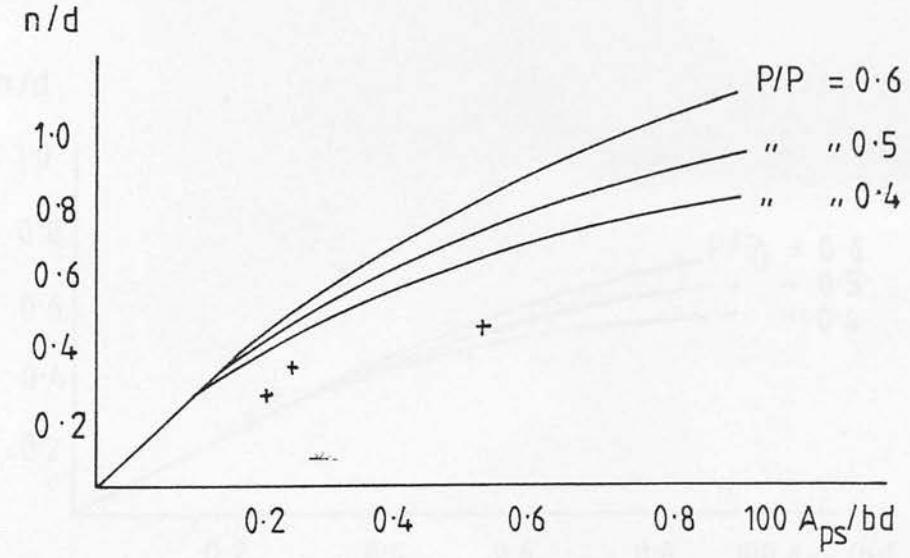

fig.5.4.3 Effect of steel % on ultimate moment and neutral axis of medium strength brick beams predicted with three course prisms.

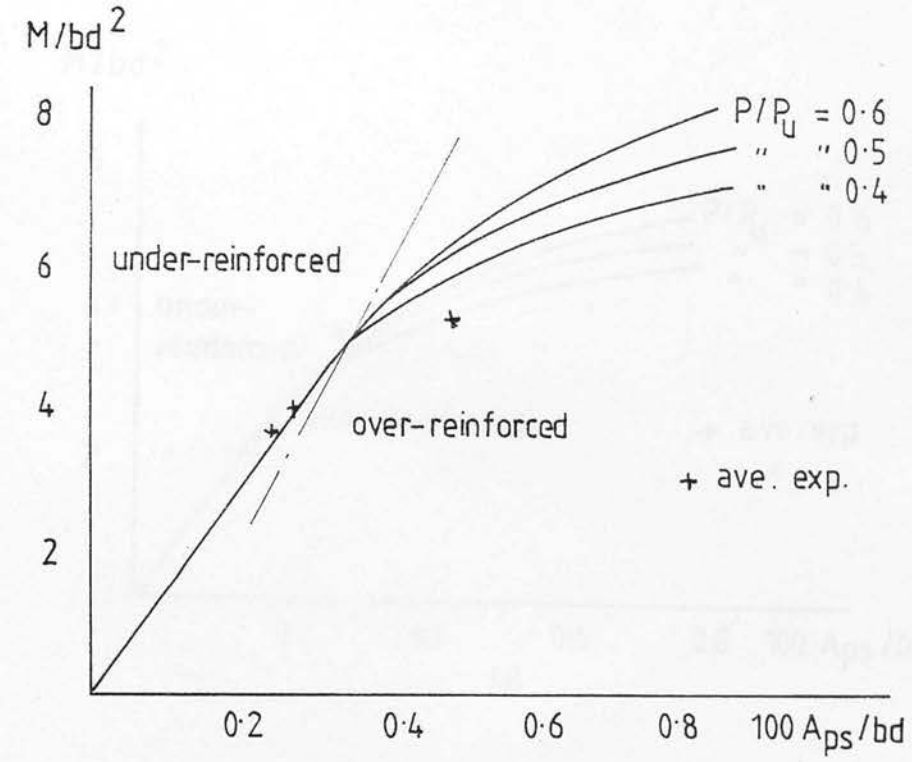

(a)

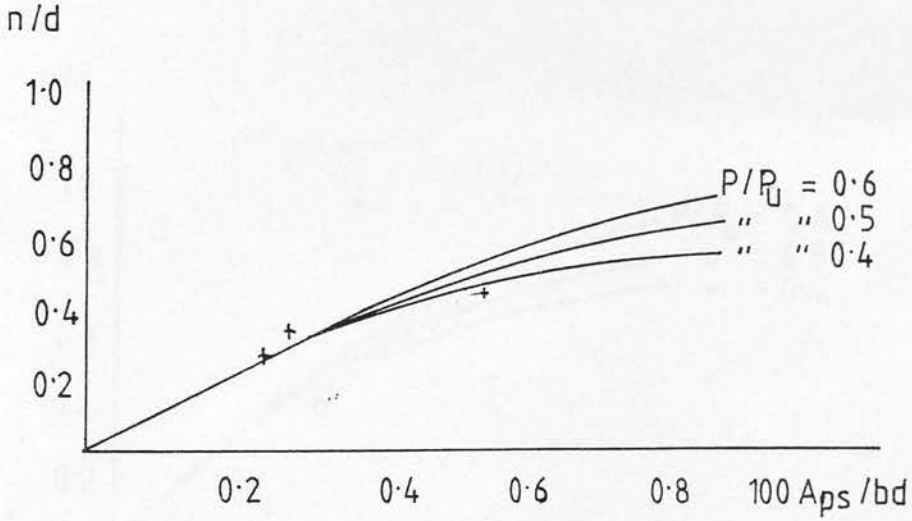

(b)

fig.5.4.4 Effect of steel % on ultimate moment and neutral axis of medium strength brick beams predicted with single course prisms.

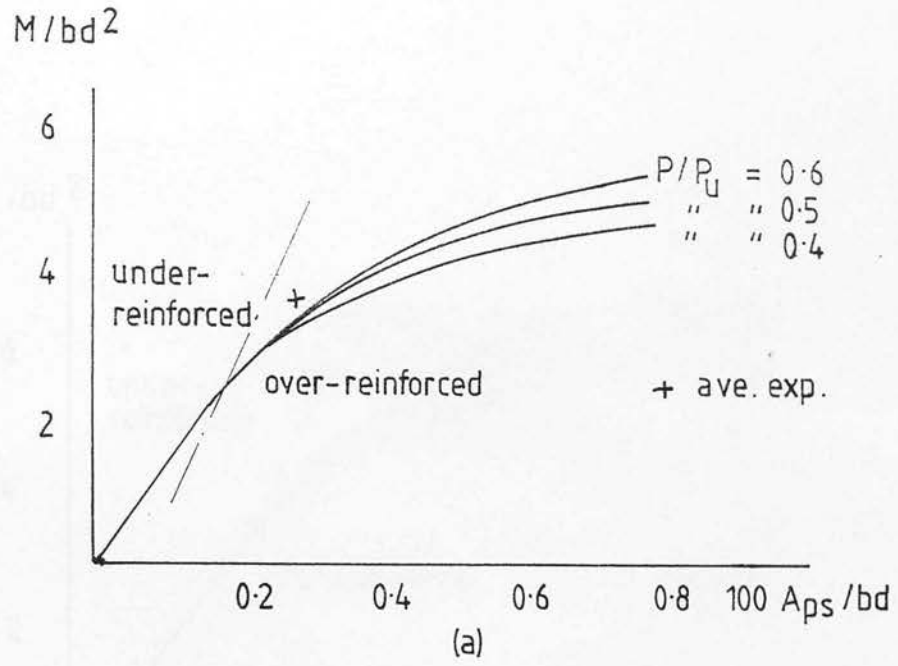

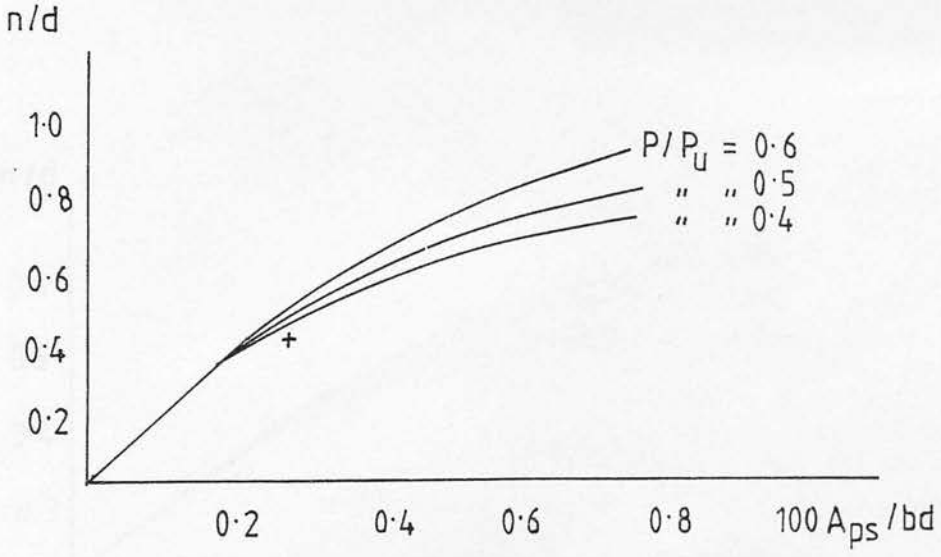

fig. 5.4.5 Effect of steel % on ultimate moment and neutral axis of medium strength brick beams in grade II mortar predicted with three course prisms.

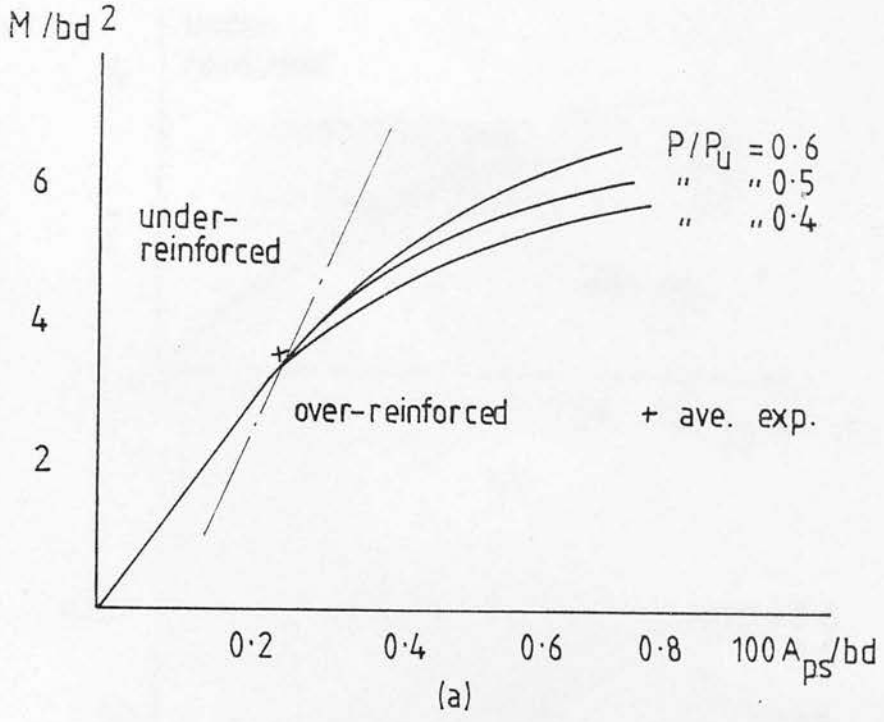

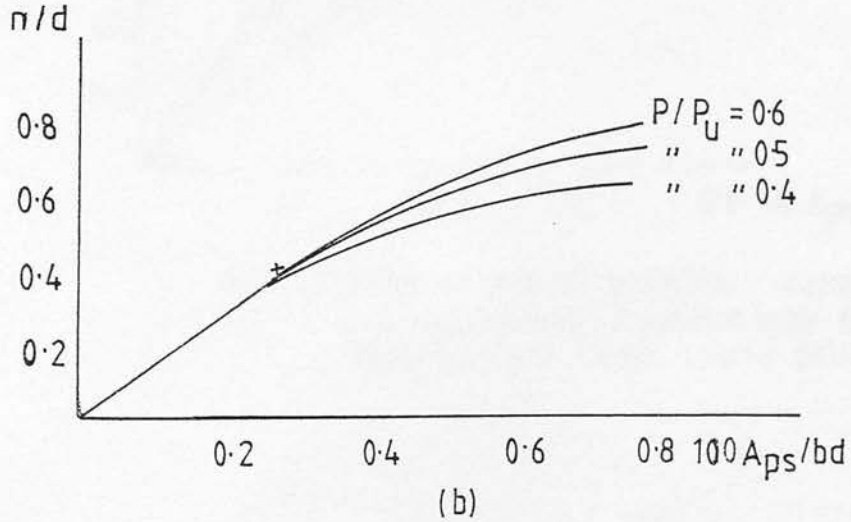

fig. 5.4.6 Effect of steel % on ultimate moment and neutral axis of medium strength brick beams in grade II mortar predicted with single course prisms.

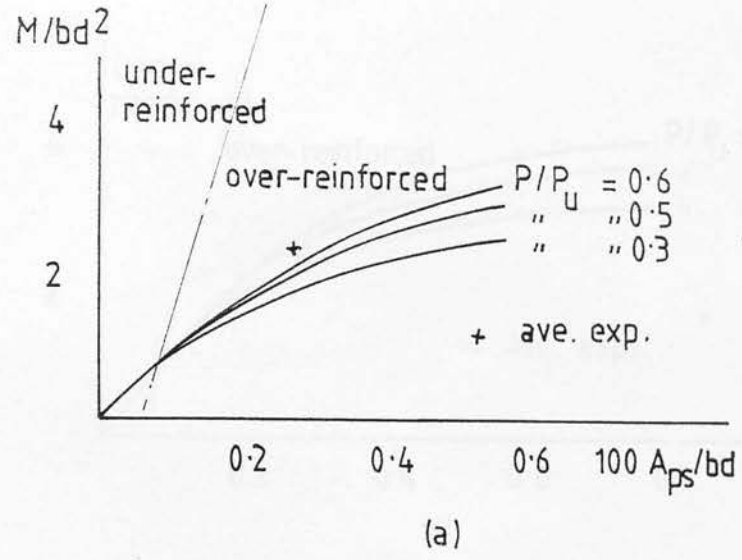

(a)

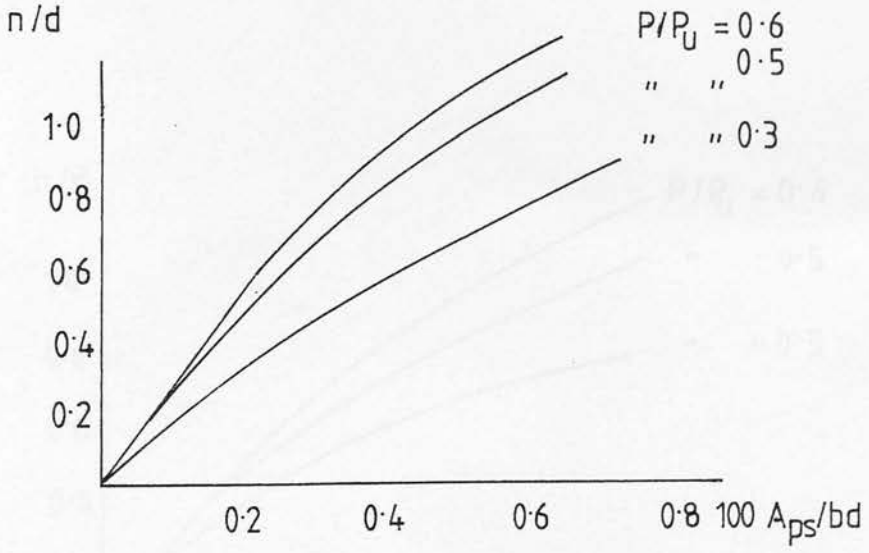

fig. 5.4.7 Effect of steel % on ultimate moment and neutral axis of common brick beams predicted with single course prisms.

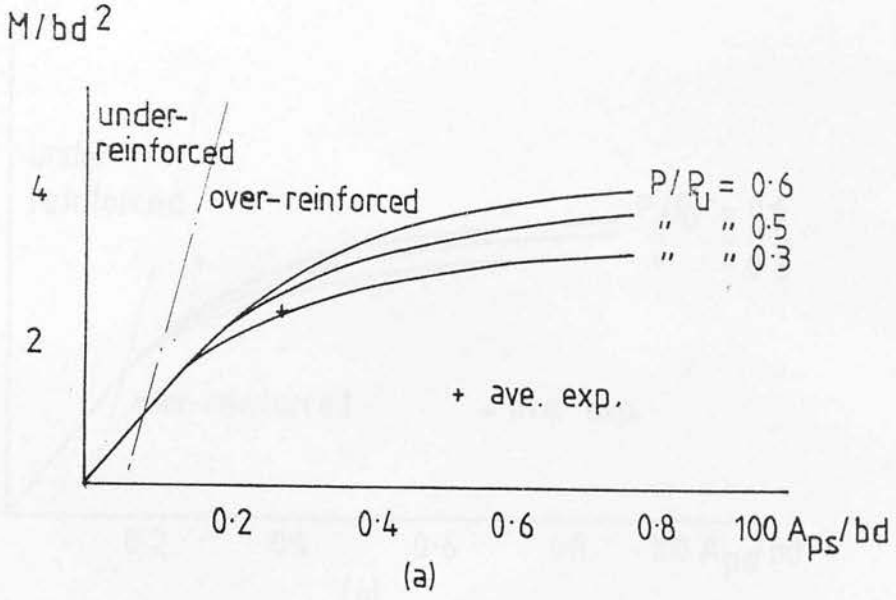

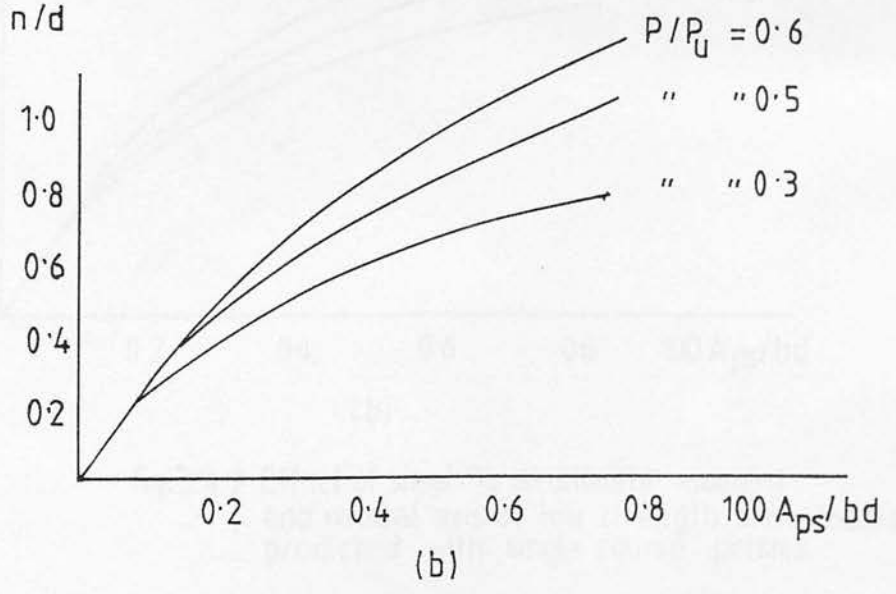

fig. 5.4.8 Effect of steel % on ultimate moment and neutral axis of common brick beams predicted with single course prisms.

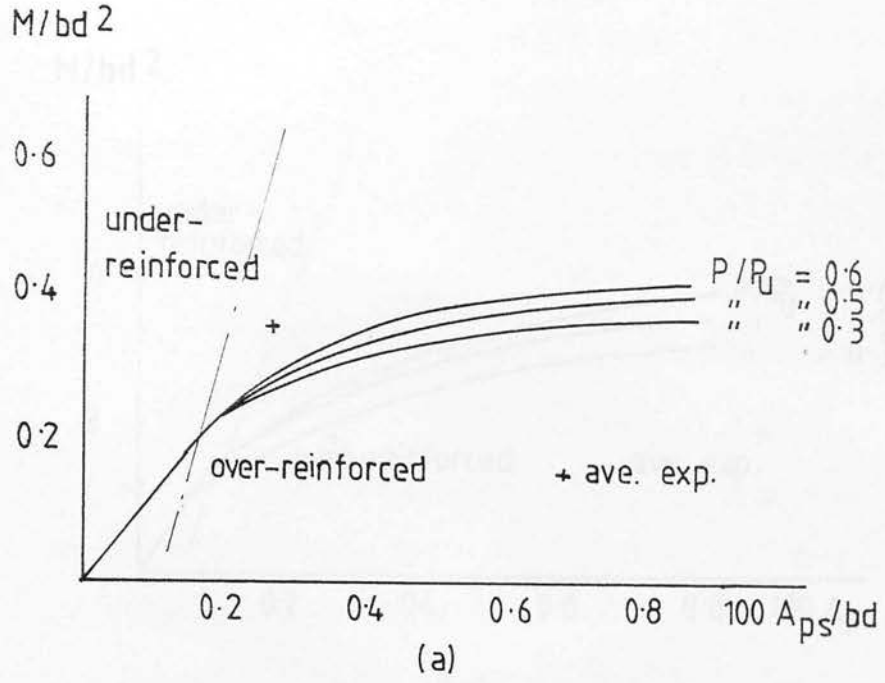

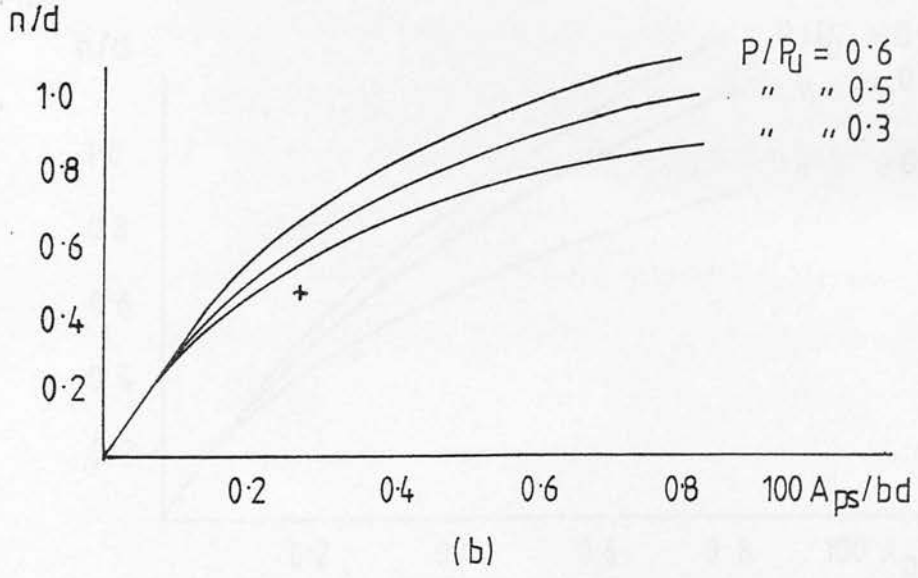

fig. 5.4.9 Effect of steel % on ultimate moment and neutral axis of low strength brick beams predicted with single course prisms.

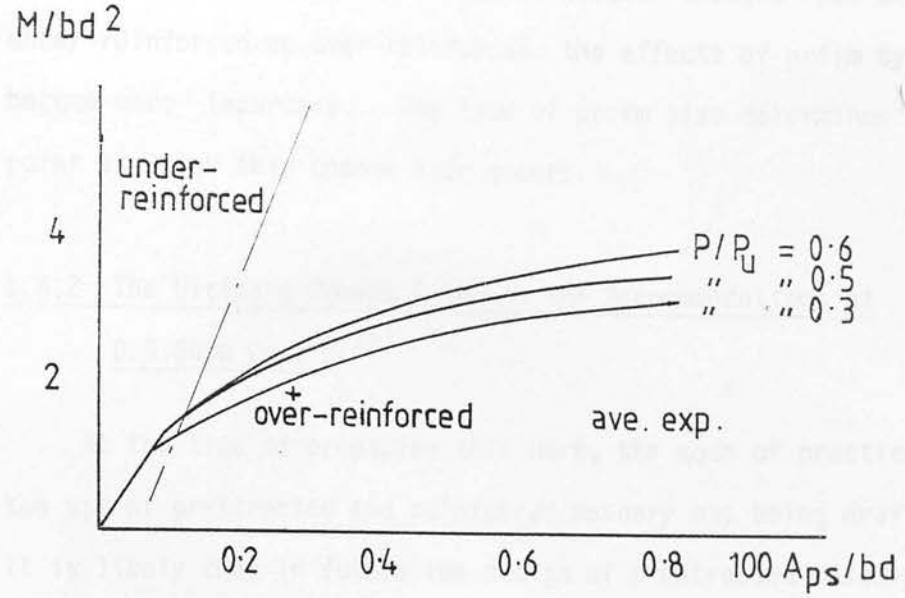

(a)

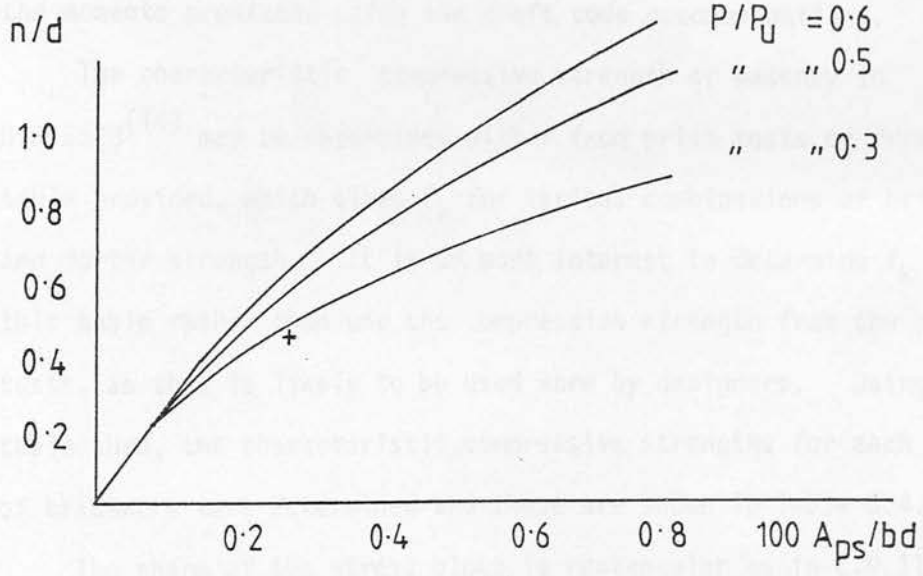

(b)

fig.5.4.10 Effect of steel % on ultimate moment and neutral axis of low strength brick beams predicted with three course prisms.

As the steel area increases the section changes from being under-reinforced to over-reinforced, the effects of prism type become more important. The type of prism also determines the point at which this change over occurs.

5.4.2 The Ultimate Moment Based on the Recommendations of B.S.5628 Part 2[14]

At the time of preparing this work, the code of practice for the use of prestressed and reinforced masonry was being drafted. It is likely that in future the design of prestressed masonry in this country will follow its recommendations. The experimental results of those beams that failed in flexure were compared with the moments predicted using the draft code recommendations.

The characteristic compressive strength of masonry in B.S.5628[14] may be determined either from prism tests or from a table provided, which gives f_k for various combinations of brick and mortar strength. It is of more interest to determine f_k from this table rather than use the compressive strength from the prism tests, as this is likely to be used more by designers. Using this table then, the characteristic compressive strengths for each type of brickwork were determined and these are shown in Table 5.4.2.

The shape of the stress block is rectangular as in C.P.110[39], i.e. $\lambda_1 = 1.0$ and $\lambda_2 = 0.5$. From Table 5.4.2, f_m from the single course prisms is greater than f_k for high and medium strength brick. The ultimate compressive strain in the brickwork is taken as 0.0035.

With the exception of the common brick, f_k is greater than f_m for the three course prisms. The stress/strain relationship for

Table 5.4.2 Compressive Strength of Brickwork Based on Recommendations of B.S.5628 Part 2

Brick/Mortar	High/Grade I	Medium/Grade I	Medium/Grade II	Low/Grade I	Common/Grade I
f_k N/mm^2	21.7	18.6	14.7	11.2	8.1
$\lambda_1 f_k$	21.7	18.6	14.7	11.2	8.1
f_k/f_m (single)	0.65	0.78	0.87	1.19	1.16
$\lambda_1 f_m$ (single)	21.23	15.9	11.7	6.6	4.2
f_k/f_m (three)	1.06	1.50	1.09	1.19	0.74
$\lambda_1 f_m$ (three)	12.5	8.05	9.2	5.3	5.9

the steel was also taken from B.S.5628. The partial safety factor for the materials, normally 2.0 for f_k and 1.15 for the steel were taken as unity. The stress/strain relationship for the steel is compared with the experimental stress/strain relationship in Figure 5.4.11, the two relationships are very similar.

Comparing the ultimate moments with the experimental results, Table 5.4.1, the predicted moments are slightly less than the experimental results, for the high strength brick. On average the experimental results were 8% greater. A closer prediction is obtained from the single course prisms. Referring to Table 5.4.2, f_k for the high strength brick is much closer to f_m from the three course prisms than the single course prisms although the predicted moments using f_k are much closer to those predicted using the single course prisms. This is caused by the greater area of the rectangular stress block, so that even though f_k is only 66% of f_m from the single course prisms the product of the stress block factor λ_1 and the compressive strength are very similar, as shown in Table 5.4.2. The slight reduction in moments predicted using B.S.5628 may be attributed to the reduction in lever arm, with $\lambda_2 = 0.5$.

The recommendations of B.S.5628[14] predict moments for the medium strength brick in grade I mortar, that are, on average with 8% of the experimental results and also agree very closely with the moments predicted from the single course prisms. From Table 5.4.2, $\lambda_1 f_k$ is slightly greater than $\lambda_1 f_m$ from the single course prisms and more than twice that for the three course prisms.

For medium strength brick in grade II mortar the B.S.5628 approach predicts higher moments than the experimental results which

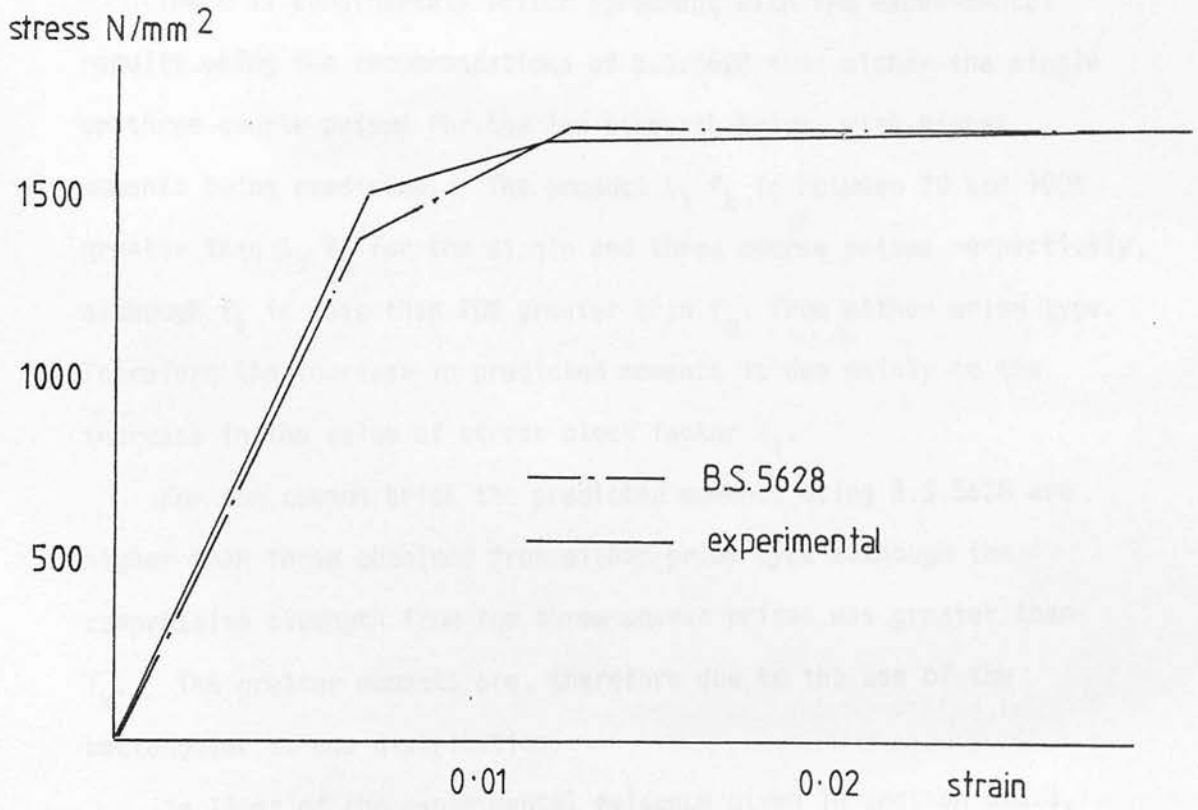

fig. 5.4.11 Comparison between stress/strain relationships for steel.

are also greater than the single course prism moments. Again it can be seen from Table 5.4.2 that $\lambda_1 f_k$ is greater than $\lambda_1 f_m$ for either prism type.

There is considerably better agreement with the experimental results using the recommendations of B.S.5628 than either the single or three course prisms for the low strength brick, with higher moments being predicted. The product $\lambda_1 f_k$ is between 70 and 100% greater than $\lambda_1 f_m$ for the single and three course prisms respectively, although f_k is less than 20% greater than f_m, from either prism type. Therefore the increase in predicted moments is due mainly to the increase in the value of stress block factor λ_1.

For the common brick the predicted moments using B.S.5628 are higher than those obtained from either prism type although the compressive strength from the three course prisms was greater than f_k. The greater moments are, therefore due to the use of the rectangular stress distribution.

In light of the experimental evidence given in section 5.3.3, the assumption that the ultimate strain in the brickwork is 0.0035 appears reasonable, particularly for the high and medium strength brick.

Generally, the range of compressive strengths obtained from B.S.5628 is narrower than that obtained experimentally and the compressive strengths for brickwork are lower than the compressive strengths of the single course prisms for the high and medium strength brick. However, due to the greater area of stress block the average compressive stress at failure is increased, which tends to cancel out the lower brickwork strengths and hence the predicted ultimate

moments are very similar to those obtained from single course prisms. For the lower strength bricks (low and common), because the beams were over-reinforced, the compressive strength and stress distribution have a more significant influence and hence the consequence of adopting a rectangular stress block is to increase the average compressive stress and hence the ultimate moment.

5.5 Summary and Conclusions

A total of 51 prestressed brickwork beams, covering a range of variables, of this number 32 failed in flexure. The experimental results show:

(i) For beams with low areas of steel failure is generally in flexure, for all strengths of bricks.

(ii) Large increases in brick strength result in only a minor increase in the ultimate strength, where the beam is under-reinforced. When a section is over-reinforced the brick strength has a more significant influence.

(iii) Increases in steel area and prestress force increase the ultimate moment of a section although the mode of failure may change.

(iv) A change in mortar from grade I to grade II does not greatly influence the ultimate strength of prestressed brickwork beams.

(v) The flexural strength of prestressed brickwork beams, built from high, medium and low strength brick can be accurately predicted using the stress block characteristics obtained from axial compression tests on single course prisms rather than the three course prisms. Also the ultimate strains and neutral axis depths at failure of the prestressed brickwork beams are more closely represented using the characteristics of the single course prisms.

(vi) The recommendations of B.S.5628 generally provide a close estimate of the ultimate strength of the beams, although not quite as accurate as the moments based on the single course prisms for the medium and high strength brick. For the low strength brick the ultimate strength is more closely predicted with the recommendations of B.S.5628 than either the single or three course prisms.

CHAPTER 6 : LOAD/DEFLECTION RESPONSE AND CRACKING OF POST-TENSIONED BRICKWORK BEAMS

6.1 Introduction

In the use of prestressed concrete beams it is quite normal to allow the prestress force to be completely neutralised under working loads. In some cases cracking may also be permitted. These types of beams are generally referred to as being partially prestressed. If cracking is not allowed then the calculation of deflections, under working loads may be based entirely on the standard 'strength of materials' approach, using either a tangent or secant modulus of elasticity. When cracking occurs the section properties, at the crack, will change and the stresses in the brickwork will increase more rapidly. This combined with the nonlinear behaviour of brickwork makes the calculation of deflections considerably more complicated. It is also of interest to study the behaviour of beams in overload conditions, as the beam approaches failure to determine whether adequate warning of impending failure would be given.

In partially prestressed beams where cracking is allowed under working loads, cracks must be kept below a prescribed limit[39], in order to prevent excessive local damage and maintain reasonably effective cover to the reinforcement, requiring a method of predicting the crack widths.

In this chapter a method of predicting the deflections of bonded prestressed brickwork beams is described. The method is based on calculating the moment-curvature relationship up to

failure, using the actual stress/strain relationships of both the steel and brickwork. Cracking and tension stiffening of the brickwork between cracks is considered. The effects of brick strength mortar grade, steel area and prestress force on the M - ϕ relationship and load/deflection response were obtained experimentally. The results thus obtained are compared with theory, using the stress/strain relationships for brickwork obtained from both single and three course prisms. A theoretical expression for the prediction of crack widths in terms of crack spacing and average strain at the level of the crack was obtained and compared with the experimental results.

6.2 Methods of Predicting the Deflection of Reinforced and Prestressed Concrete Beams

There have been three main methods developed for the calculation of deflections of reinforced and prestressed concrete beams and each is dealt with briefly in sections 6.2.1-3.

6.2.1 Based on Moment of Inertia

In an elastic beam the curvature[51] may be determined from:

$$\phi = M/EI \qquad (6.2.1)$$

If the bending moment diagram for the beam is known then the distribution of curvature along the beam is easily obtained. The deflection can then be found by considering the differential

equation for beam bending

$$M/EI = - d^2y/dx^2 \qquad (6.2.2)$$

resulting in the 'strenth of materials' deflection formulae.

However when cracking occurs in a reinforced or prestressed concrete beam the stiffness at a cracked section is reduced, Figure 6.2.1, causing greater curvatures and hence deflections.

This has led a number of researchers[52,53] to develop methods of calculating the deflections by taking the properties of the cracked section into account in calculating the moment of inertia, I. A value of elastic modulus is often taken which reflects the level of stress in the beam. This approach then has the simplicity of enabling the deflections to be calculated from standard methods assuming elastic, uncracked behaviour.

The more popular formulations for concrete have been reviewed by Branson[52] and Beeby[53].

Essentially the moment-curvature relationship takes an idealised bi-linear form (figure 6.2.2). Each part of the relationship is based on cracked and uncracked moment of inertias.

Up to the cracking moment the moment of inertia based on the uncracked section is normally calculated by one of the two different methods. The first of these considers only the dimensions of cross-section, ignoring the presence of the reinforcement, the second method considers the reinforcement as a transformed area of concrete (area of reinforcement multiplied by modular ratio). After cracking, the moment of inertia is calculated using the area of

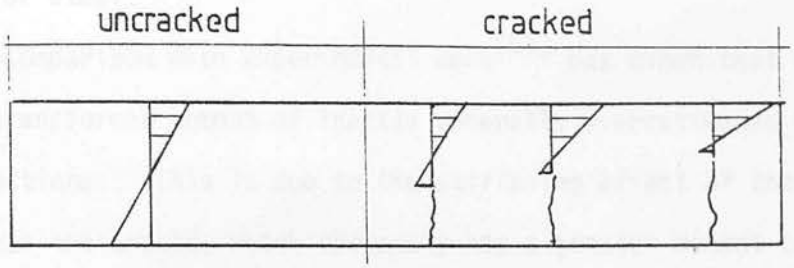

fig. 6.2.1 Conditions in a cracked beam.

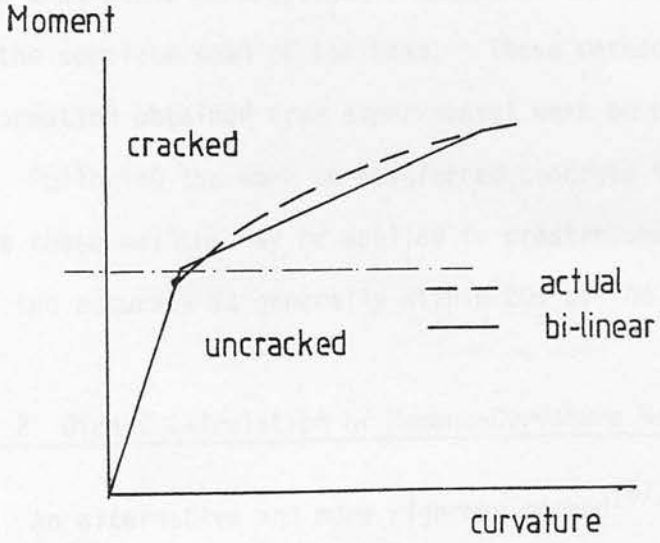

fig. 6.2.2 Bi-linear Moment-curvature relationship.

concrete in compression above the neutral axis and the transformed area of steel.

Comparison with experimental work[53] has shown that using the transformed moment of inertia generally overestimates the deflections. This is due to the stiffening effect of the concrete between the cracks, which obviously has a greater moment of inertia, and also those sections of the beam's span that are lightly loaded and remain uncracked in flexure.

There are a number of ways in which these effects are allowed for. These include multiplying the deflections by a reduction factor or by using an effective moment of inertia which is greater than that based on the cracked moment of inertia and is applicable to the complete span of the beam. These methods generally require information obtained from experimental work on beams.

Following the work on reinforced concrete it has been shown that these methods may be applied to prestressed concrete[54,55,56] and the accuracy is generally within 20% of the actual deflections.

6.2.2 Direct Calculation of Moment-Curvature Relationship

An alternative and more rigorous method[57,58] to that described in section 6.2.1, in which an idealised, bi-linear moment-curvature relationship was considered, has been used for reinforced and prestressed concrete. This method employs the actual stress/strain relationships for the concrete and steel.

Up to the cracking moment the beams are normally considered as elastic and the M - ϕ relationship is obtained from equation

6.2.1. The cracking moment, M_{cr} may be determined from:

$$M_{cr} = (P \cdot (1/A + e/Z) + f_r) Z \qquad (6.2.3)$$

where Z is the section modulus and e is the eccentricity of the prestressing force, P, and f_r is the modulus of rupture. By applying increments of strain to the beam section and assuming cracked conditions the strain distribution necessary to ensure equilibrium of the internal forces can be found. The moments and curvatures up to failure are then easily obtained. For a particular loading the distribution of curvature along the beam is obtained from the computed moment curvature relationship. The deflection at any point may then be obtained by double integration of the curvature along the span.

This method[57,58,59] has previously been used to study the effects of prestress force, % of steel etc., on the behaviour of prestressed concrete beams. Although the determination of the M - ϕ relationship may be considered as one step in the calculation of deflections, consideration of the M - ϕ relationship itself is often of more use as it yields valuable information on the ductility of the sections. Warwaruk et al[58] and later Burns[57] used M - ϕ relationships to study the influence of % steel area on prestressed concrete sections. For low % of steel there are three phases to the M - ϕ relationship, Figure 6.2.3, 0-1 the beam is elastic and uncracked, 1-2 the beam is cracked but the stress in the reinforcement is less than the yield stress, 2-3 the yield point of the steel has been exceeded and the curvature increases with very little increase

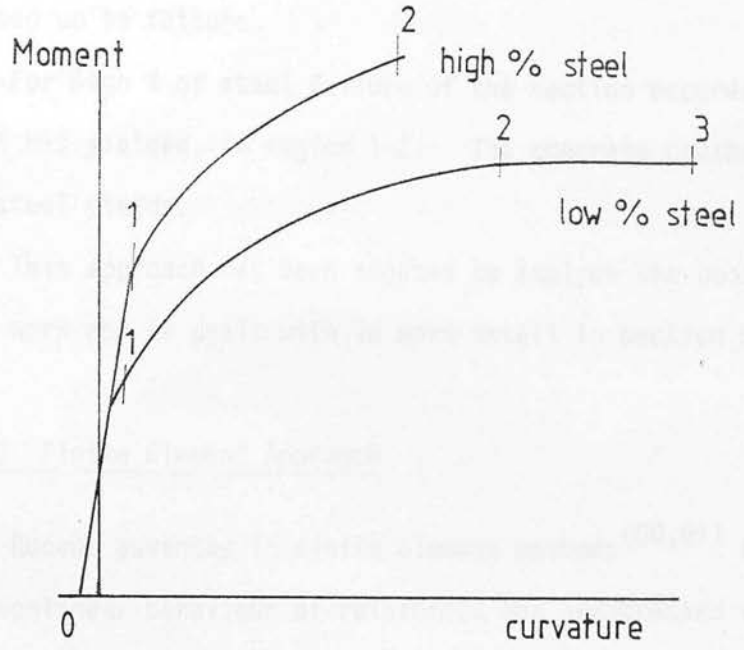

fig. 6.2.3 Effect of % of steel on the M-ϕ relationship of prestressed concrete beams.

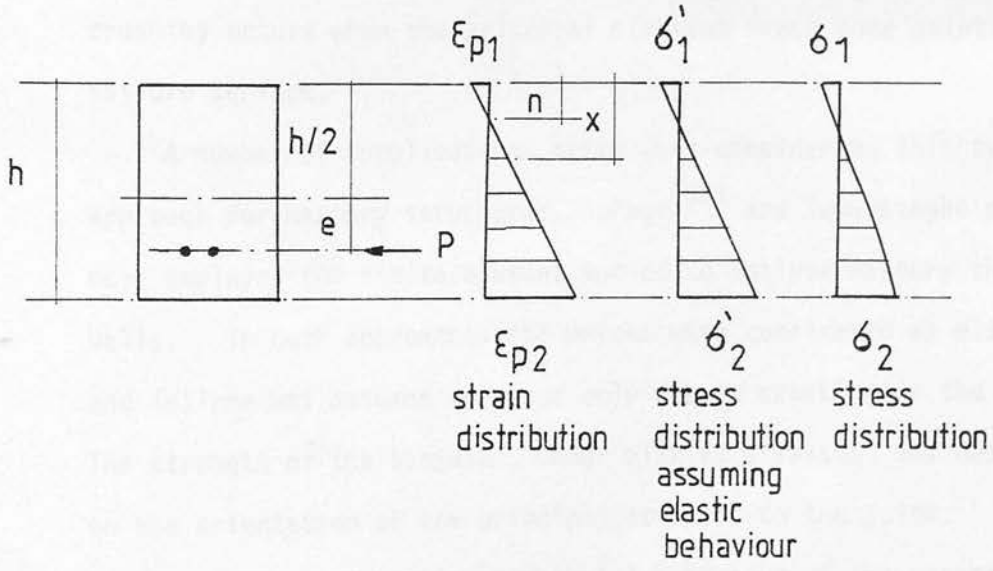

fig. 6.3.1 Stress conditions in beam due to prestress.

in load up to failure.

For high % of steel failure of the section occures before the steel has yielded, in region 1-2. The concrete crushes before the steel yields.

This approach has been adopted to analyse the beams in this work and is dealt with in more detail in section 6.3.

6.2.3 Finite Element Approach

Recent advances in finite element methods[60,61] have enabled the nonlinear behaviour of reinforced and prestressed concrete beams to be studied by such techniques. The effects of cracking, non-linear material behaviour, bond-slip and dowel action on the load-deflection response have been considered. Normally, the beams are considered as being in a state of plane stress and so the failure surface under biaxial stresses is required. Cracking or crushing occurs when the principal stresses reach some point on the failure surface.

A number of complications arise when considering this type of approach for masonry structures. Page[62] and Samarsinghe et al[63] have employed the finite element method to analyse masonry shear walls. In both approaches the bricks were considered as elastic and failure was assumed to occur only due to cracking in the bedjoints. The strength of the bedjoint, under biaxial stresses, was dependent on the orientation of the principal stresses to the joint. Crushing of the masonry and nonlinear material behaviour of the masonry was not considered and cracking, although it is normally initiated at a mortar joint, may also occur through bricks. Hence to define a

failure surface which would accurately model the behaviour of brickwork beams would, necessarily, have to be very complicated and could only be obtained from a very comprehensive and detailed experimental investigation.

6.3 Theoretical Determination of Moment-Curvature Relationship of Prestressed Brickwork Beams

The M - ϕ relationship of prestressed brickwork beams was calculated from the direct method, somewhat similar to that described in section 6.2.2. The methods described in section 6.2.2 assumed linear elastic behaviour up to cracking, which is not strictly valid for the stress/strain relationship of brickwork obtained in Chapter 3. Hence in this proposed method the actual stress/strain relationship is used to calculate the deformation from prestressing up to ultimate. The method of finite differences is used to calculate the deflections from the M - ϕ relationship.

It is assumed that the strain distribution through the section is linear at any level of applied load and that full bond exists between steel, grout and brickwork. It is further assumed that the modulus of elasticity of brickwork in tension is linear and is equal to the initial tangent modulus of brickwork in compression. The stress/strain relationship of steel can be represented by a tri-linear model, Figure 3.5.2, and the stress/strain relationship of brickwork in compression can be represented by a polynomial as given in section 3.4.5. The strength of brickwork can be determined by uni-axial tests.

The applied loading of the beam is considered in three stages:

(i) prestressing,

(ii) from prestressing up to cracking,

(iii) postcracking up to ultimate load,

each of which is dealt with in the next three sections.

6.3.1 Prestressing

Figure 6.3.1 shows the distribution of stress and strain in a rectangular prestressed brickwork due to prestressing. Initially the beam is considered as elastic and so the stresses in the outermost fibres due to prestress are obtained from:

$$\sigma_1' \; \sigma_2' = P/A \pm P \cdot e/Z \qquad (6.3.1)$$

By assuming an initial value of elastic modulus E' the corresponding strains in the outermost fibres, ε_{p1} and ε_{p2} may be found. Using these strains the total compressive force in the section is calculated

$$C = \int_{n}^{h} b \cdot F_m(\varepsilon) \, d(x) \qquad (6.3.2)$$

where $\varepsilon = \varepsilon_{p1} + (\varepsilon_{p2} - \varepsilon_{p1}) \frac{x}{h}$.

The grout surrounding the steel in the duct is assumed to have the same properties as the brickwork. $F_m(\varepsilon)$ is the stress/strain relationship of brickwork. The ratio of ε_{p1} to ε_{p2} may be expressed as:

$$r_t = \varepsilon_{p1}/\varepsilon_{p2} \qquad (6.3.3)$$

For equilibrium the compressive forces in the section must equal the applied prestress force, i.e.:

$$C = P \qquad (6.3.4)$$

if $C \neq p$ then the initial value of elastic modulus is modified:

$$E = E' \, (C/P) \qquad (6.3.5)$$

The strain ratio, r_t is always kept constant but the magnitude of ε_{p1} and ε_{p2} are changed according to the revised value of E. Equations 6.3.2, 6.3.4 and 6.3.5 are applied until 6.3.4 is satisfied. This assumed to occur if:

$$0.98 < C/P < 1.02 \qquad (6.3.6)$$

The curvature due to prestressing is then:

$$\phi_p = \frac{\varepsilon_{p1} - \varepsilon_{p2}}{h} \qquad (6.3.7)$$

6.3.2 M - ϕ Relationship up to Cracking Moment

Figure 6.3.2 shows the distribution of stresses and strain prior to cracking. Cracking will occur once the decompression of prestress has taken place and the flexural tensile strength of the brickwork, at the extreme fibre is exceeded.

The strain distribution may be considered as the sum of the strains due to prestress and applied load, Figure 6.3.3. The

additional strain necessary to decompress the strain in the bottom fibre must be equal and opposite to that initially applied. At this stage in the loading there is zero strain at soffit level. Further increases in load will result in tensile stresses developing. The magnitude of the strain that may be sustained before cracking is then soley governed by the flexural tensile strength of the brickwork, most often referred to as the modulus of rupture, f_r. The ultimate strain in tension ε_r may be defined as:

$$\varepsilon_r = f_r/E' \qquad (6.3.8)$$

Hence the total strain required to cause cracking in the extreme fibre, from prestressing is:

$$\varepsilon_{cr} = \varepsilon_{p2} + \varepsilon_r \qquad (6.3.9)$$

The total compressive force in the section is:

$$C = b \int_0^n F_m(\varepsilon)\, dx \qquad (6.3.10)$$

where $\varepsilon = \varepsilon_1 - (\varepsilon_1 \cdot x/n)$ and $n = \left(\frac{\varepsilon_1}{\varepsilon_1 + \varepsilon_2}\right) h$. The total strain in the steel consists of the initial strains due to prestress, ε_{ps} and the applied steel stress, ε_{sa} caused by the applied loading, Figure 6.3.3:

$$\varepsilon_{sa} = \varepsilon_{a2} \left(\frac{d - n_r}{h - n_r}\right) \qquad (6.3.11)$$

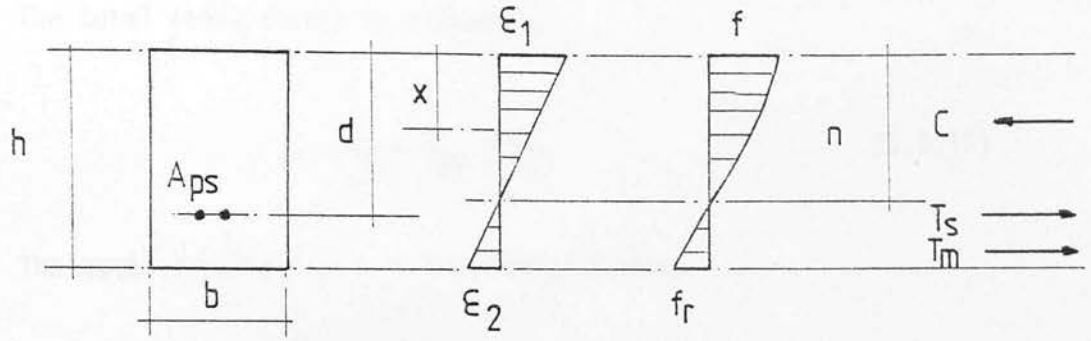

fig. 6.3.2 Conditions immediately prior to cracking.

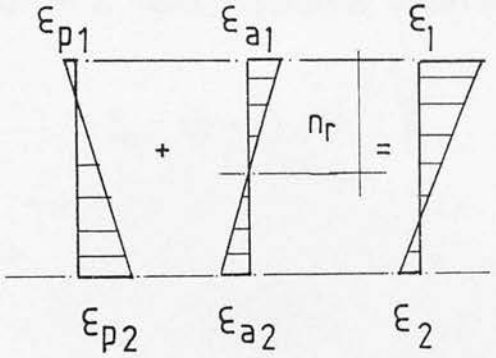

fig. 6.3.3 Strains in prestressing strand.

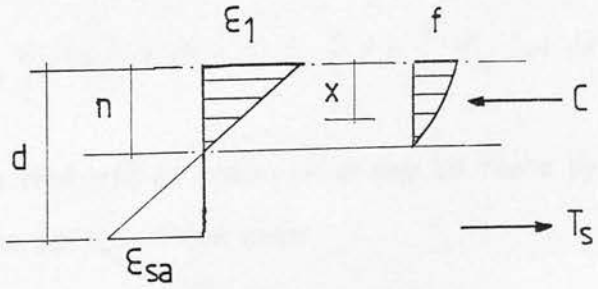

fig. 6.3.4 Conditions at a cracked section.

The total steel strain is therefore:

$$\varepsilon_s = \varepsilon_{ps} + \varepsilon_{sa} \qquad (6.3.12)$$

The total tensile force in the steel is then:

$$T_s = A_{ps} \cdot F_s\ (\varepsilon_s) \qquad (6.3.13)$$

The tensile force in the brickwork is, with the same assumptions for the distribution of tensile stresses as before:

$$T_m = (h - n) \cdot f_r \cdot \frac{b}{2} \qquad (6.3.14)$$

for equilibrium:

$$C = T_s + T_m \qquad (6.3.15)$$

i.e.:

$$A_{ps}\ F_s\ (\varepsilon_s) + (h - n)\ f_r\ \frac{b}{2} = b \int_o^n F_m\ (\varepsilon)\ dx \qquad (6.3.16)$$

The centroid of compression may be found by taking moments about the soffit of the beam:

$$l_a = \frac{(b \int_o^n F_m\ (\varepsilon)\ (h - x)\ dx)}{C} \qquad (6.3.17)$$

The cracking moment is calculated also by taking moments about the soffit of the beam:

$$M_{cr} = C \cdot I_a - T_s (h - d) - T_m (h - n)/3 \qquad (6.3.18)$$

The curvature immediately prior to cracking is:

$$\phi = (\varepsilon_1 - \varepsilon_2)/h \qquad (6.3.19)$$

In concrete beams, linear elastic behaviour is often assumed up to cracking and the curvatures obtained from a gross moment of inertia. In which case the position of the neutral axis depth of applied strains, n_r, neglecting the strains due to prestressing, Figure 6.3.3, is h/2, or the uncracked transformed section is used in which n_r is greater than h/2 and is constant at the centroid of the section. However in using a stress/strain relationship for the brickwork that exhibits a continually falling modulus then the position of n_r will change with the applied loading.

This is taken account of by applying the strain in the bottom fibre in increments up to ε_{cr}. For the first increment n_r is obtained by considering the uncracked, transformed section. The modular ratio of brickwork and steel is defined as:

$$m_r = E_s/E' \qquad (6.3.20)$$

ignoring the reduction in cross-section due to area of steel, n_r is then:

$$n_r = (bh^2/2 + A_{ps}\, m_r\, d) \,/\, (bh + m_r\, A_{ps}) \qquad (6.3.21)$$

ε_{a1}, the applied strain in the top fibre is:

$$\varepsilon_{a1} = \left(\frac{n_r}{h - n_r} \right) \varepsilon_{a2} \qquad (6.3.22)$$

The internal forces in the section are obtained from the Equations 6.3.10, 6.3.13 and 6.3.14. If 6.3.15 is not satisfied then n_r is modified and ε_{a1} obtained from 6.3.22. The process is repeated until equilibrium is attained. The moments and curvatures are then found from equations 6.3.18 and 6.3.19, replacing M_{cr} with M.

6.3.3 M - ϕ Relationship After Cracking at a Crack

Once cracking has occurred the crack is assumed to extend up to the neutral axis depth, Figure 6.3.4. Due to the tensile strength of the masonry the depth of the crack penetration will actually be slightly lower. However, the influence of this on the moment is minimal and ignored in this analysis.

At the cracking moment there are two possible states, uncracked and cracked. The uncracked state is defined in section 6.3.2. As the tensile strength of the brickwork has been exceeded then there is an increase in steel stress and strain accompanied with a decrease in neutral axis depth resulting in an increase in compressive strain and stresses in brickwork. Equation 6.3.16 becomes:

$$A_{ps} F_s (\varepsilon) = b \int_0^n F_m (\varepsilon) \, dx \qquad (6.3.23)$$

where $\varepsilon = \varepsilon_1 - (\varepsilon_1 \cdot x/n)$ and 6.3.18 becomes:

$$M_{cr} = C \cdot l_a - T_s (h - d) \qquad (6.3.24)$$

The strains ε_{sa} and ε_1, Figure 6.3.4, are not readily known and are obtained by simultaneous solution of 6.3.23 and 6.3.24.

The M - ϕ relationship from cracking up to ultimate load is obtained by applying compressive strains to the top fibre in increments, up to the ultimate compressive strain of brickwork ε_m. The additional strain in the steel is calculated from:

$$\varepsilon_{sa} = \varepsilon_1 \left(\frac{d - n}{n}\right) \qquad (6.3.25)$$

The total steel strains and tensile force are again obtained from the Equations 6.3.12 and 6.3.13 and the total compressive force from Equation 6.3.10. If $C \neq T$ the neutral axis depth, n, is modified. This is assumed to be satisfied when:

$$0.98 < C/T < 1.02 \qquad (6.3.26)$$

The moment is obtained from 6.3.24 replacing M_{cr} with M, the curvature is:

$$\phi_{cr} = (\varepsilon_1 + \varepsilon_{sa})/d \qquad (6.3.27)$$

6.3.4 Effect of Tension Stiffening

In a cracked beam the stress distribution away from a crack is different than at a crack, Figure 6.3.5, caused by the stiffening effect of the tension carried by the masonry between the cracks,

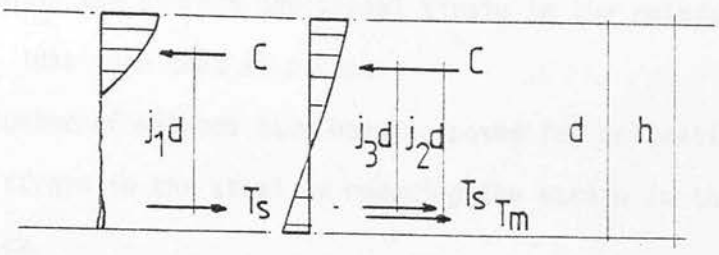

fig. 6.3.5 Forces in a cracked beam.

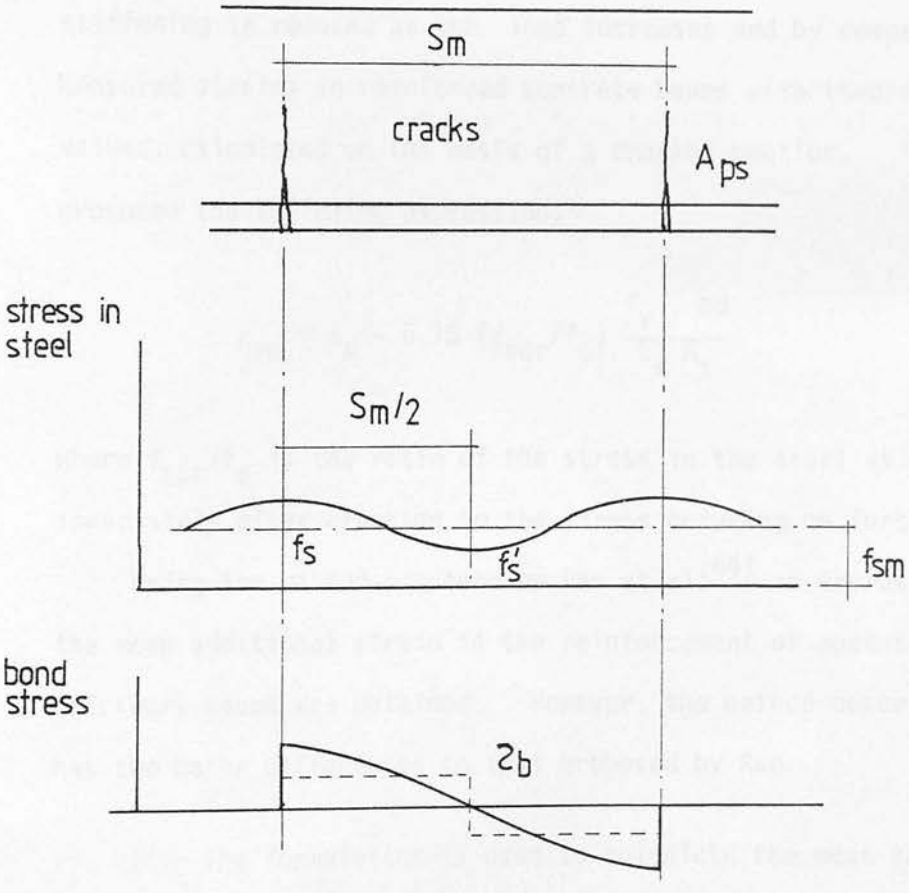

fig. 6.3.6 Stress distribution between cracks.

consequently the average additional strain in the reinforcement will be less than that at a crack.

A number of methods have been proposed for estimating the average strain in the steel by reducing the strain in the steel at a crack.

Beeby[53] proposed a constant reduction in steel strain such that:

$$\varepsilon_{sm} = \varepsilon_s - (4\ b\ .\ d/A_s) \times 10^{-6} \qquad (6.3.28)$$

Rao and Subrahmanyam[64] suggested that the effect of tension stiffening is reduced as the load increases and by comparing measured strains in reinforced concrete beams with theoretical values, calculated on the basis of a cracked section. They produced the following expression:

$$\varepsilon_{sm} = \varepsilon_s - 0.18\ (f_{scr}/f_s)\ \frac{f_r\ .\ bd}{E_s\ A_s} \qquad (6.3.29)$$

where f_{scr}/f_s is the ratio of the stress in the steel at a crack, immediately after cracking to the stress occuring on further loading.

Using the method proposed by Rao et al[64] an expression for the mean additional strain in the reinforcement of post-tensioned brickwork beams was obtained. However, the method described here has two major differences to that proposed by Rao.

(i) The formulation is used to calculate the mean <u>additional</u> strain in the reinforcement as opposed to the mean strain in the reinforcement.

(ii) Rather than calculating the additional strain at a crack, using theoretical considerations for the behaviour of the brickwork the additional strains are obtained from measurements on the beams.

The variation in steel stress between cracks is due to bond stresses between steel and grout. The variation of bond stresses between cracks is extremely difficult to determine. Referring to Figure 6.3.6 and considering a section midway between two cracks then:

$$a_o \, S_m/2 \, \tau_b = A_{ps} \, (f_s - f_s') \qquad (6.3.30)$$

where S_m is the distance between cracks, a_o the sum of the perimeters of the reinforcement and τ_b the average bond stress. The difference in steel strain at this point is:

$$\varepsilon_{sa} - \varepsilon_{sa}' = (f_s - f_s')/E_s \qquad (6.3.31)$$

The mean additional strain between the crack is then,

$$\varepsilon_{sam} = \varepsilon_{sa} - C_o \, (f_s - f_s')/E_s \qquad (6.3.32)$$

where C_o is a bond factor.

The internal resisting moment midway between cracks must equal the moment at a crack thus referring back to Figure 6.3.5:

$$A_{ps} \, f_s \, j_1 \, d = A_{ps} \, f_s' \, j_3 \, d + A_e \, f_{mt} \, j_2 \, d \qquad (6.3.33)$$

A_e is the area of brickwork in tension and may be expressed as C_1 b d, f_{mt} is the mean tensile stress in the brickwork and can be redefined as C_2 f_r. Also j_3 d $\simeq$ j_1 d. Rearranging Equation 6.3.33:

$$(f_s - f_s') = C_1 C_2 j_2/j_1 f_r b d/A_{ps} \qquad (6.3.34)$$

Substituting 6.3.34 in 6.3.32:

$$\varepsilon_{sam} = \varepsilon_{sa} - (C_o/E_s C_1 C_2 j_2/j_1 f_r b d/A_{ps}) \qquad (6.3.35)$$

if $k = C_0 C_1 C_2 j_2/j_1$ then:

$$\varepsilon_{sam} = \varepsilon_{sa} - k f_r/E_s b d/A_{ps} \qquad (6.3.36)$$

The values of C_0, C_1, C_2 and j_2/j_1 are not easily found but rearranging 6.3.36:

$$k = (\varepsilon_{sa} - \varepsilon_{sam}) E_s A_{ps}/(f_r b d) \qquad (6.3.37)$$

The additional strains were obtained from measurements, using electrical resistance gauges, on the strand, at random points in the constant moment zone. k was determined from Equation 6.3.37. The average value of k was obtained by averaging the results between limits of f_{scr}/f_s.

Figure 6.3.7 shows the relationship between k and f_{scr}/f_s. This appears to be approximately linear and the following expression for k in terms of f_{scr}/f_s was found:

$$k = 1.0 - 0.97\, f_{scr}/f_s \qquad (6.3.38)$$

From Figure 6.3.7 k increases as f_{scr}/f_s decreases, i.e. as the load after cracking increases the difference between the strain in the steel at a crack and the average steel strain increases. This is contrary to 6.3.29 as proposed by Rao et al[64].

Once a stable crack pattern has formed provided that there is no significant loss of bond, then as the load increases the additional strain in the reinforcement at a crack and between cracks will increase at different rates, this is illustrated in Figure 6.3.8, hence the difference between the two strains, $\varepsilon_{sa} - \varepsilon_{sam}$ will increase.

The strain in the outer compression fibres will be greater at a crack than between, however the difference between the two strains is small and is neglected. Thus the average curvature is:

$$\phi_{av} = (\varepsilon_1 + \varepsilon_{sam})/d \qquad (6.3.39)$$

Hence the average M - ϕ relationship from cracking up to the ultimate moment is obtained by reducing the additional strains from the M - ϕ relationship across a crack using Equations 6.3.36 and 6.3.38. The average curvature is then recalculated using Equation 6.3.39.

6.3.5 Calculation of Deflection from the M - ϕ Relationship

Once the M - ϕ relationship from prestressing to ultimate has been determined, then, providing that the bending moment diagram is known, such as in simple beams, the curvature at any point can

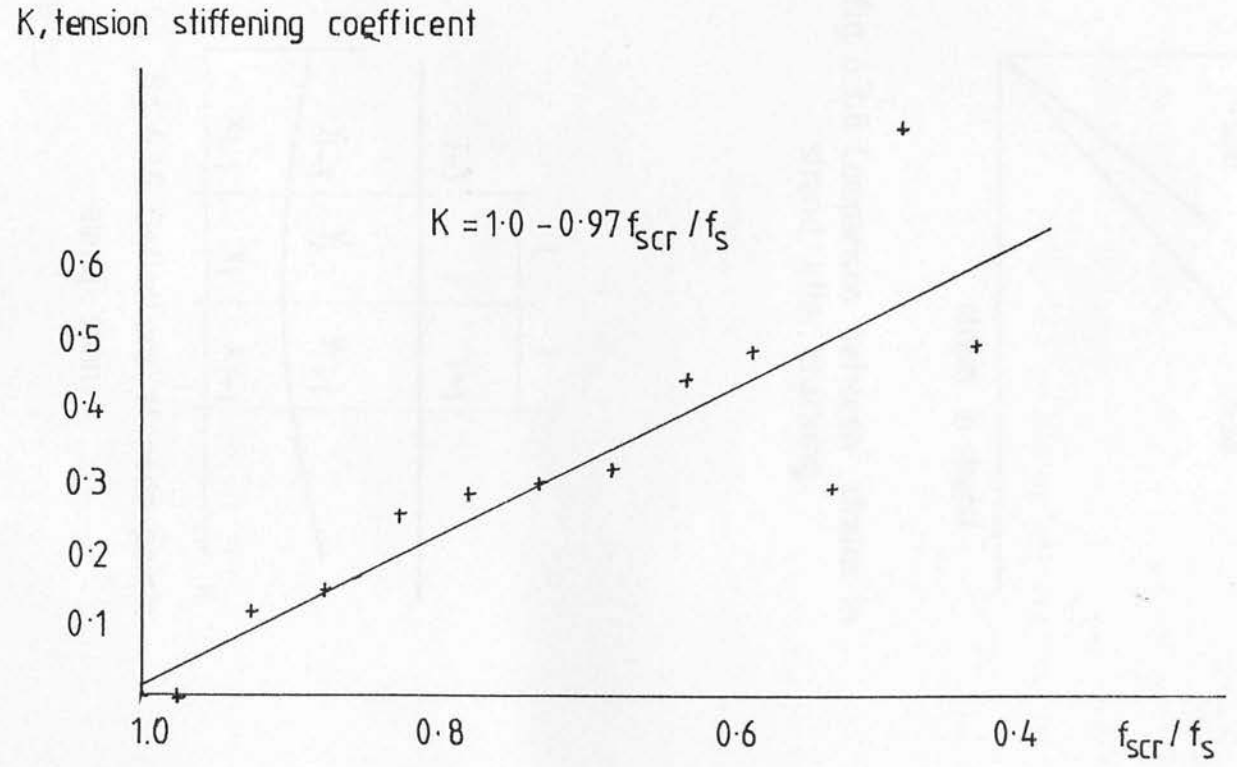

fig. 6.3.7 Relationship between tension stiffening, K and degree of cracking, f_{scr}/f_s.

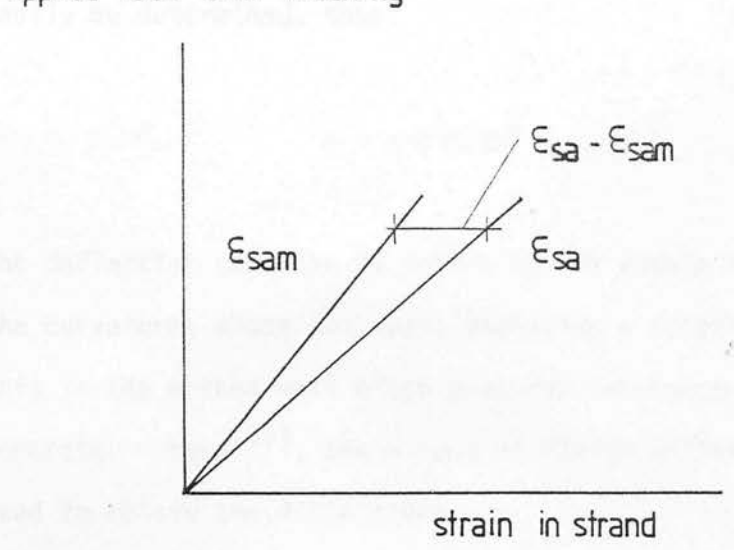

fig. 6.3.8 Comparison between strains in strand after cracking.

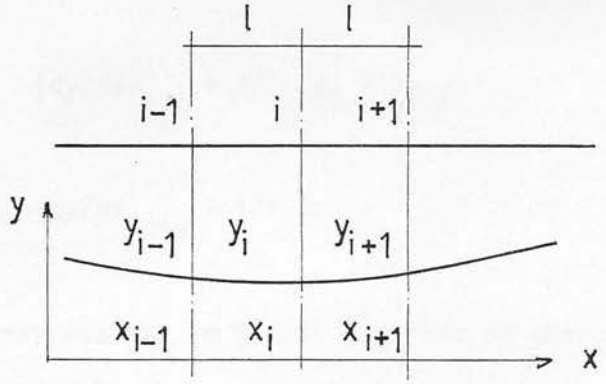

fig. 6.3.9 Deflections at node points along span.

easily be determined, thus:

$$\phi = - d^2y/dx^2 \qquad (6.3.40)$$

The deflection can then be determined by double integration of the curvatures along the span, employing a numerical integration. This is the method most often used for reinforced and prestressed concrete. Here[65], the method of finite differences has been used to obtain the deflections.

The second derivative in Equation 6.3.40 can be expressed in a finite difference form. Figure 6.3.9 shows the deflected shape of a particular beam. The beam is divided into nodes at equally spaced points. The deflections at three consecutive nodes are y_{i-1}, y_i and y_{i+1}. The slope at the points midway between i-1 and i and i and i+1, i.e. at $x_{i-\frac{1}{2}}$ and $x_{i+\frac{1}{2}}$ may be approximated by:

$$(dy/dx)_{i-\frac{1}{2}} \simeq 1/\ell\ (y_i - y_{i-1}) \qquad (6.3.41(a))$$

$$(dy/dx)_{i+\frac{1}{2}} \simeq 1/\ell\ (y_{i+1} - y_i) \qquad (6.3.41(b))$$

Using the expressions in 6.3.41 the rate of change of slope at x_i is approximated by:

$$(d^2y/dx^2)_i \simeq 1/\ell^2 \left[\left(\frac{dy}{dx}\right)_{i+\frac{1}{2}} - \left(\frac{dy}{dx}\right)_{i-\frac{1}{2}} \right] \qquad (6.3.42)$$

which is equivalent to:

$$(d^2y/dx^2)_i \simeq 1/\ell^2\ (y_{i+1} - 2y_i + y_{i-1}) \qquad (6.3.43)$$

Substituting 6.3.43 into 6.3.40 for i = 1 to n then a series of simultaneous equations is obtained which may then be expressed in matrix form:

$$\begin{bmatrix} -2 & 1 & 0 & 0 & \cdots \\ 1 & -2 & 1 & 0 & \cdots \\ 0 & 1 & -2 & 1 & \cdots \\ \cdot & \cdot & \cdot & \cdot & \cdots \\ \cdot & \cdot & \cdot & \cdot & \cdots \\ \cdot & \cdot & \cdot & \cdot & \cdots \end{bmatrix} \begin{bmatrix} y_1 \\ y_2 \\ y_3 \\ \cdot \\ \cdot \\ y_n \end{bmatrix} = \ell^2 \begin{bmatrix} \phi_1 \\ \phi_2 \\ \phi_3 \\ \cdot \\ \cdot \\ \phi_n \end{bmatrix} \qquad (6.3.44)$$

At the supports, in a simple beam, the deflection will be zero and hence these terms may be eliminated from 6.3.44.

$\phi_1 - \phi_n$ are the average curvatures obtained from the M - ϕ relationship. Solution of Equation 6.3.44 yields the deflections at each node point. The load/deflection response is therefore obtained by applying the load in increments, calculating the bending moment at the nodes, then using the M - ϕ relationship to find the curvatures at the nodes. These are then substituted in Equation 6.3.44 and the corresponding deflections are found. This process is repeated until the ultimate load of the beam has been attained.

The sequence of calculations from 6.3.1 to 6.3.44 entails a large amount of iterative and matrix operations and hence a computer programme was written which employs all these steps, to facilitate the analysis. The programme, along with instructions for data input, is presented in Appendix I.

6.4 Comparison of Experimental and Theoretical Results

The theoretical analysis presented in section 6.3 may be conveniently sub-divided into three parts, namely, the determination of the M - ϕ relationship across a crack, the averaged M - ϕ relationship and the calculation of the deflections from the average M - ϕ relationship. This provides a suitable means by which the experimental and theoretical results may be compared.

The theoretical curvatures and deflections were calculated using the stress/strain relationships obtained from both the single and three course prisms for each type of brickwork, from Chapter 3.

6.4.1 M - ϕ Relationship Across a Crack

The experimental M - ϕ relationships were obtained from strains measured on the surface of the beams where a crack formed within the gauge length. By applying linear regression analysis to the measured strains in a vertical, cracked section, the gradient of the strain distribution was found, which is equal to the curvature.

Where the curvatures were measured at a number of cracked sections, the average of these was taken as the curvature across the cracks. In one of two beams cracks did not form within the gauge length and consequently the curvatures across the cracks could not be obtained.

Figures 6.4.1-5 show the experimental M - ϕ relationship across a crack for beams of high strength brick. The beams with two strands (% steel 0.274), Figure 6.4.1, and three strands (% steel

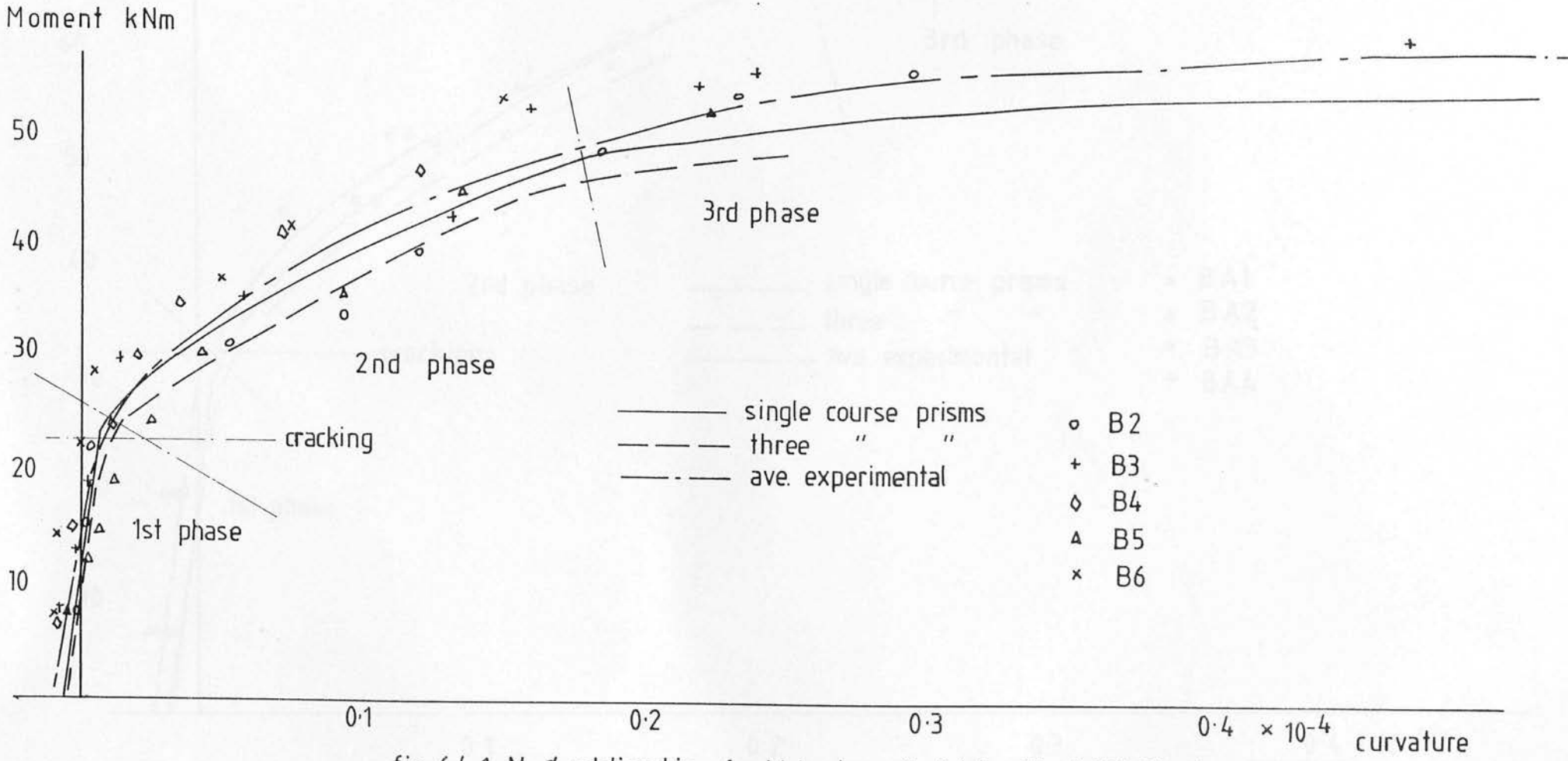

fig. 6.4.1 M-ϕ relationship for high strength brick with 0.274 % steel across cracks.

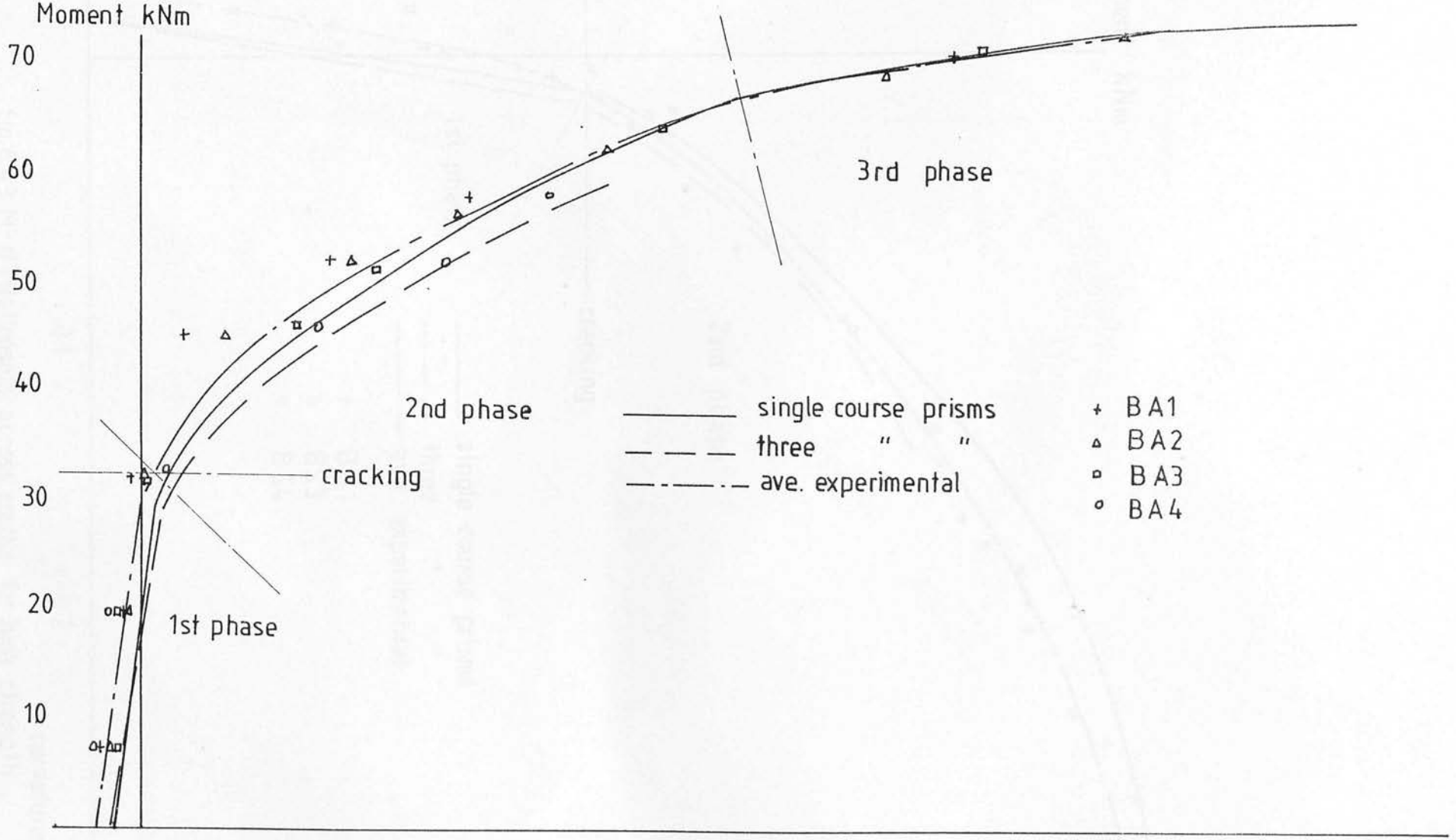

fig.6.4.2 M-ϕ relationship across cracks for high strength brick beams with 0·411 % steel.

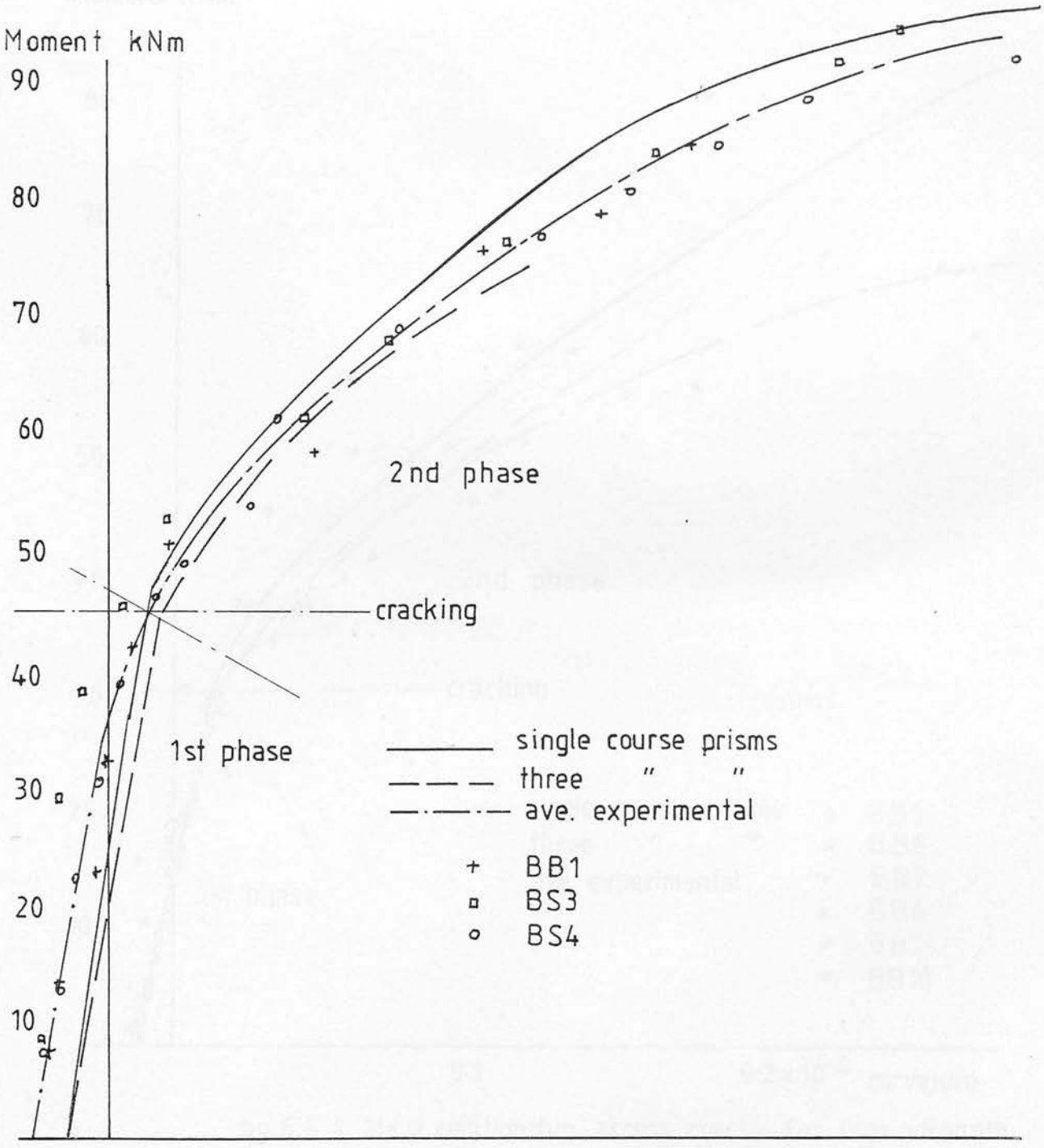

fig.6.43 M-Ø relationship across cracks for high strength brick beams with 0·548 % steel.

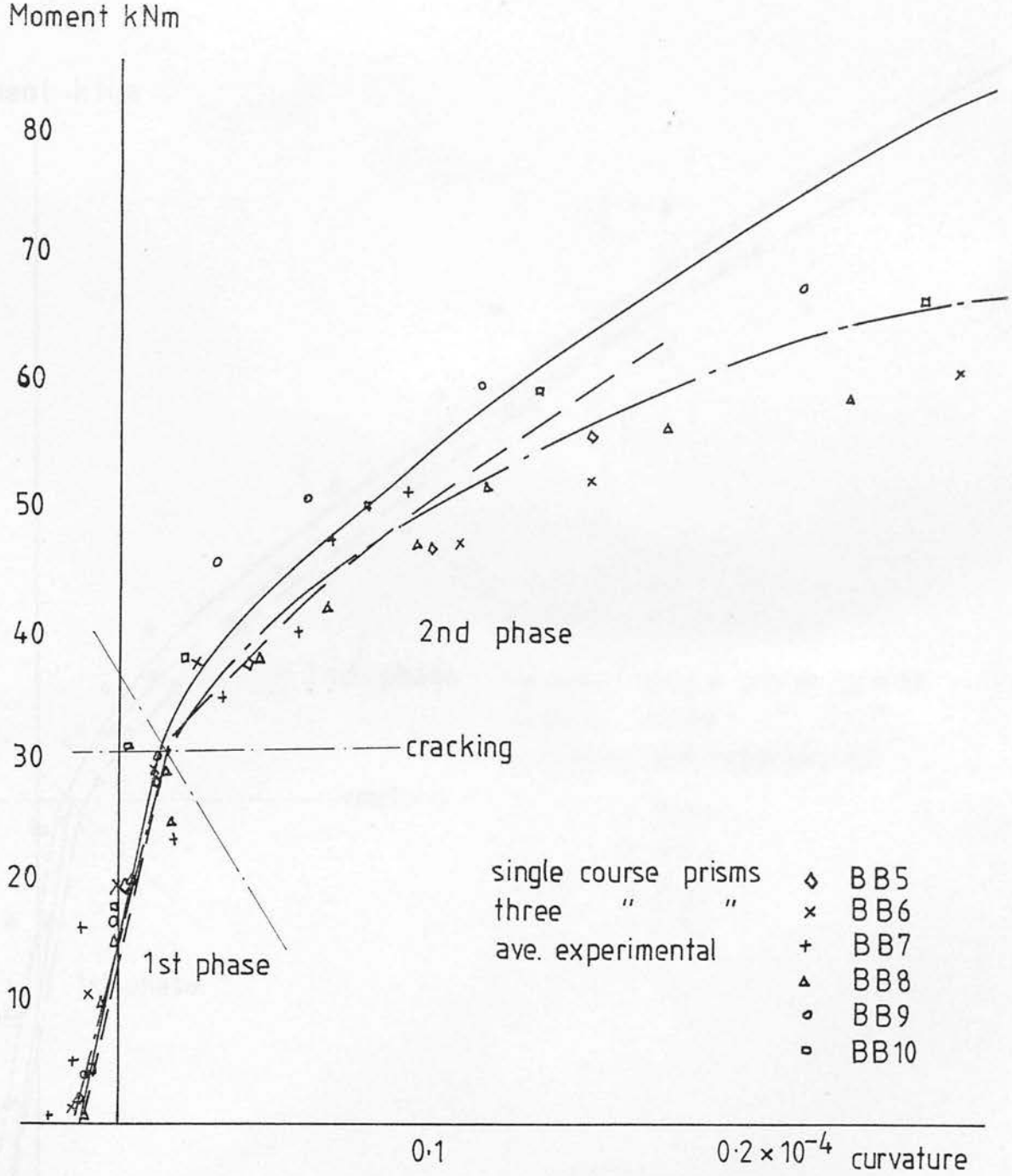

fig. 6.4.4 M - ϕ relationship across cracks for high strength brick beams with 0·548 % steel.

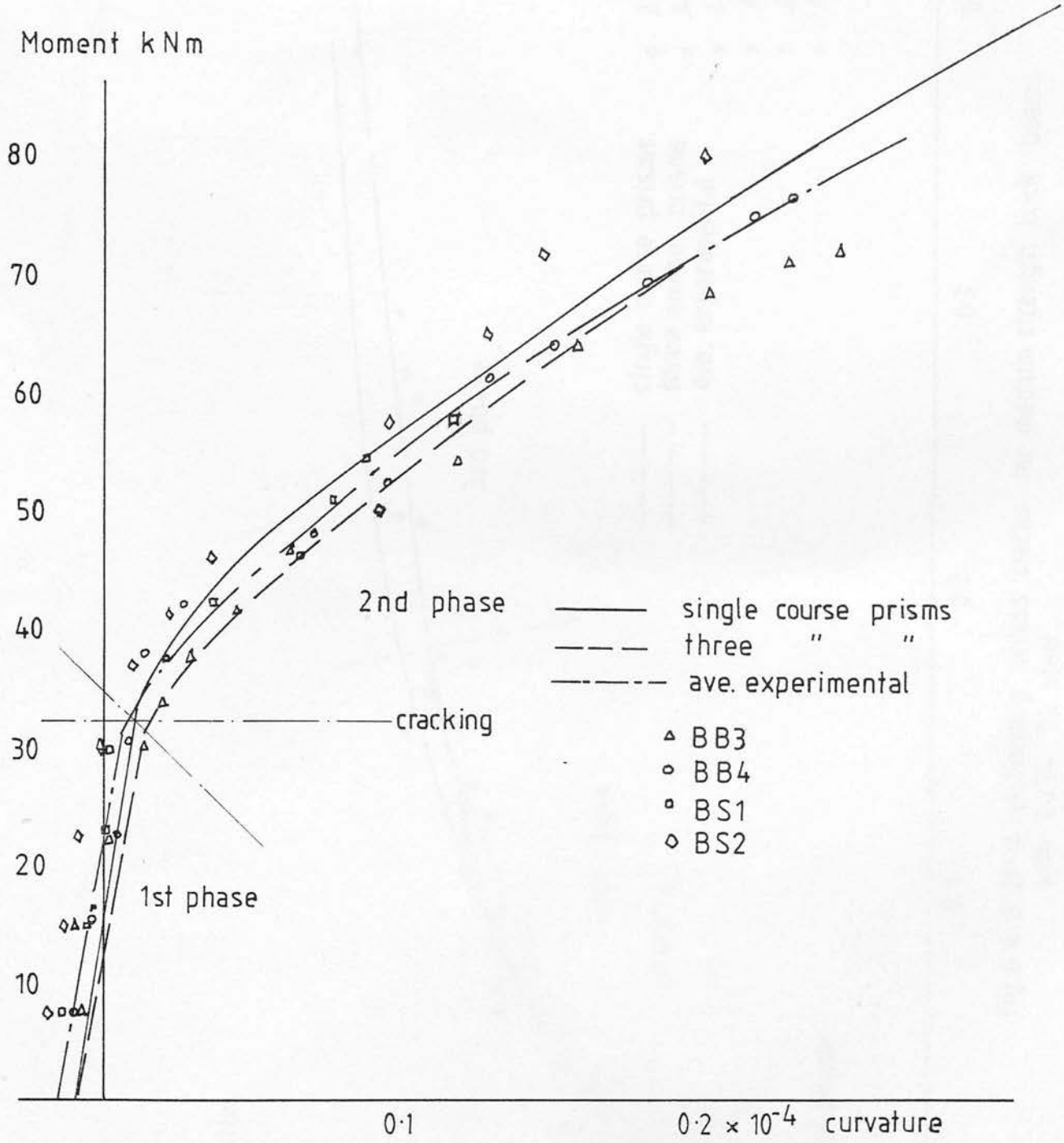

fig. 6.4.5 M-ϕ relationship across cracks for high strength brick beams with 0·548 % steel.

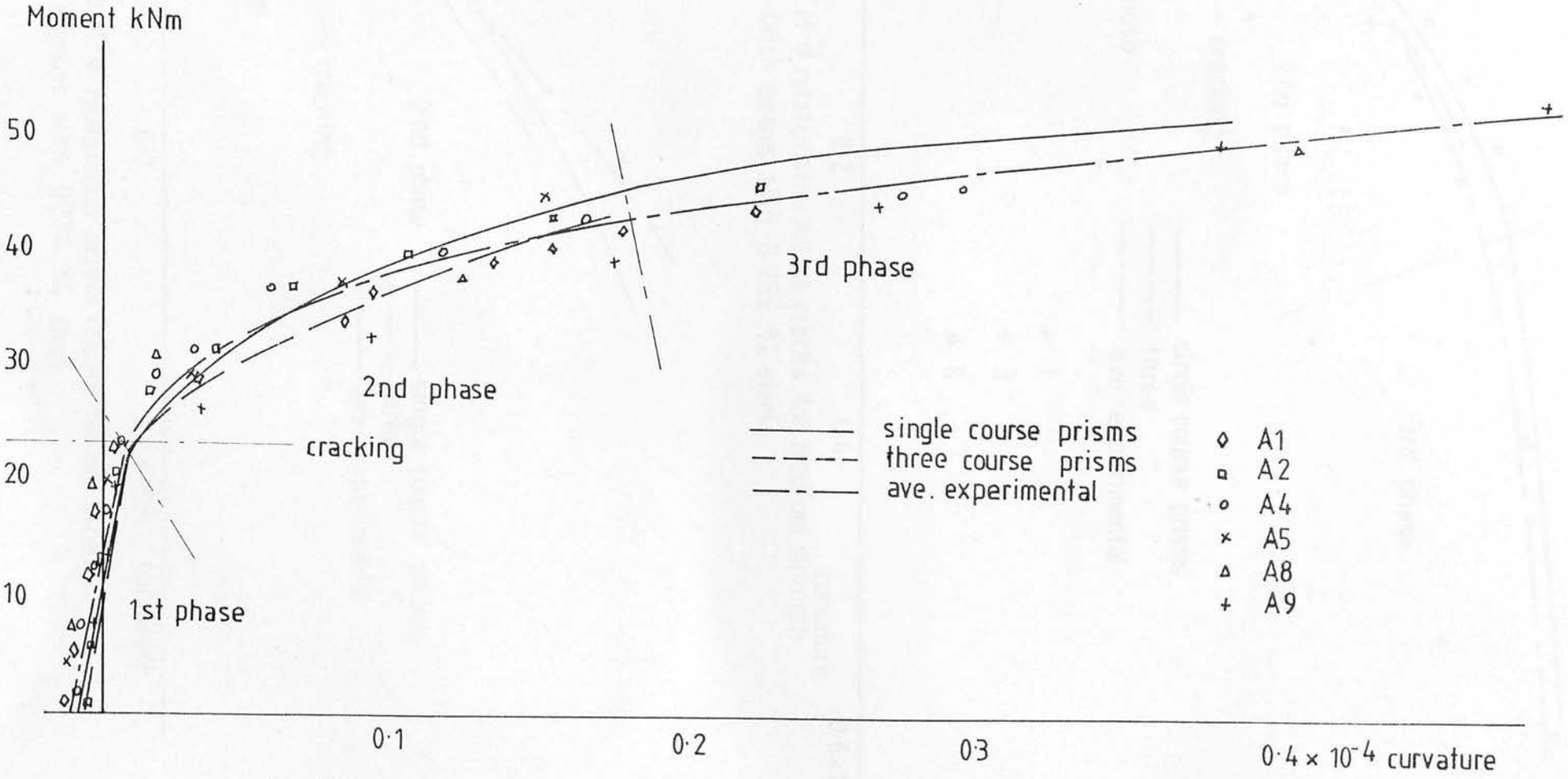

fig.6.4.6 M-ϕ relationship across cracks for medium strength brick beams with 0·274 % steel.

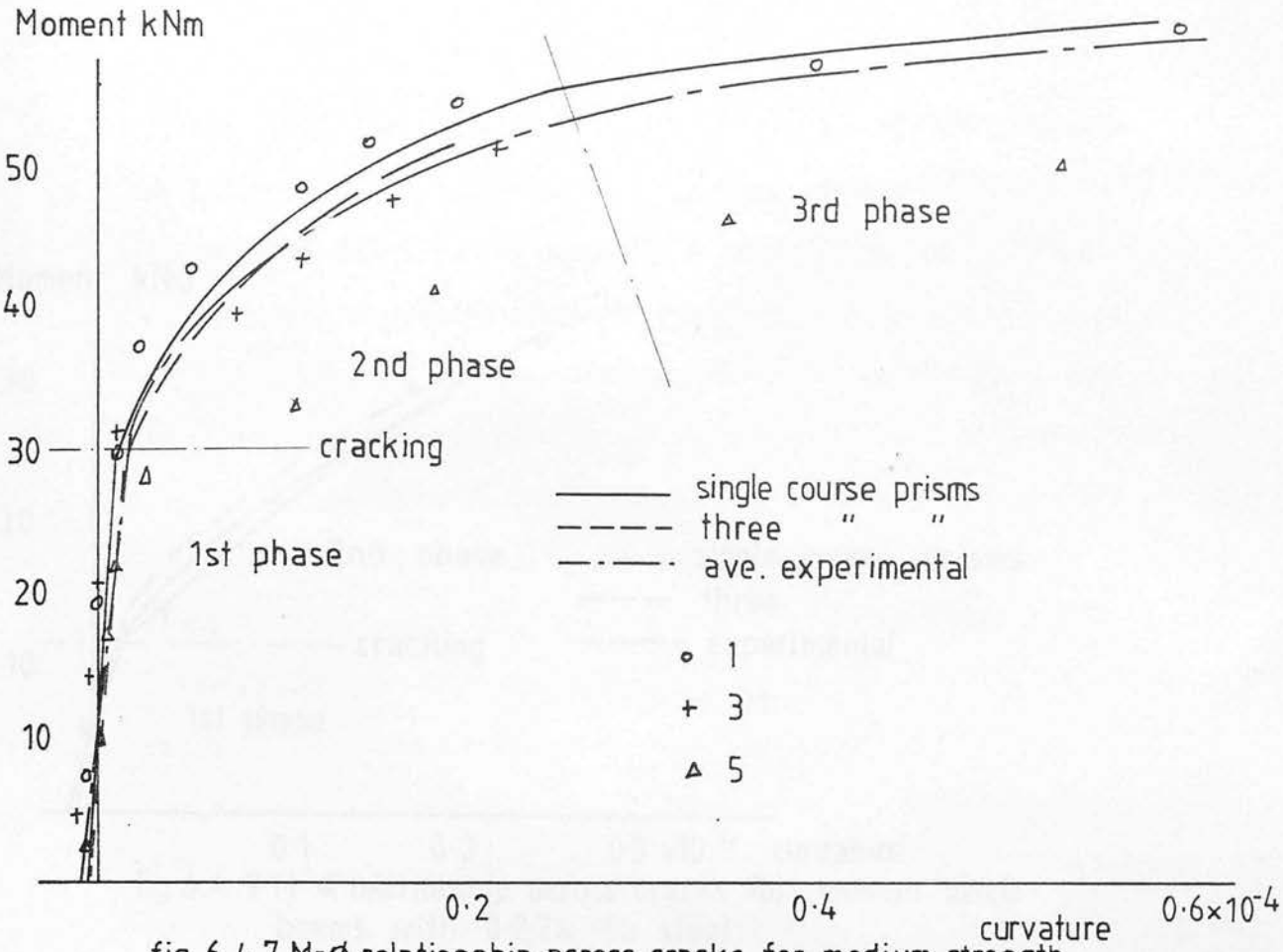

fig. 6.4.7 M-ϕ relationship across cracks for medium strength brick beams with 0·255 % steel.

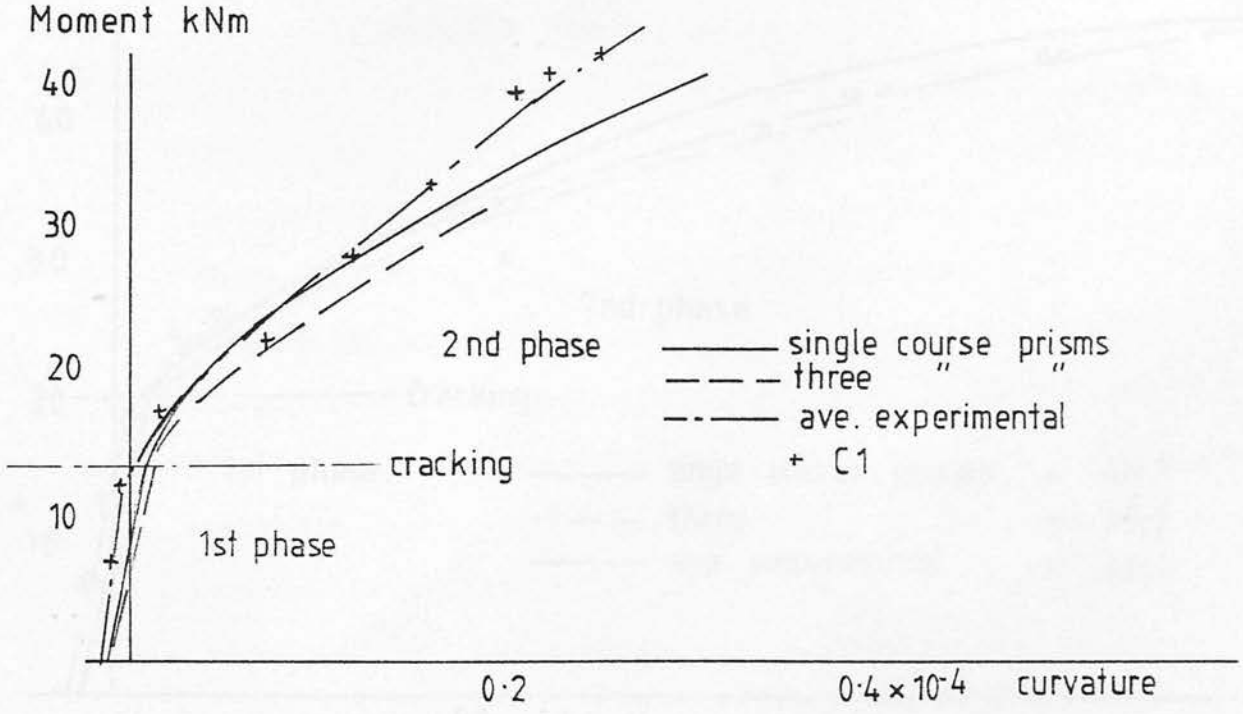

fig 6.4.8 M-ϕ relationship across cracks for low strength brick beams with 0·274 % steel.

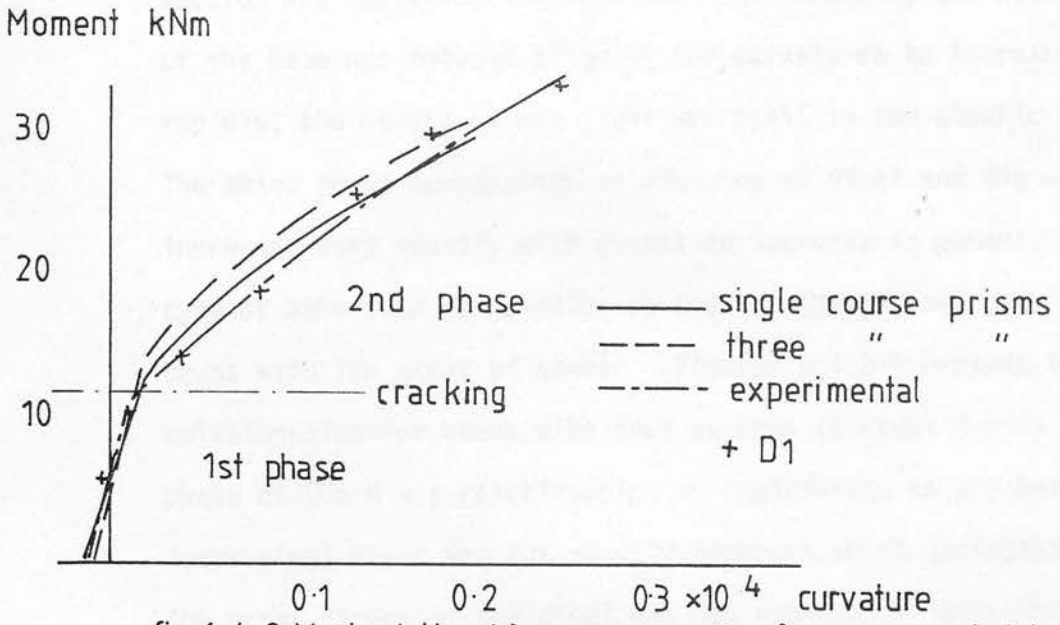

fig. 6.4.9 M-Φ relationship across cracks for common brick beams with 0·274 % steel.

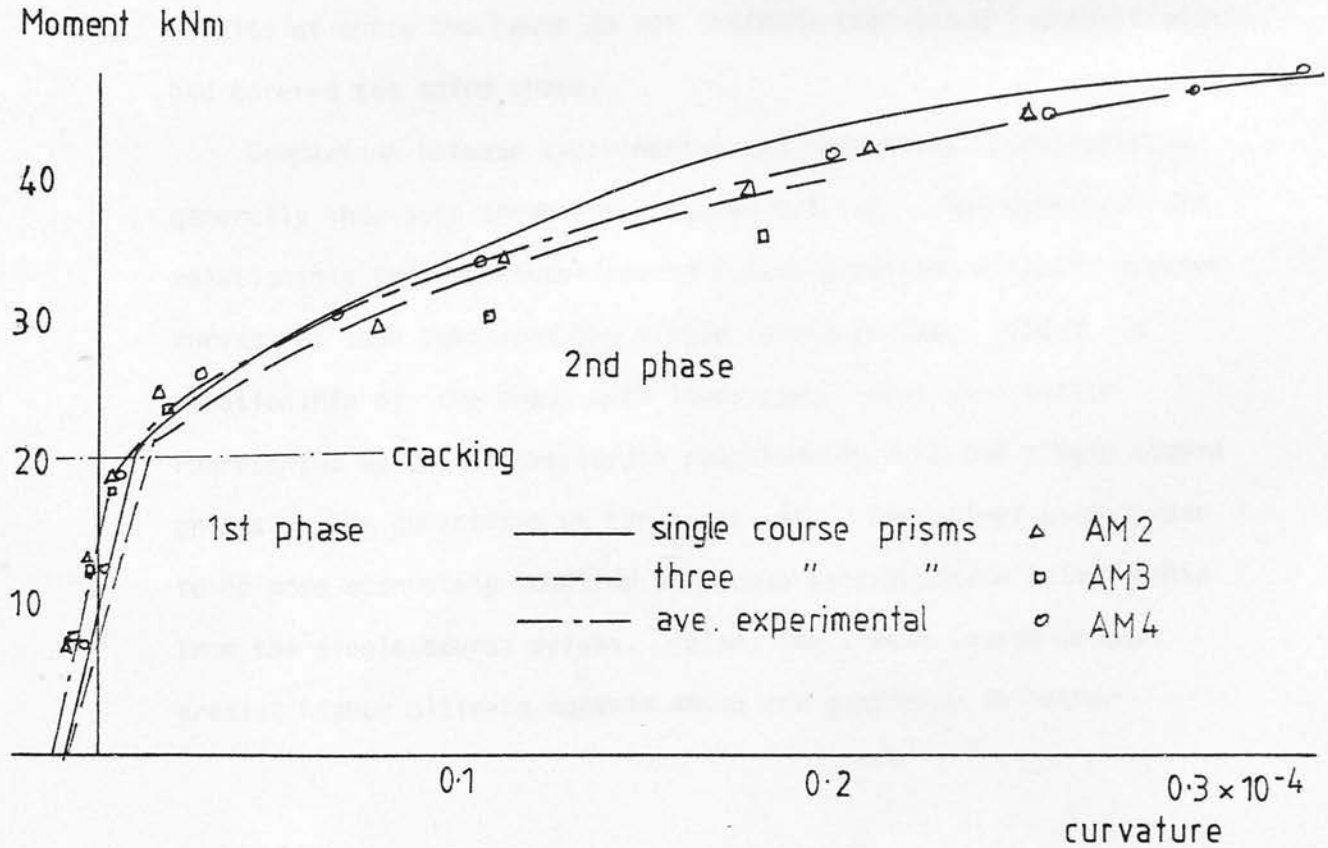

fig. 6.4.10 M-Φ relationship across cracks for medium strength brick beams in grade II mortar with 0·274 % steel.

0.411), Figure 6.4.2, exhibit an M - ϕ relationship which took a well defined three phase form. Prior to cracking the whole section was resisting the moments, after cracking the stiffness of the beam was reduced allowing the curvatures to increase more rapidly, the stress in the steel was still in the elastic range. The third phase corresponds to yielding of steel and the curvatures increased very rapidly with almost no increase in moment. This type of behaviour was similar to that of prestressed concrete beams with low areas of steel. Figures 6.4.3-5 present the M - ϕ relationships for beams with four strands (% steel 0.548) the third phase of the M - ϕ relationship, as experienced in the beams with lower steel areas was not readily apparent which indicated that the proof stress of the steel was not exceeded. With the exception of BS1 and BS2, all the beams in Figures 6.4.3-5 failed in shear, hence the full flexural capacity was not reached, however the results of these two beams do not indicate that the M - ϕ relationship had entered the third phase.

Comparison between experimental and theoretical curvatures generally show good agreement, Figures 6.4.1-5. The stress/strain relationship from the three course prisms predicted slightly greater curvatures than that from the single course prisms. The M - ϕ relationship of the beams with lower steel areas were better represented by the stress/strain relationship from the single course prisms. The curvatures of the beams with 0.548% steel also appear to be more accurately modelled using the stress/strain relationship from the single course prisms. Also, the single course prisms predict higher ultimate moments which are generally in better

agreement with the experimental results and consequently more able to predict curvatures up to ultimate load. This is apparent from Figures 6.4.3-6.4.5, where, even though the majority of these beams failed in shear the three course prisms were not able to predict curvatures up to failure.

Behaviour similar to the high strength bricks with two strands can be observed for beams built of medium strength brick, Figures 6.4.6-7. As with the high strength brick a three phase form to the M - ϕ relationship may be discerned. For this type of brickwork also, the single course prisms predicted slightly lower curvatures suggesting a stiffer section than that obtained from the three course prisms and much greater curvatures near failure which was in better accordance with the experimental results.

Figures 6.4.8 and 9 present the experimental curvatures for the low strength and common brick beams. The curvatures across cracks were obtained only for one of each type of beam. Cracking occurred earlier in these beams than in similar beams of high and medium strength brick, due to the reduced prestress force. There appears to be a slight flattening of the M - ϕ relationship as failure occurs, however evidence of the relationship entering the third phase was not nearly as well defined as in the higher strength brick beams.

The computed curvatures for the low strength brick beams, Figure 6.4.8, show very good agreement up to approximately 75% of the ultimate load, where after the theoretical curvatures tend to overestimate the experimental results. Again the single course prisms predict slightly lower curvatures than the three course

prisms and are more capable of predicting curvatures up to failure.

For the high, medium and low strength brick, the three course prisms consistently predict slightly greater curvatures and lower ultimate moments than the single course prisms. The reverse is true for the beams built of common brick although the single course prisms appear to give a better correlation between the theoretical and experimental results.

Figure 6.4.10 illustrates the medium strength brick beams in 1:½:4½ mortar. The behaviour is very similar to the beams in 1:¼:3 mortar, Figure 6.4.6, although corresponding curvatures are slightly greater. The curvatures calculated from both prism types are very similar and closer than the curvatures predicted for medium strength brick in 1:¼:3 mortar, obviously due to the closer similarities in the stress/strain relationships obtained from both prism types.

6.4.2 Averaged M - ϕ Relationship

After cracking the neutral axis depth at a crack, in a prestressed brickwork beam, rises. Prior to this the tensile strength of the brickwork assists in resisting the tensile forces caused by flexure and is then lost. In order to sustain the same moment the stresses in the steel must increase, which causes an increase in brickwork strain and rise in neutral axis depth. The rise in neutral axis depth will vary from points at cracks and between cracks. In a number of beams the strains were measured at five or six sections in the constant moment zone. The resulting

variations in neutral axis depth along this region are shown, for typical beams in Figures 6.4.11-13. Also shown is the corresponding strain in the top fibre of the beams and curvatures measured at each section. The dashed line in (a) represents the neutral axis depth calculated using the additional strain in the reinforcement and the average compressive strain in the top fibre, i.e.:

$$n = \left(\frac{\varepsilon_1}{\varepsilon_1 + \varepsilon_{sam}}\right) d \qquad (6.4.1)$$

The dashed line in (b) shows the averaged strain in the top fibre and the dashed line in (c) the average curvature calculated again using the additional measured strain in the strain and the average compressive strain as given in Equation 6.3.39.

As the load increases the variation in the neutral axis depth tends to decrease. The neutral axis depth calculated as per Equation 6.4.1 is generally within the range of variability of the neutral axis depth. The variation of compressive strain in the constant moment zone increases with increasing load as does the curvature. However, the curvature calculated by Equation 6.3.39 gives a good estimation of the probable average curvature. In section 6.3.4, it was stated that in calculating the average curvature the strain in the top fibre at a crack, obtained by theory is then combined with the average strain at the level of the steel, therefore assuming that the average strain in the compression fibre is equal to that at a crack.

This assumption may have a considerable effect on the accuracy

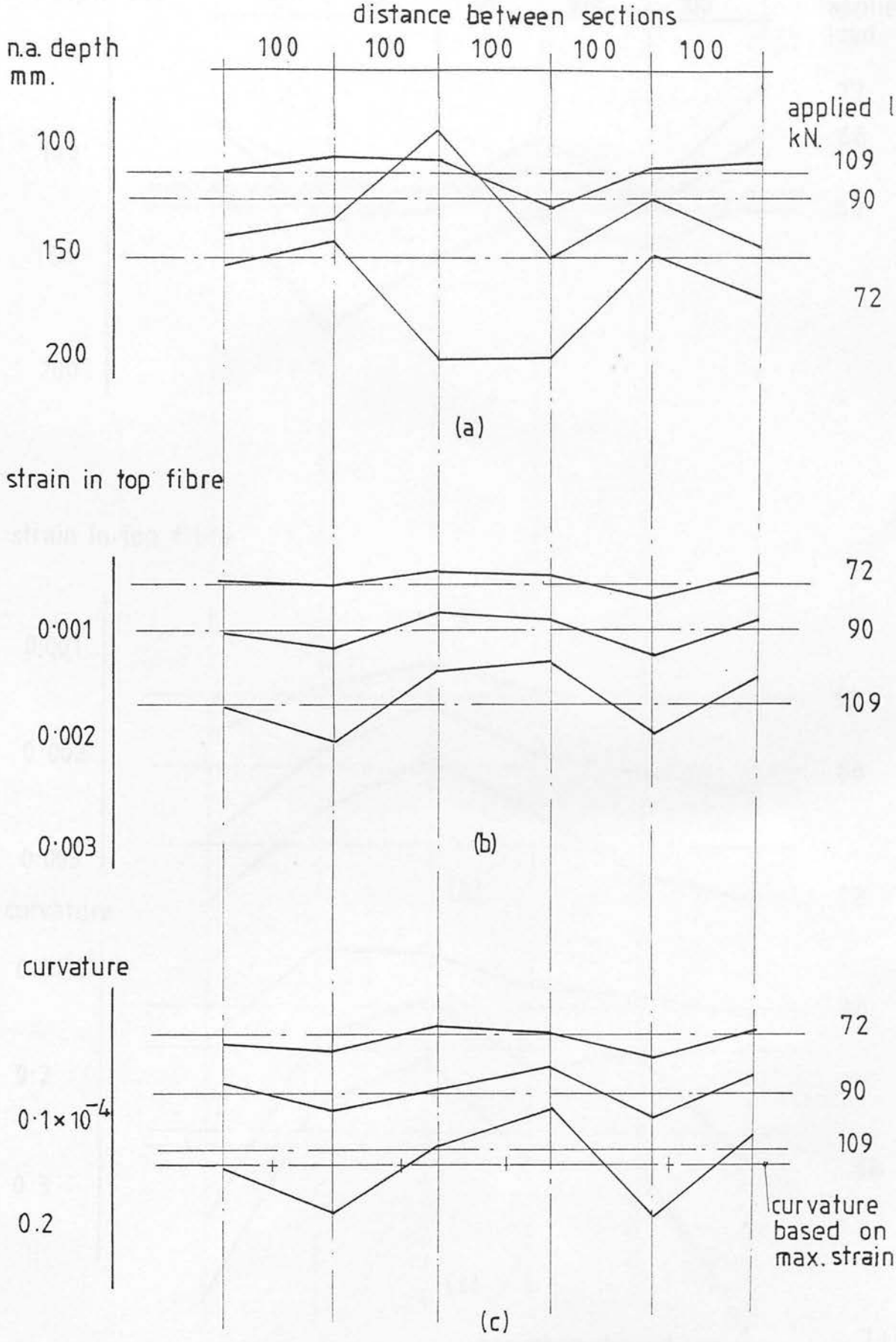

fig. 6.4.11 Variations in n.a. depth, strain & curvature for beam BB5, 0·548 % steel.

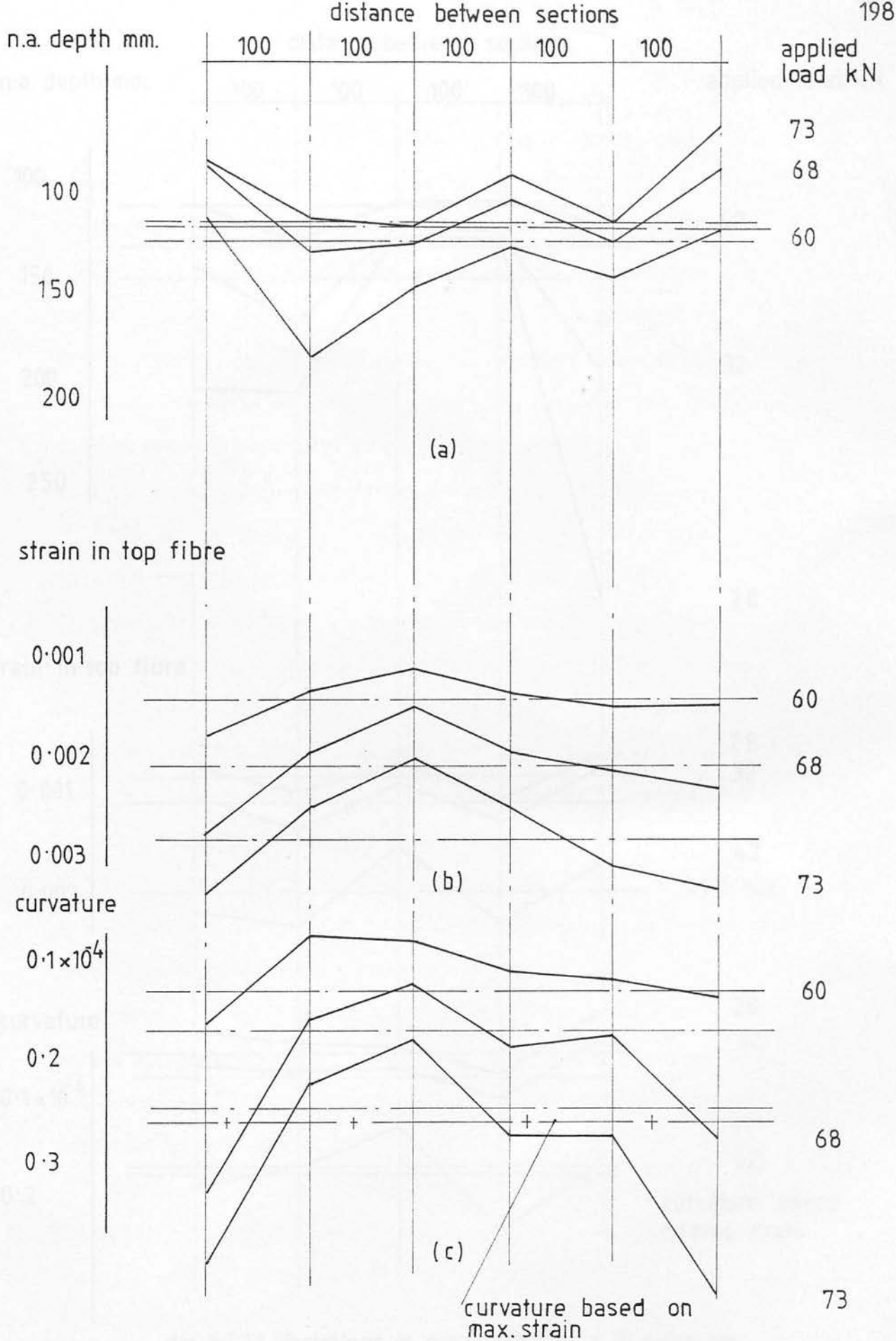

fig. 6.4.12 Variations in n.a. depth, strain & curvature for beam BB10, 0·548 % steel.

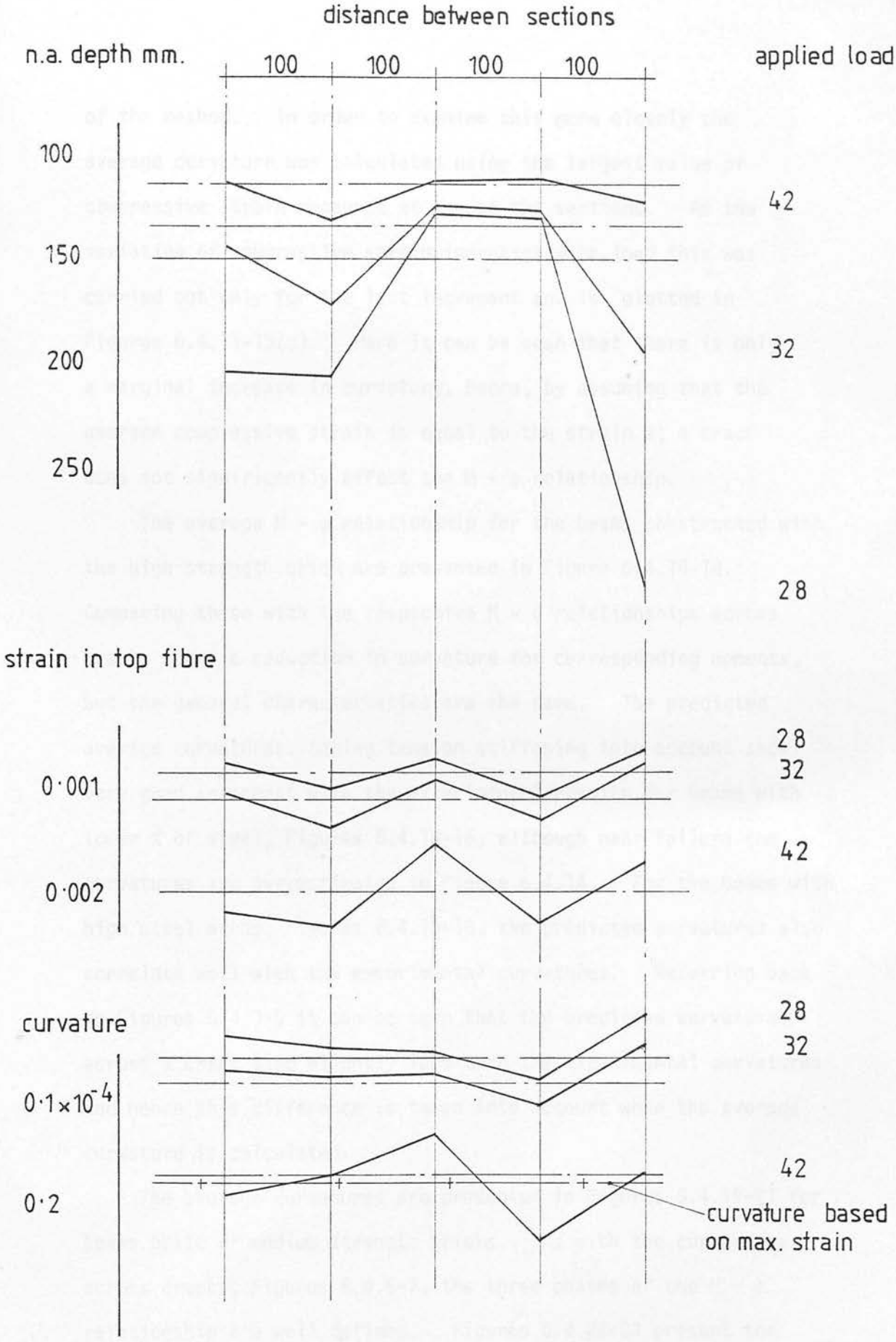

fig. 6.4.13 Variations in n.a.depth, strain & curvature for beam BA3, 0·411 % steel.

of the method. In order to examine this more closely the average curvature was calculated using the largest value of compressive strain measured at any of the sections. As the variation of compressive strain increases with load this was carried out only for the last increment and is plotted in Figures 6.4.11-13(c). Here it can be seen that there is only a marginal increase in curvature, hence, by assuming that the average compressive strain is equal to the strain at a crack does not significantly affect the M - ϕ relationship.

The average M - ϕ relationship for the beams constructed with the high strength brick are presented in Figure 6.4.14-18. Comparing these with the respective M - ϕ relationships across cracks shows a reduction in curvature for corresponding moments, but the general characteristics are the same. The predicted average curvatures, taking tension stiffening into account show very good agreement with the experimental results for beams with lower % of steel, Figures 6.4.14-15, although near failure the curvatures are overestimated in Figure 6.4.14. For the beams with high steel areas, Figures 6.4.16-18, the predicted curvatures also correlate well with the experimental curvatures. Referring back to Figures 6.4.3-5 it can be seen that the predicted curvatures across a crack also slightly less than the experimental curvatures and hence this difference is taken into account when the average curvature is calculated.

The average curvatures are presented in Figures 6.4.19-21 for beams built of medium strength bricks. As with the curvatures across cracks, Figures 6.4.6-7, the three phases of the M - ϕ relationship are well defined. Figures 6.4.22-23 present the

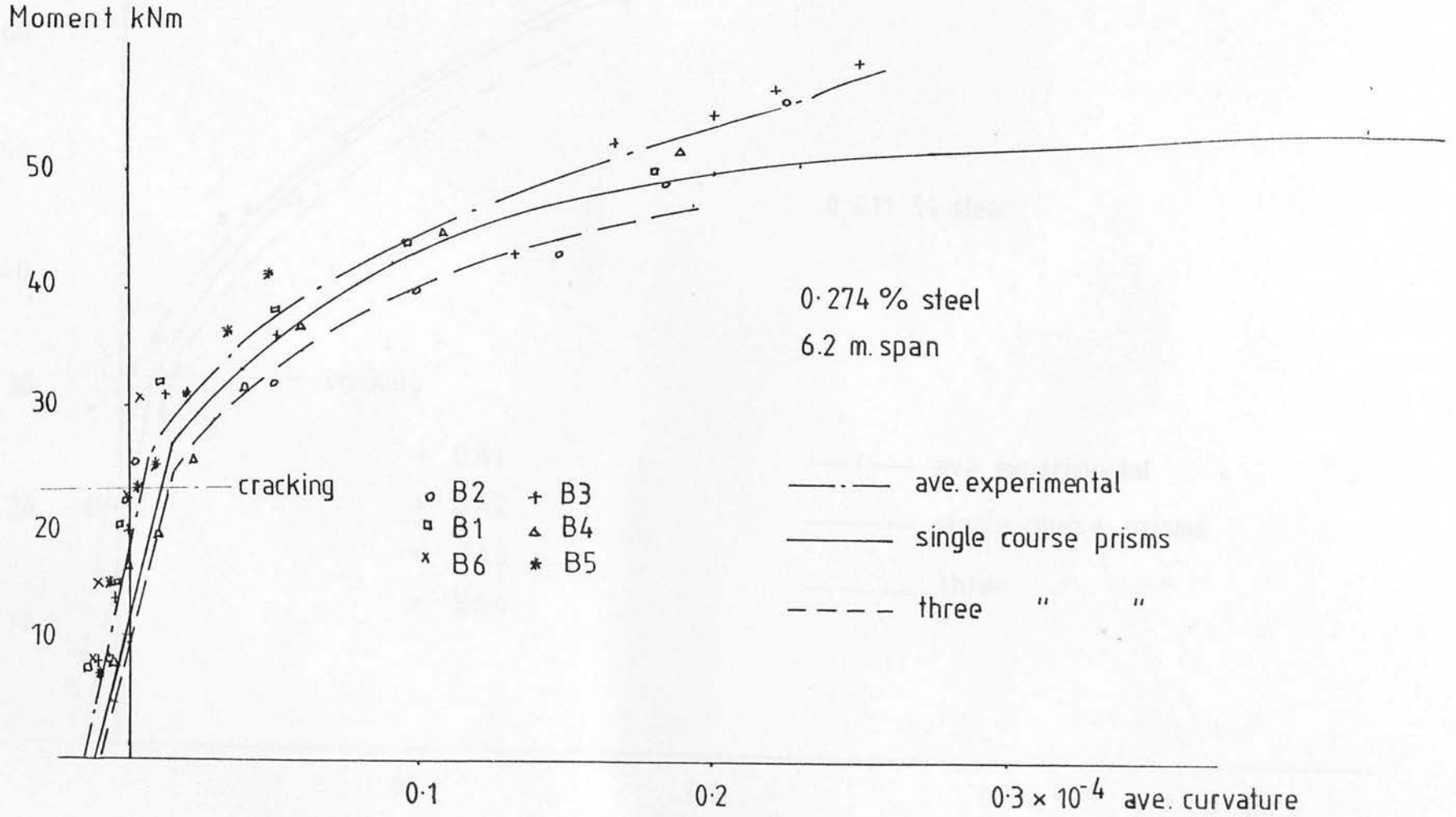

fig. 6.4.14 Averaged M - ϕ relationship for high strength brick beams.

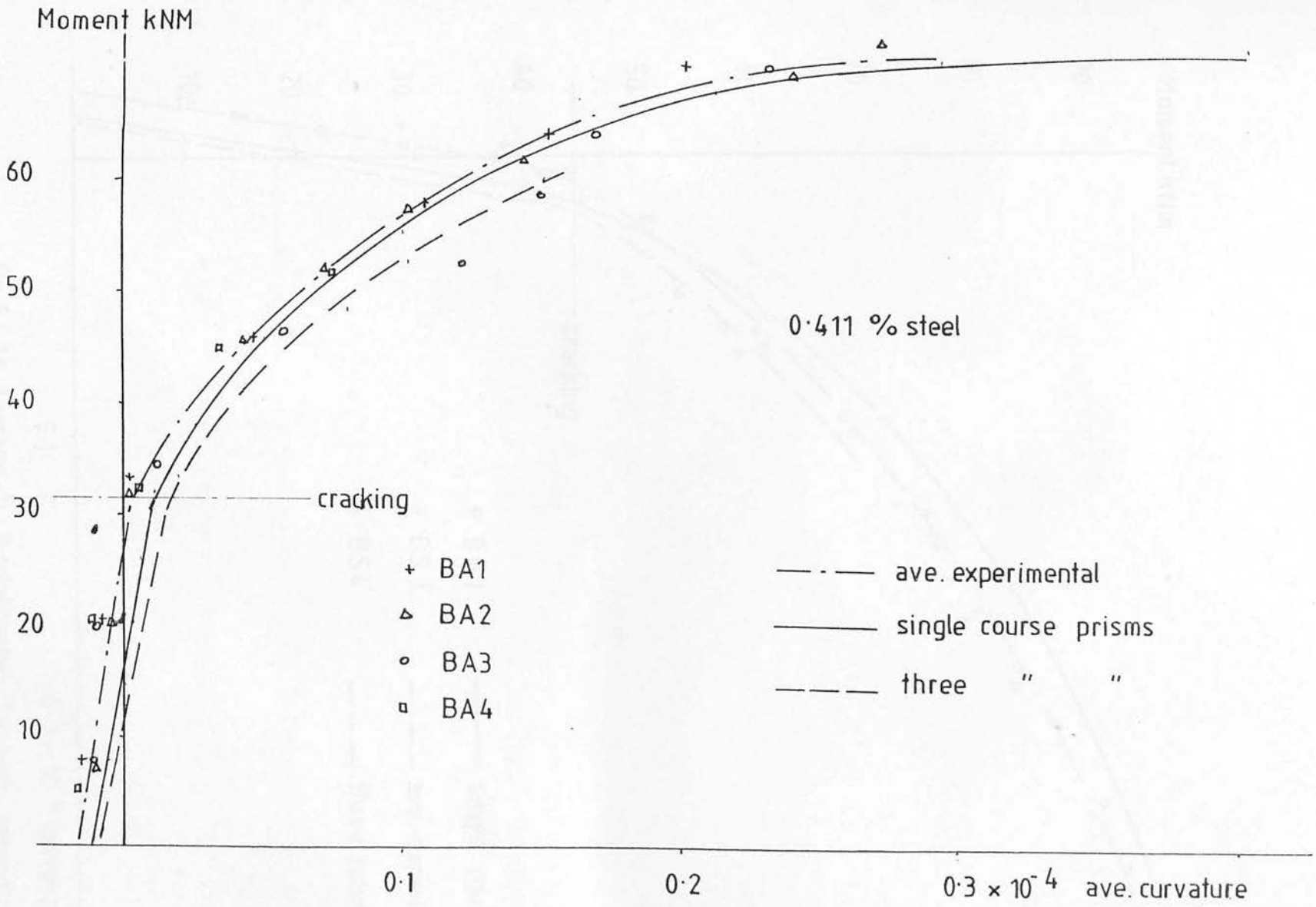

fig. 6.4.15 Average M-ϕ relationship for high strength brick beams.

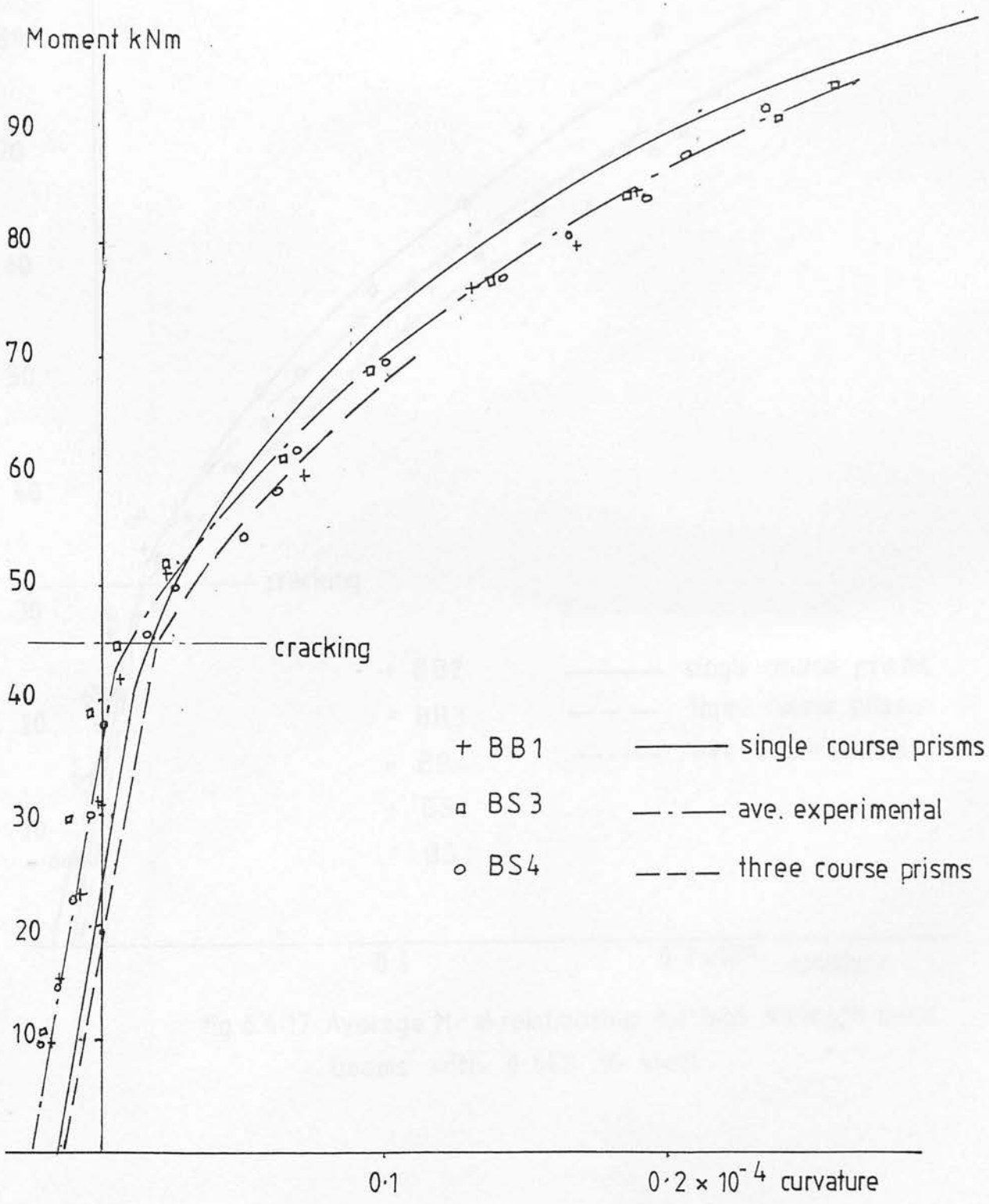

fig. 6.4.16 Average M - ϕ relationship for high strength brick beams with 0·548 % steel.

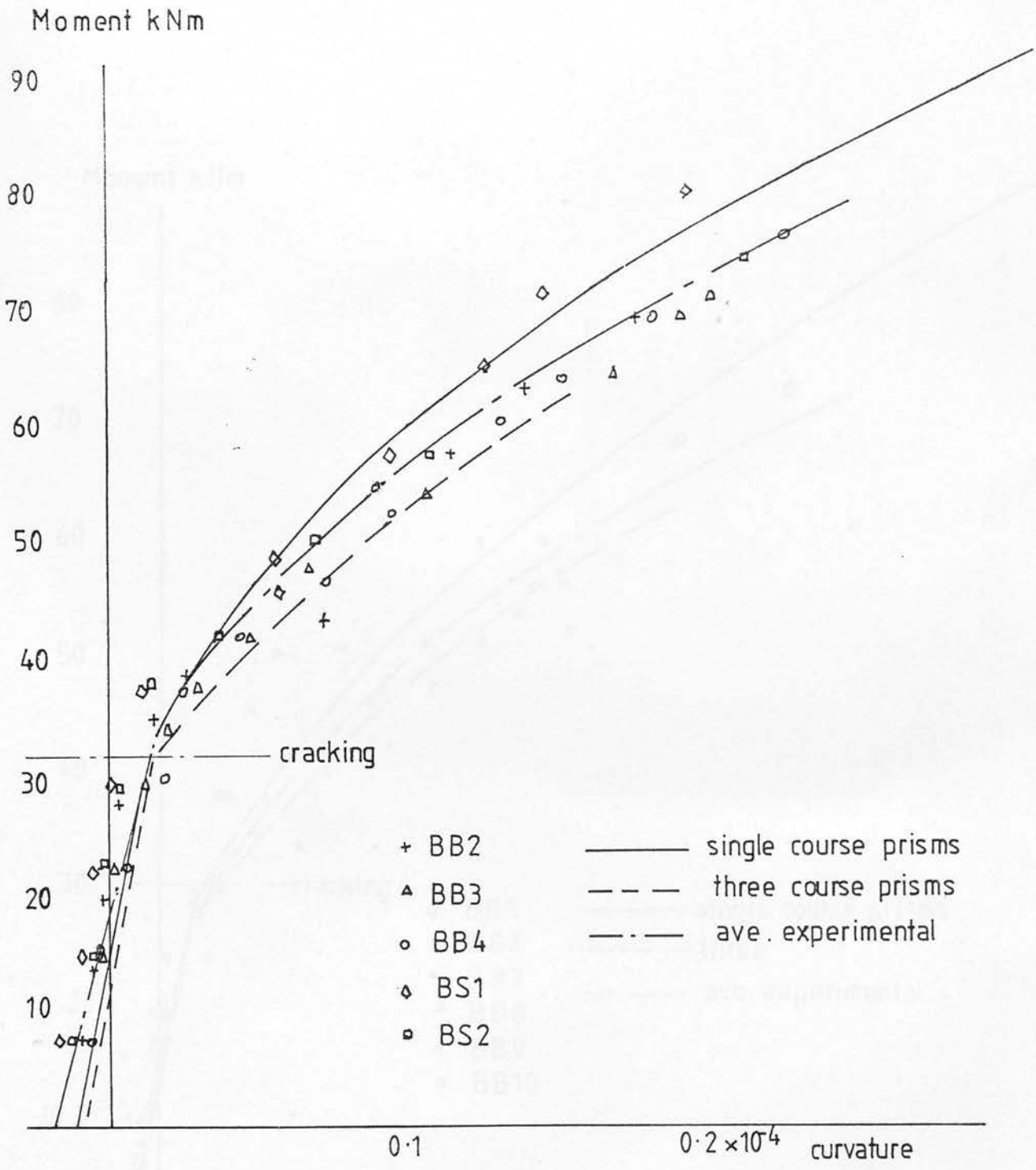

fig. 6.4.17 Average M - ϕ relationship for high strength brick beams with 0·548 % steel.

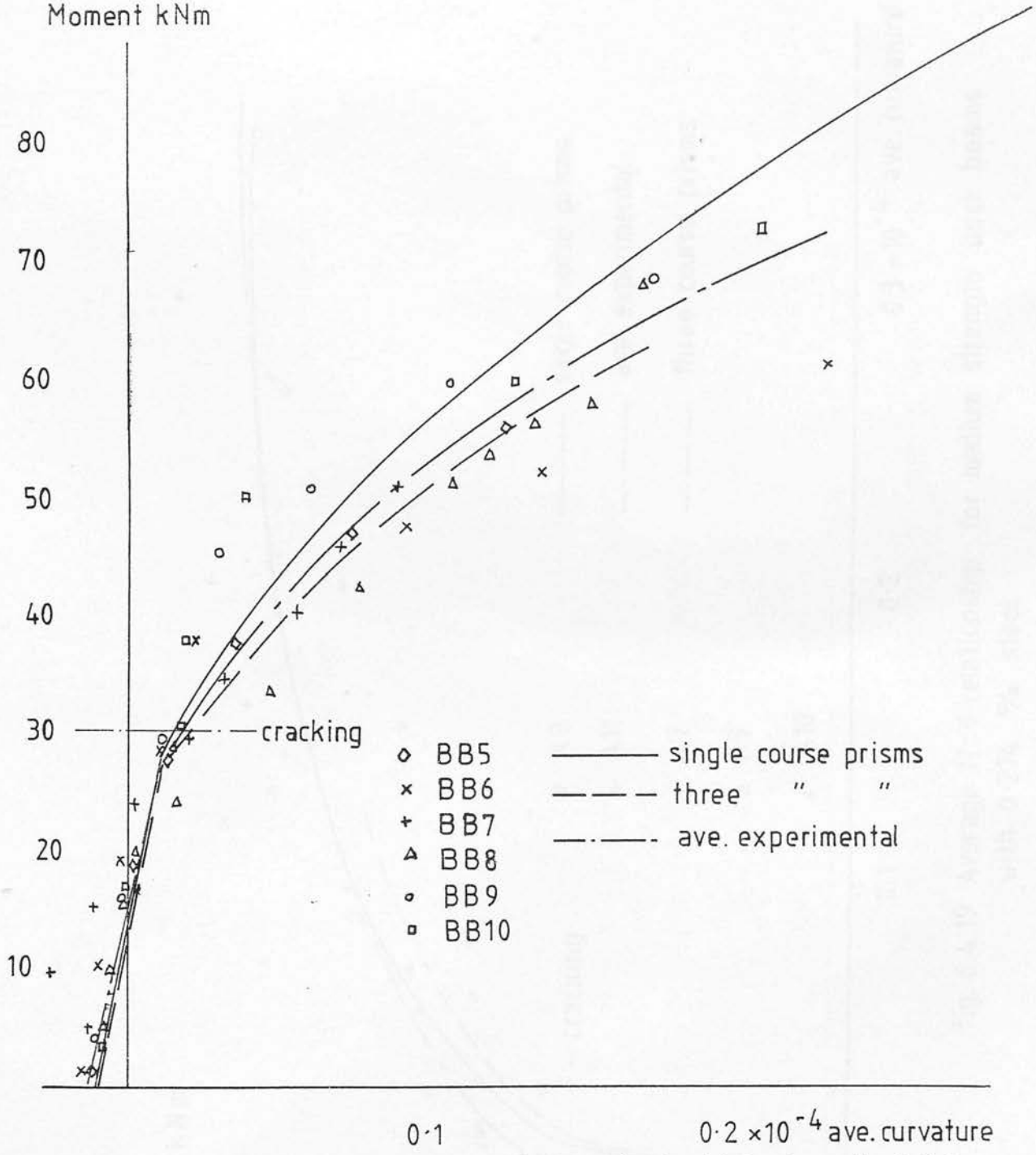

fig. 6.4.18 Average M-Φ relationship for high strength brick beams with 0·548 % steel.

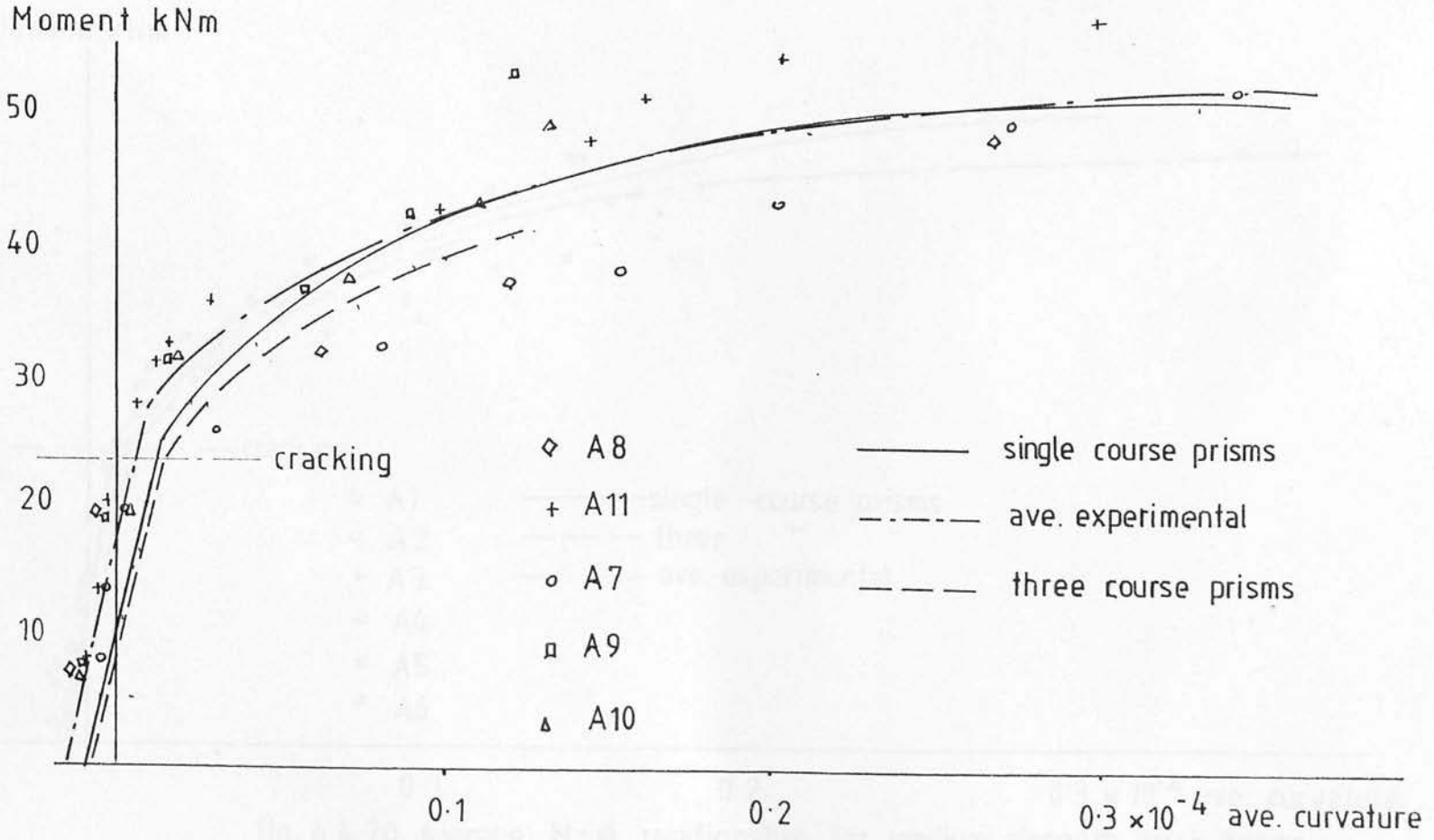

fig. 6.4.19 Average M-φ relationship for medium strength brick beams with 0·274 % steel.

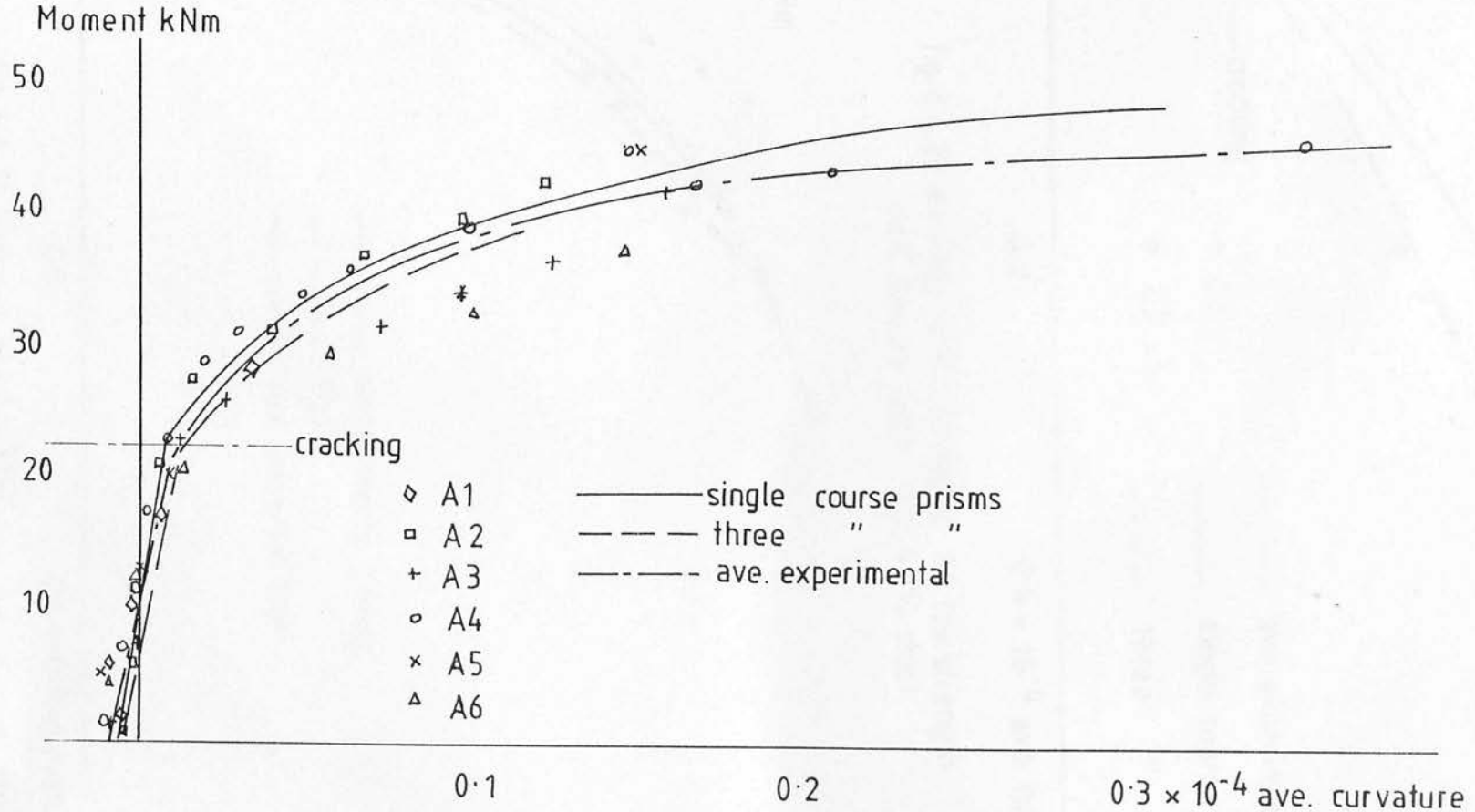

fig. 6.4.20 Average M - ϕ relationship for medium strength brick beams with 0·274 % steel.

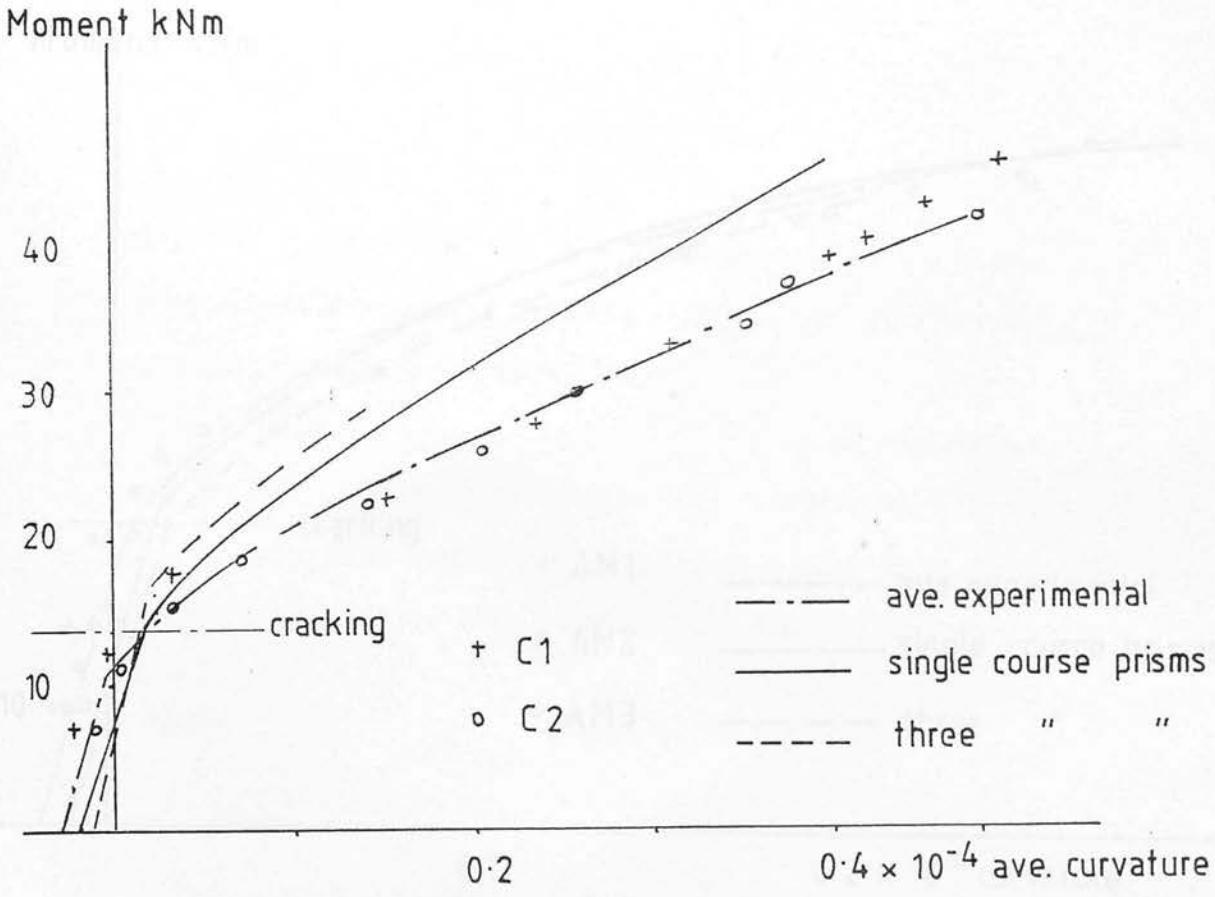

fig. 6.4.22 Average M-Φ relationship for low strength brick beams with 0·274 % steel.

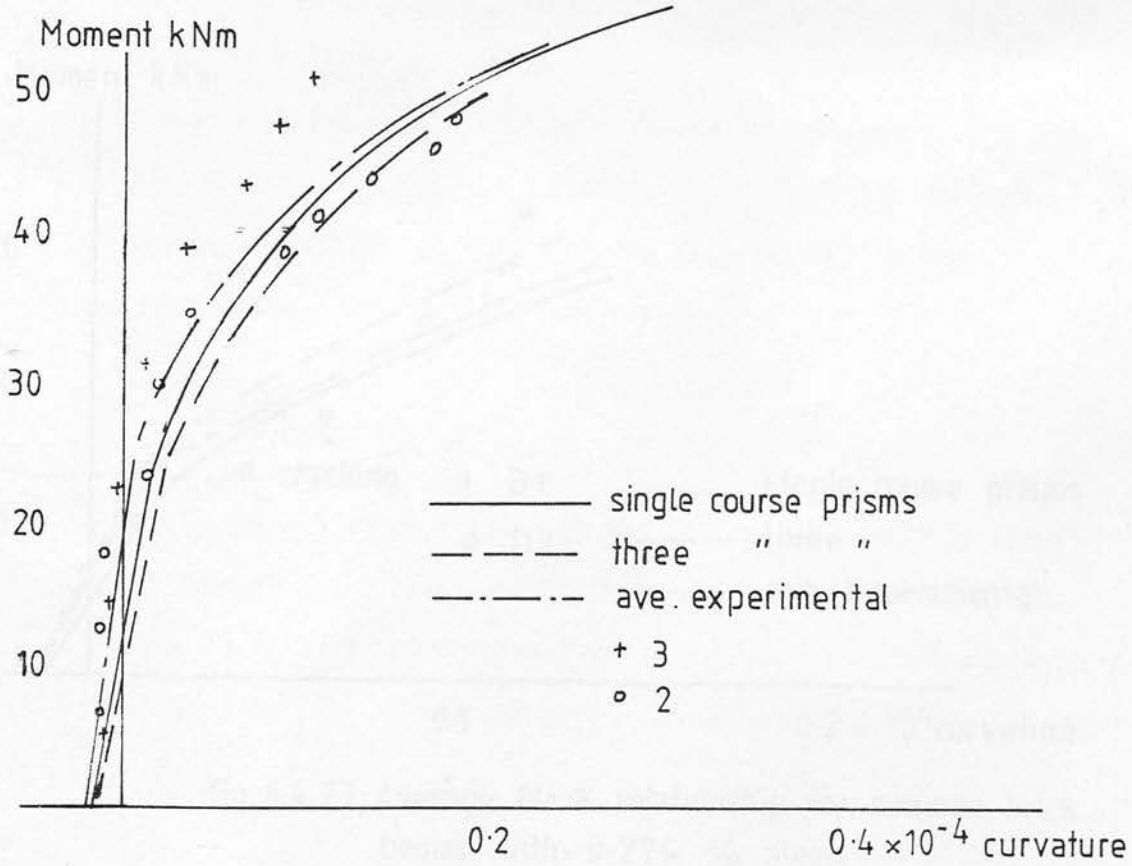

fig. 6.4.21 Average M-Φ relationship for medium strength brick beams with 0·255 % steel.

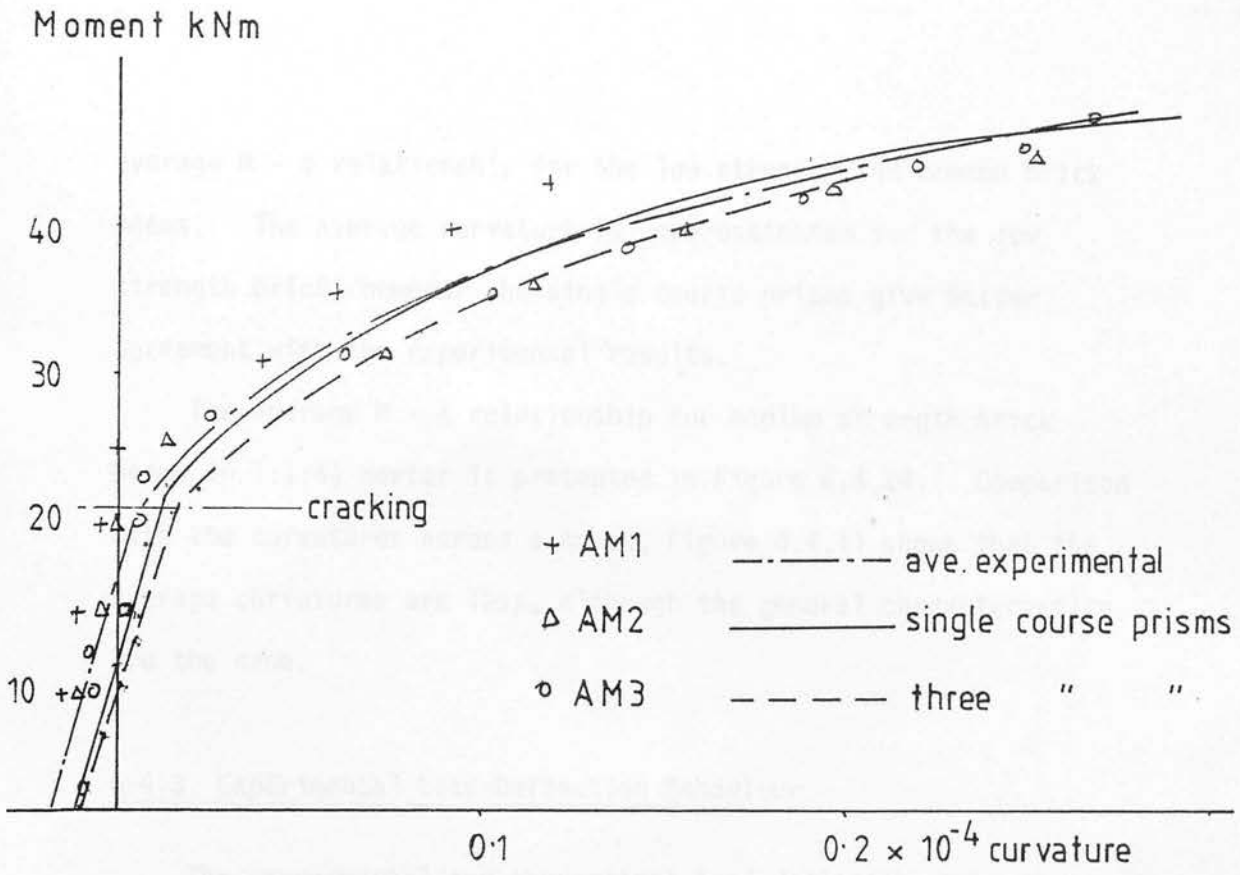

fig 6.4.24 Average M-ϕ relationship for medium strength, in grade II mortar, brick beams with 0·274 % steel.

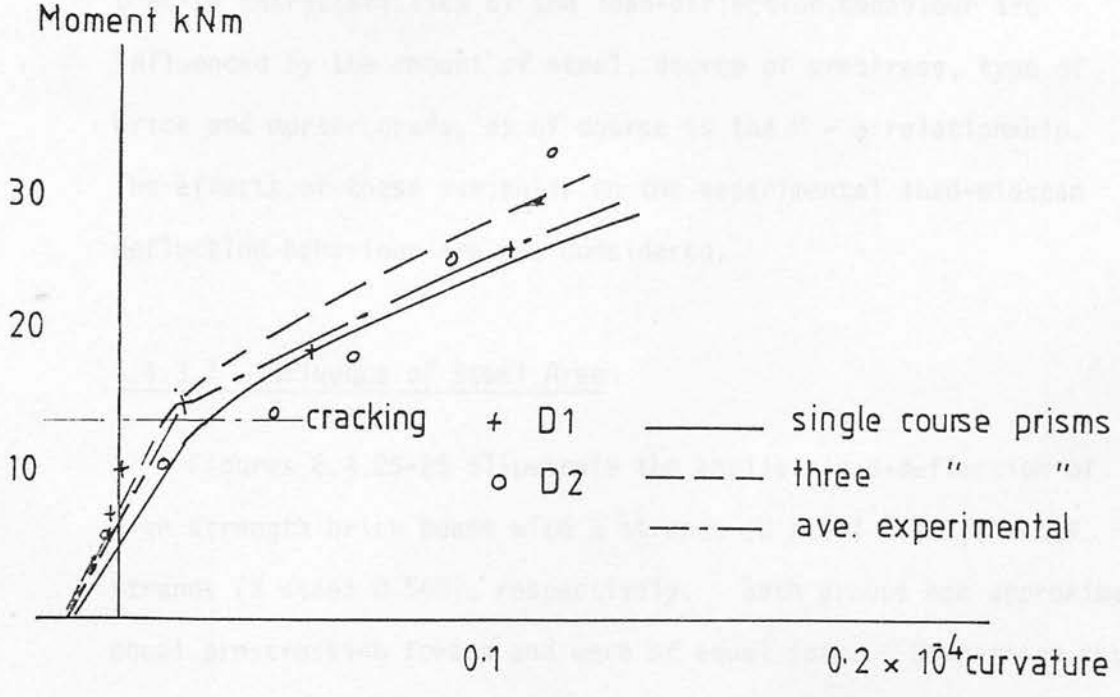

fig. 6.4.23 Average M-ϕ relationship for common brick beams with 0·274 % steel.

average M - ϕ relationship for the low strength and common brick beams. The average curvature is underestimated for the low strength brick, however the single course prisms give better agreement with the experimental results.

The average M - ϕ relationship for medium strength brick beams in 1:$\frac{1}{2}$:4$\frac{1}{2}$ mortar is presented in Figure 6.4.24. Comparison with the curvatures across a crack, Figure 6.4.11 shows that the average curvatures are less, although the general characteristics are the same.

6.4.3 Experimental Load-Deflection Behaviour

The experimental and theoretical load-deflection behaviour are given in Figures 6.4.25-41. For all beams the load-deflection response is initially linear, up to the point where cracking occurs after which the deflection increases more rapidly with load. The precise characteristics of the load-deflection behaviour are influenced by the amount of steel, degree of prestress, type of brick and mortar grade, as of course is the M - ϕ relationship. The effects of these variables on the experimental load-midspan deflection behaviour are now considered.

6.4.3.1 Influence of Steel Area

Figures 6.4.25-26 illustrate the applied load-deflection of high strength brick beams with 3 strands (% steel 0.411), and 4 strands (% steel 0.548), respectively. Both groups had approximately equal prestressing forces and were of equal span. Comparison shows

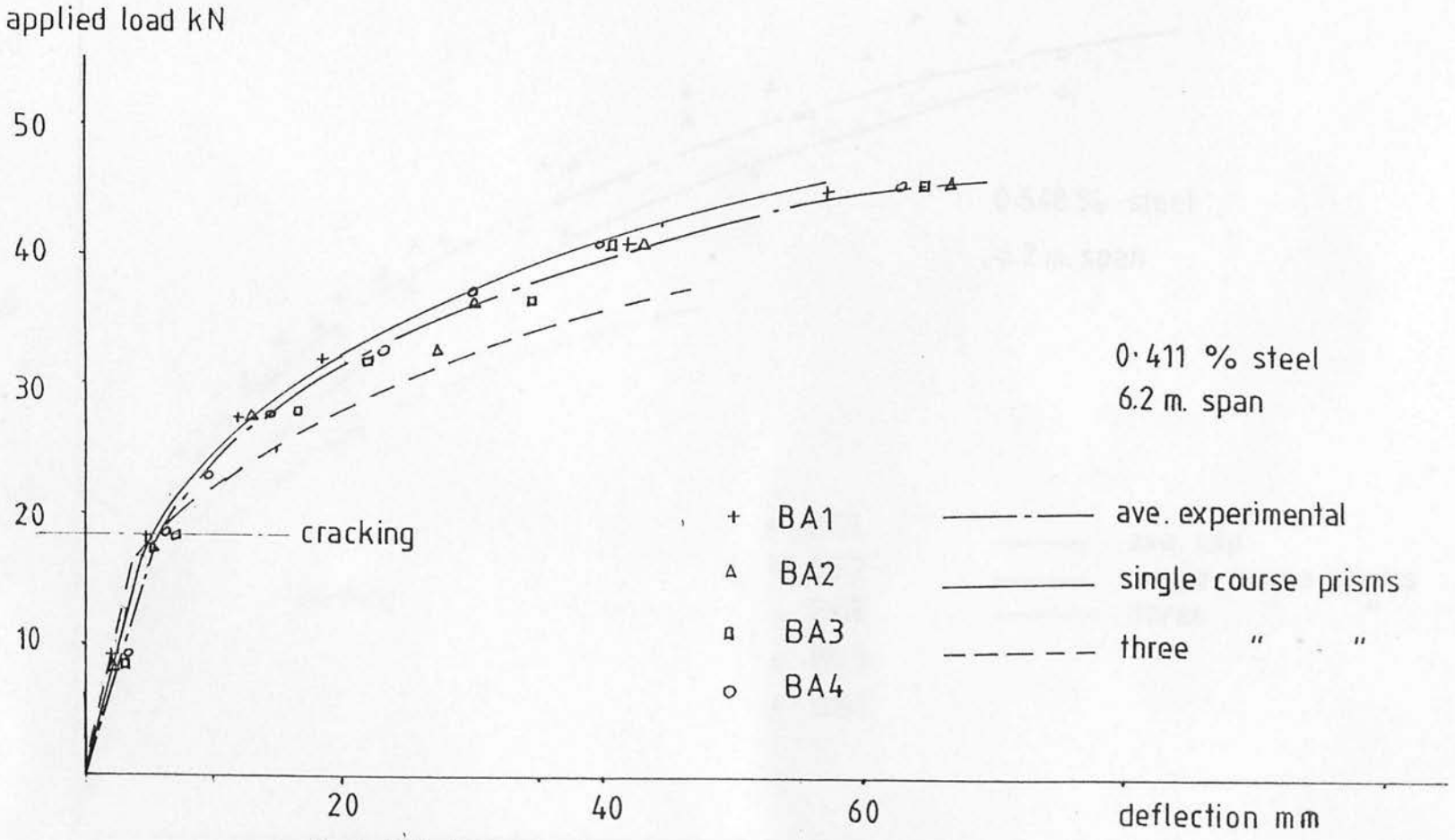

fig 6.4.25 Load/deflection response, high strength brick.

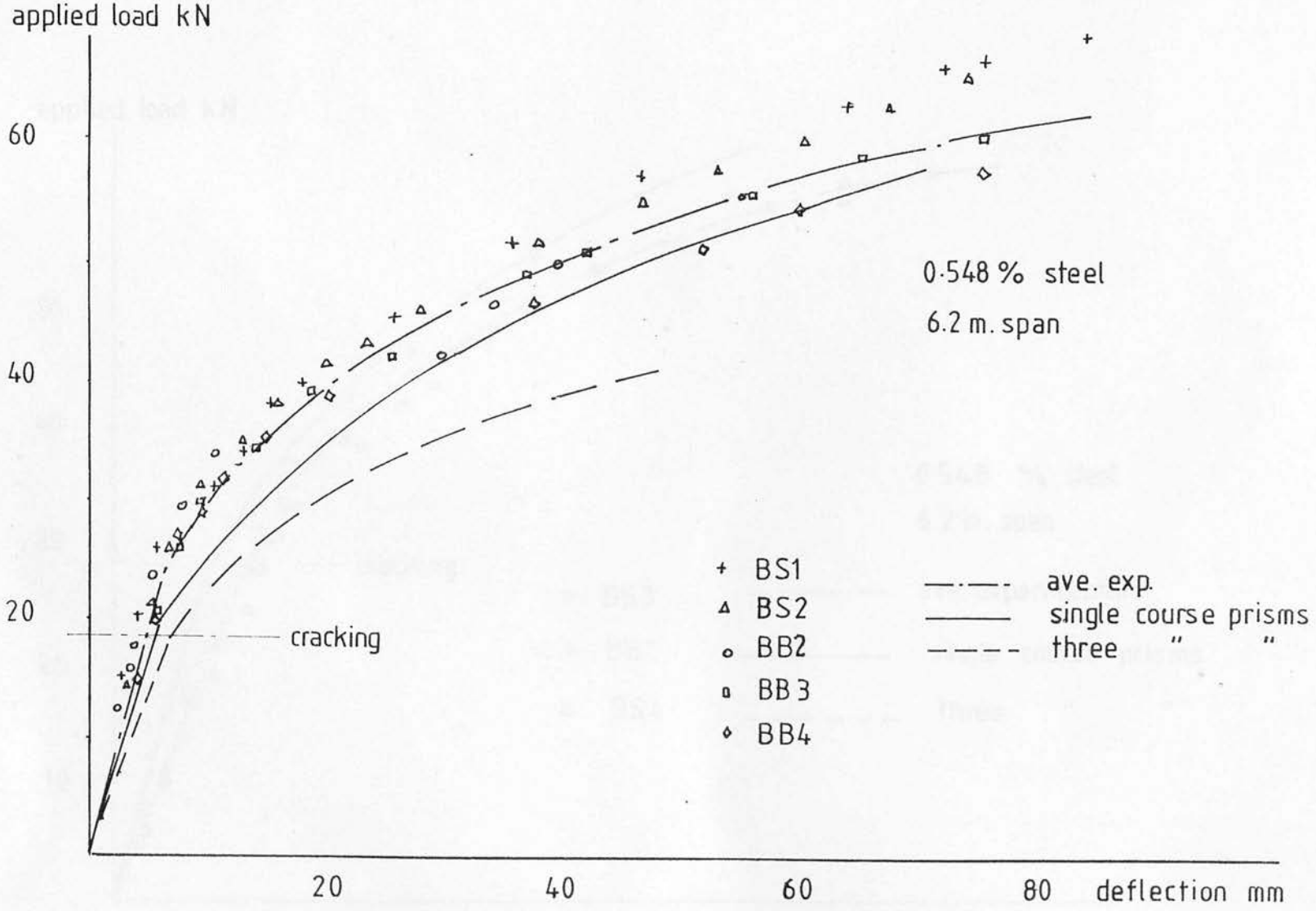

fig. 6.4.26 Load/deflection response, high strength brick

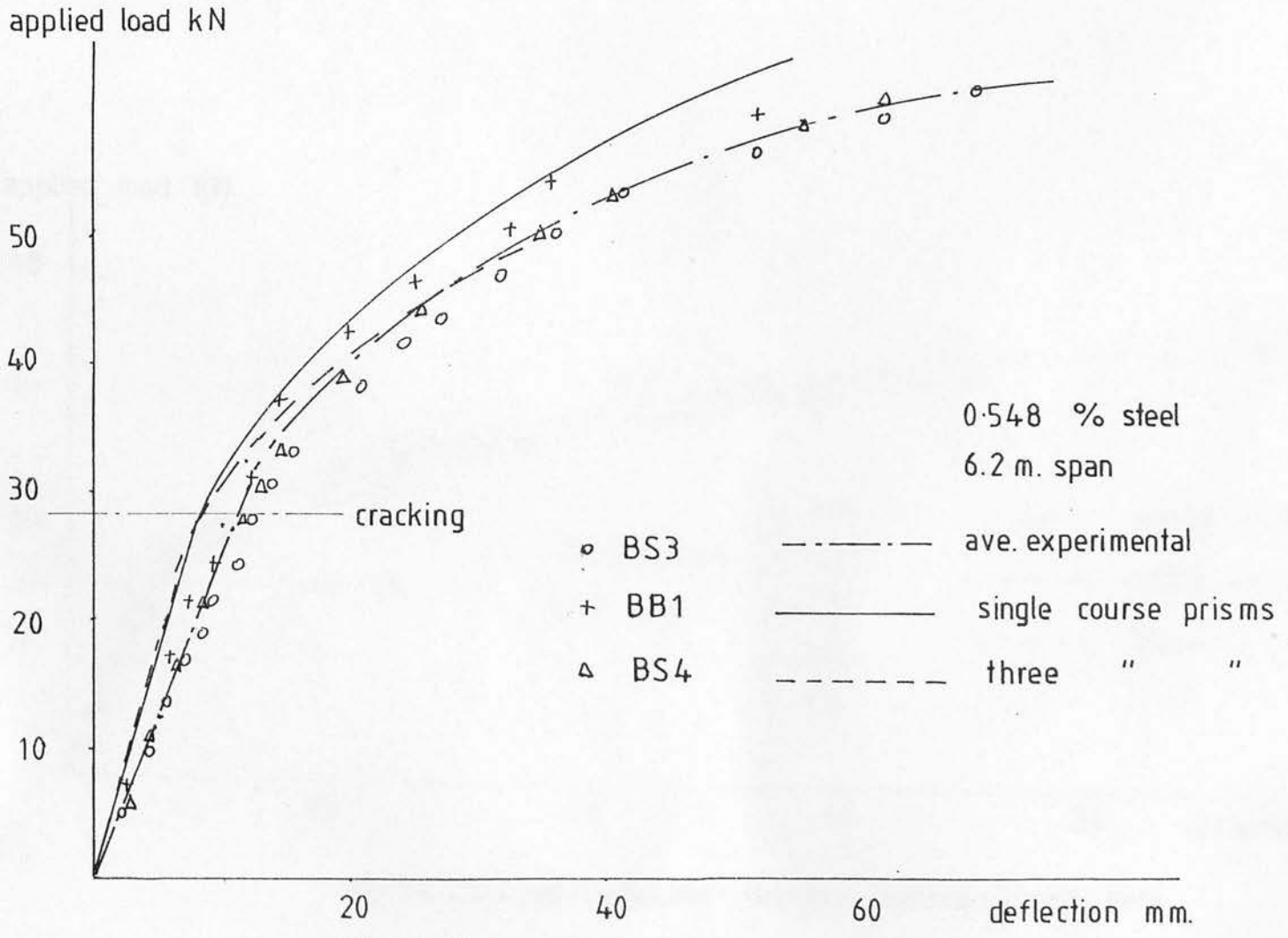

fig. 6.4.27 Load/deflection response for high strength brick.

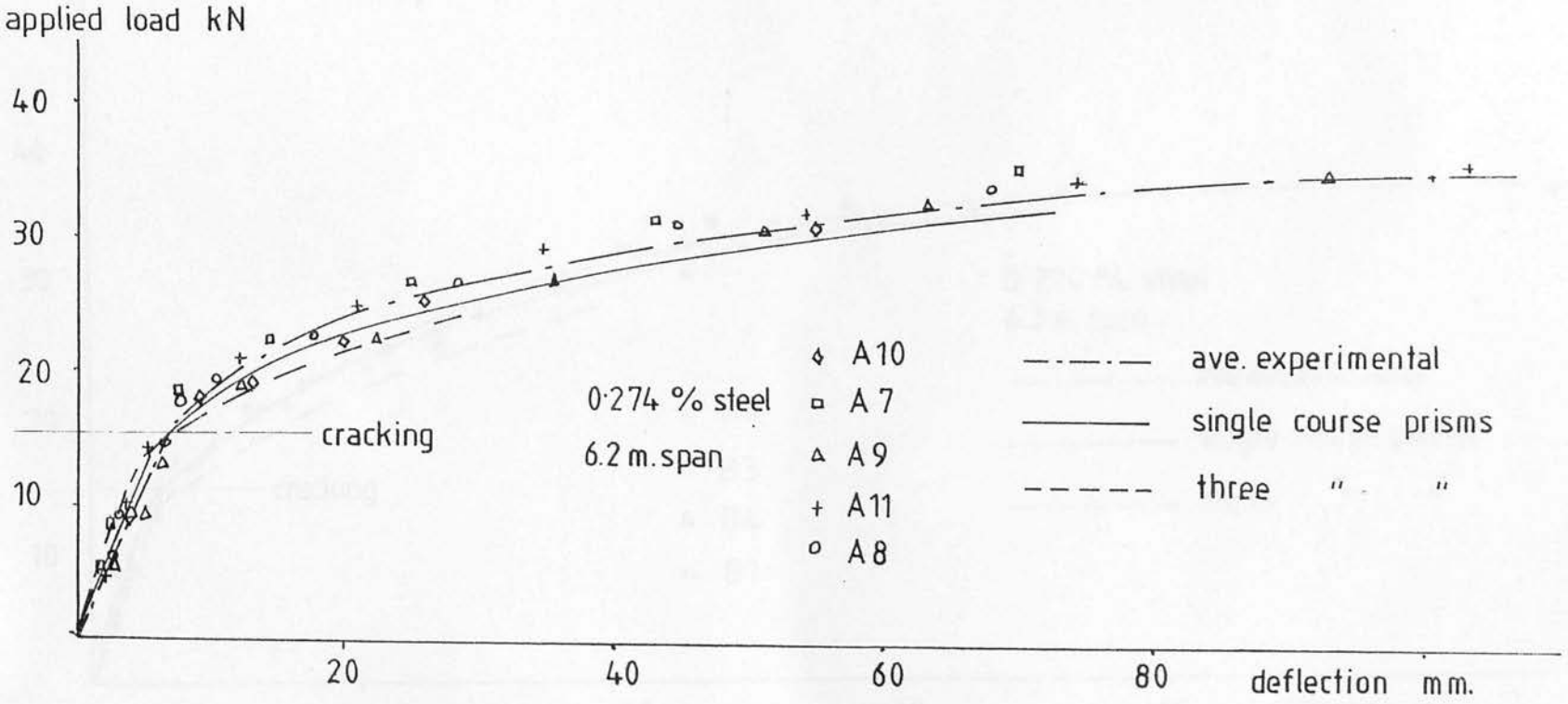

fig. 6.4.28 Load/deflection response, medium strength brick.

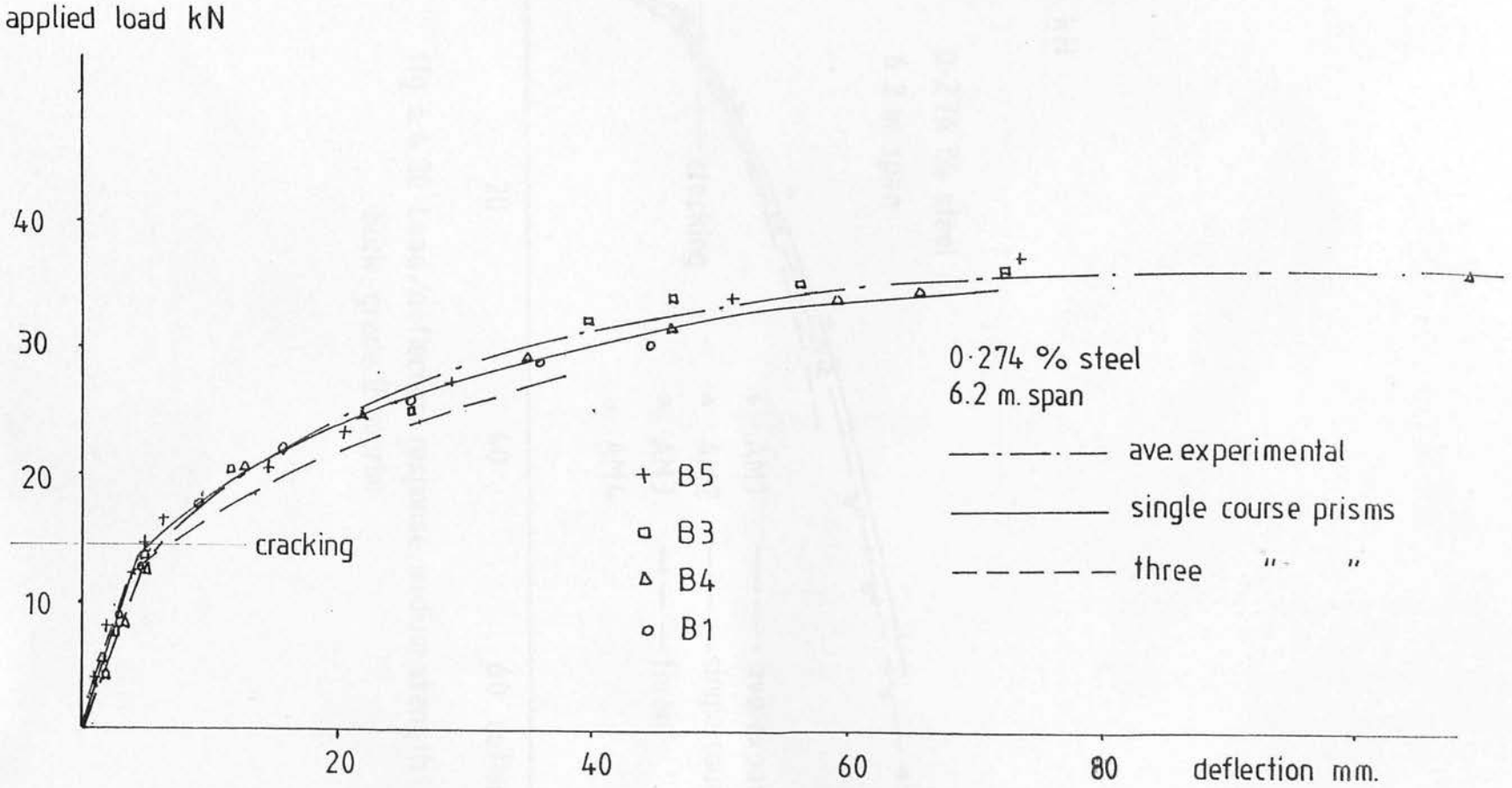

fig. 6.4.29 Load/deflection response, high strength brick.

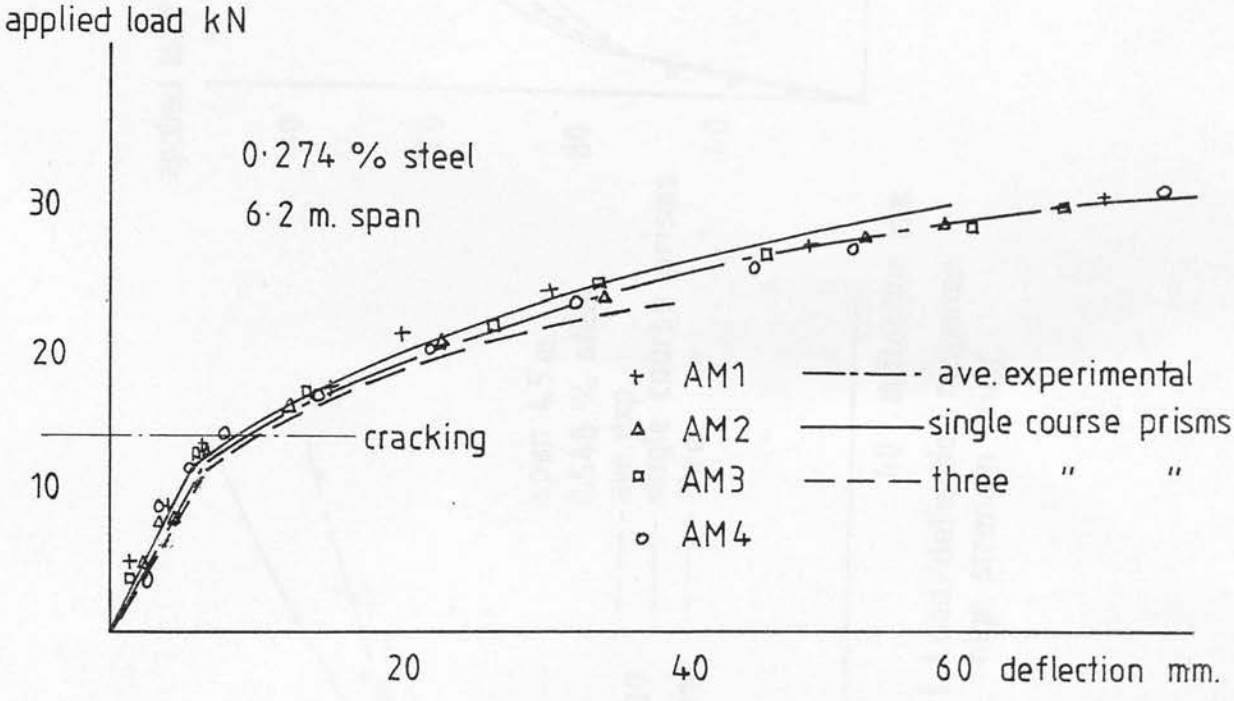

fig. 6.4.30 Load/deflection response, medium strength brick, grade II mortar.

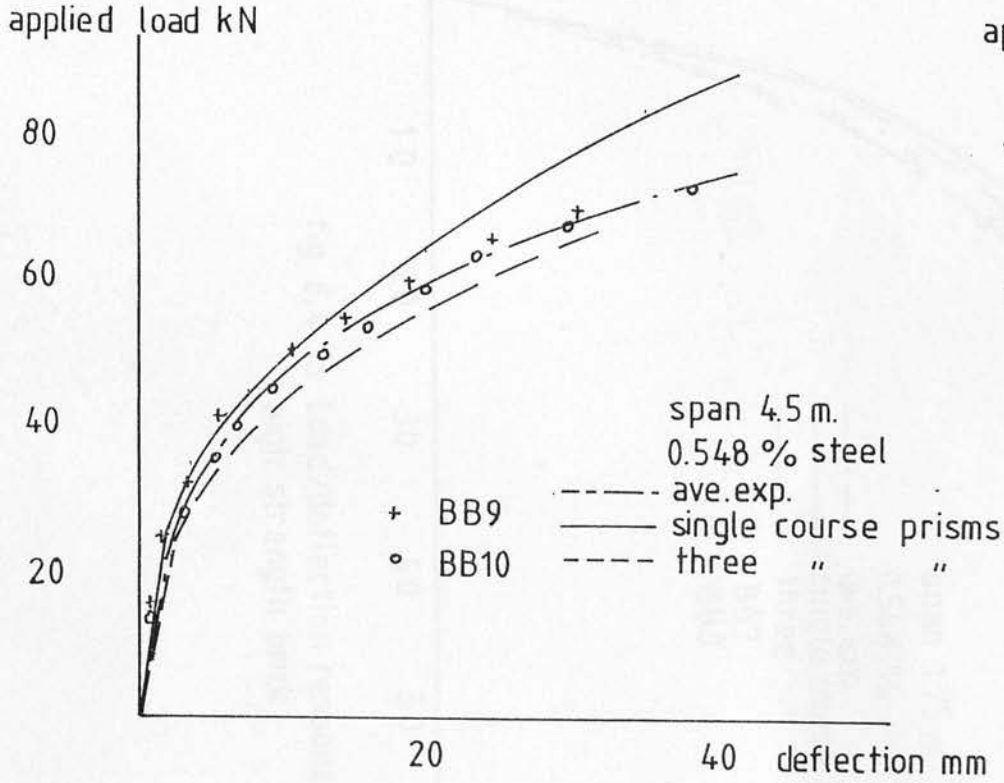

fig. 6.4.31 Load/deflection response high strength brick.

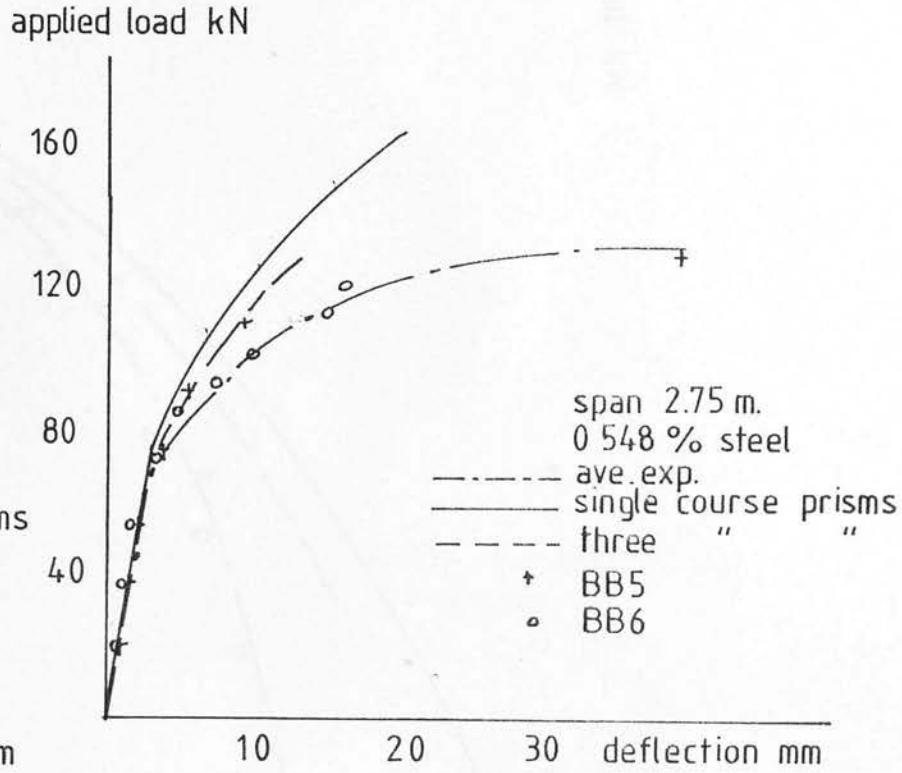

fig. 6.4.32 Load/deflection response high strength brick.

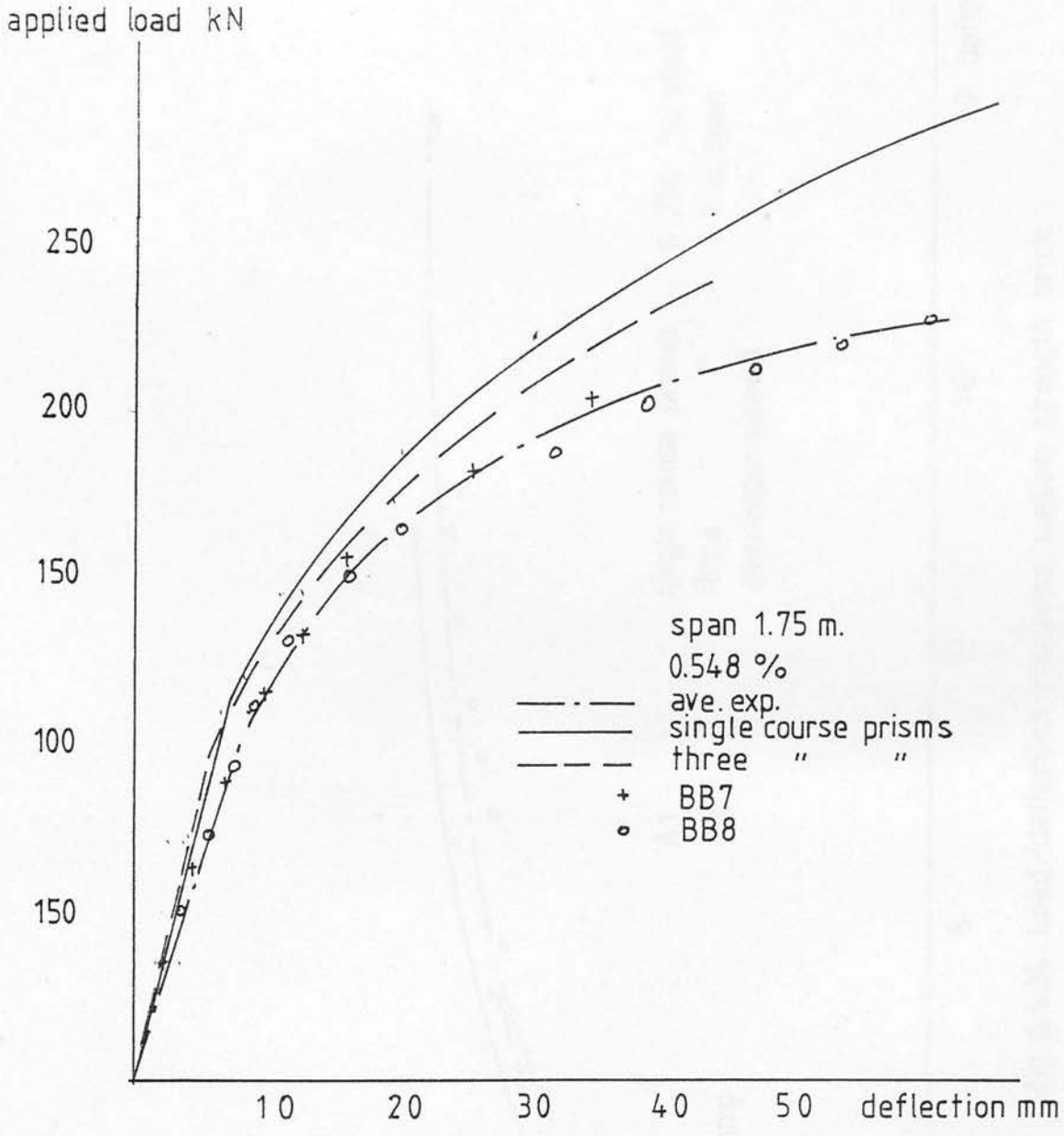

fig 6.4.33 Load/deflection response
high strength brick

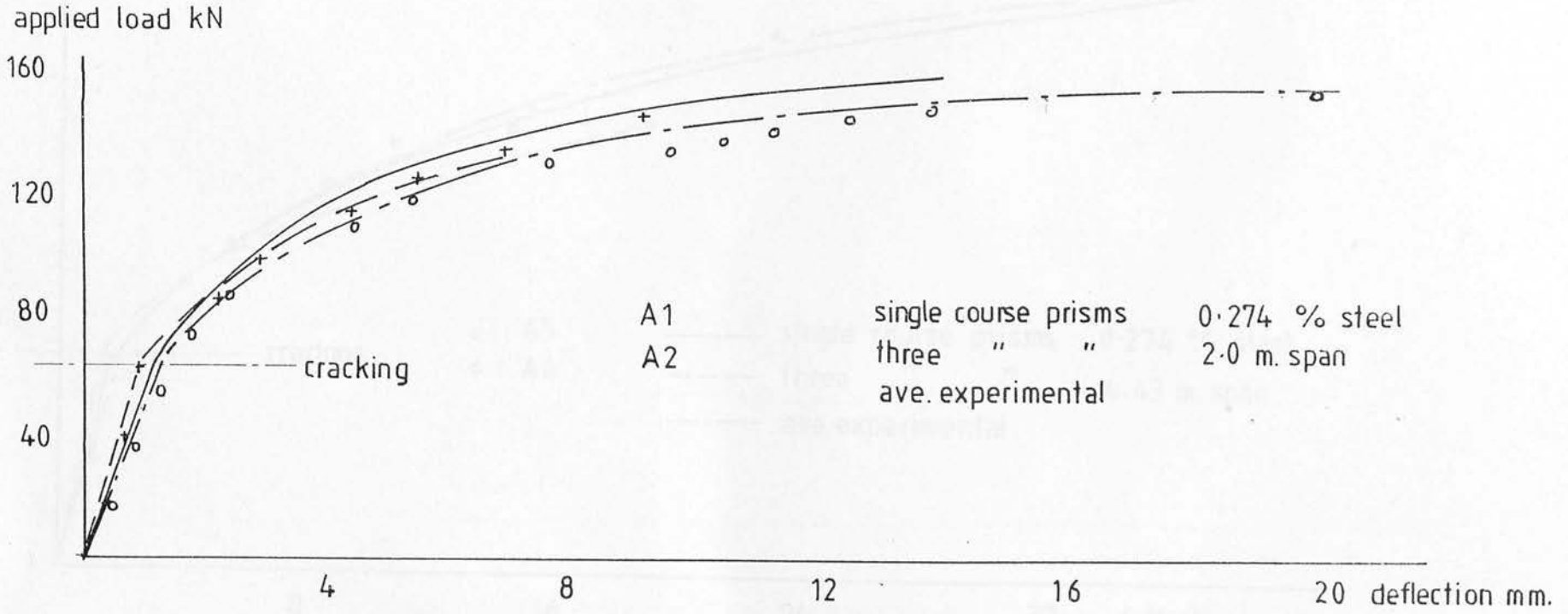

fig. 6.4.34 Load/deflection response, medium strength brick.

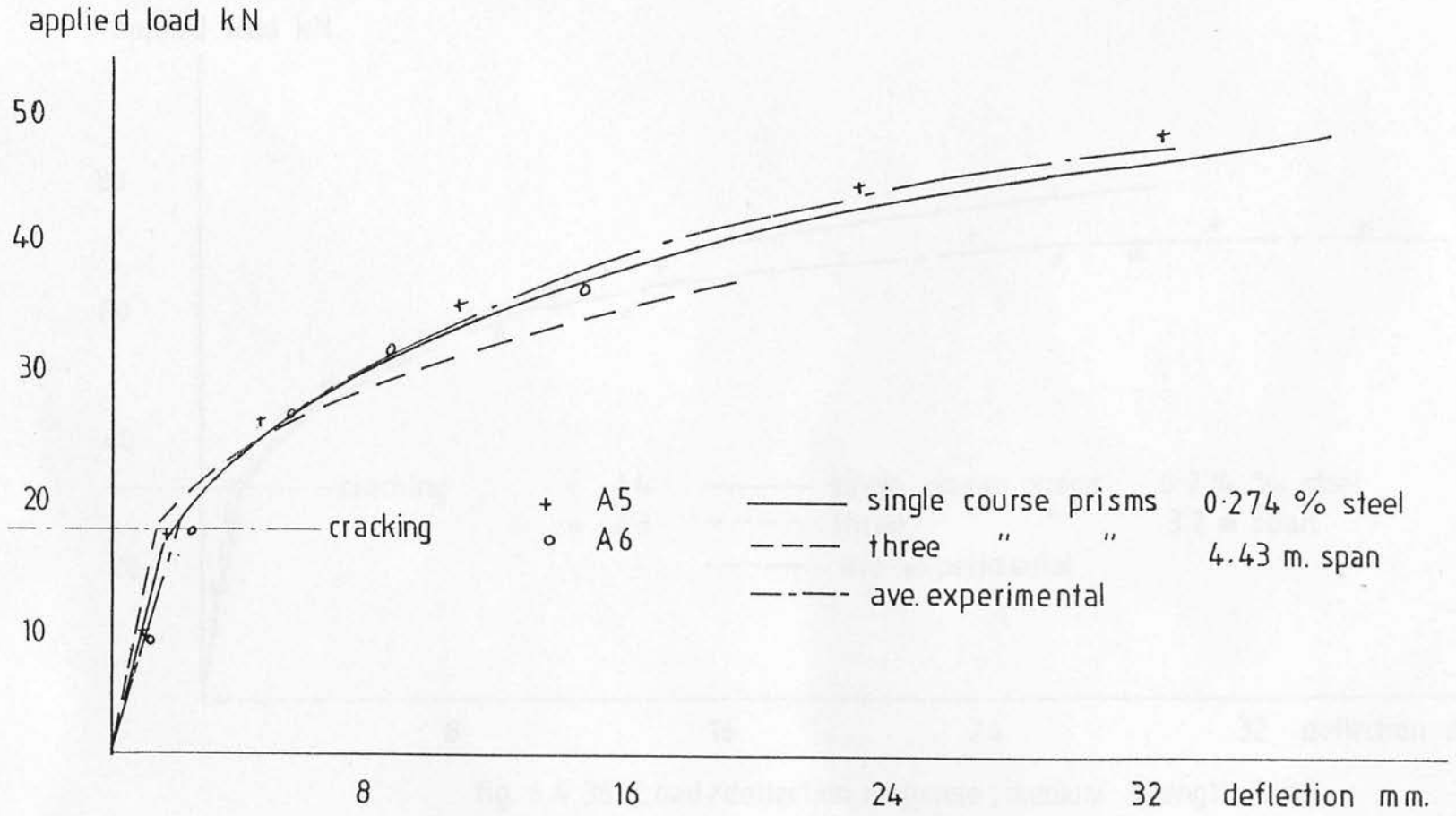

fig. 6.4.35 Load/deflection response, medium strength brick

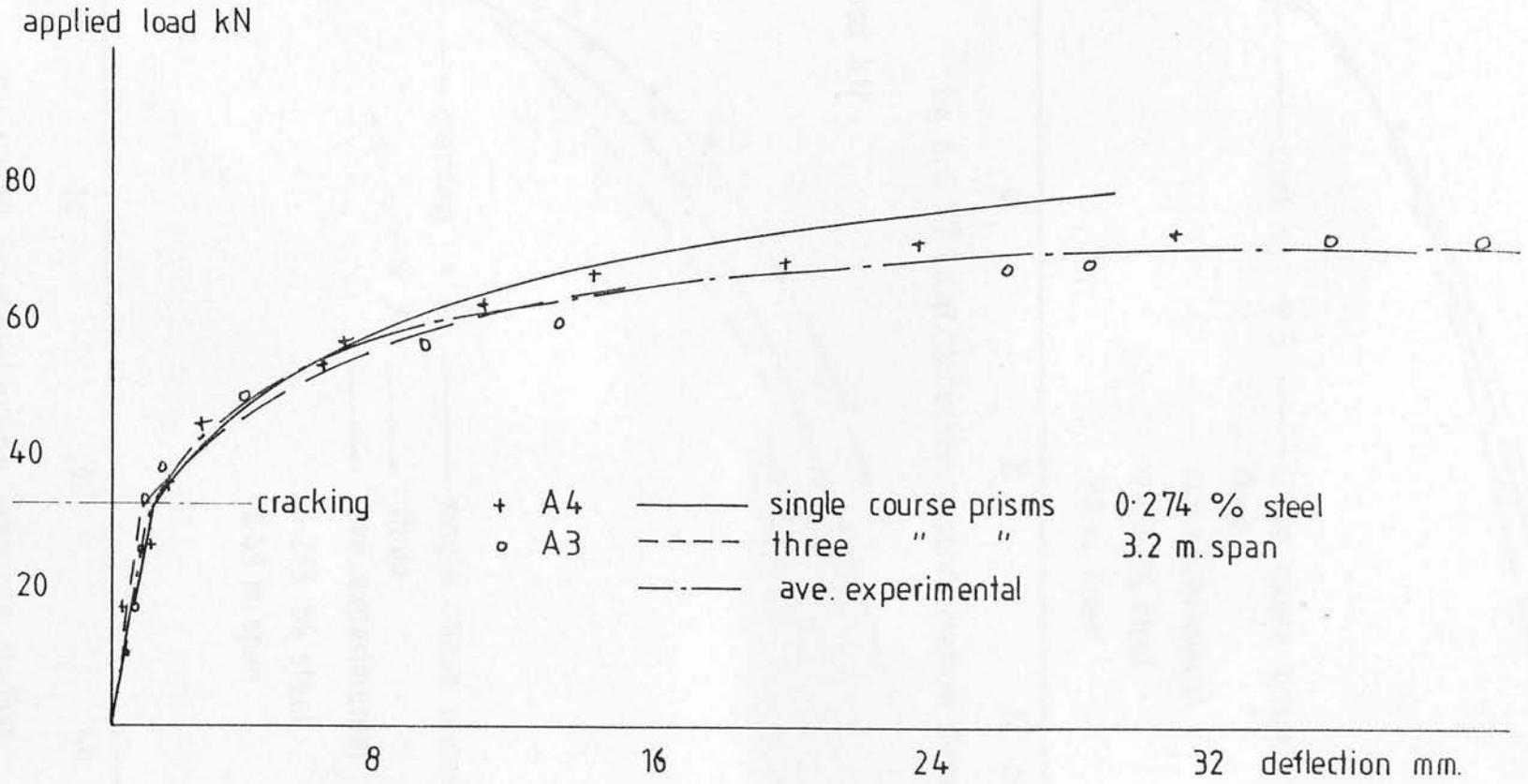

fig. 6.4.36 Load/deflection response, medium strength brick.

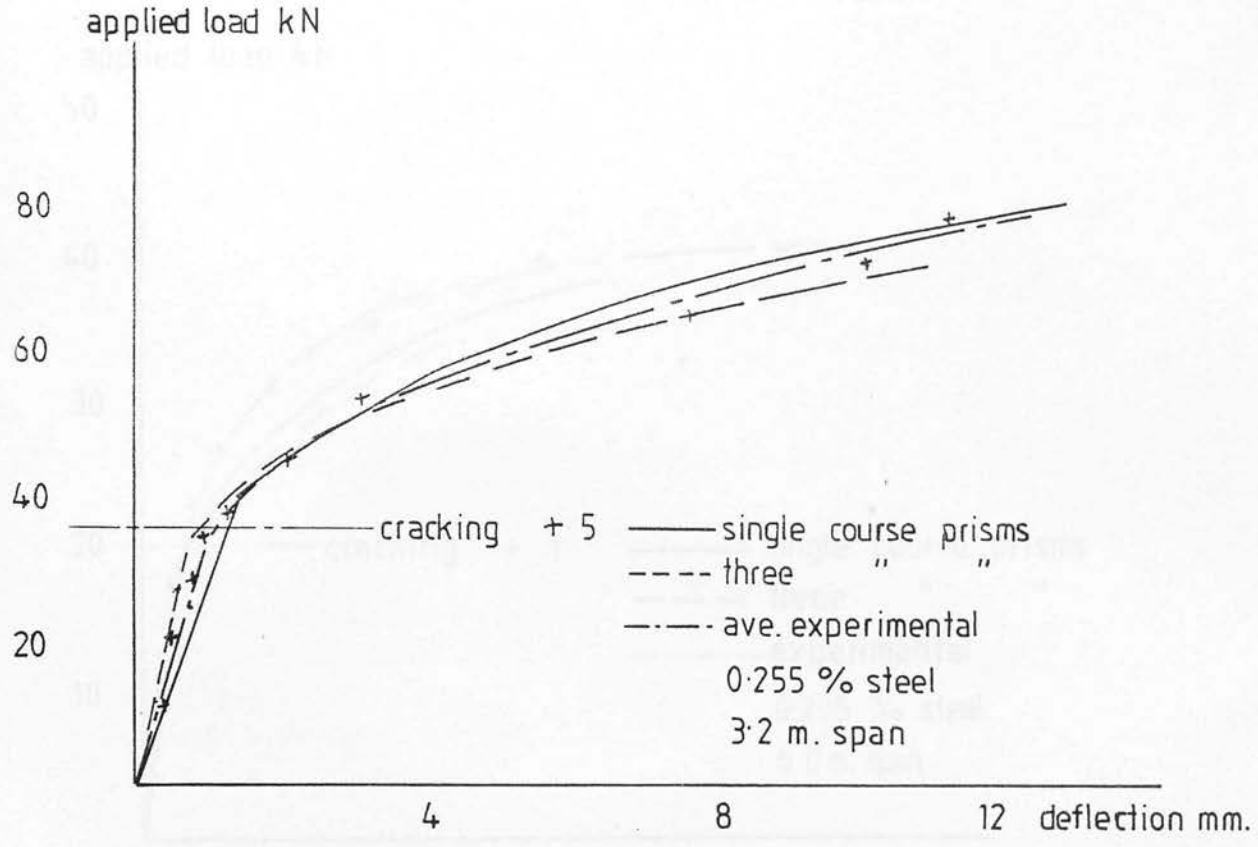

fig. 6.4.37 Load/deflection response, medium strength brick.

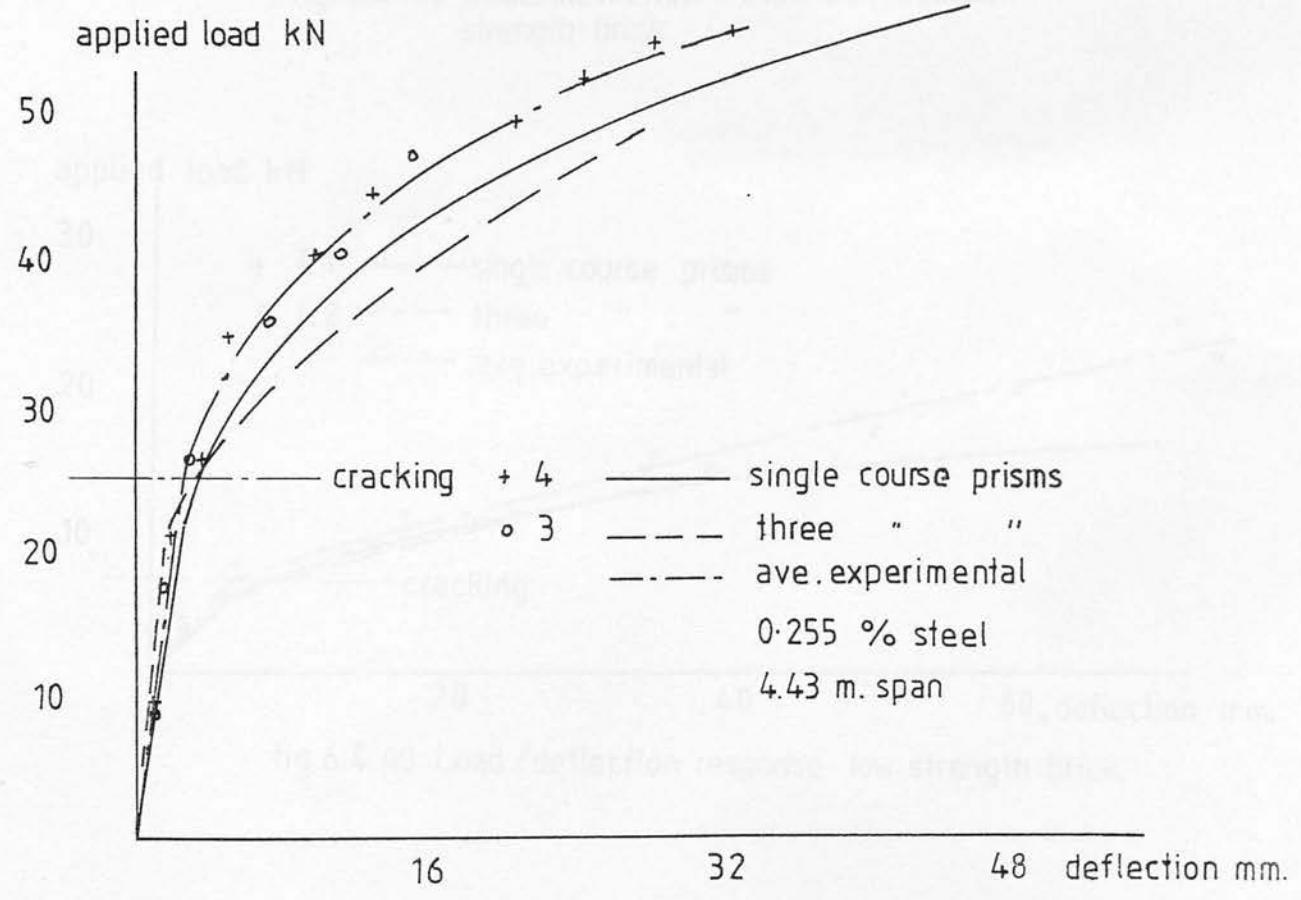

fig. 6.4.38 Load/deflection response, medium strength brick.

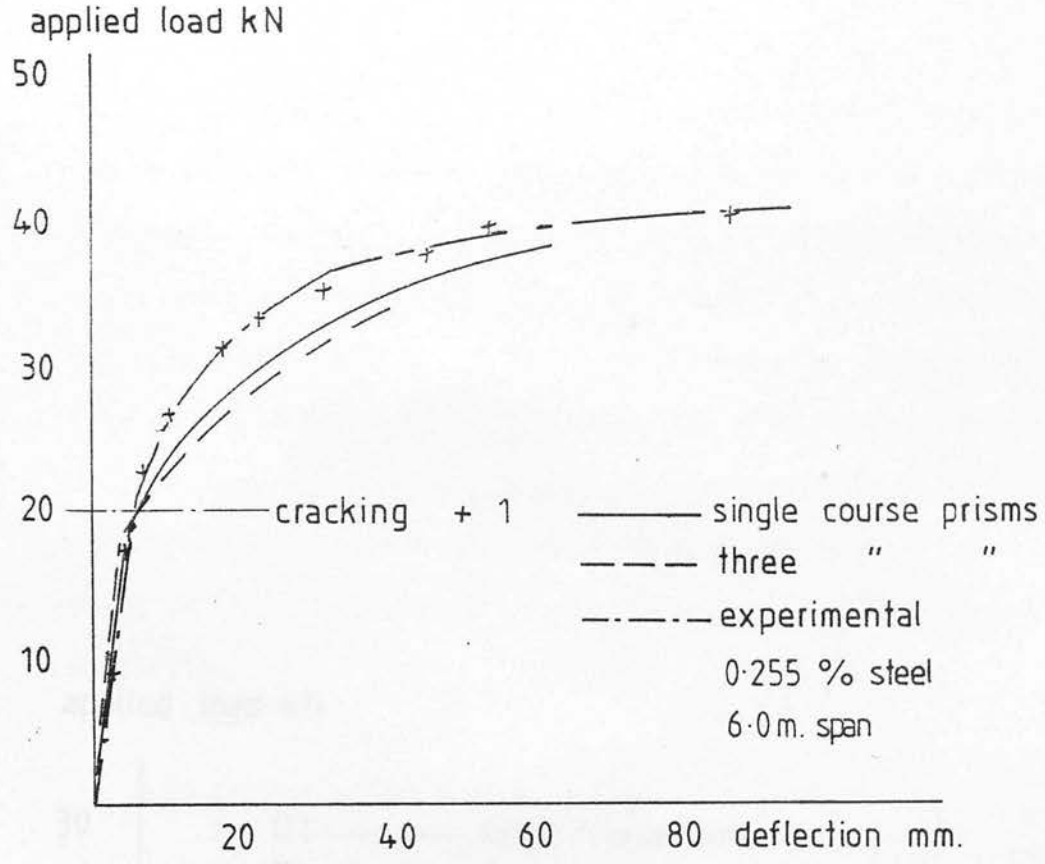

fig. 6.4.39 Load/deflection response, medium strength brick.

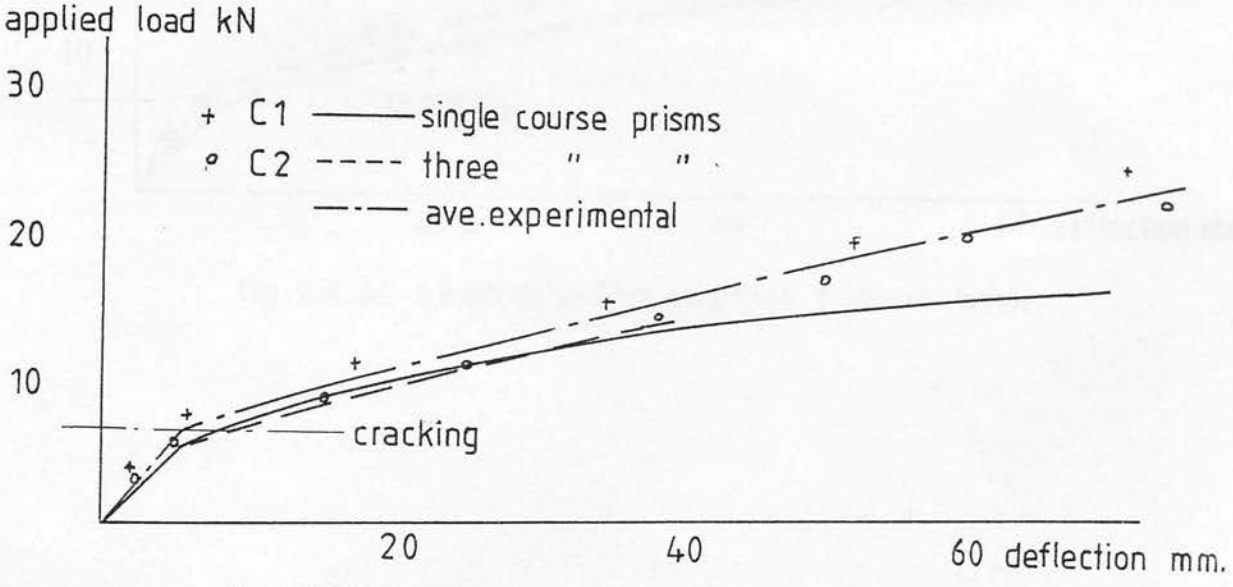

fig. 6.4.40 Load/deflection response low strength brick.

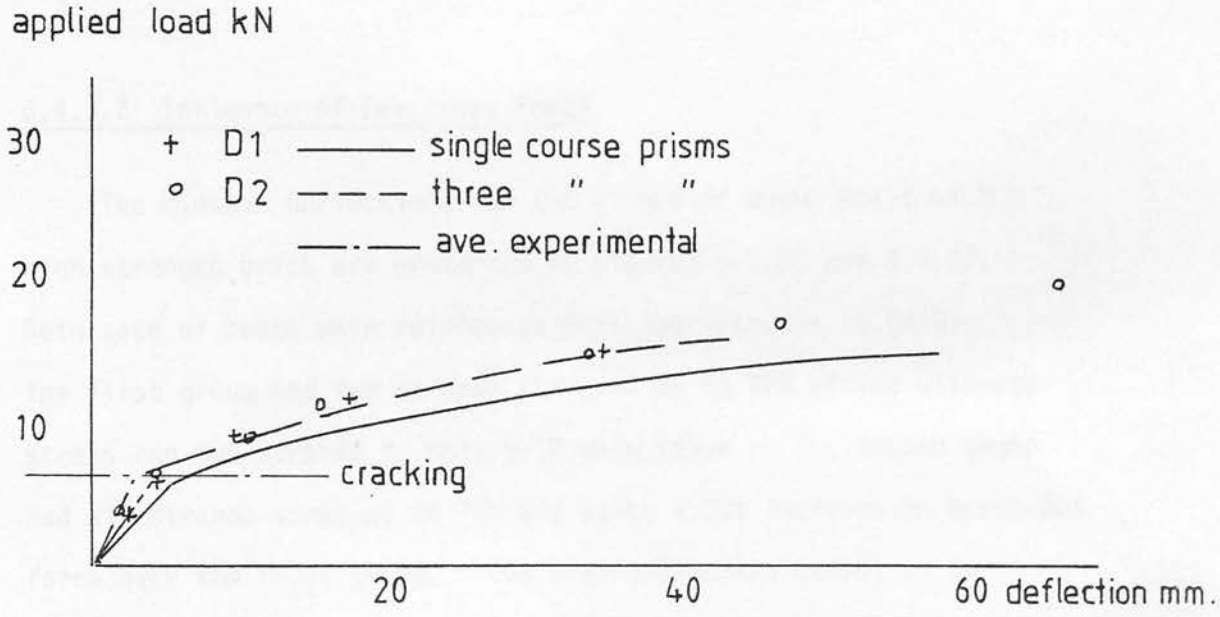

fig. 6.4.41 Load/deflection response, common brick.

that up to cracking which occurs at the same load, the behaviour was very similar. Post-cracking behaviour, however, was somewhat different. The midspan deflection of the beams with the lower steel areas (75% of the other beams), Figure 6.4.25, is considerably greater. Comparison of the M - ϕ relationship for both groups, Figures 6.4.15 and 6.4.17, shows a similar trend. The 25% reduction in steel area caused the stress in the steel to increase in order for the beams to sustain the same moment as the other group, resulting in an increase in strain and consequently curvature and deflection.

6.4.3.2 Influence of Prestress Force

The midspan deflections for two groups of beams built with high strength brick are presented in Figures 6.4.26 and 6.4.27. Both sets of beams were reinforced with four strands (0.548%). The first group had two strands stressed up to 70% of the ultimate stress and two strands to only half this value. The second group had all strands stressed to 70% and hence a 33% increase in prestress force over the first group. The load-deflection curve, up to cracking is approximately equal for both groups of beams, although cracking occurred at different loads, occurring first in the beams with the lower prestress force. The deflections after cracking were therefore greater in these beams. If immediately after cracking the stress in the steel was still in the elastic range as was normally the case, then the increase in deflection for a given load increment will be the same irrespective of the load at which cracking occurred. Comparison of the M - ϕ relationship

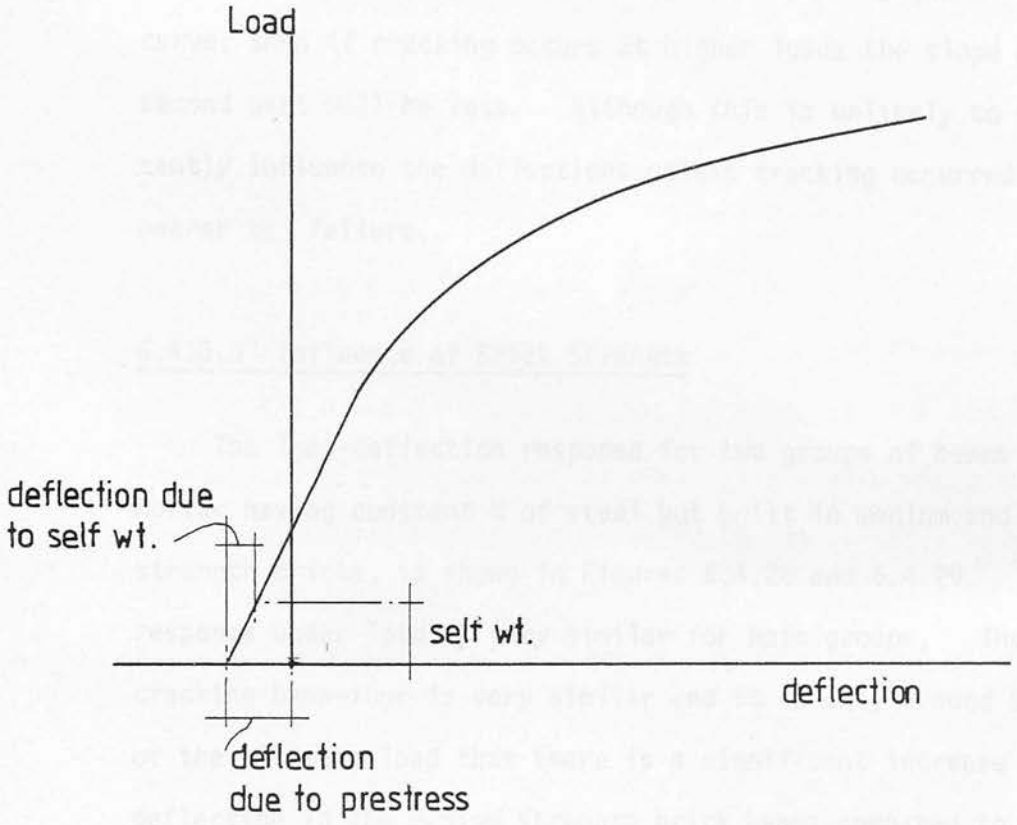

fig. 6.4.42 Effect of prestress on load/deflection response.

Figures 6.4.16 and 6.4.17, show that if they were idealised by a bi-linear curve then the slope of both sections would be approximately equal. Of course due to the non-linear stress/strain relationship of brickwork, this is not strictly correct. Therefore, if the elastic modulus is taken as the slope of the stress/strain curve at the level of stress occurring at cracking and was then used to calculate the second part of the bi-linear curve, then if cracking occurs at higher loads the slope of the second part will be less. Although this is unlikely to significantly influence the deflections unless cracking occurred much nearer to failure.

6.4.3.3 Influence of Brick Strength

The load-deflection response for two groups of beams in 1:¼:3 mortar having constant % of steel but built in medium and high strength bricks, is shown in Figures 6.4.28 and 6.4.29. The response under load is very similar for both groups. The post-cracking behaviour is very similar and it is only around 80-85% of the ultimate load that there is a significant increase in deflection in the medium strength brick beams compared to beams built from high strength brick. This is also reflected in the M - ϕ relationship as given in Figures 6.4.14 and 6.4.19.

6.4.3.4 Influence of Mortar Grade

Figures 6.4.28 and 6.4.30 show the load-deflection response for beams built from medium strength bricks in 1:¼:3 (grade I) and

1:½:4½ (grade II) mortar. Although the prestressing forces were almost identical, it can be seen that the beam built with grade II mortar cracked earlier than those built with grade I mortar. The tensile strength of brickwork is influenced by the mortar grade and this may be the cause for the earlier cracking. In the same vein as previous comparisons, this trend is also highlighted in the M - ϕ relationships, as shown in Figures 6.4.19 and 6.4.24.

6.4.4 Comparison of Experimental and Theoretical Midspan Deflections

Figures 6.4.31-41 compare the predicted deflection with the experimental results for the remaining beams not discussed in section 6.4.3.1-4. These include the beams of high and medium strength of the same section as previous but with different spans, the medium strength brick beams built in the slightly deeper section and those built in low strength and common brick. The M - ϕ relationship, as calculated takes into account the curvatures caused by prestressing and as such predicts an initial upward deflection. During the experiments the deflection caused by self weight cannot be determined. Figure 6.4.42 shows the complete load-deflection behaviour for a prestressed brickwork beam. Normally the absolute deflection caused by self weight will be still upward if measured from a position prior to prestressing. This is the point from which the measured deflections were taken and were all downward. Therefore in order to compare theory with deflections, the theoretical deflections are modified to allow for the self weight.

Comparing the measured deflections with the computed deflections for the high strength brick beams, Figures 6.4.25-27, 6.4.29 and 6.4.31-33, with the exception of Figures 6.4.32-33, the stress/strain relationship from single course prisms gives a better agreement with the experimental results and follows the deflection response up to higher loads. At higher levels of load the deflections are overestimated for beams with lower steel areas with the three course prisms, Figures 6.4.29 and underestimated in Figures 6.4.31-6.4.33. This is caused by differences in predicted M - ϕ relationships as shown in Figures 6.4.14 and 6.4.17. The computed deflections for the medium strength brick beams in 1:$\frac{1}{4}$:3 mortar, Figures 6.4.28 and 6.4.34-39, again showed the best agreement with the experimental results using the relationship from the single course prisms. In two cases the deflections are slightly underestimated, Figures 6.4.34 and 6.4.36, as with the high strength brick beams this may be traced back to the M - ϕ relationship predicting a slightly stiffer section than that obtained experimentally, Figure 6.4.19.

For the remaining beams, Figures 6.4.30, 6.4.40-41, the stress/strain relationship based on single course prisms gives a better representation of the experimental results than the three course prisms for the beams built from low strength brick and medium strength brick in 1:$\frac{1}{2}$:4$\frac{1}{2}$ mortar. The stress/strain relationship from the three course prisms appears to give better agreement with the experimental results for the beams built from common brick, Figure 6.4.41.

The assumptions involved in obtaining the stress/stain relation-

ship from the prisms, i.e. axial load etc., were sensibly, more valid up to higher levels of load for the single course prisms in high, medium and low strength brick as described in Chapter 3. It also appears from Chapter 5 that greater strains measured in the single course prisms are closer to those observed during the experiments. These two factors support the evidence in this section that the single course prisms generally predict the M - ϕ relationship more accurately than the three course prisms.

6.4.5 Deflections in the Shear Span

In normal circumstances, the maximum deflection of a beam, which in this case occurs at midspan, generally received the most consideration. However in some cases it might be necessary to calculate the deflections at other points in the span, i.e. where excessive deflections might interfere with services. The method of calculating the deflections from the M - ϕ relationship using finite differences calculates the deflections at each node point and it is therefore of interest to compare these with measured deflections at points along the shear span. Figure 6.4.43 shows a typical deflection profile for the half span of a high strength brick beam with 0.411% steel. The deflections were measured at 1.0 m, 2.0 m from the support as well as at midspan. It can be seen that the single course prisms predict the deflected shape of the beam more closely than the three course prisms and show good agreement with the experimental results.

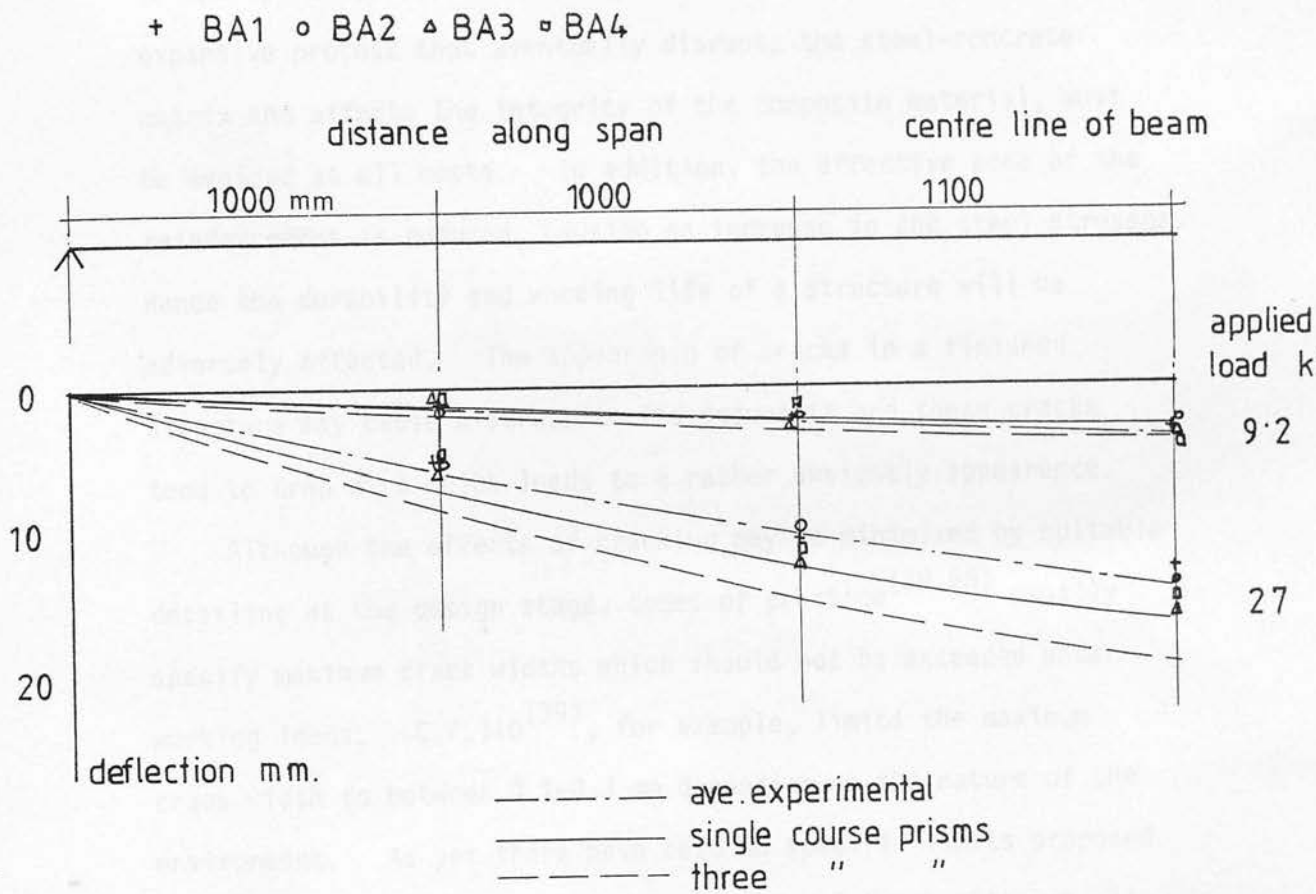

fig. 6.4.43 Typical deflections in shear span for high strength brick beams with 0·411 % steel.

6.5 Cracking of Prestressed Brickwork Beams

6.5.1 General

The control of cracks is recognised as a major problem for the design of reinforced and prestressed concrete. The nature of cracking, its occurrence and magnitude may play an important part in the corrosion of reinforcement. Corrosion, which is an expansive process that eventually disrupts the steel-concrete matrix and affects the integrity of the composite material, must be avoided at all costs. In addition, the effective area of the reinforcement is reduced, causing an increase in the steel stresses. Hence the durability and working life of a structure will be adversely affected. The appearance of cracks in a finished structure may cause distress to its occupants and these cracks tend to trap dirt which leads to a rather unsightly appearance.

Although the effects of cracking may be minimised by suitable detailing at the design stage, codes of practice[39,66] usually specify maximum crack widths which should not be exceeded under working loads. C.P.110[39], for example, limits the maximum crack width to between 0.1-0.3 mm depending on the nature of the environment. As yet there have been no specific limits proposed for the maximum crack width in reinforced brickwork although it does not appear unreasonable that similar limits would be applied. Therefore, it is important to consider methods of calculating the crack widths in reinforced brickwork.

To the author's knowledge there has not been a major study into the factors, viz. type of bars, cover etc., on cracking in

reinforced brickwork. Although, this study was not concerned with this particular aspect which itself can form the basis of a detailed investigation, a semi-empirical method has been suggested similar to that adopted for concrete, based on the results of this work.

6.5.2 Calculation of Crack Widths

Generally, there are two principal methods adopted for calculating the crack widths in reinforced concrete:

Method 1 : This is based on relating the crack width to a 'fictious' tensile stress in the concrete[67,68], assuming that the section were to remain uncracked. An equation of general form is proposed:

$$W = k_1 \, c \, f_{ct} \qquad (6.5.1)$$

where k_1 is a constant obtained experimentally and f_{ct} is the fictious tensile stress in the concrete.

Method 2 : The crack width is related[69] to the average strain, ε_{sm}, in the reinforcement. If the average spacing of the cracks is known then the average crack width is given by:

$$W = S_m \, \varepsilon_{sm} \qquad (6.5.2)$$

This is not strictly correct as there is a recovery of strain in the concrete, away from the steel that will reduce ε_{sm}. This, however, is generally small in comparison with ε_{sm} and is usually ignored.

It has been shown[70] that the crack width in a flexural member is closely related to the strain in the steel, after cracking and so method 2 is inherently more accurate than method 1 in which the effect of steel area is not allowed for. Method 1 has in its favour that it is much simpler to calculate the fictious tensile stress in an uncracked section than the strain in the reinforcement in a cracked section and is therefore more suited to design. In this work the strains in the reinforcement were obtained as part of the process of calculating the M - ϕ relationship and were used in predicting the crack widths to compare with the experimental results.

6.5.3 Crack Spacing

From the Equation 6.5.2 it can be seen that to determine the crack width from the average strain in the reinforcement it is necessary to know the average spacing of the cracks. If a crack forms in a beam, Figure 6.5.1, then there is a minimum distance away from the crack required before another crack can form, S_o. If a second crack forms at a distance greater than 2 S_o, then it is possible for a further crack to form in between these two. If, however, the second crack forms at a distance less than 2 S_o then

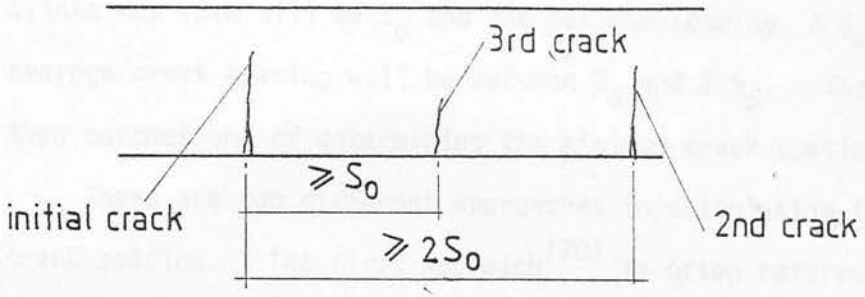

fig.6.5.1 Spacing of cracks

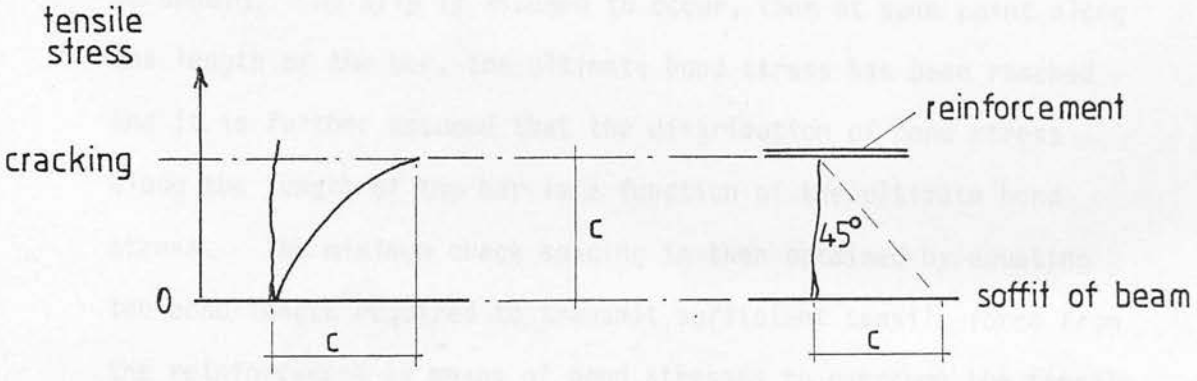

fig. 6.5.2 Effect of crack on stress in beam.

it will not be possible for a third crack to form between these two, as the distance from this third crack to the other two will be less than S_o. Therefore, the minimum spacing at which cracks may form will be S_o and the maximum spacing, $2\ S_o$. The average crack spacing will be between S_o and $2\ S_o$. The problem then becomes one of determining the minimum crack spacing, S_o.

There are two different approaches in calculating the minimum crack spacing. The first approach[70] is often referred to as the 'classical' approach. It is assumed that at a crack plane sections remain plane before and after cracking this then requires slip between reinforcement and concrete in order for this condition to be upheld. As slip is assumed to occur, then at some point along the length of the bar, the ultimate bond stress has been reached and it is further assumed that the distribution of bond stress along the length of the bar is a function of the ultimate bond stress. The minimum crack spacing is then obtained by equating the bond length required to transmit sufficient tensile force from the reinforcement by means of bond stresses to overcome the tensile strength of the concrete. Usually there is some difficulty in defining exactly what area of the concrete is actually effective in resisting the tensile forces and an arbitrary assessment was made which was then correlated with experimental results.

The second method is sometimes called the 'no-slip' approach, in contradiction to the previous method, it is assumed that there is no slip between steel and concrete and that plane sections do not remain planeafter cracking. As there is no slip it is implied that the crack has zero width at the steel-concrete interface and

increases with distance towards the surface of the beam. From elastic theory it can be shown that the distance at which the presence of the crack no longer affects the stresses in the concrete is equal to the cover to the reinforcement, Figure 6.5.2. The stresses in the concrete will be relived at a crack and another crack will only form once sufficient stresses have developed in the concrete and this will only occur at distances greater than or equal to the cover to the steel. Hence S_o is defined as being equal to the cover.

Beeby[71] then considered the actual development of crack spacing as being a combination of both effects. Since the stresses are relieved by the crack plane sections will not remain plane and deformation predicted by the no-slip approach will occur. However, there is likely to be some bond failure causing the stresses around the crack to be further relieved, which is likely to increase the minimum crack spacing. The foregoing methods have been developed by considering an axially loaded tension member and it was normally assumed that these conditions were applicable to the tension zones of flexural members, which does not necessarily follow.

In an un-reinforced concrete column[71] with a load at sufficient eccentricity to cause tension in one face, Figure 6.5.3, then if the load is increased cracks will develop perpendicular to the direction of load. The crack will form to an initial height, h_{cr}. In a similar manner to that of the crack reaching the reinforcement in the 'no-slip' approach the distance at which the stresses in the column are no longer affected by the presence of the crack is equal to the crack height, both of which are analagous

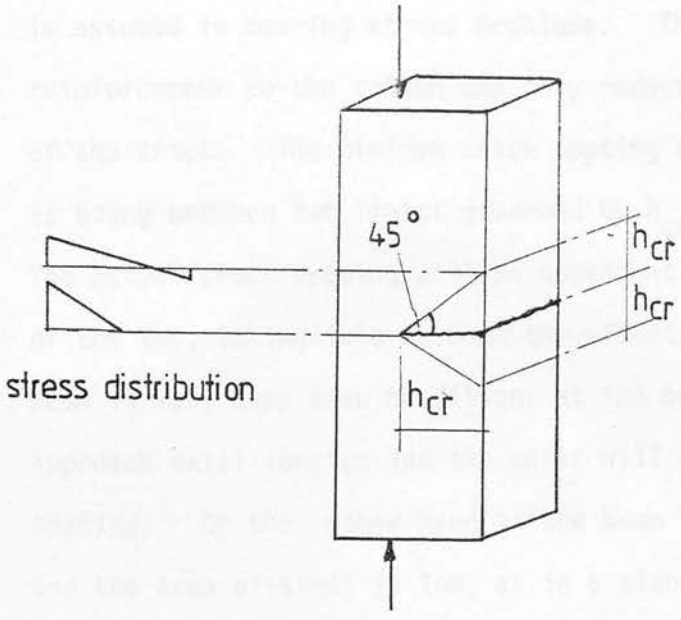

fig. 6.5.3 Cracking in an unreinforced column.

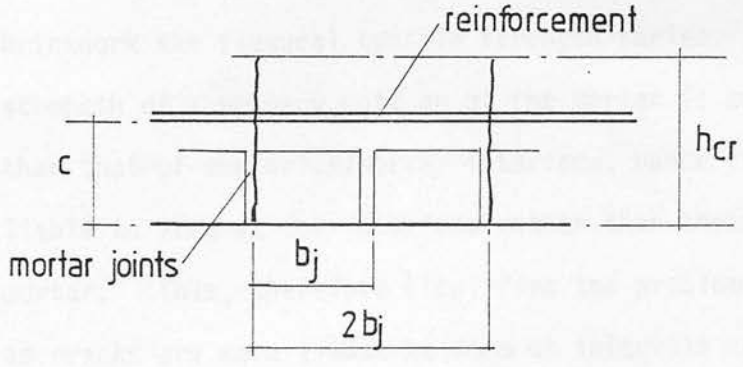

fig. 6.5.4 Crack spacing in brickwork beam.

to taking a 45^{o} dispersion from the edge of the loaded area as is assumed in bearing stress problems. The effect of adding reinforcement to the column can only reduce the initial height of the crack. The minimum crack spacing can then be defined as being between two limits governed by h_{cr} and the cover, c. The actual crack spacing will be dependent on the interaction of the two, taking into account the effects of bond slip. If a beam is very deep then conditions at the bottom of the beam may approach axial tension and the cover will dominate the crack spacing. On the other hand if the beam is relatively shallow and the area of steel is low, as in a slab, then crack spacing will be governed by the initial height of the cracks.

In reinforced or prestressed brickwork, the situation is somewhat different than concrete. In concrete the tensile strength is relatively uniform along the length of the beam, whereas in brickwork the flexural tensile strength varies. The tensile strength of a masonry unit or of the mortar is considerably higher than that of the brick/mortar interface, hence cracking is more liable to form at the interface rather than through brick or mortar. This, therefore simplifies the problem of crack spacing as cracks are more liable to form at intervals coincident with the mortar joints. The cracks may not necessarily form at every brick/mortar interface, but at multiples of the distance between two adjacent joints, b_j, Figure 6.5.4. If the cover to the reinforcement is greater than the smallest joint distance then the average crack spacing must be greater than b_j and if h_{cr} is greater than $2\ b_j$ but less than $3\ b_j$, the average crack spacing will be $2\ b_j$.

For the beams tested in this work the distance, b_j, is equal to 110 mm (the width of one brick and the thickness of a mortar joint). The average crack spacing can then be obtained by comparing the upper and lower limits of crack spacing as predicted by the theory for concrete with the range of possible spacings determined by the bonding pattern. The cover to the strand varied from between 90-128 mm depending on the section considered and the amount of reinforcement. The initial crack height was obtained as part of the process of calculating the M - ϕ relationship, using the single course prisms and was taken as:

$$h_{cr} = h - n \qquad (6.5.3)$$

where n is the neutral axis depth at a crack immediately after cracking.

Table 6.5.1 shows the predicted crack spacing, using this method for the beams in this work.

In the experiments all cracks initiated at the brick/mortar interface and consequently the experimental crack spacings were all multiples of b_j. In the third column of Table 6.5.1 there is a range of crack heights computed for beams with % areas of steel of 0.274. In this group of beams there was a range of brick strengths (high-low) used in the construction of the beams and the corresponding crack heights will vary due to this. From this table it may be seen that the average crack spacing decreased as the % of steel or cover increased. The last column of Table 6.5.1 shows the most commonly occurring crack spacing for the different %

Table 6.5.1 Predicted Average Crack Spacing

% Area of Steel	Cover (mm)	h_{cr} (mm)	Average Crack Spacing (mm)	Experimental Most Common Spacing (mm)
0.274	116	220-255	220	220
0.248	128	222	220	220
0.411	90	192	110	220
0.548	90	171	110	110

of steel, these crack spacings were all taken in the constant moment zone. Figure 6.5.5 shows the distribution of the crack spacings for different % of steel, from which the last column of Table 6.5.1 was obtained. The results from the two groups with 0.274 and 0.248% steel are combined in Figure 6.5.5(c). From this figure it is apparent that the average crack spacing increased as the % steel decreases, however the influence that the differences in the cover have on this trend cloud the issue somewhat. From Figure 6.5.5(a), 55% of the crack spacings are of length b_j while 92% are either b_j or 2 b_j. In Figure 6.5.5(b), the % area of steel has decreased by 25% and only 37% of the spacings are of length b_j, the most commonly occurring spacing being 2 b_j at 53%, however the majority of spacings are either b_j or 2 b_j. In Figure 6.5.5(c), the situation was different, the vast majority of spacings were either 2 b_j or 3 b_j at 84% of the total and the most commonly occurring was 2 b_j at 49%. Bearing in mind that there was only a limited number of specimens tested with 0.411% steel and that the minimum cover was the same as the beams with the higher steel areas, then, although the majority of the spacings lie in the same range the most commonly occurring spacing has increased, suggesting that this was due to the difference in steel areas, which result in a difference in the initial crack height.

Looking at Figure 6.5.5 generally, the greater proportion of the results lie within a range of 2 b_j rather than one particular crack spacing dominating completely and this was probably due to the variability of the strength of the brick/mortar interface, which is affected by such factors as moisture content of bricks

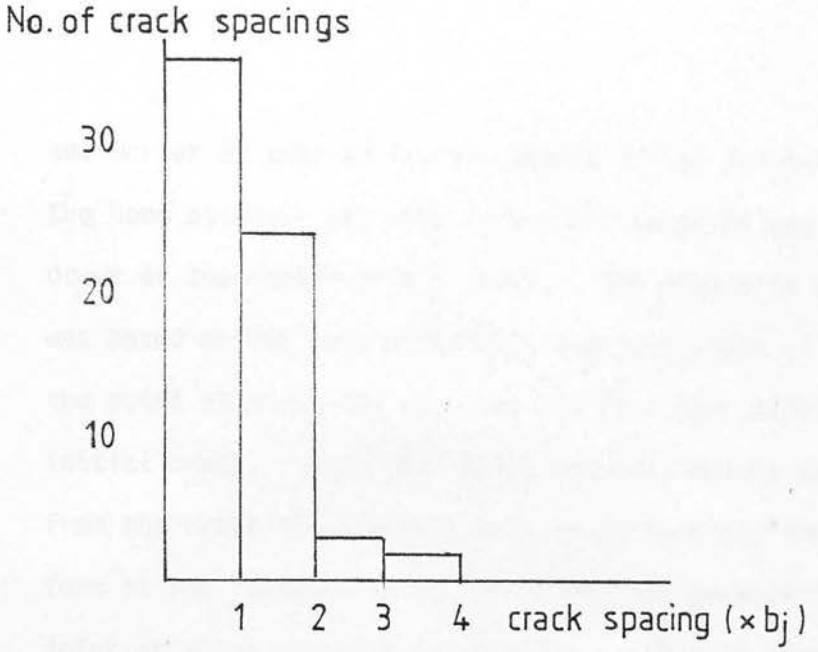

(a) % area of steel 0·548.

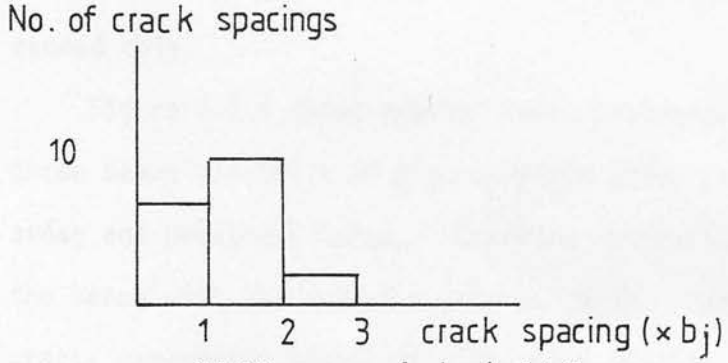

(b) % area of steel 0·411.

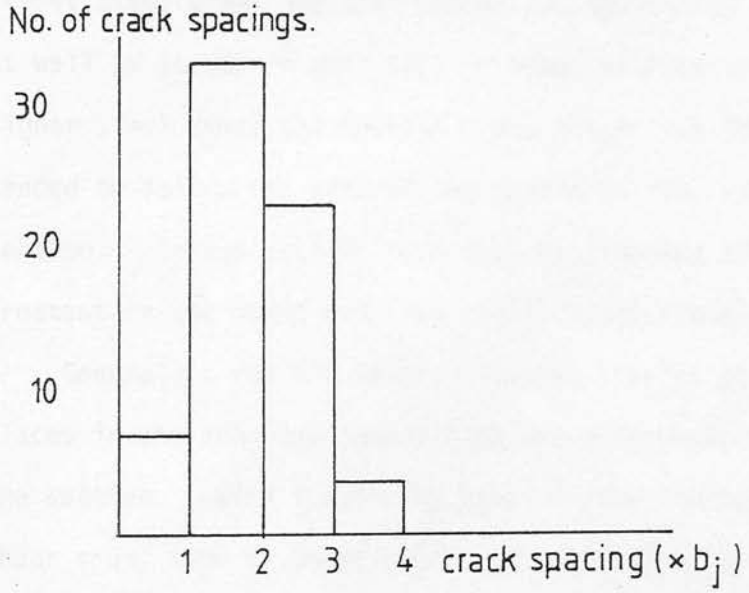

(c) % area of steel 0·274

fig.6.5.5 Distribution of crack spacing.

and mortar at time of laying, poorly filled joints etc., and so the bond strength may vary from joint to joint and cracking will occur at the weaker joints first. The predicted crack spacing was based on the assumption that the next crack will form after the point at which the stresses are no longer affected by the initial crack. From this point onwards, moving further away from the crack the stresses will be uniform and the next crack will form at the weakest joint, which may not necessarily be the first joint at which cracking is possible. Clearly then the predicted crack spacings are the most likely minimum spacings and there is the possibility that a proportion of the actual crack spacings may exceed this.

Figure 6.5.6 shows typical crack propagation patterns for three beams all built of high strength brick but varying steel areas and prestress force. Cracking obviously occurs first in the beams with the lowest prestress force. On first cracking, the cracks penetrated higher into the beam section, in the beams with lowest steel areas and most cracks ran vertically through bricks as well as joints in this type of beam, whereas in those with higher steel areas the initial crack height was lower and the cracks tended to follow the path of the joints as they rose through the section. It can also be seen that the spacing of the cracks was greatest in the beams with the lowest steel areas.

Generally, for all beams, cracking started at one or two places in the constant moment zone and progressed upward through the section. With increasing load, cracks started to form in the shear span, some of these cracks moving diagonally towards the

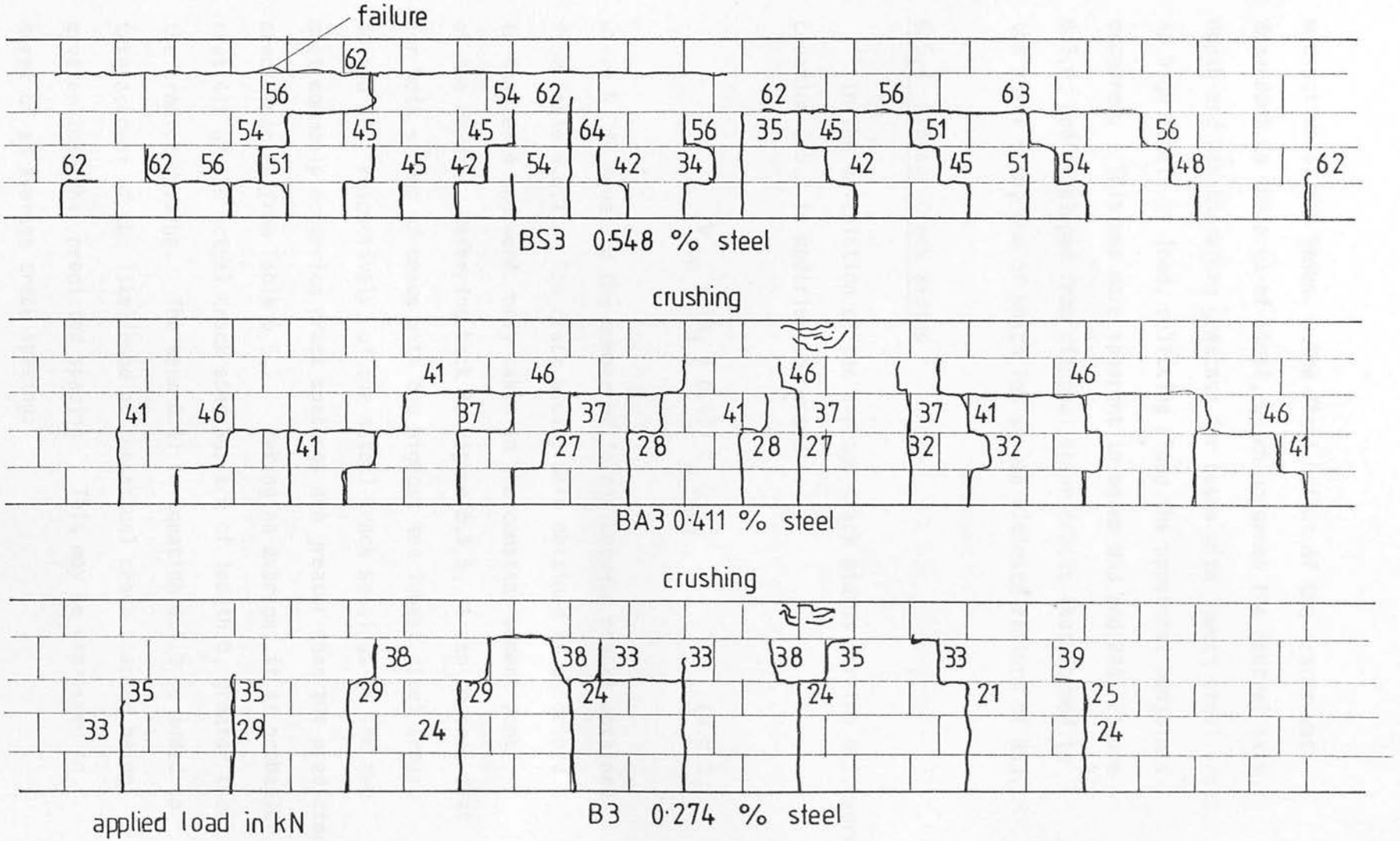

fig. 6.5.6 Typical crack patterns for high strength brick beams.

midsection of the beams. The final height of the cracks was dependent on the area of steel, which governed the neutral axis depth and was therefore greatest for beams with lowest steel areas. At high levels of load, splitting along the uppermost bedjoints occurred. This was more apparent in beams BS3 and BA3, Figure 6.5.6, and developed from diagonal shear cracks that formed in the shear span, one of which led to the ultimate failure of BS3.

6.5.4 Average Crack Widths

In the calculation of the average crack widths for the brickwork, Equation 6.5.2 is modified to become:

$$W_{ave} = (N_j + 0.41)\, b_j\, \varepsilon_{smb} \qquad (6.5.3)$$

where N_j is equal to the number of joints between cracks obtained from Table 6.5.1. The crack widths were obtained as described in Chapter 4 and were only taken in the constant moment zone of the beams. Referring back to Figure 6.5.5, it can be seen that for both groups of beams with the highest and lowest steel areas, 40 and 42%, respectively, of the actual crack spacings of the two most commonly occurring crack spacings are greater than the predicted crack spacing from Table 6.5.1. Taking an average, it is probable that 41% of the actual crack spacings are of length b_j greater than the predicted value. The term 0.41 in Equation 6.5.3 is added to take account of the likelihood of the actual crack spacing being greater than the predicted spacing. This may be expressed in terms of an average crack spacing:

$$S_m = \left(\frac{0.59\ N_j + 0.41\ (N_j + 1)}{N_j}\right) N_j\ b_j \qquad (6.5.4)$$

or

$$S_m = (n_j + 0.41)\ b_j \qquad (6.5.5)$$

The results of Figure 6.5.5(b) for the beams with 0.411% steel were ignored in obtaining Equation 6.5.5 due to the comparatively small number of results in relation to the two other groups.

In Equation 6.5.3 ε_{smb} is the average strain at where cracking is considered. This was obtained from the average additional strain at the level of the strand, calculated using the stress/strain relationship from the single course prisms, and the following Equation 6.5.6:

$$\varepsilon_{smb} = \left(\frac{d_1 - n}{d - n}\right) \varepsilon_{sam} \qquad (6.5.6)$$

where d_1 is the distance from the top fibre of the beam to the point at which the crack is considered.

During the experiments it was not possible to measure the crack widths at the soffit of the beams and so all crack widths were taken at approximately 25 mm from the soffit. In some instances the sides of the crack were quite smooth, in others, the side of the crack on the mortar joint was very ragged. When the latter occurred the crack width was measured at a point where the irregularities appeared to be a minimum. Crack widths were not measured in the first series of beams 1-7, and only a limited

number on the low strength and common brick beams. A typical relationship between average crack width and ε_{smb} for high strength brick with 4 strands is shown in Figure 6.5.7. Given the scatter of the experimental results there is a linear variation of average crack width and average strain. Comparisons of the measured crack widths and predicted crack widths using Equation 6.5.3 are shown for the high and medium strength brick beams in Figures 6.5.8-13. In some instances, especially in beams with lower steel areas, the crack widths at higher levels of load became very wide, up to 3 or 4 mm. However, as previously mentioned the limits on crack widths would be much lower and therefore crack widths up to 0.8 mm only were considered. The crack widths in Figure 6.5.8-13 are plotted against the applied moment after cracking. By adopting this approach slight variations in prestressing forces are allowed for. There is a considerable scatter of the experimental results, especially in Figure 6.5.9. Given this variation, Equation 6.5.3 provides a reasonably accurate prediction of the actual behaviour. The predicted crack widths generally over-estimate the experimental results, slightly in the earlier stages of cracking. A possible explanation of this is as follows. Once the cracking moment has been reached only one crack forms initially, therefore, the relationship between the crack width and crack spacing is not valid. The crack width is then related to the average strain at this level along the total length of the beam minus the average strain prior to cracking. As there is only one crack formed at this stage then the difference between the strains before and after cracking will be small and the influence of the

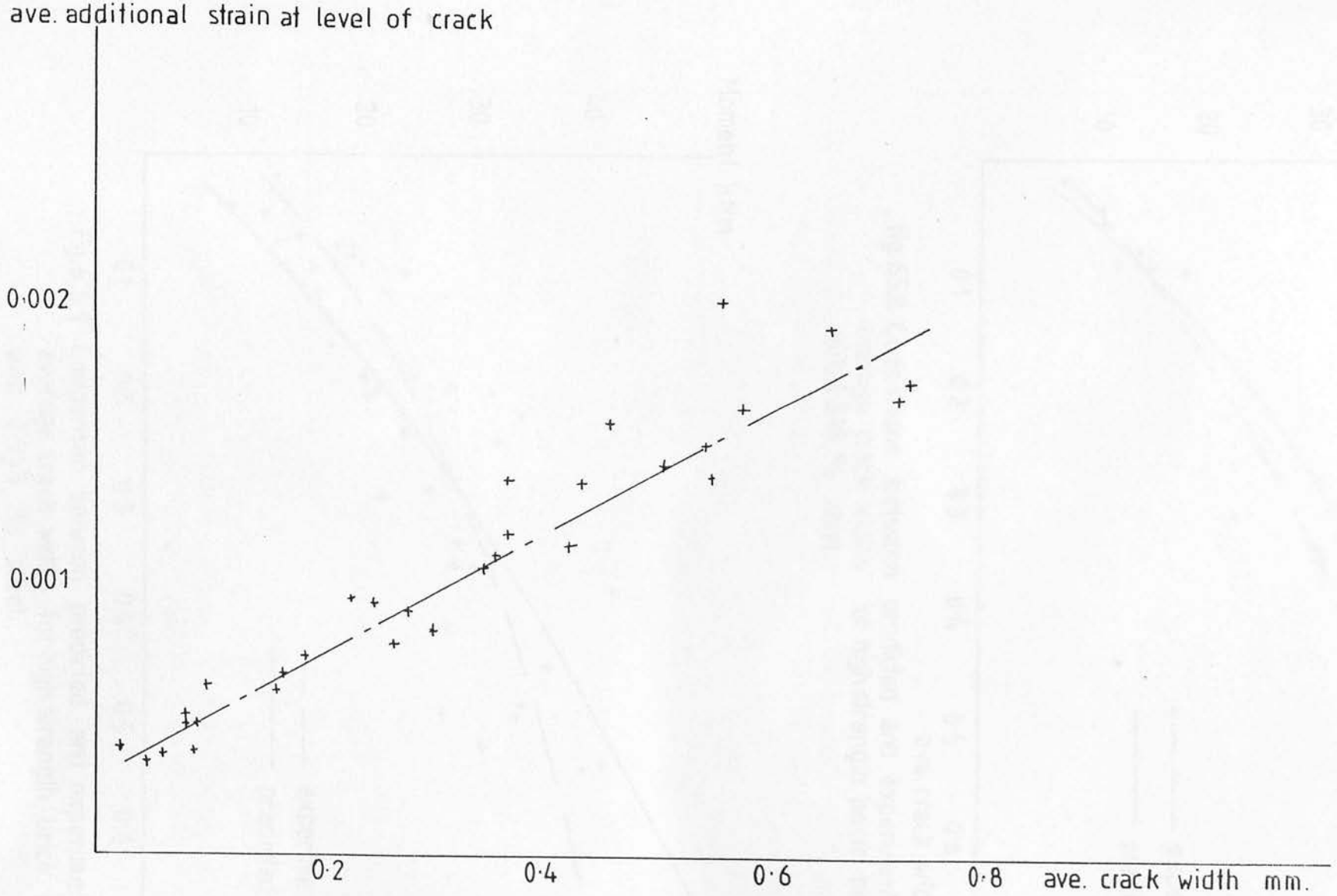

fig. 6.5.7 Typical relationship between strain and ave. crack width for high strength brick beams with 0·548 % steel.

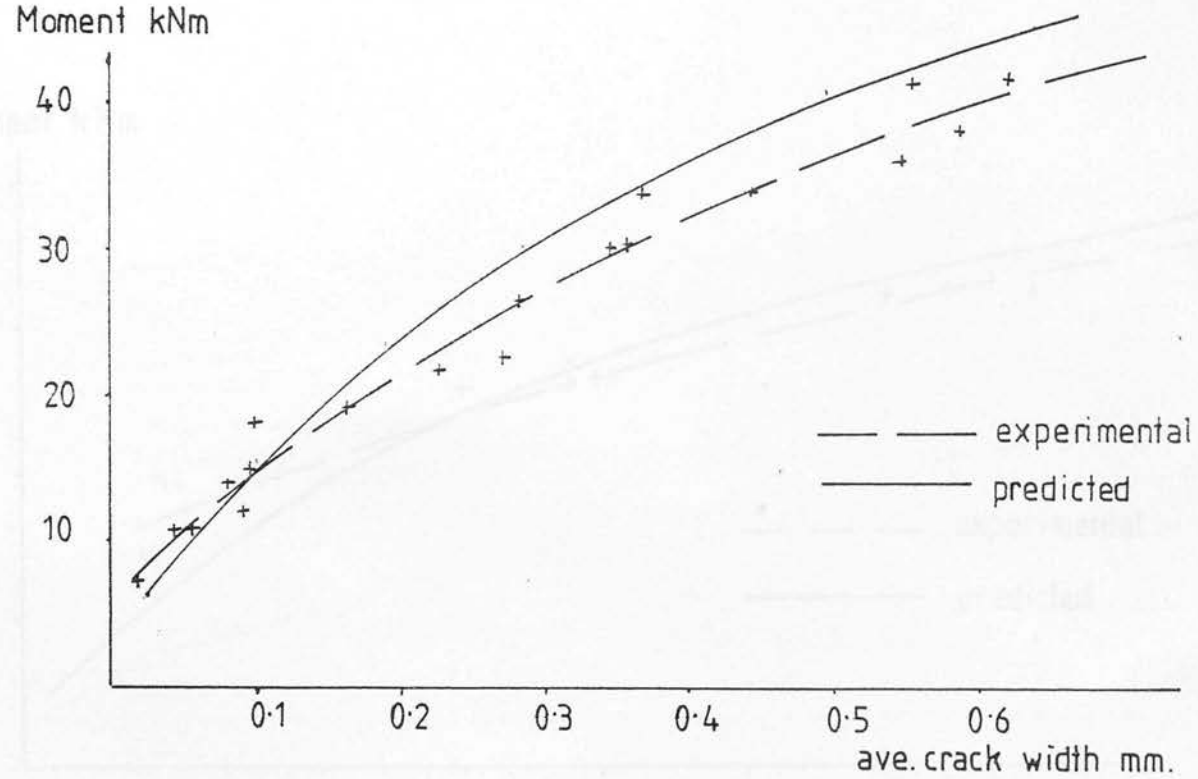

fig.6.5.8 Comparison between predicted and experimental average crack widths for high strength brick beams with 0·548 % steel.

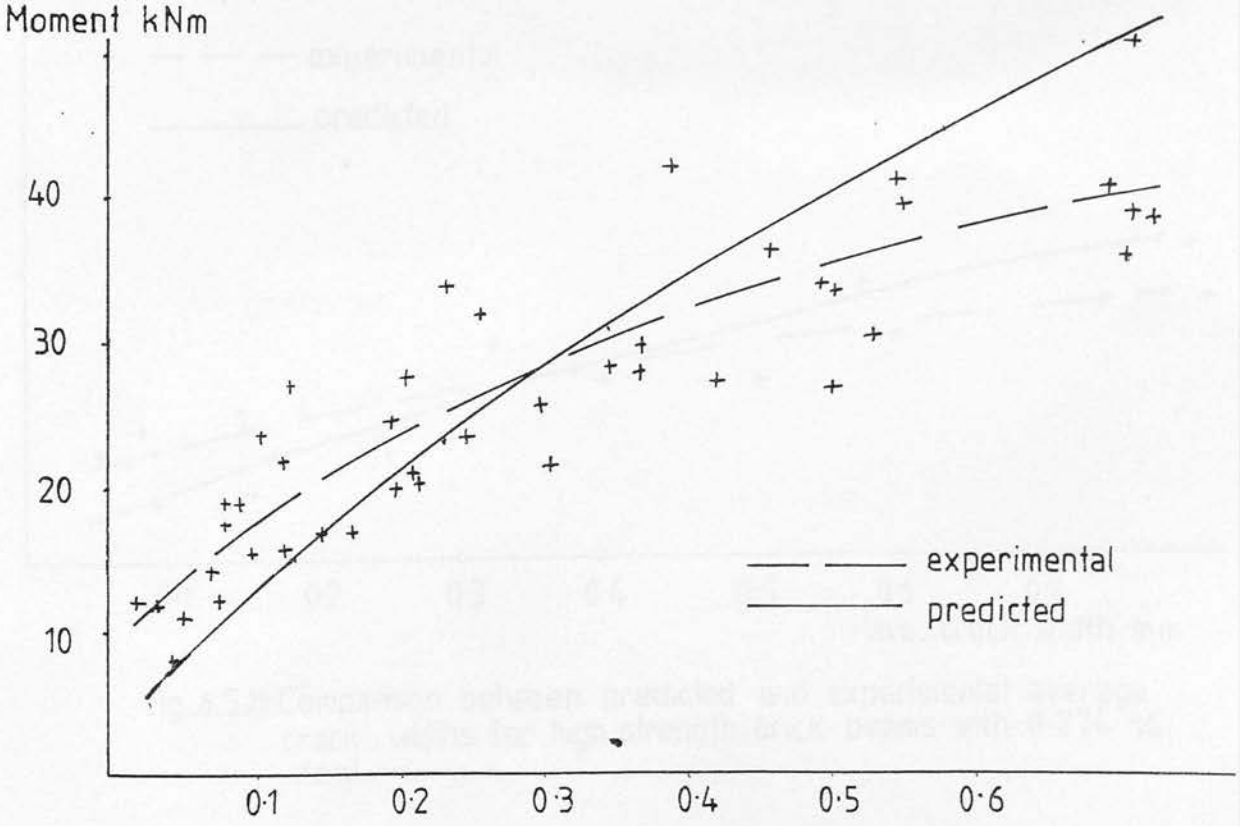

fig.6.5.9 Comparison between predicted and experimental average crack widths for high strength brick beams with 0·548 % steel.

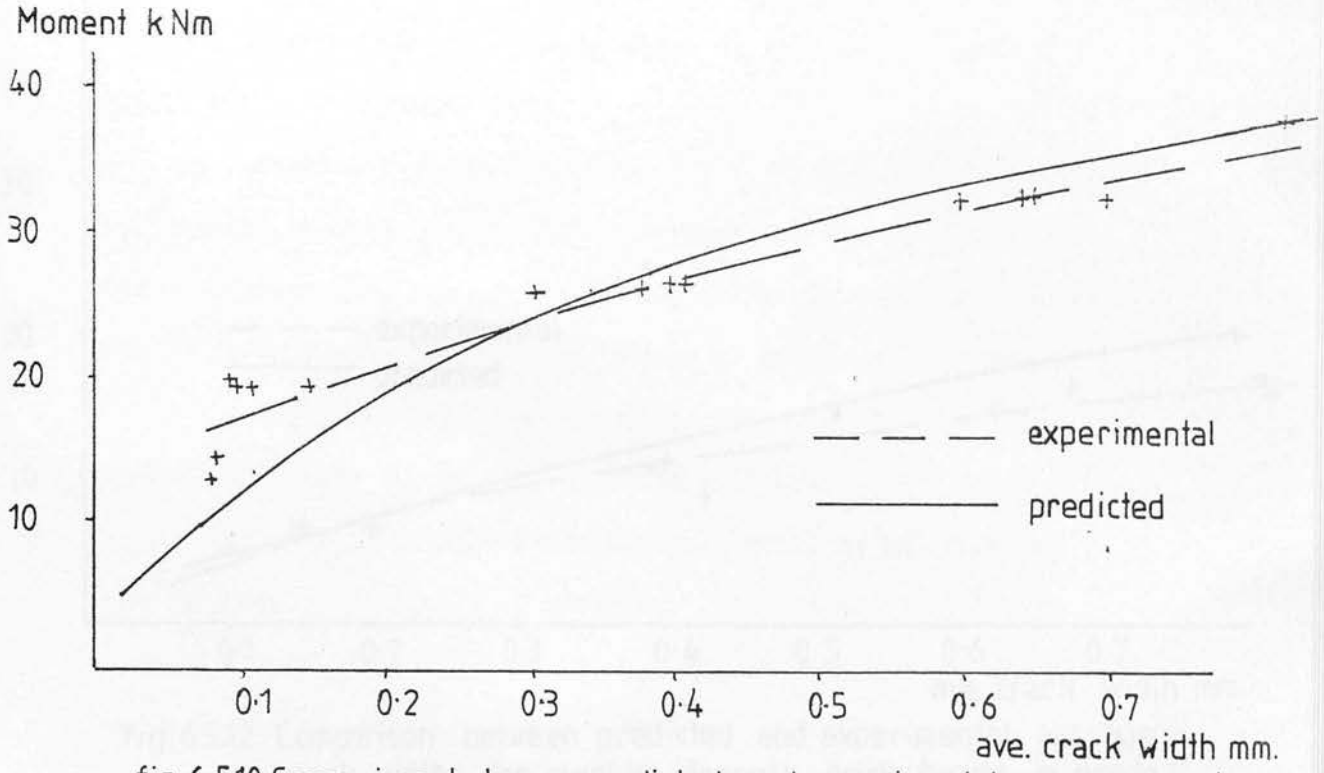

fig.6.5.10 Comparison between predicted and experimental average crack widths for high strength brick beams with 0·411 % steel.

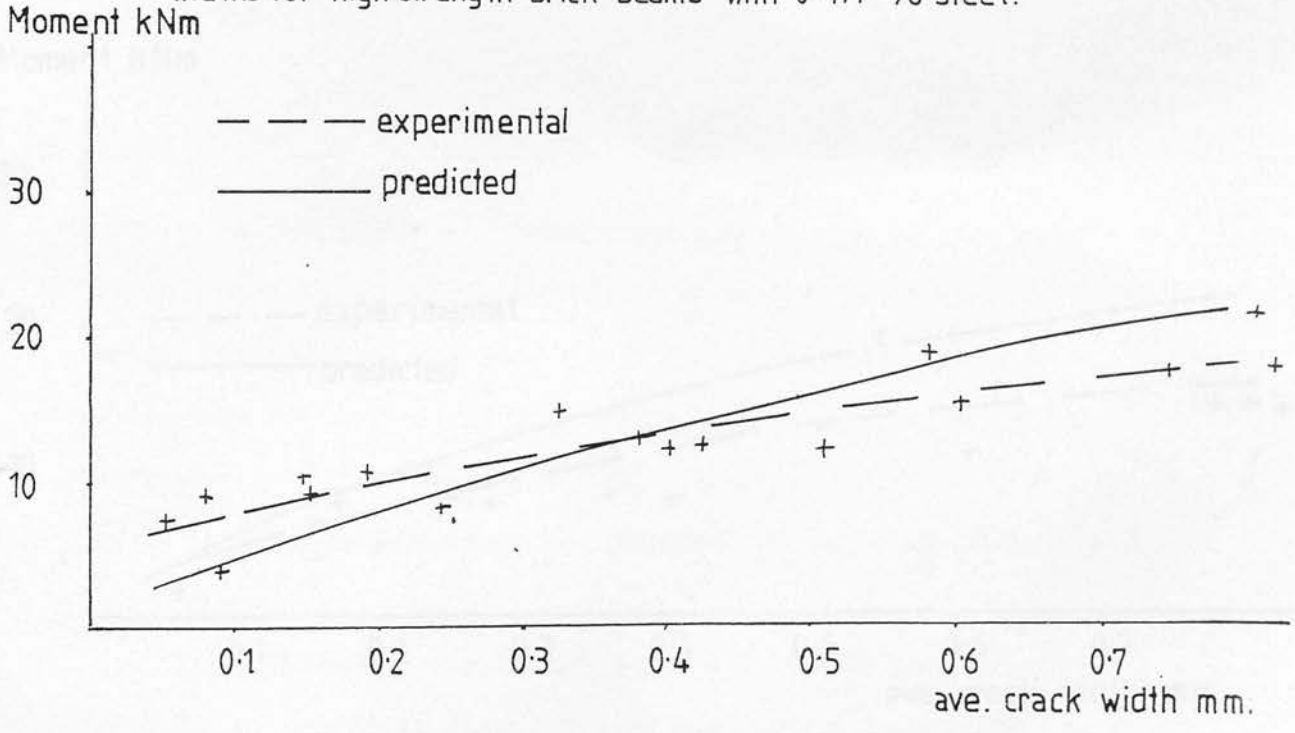

fig.6.5.11 Comparison between predicted and experimental average crack widths for high strength brick beams with 0·274 % steel.

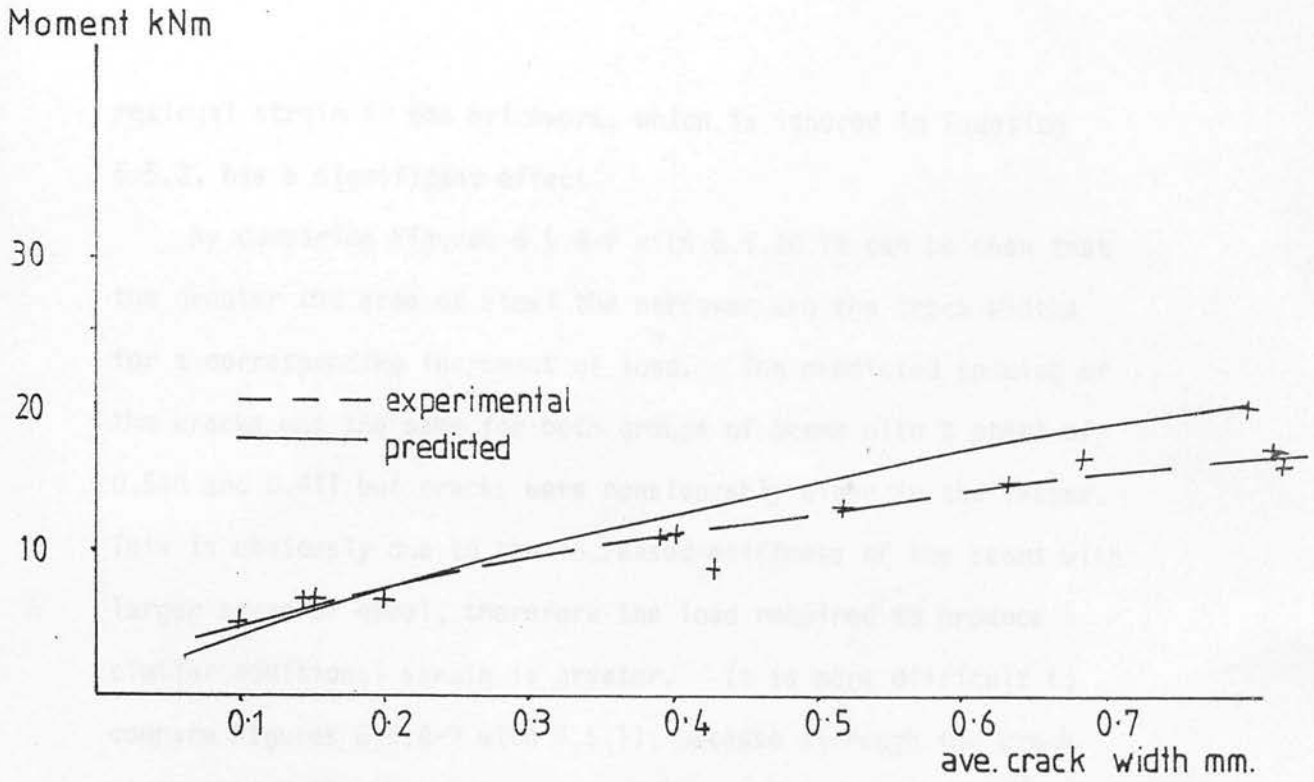

fig.6.5.12 Comparison between predicted and experimental average crack widths for medium strength brick beams in grade II mortar with 0·274 % steel.

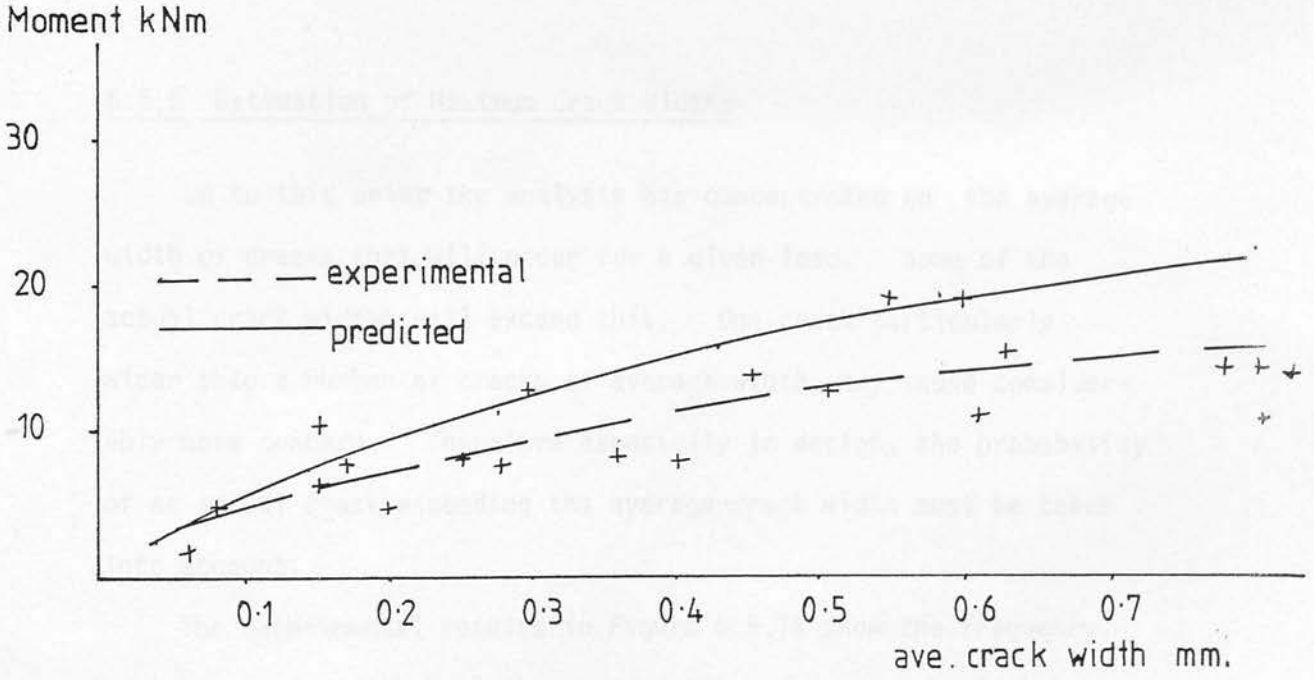

fig.6.5.13 Comparison between predicted and experimental average crack widths for medium strength brick beams in grade I mortar with 0·274 % steel.

residual strain in the brickwork, which is ignored in Equation 6.5.3, has a significant effect.

By comparing Figures 6.5.8-9 with 6.5.10 it can be seen that the greater the area of steel the narrower are the crack widths for a corresponding increment of load. The predicted spacing of the cracks was the same for both groups of beams with % steel of 0.548 and 0.411 but cracks were considerably wider in the latter. This is obviously due to the increased stiffness of the beams with larger areas of steel, therefore the load required to produce a similar additional strain is greater. It is more difficult to compare Figures 6.5.8-9 with 6.5.11, because although the crack width in 6.5.11 were much greater the cover was also greater and hence the increase is caused by a change in two variables, cover and steel area.

6.5.5 Estimation of Maximum Crack Widths

Up to this point the analysis has concentrated on the average width of cracks that will occur for a given load. Some of the actual crack widths will exceed this. One crack particularly wider than a number of cracks of average width, may cause considerably more concern. Therefore especially in design, the probability of an actual crack exceeding the average crack width must be taken into account.

The experimental results in Figure 6.5.14 show the frequency that the maximum crack width exceeded the average crack width by a given amount. The maximum crack width was most often between 1.1 and 1.2 times the average crack width with 76% of the results

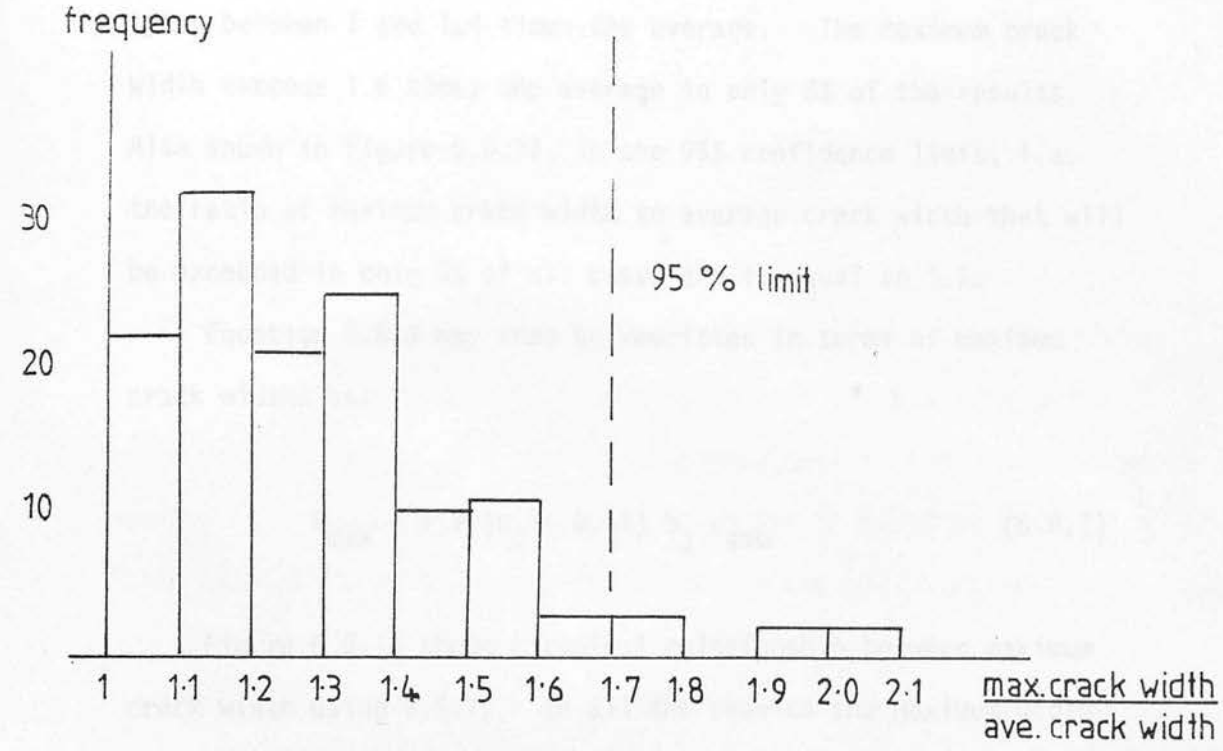

fig. 6.5.14 Distribution of maximum crack widths.

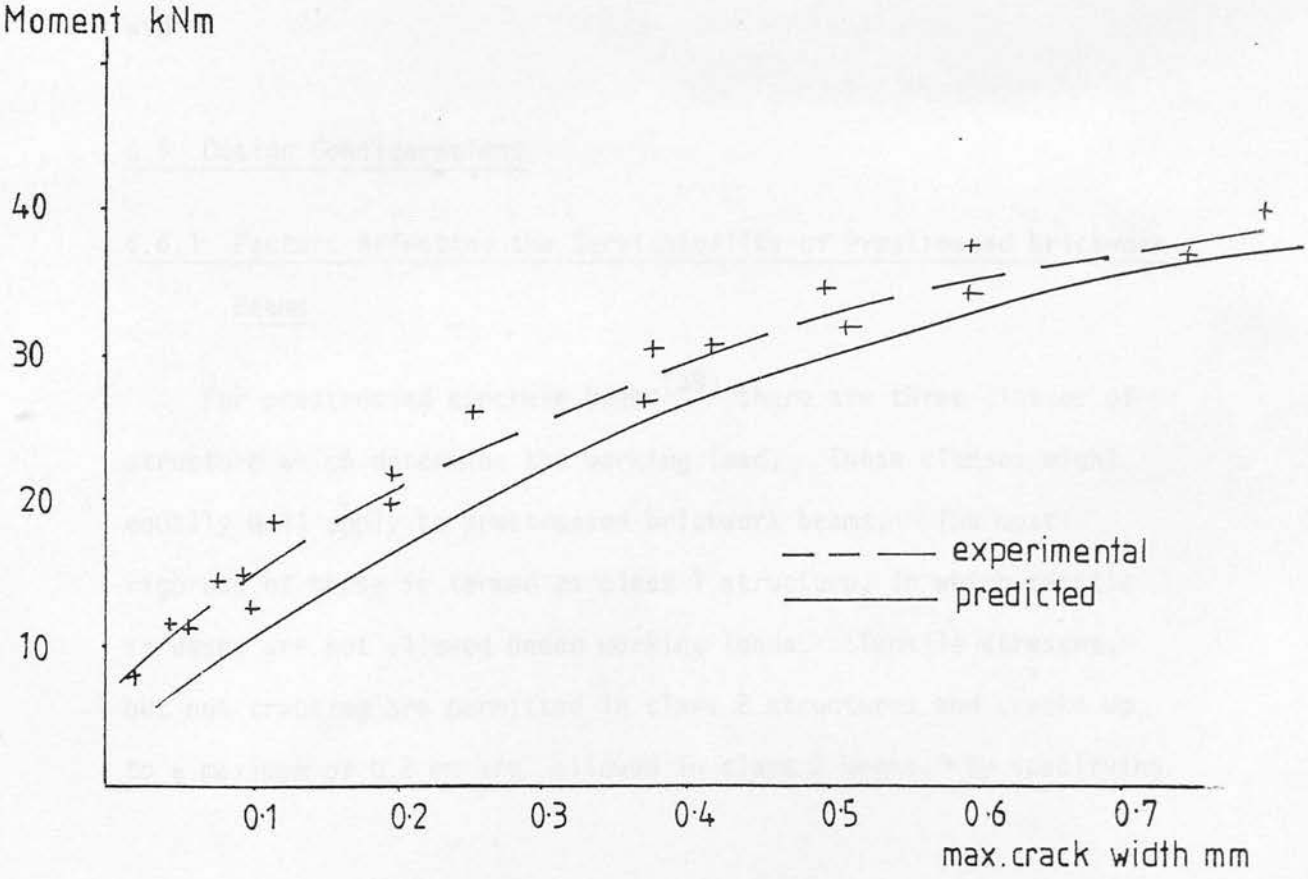

fig.6.5.15 Typical comparison between predicted and experimental maximum crack widths for high strength brick beams with 0·548 % steel.

lying between 1 and 1.4 times the average. The maximum crack width exceeds 1.6 times the average in only 8% of the results. Also shown in Figure 6.5.14, is the 95% confidence limit, i.e. the ratio of maximum crack width to average crack width that will be exceeded in only 5% of all cases and is equal to 1.7.

Equation 6.5.3 may then be rewritten in terms of maximum crack widths as:

$$W_{max} = 1.7\ (n_j + 0.41)\ b_j\ \varepsilon_{smb} \qquad (6.5.7)$$

Figure 6.5.15 shows a typical relationship between maximum crack width using 6.5.7. In all the results the maximum width predicted is greater than that obtained experimentally. Equation 6.5.7 will therefore provide a 'safe' estimate of the maximum crack width.

6.6 Design Considerations

6.6.1 Factors Affecting the Serviceability of Prestressed Brickwork Beams

For prestressed concrete beams[39] there are three classes of structure which determine the working load. These classes might equally well apply to prestressed brickwork beams. The most rigorous of these is termed as class 1 structure, in which tensile stresses are not allowed under working loads. Tensile stresses, but not cracking are permitted in class 2 structures and cracks up to a maximum of 0.2 mm are allowed in class 3 beams. By specifying

any one of these three classes it is possible for a beam to have three different working loads. It is always of prime importance that the beam has an adequate factor of safety against collapse and it is obvious that if the working load of a given beam is increased then the overall factor of safety will decrease.

It is of interest to study, briefly, the effect that specifying different working loads would have on some of the beams tested in this work. Table 6.6.1 compares the predicted working loads based on the 3 previous conditions, for the series of beams built in high strength brick with different steel areas and prestress forces. It is assumed that the beams are adequately reinforced against shear to ensure that the full flexural capacity is reached. The maximum crack width is obtained using Equation 6.5.7. The last column of Table 6.6.1 shows that the deflections are within allowable limits[39] when cracking is allowed under working load.

If the beams were designed as class 1 members then from Table 6.6.1 it can be seen that the ratio of $Mult/M_{c1}$ varies from 2.7-4.27. If, however, tension is allowed to develop, up to the flexural tensile strength of the brickwork then there is an increase in working load from 19-39%, this increase being greatest for beams with lower prestress. The factor of safety is consequently reduced to between 2.16 and 3.26. Allowing cracking to a maximum width of 0.2 mm results in an increase in working load over that based on class 1 conditions of between 62-82%. This is a very substantial increase but the factor of safety drops to below 2.0 in all but one case.

It is uneconomic to have too great a factor of safety and if,

Table 6.6.1 Serviceability Conditions for Prestressed Brickwork Beams

% Steel	Prestress Force kN	Pred. Ult. Moment kNm, Mult	Working Load Moments Class 1 M_{c1}	Class 2 M_{c3}	Class 3 M_{c3}	$\frac{Mult}{Mc_1}$	$\frac{Mult}{M_{c2}}$	$\frac{Mult}{M_{c3}}$	Span at Defl M_{c3}
0.548	300	101.0	37.4	44.6	60.6	2.70	2.27	1.67	365
0.548	200	98.7	23.1	30.3	43.3	4.27	3.26	2.28	590
0.411	210	76.6	24.5	31.7	42.7	3.10	2.40	1.78	563
0.274	138	55.0	18.3	25.5	30.5	3.01	2.16	1.80	776

for the purpose of discussion only, a factor of safety over the collapse load of 2.0 is considered as the minimum required, then it can be seen that the only beam which satisfies this in the cracked state is the beam with 0.548% steel and the lower prestress force. However it may also be seen that almost an identical working load may be obtained, without cracking, by increasing the prestress force and with approximately the same factor of safety. It will not always be possible to increase the service load by increasing the prestress force as problems with excessive camber and the stresses in the anchorage zones may arise. In this situation it is possible to increase the factor of safety and hence working load by increasing the steel area. This is illustrated in Table 6.6.1 where a 33% increase in steel area for beams of approximately equal prestress results in an increase in factor of safety from 1.78-2.28, when cracking is allowed.

The three beams which have factors of safety less than 2.0 at the limiting crack width of 0.2 mm were the beams in which the reinforcement was stressed to the maximum allowable. Therefore, it appears that it is not suitable to allow cracking to develop under working loads when the reinforcement is fully stressed. On the other hand, if it is not possible to fully prestress all the reinforcement then it is more efficient to allow limited cracking under working loads.

6.6.2 Prediction of Deflections in Design

The method of predicting the deflection of prestressed brickwork beams using the M - ϕ relationship is rather too cumbersome for

use in design. The deflection is normally only required under the working load and as shown in section 6.6.1, the working load may be influenced by whether tension or cracking is allowed. If the design of prestressed brickwork beams is limited to class 1 or class 2 type structures then the calculation of deflections may be based solely on the properties of the uncracked section. In class 3 type structures then the calculation of deflections has to recognise that the beam will be cracked for some portion of its length. Figure 6.6.1 compares the experimental and theoretically predicted deflections, using the single course prisms, for typical prestressed brickwork beams, with the deflections predicted using the method for calculating the effective moment of inertia proposed by Branson[52]. This expression or the effective moment of inertia is given in Equation 6.6.1:

$$I_e = \left(\frac{M_{cr}}{M}\right)^3 I_g + \left(1 - \left(\frac{M_{cr}}{M}\right)^3\right) I_{cr} \qquad (6.6.1)$$

I_g and I_{cr} are the moments of inertia based on the gross cross-section and the cracked section, respectively. M_{cr} is the moment required to cause cracking from the position of zero net deflection of the beam and M is the applied moment. I_e, from Equation 6.6.1, applies to the complete span of beam and takes account of tension stiffening and the sections of the beam that remains uncracked.

Figure 6.6.1 shows that this method shows very good agreement with both the previous results up to cracking but tends to over-estimate the deflections after cracking. However, in design, it is more desirable that any method should overestimate rather than

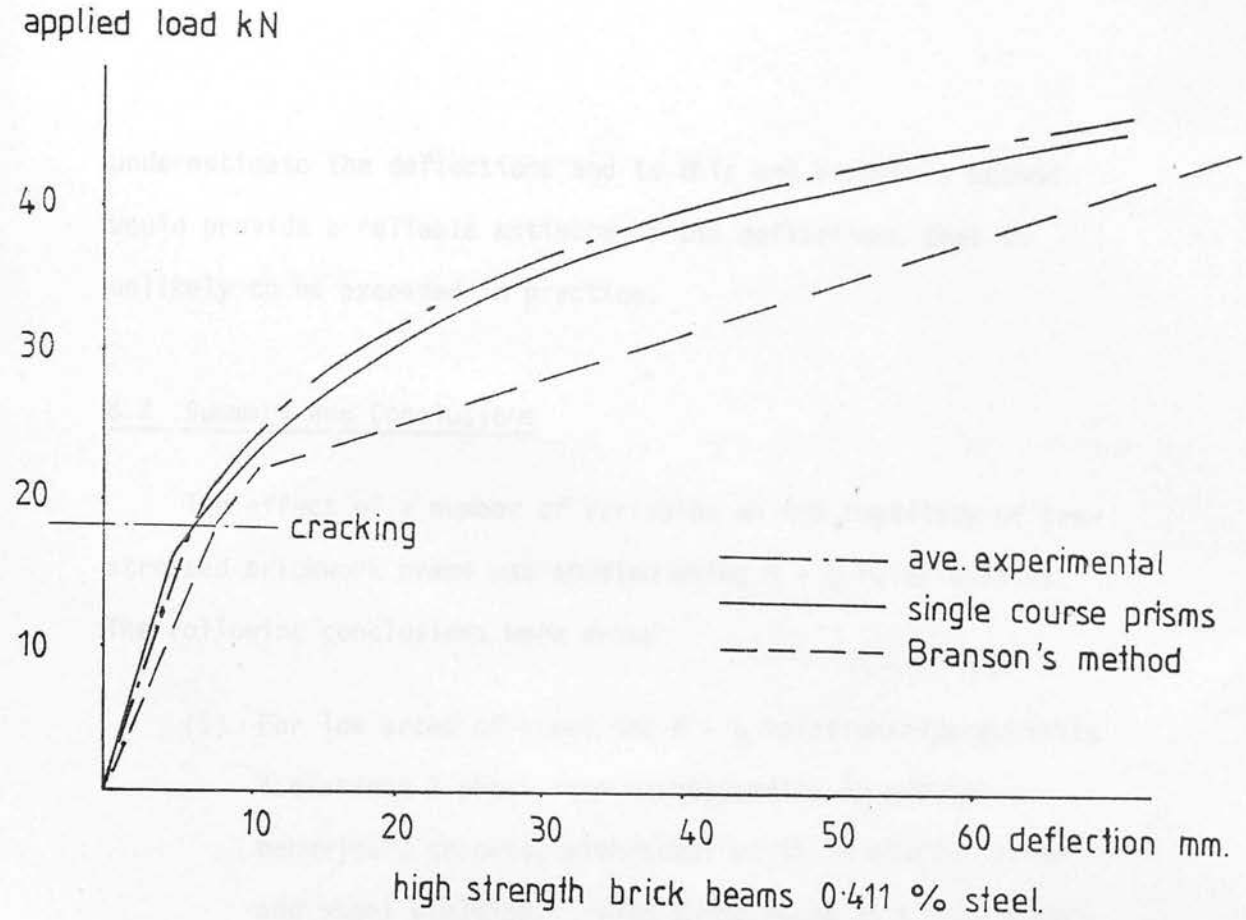

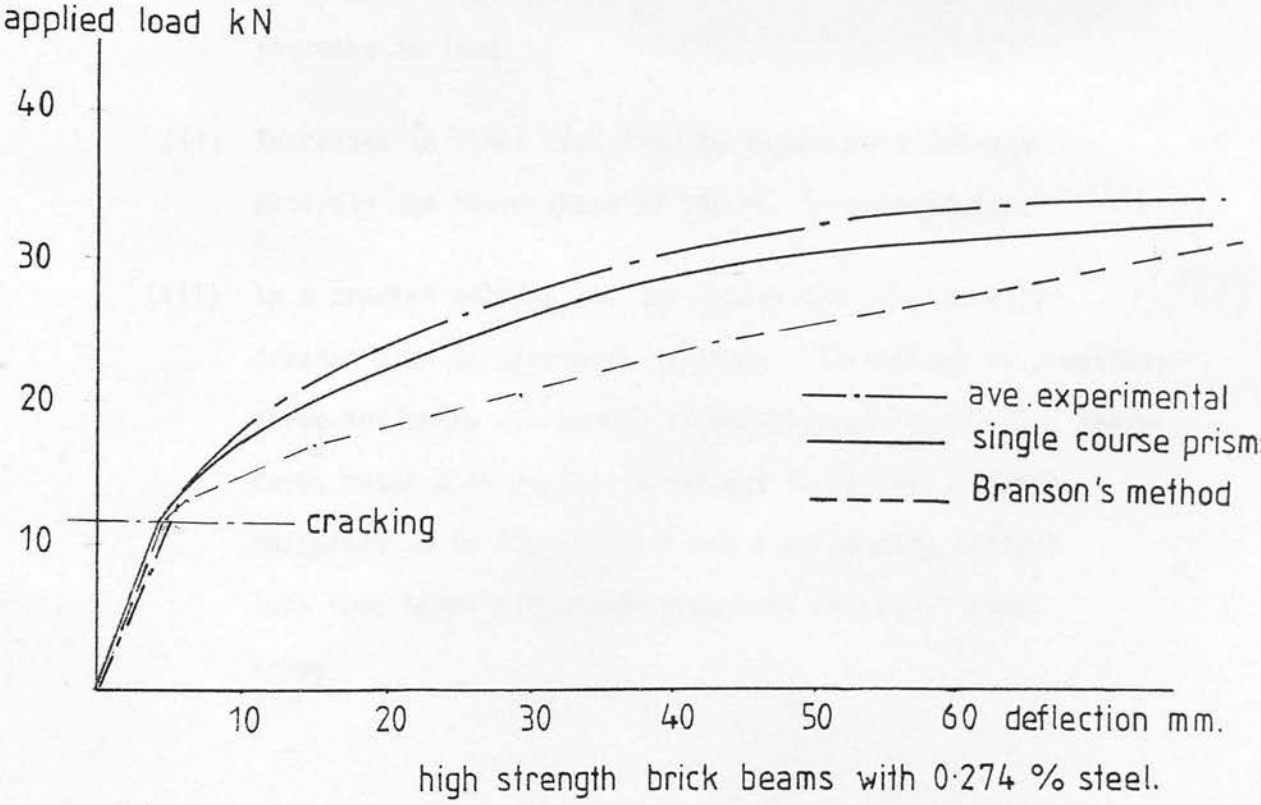

fig. 6.6.1 Typical load/deflection response using Branson's method.

underestimate the deflections and to this end Branson's method would provide a reliable estimate of the deflections that is unlikely to be exceeded in practice.

6.7 Summary and Conclusions

The effect of a number of variables on the ductility of prestressed brickwork beams was studied using M - ϕ relationships. The following conclusions were drawn:

(i) For low areas of steel the M - ϕ relationships exhibits a distinct 3 phase form corresponding to uncracked behaviour, cracked, with steel still in elastic range and steel yielding. This third phase is hightlighted in the latter stages of the load/deflection response where very large deflections occur with little or no increase in load.

(ii) Increases in steel area tend to reduce or eliminate entirely the third phase of the M - ϕ relationship.

(iii) In a cracked section the curvatures are considerably greater than an uncracked section. Variations in prestress force influence the moment at which cracking occurs. Therefore, beams with greater prestress forces will remain uncracked up to higher loads and consequently deflect less than beams with lower prestress but equal steel areas.

(iv) The main influence that a change in mortar, from a grade I to a grade II has on the M - ϕ relationship is to reduce the tensile strength of the brickwork and so reduce the cracking moment.

(v) For the high and medium strength brick the brick strength does not influence the M - ϕ relationship greatly and hence the load/deflection response.

(vi) The M - ϕ relationship and the load/deflection response of prestressed brickwork beams can be closely modelled using the proposed method, taking account of the non-linear stress/strain relationship of brickwork and tension stiffening. To this end the single course prism yields closer agreement with the experimental results than the three course prisms.

(vii) Flexural cracks in prestressed brickwork beams initiate at the brick/mortar interface. The average crack width is directly related to the average strain in the steel. The average crack width can be predicted using the proposed equation.

CHAPTER 7 : THE SHEAR STRENGTH OF PRESTRESSED BRICKWORK BEAMS

7.1 Introduction

By far the aspect of structural concrete behaviour that has attracted the most concern of researchers has been the problem of shear in reinforced and prestressed concrete beams. Shear failure may occurs at a lower load than the flexural strength of the beam and is generally sudden and devasting.

It is very well known that the shear strength of concrete beams increases with decreasing shear span/effective depth ratio and increasing % of steel area. Various theories have been developed for the shear strength of reinforced and prestressed concrete beams but they generally depend on correlation with specific test results.

Researchers[45,72,73] in structural brickwork have found themselves in a similar situation concerning shear in brickwork beams. Sinha[72,45], Suter and Hendry[73] have shown experimentally, that the shear strength of reinforced brickwork, like concrete, increases with decreasing shear span/effective depth ratio and increasing steel areas. More recently work has been carried out by Osman and Hendry[74] on the contribution of dowel action, compression zone transmission and aggregate interlock to the shear strength of reinforced, grouted cavity brickwork beams. They found that the greatest proportion of the shear was carried by compression zone transmission. Although interest in this area is growing the present state of knowledge is still lagging far behind the work on concrete and a complete understanding of shear in brickwork is still far away.

From the previous chapters, it was shown that the prestressed brickwork beams with 0.274% failed in flexure. However, it was felt that if the % of steel is increased the mode of failure may shift from flexural to shear. In the design of prestressed brickwork beams it is very important to have some idea when shear failure will predominate. It was decided, therefore, to test a limited number of beams with % steel areas greater than 0.274% to study the effect of the following variables:

(i) shear span/effective depth ratio (a/d), 2-11,

(ii) percentage area of steel, 0.548-0.411%,

(iii) shear reinforcement,

on the ultimate shear strength of prestressed brickwork beams. With the given section of the beams and the size of the prestressing strands further increases in steel areas were limited to increasing the steel areas to 0.411 or 0.548%, corresponding to 3 or 4 strands respectively. From Figures 5.4.1-5.4.10 such increases in steel area will result in grossly over-reinforced sections for all but the beams built with high strength brick. As these would normally be considered undesirable in design all the beams were built from high strength brick to study the variables (i) to (iii). The addition of shear reinforcement to prestressed brickwork beams is considerably more difficult than for concrete beams. However, in an effort to prevent shear failure, four beams with shear reinforcement were tested, as shown in Figure 4.2.2(b).

Quite recently, plastic methods for determining the shear strength of prestressed concrete beams without shear reinforcement have been

developed by Nielsen et al[26,75]. The method predicts the shear strength by employing an empirical factor on compressive strength and excellent agreement with experimental results was obtained. The inherent simplicity of this method proved a powerful argument for its application to the prestressed brickwork beams in this study. Since it has been shown that the single course prisms predict the flexural behaviour accurately, the compressive strength from these prisms were used in the analysis of the shear strength. The method was further verified by comparison with previous work on reinforced brickwork beams[72,73].

7.2 The Shear Strength of Brickwork Beams Without Shear Reinforcement

The plastic methods proposed by Nielsen et al[26,75] are given in greater detail elsewhere and only those aspects specifically related to the shear strength of beams without shear reinforcement are considered here.

Implicit in the use of plastic theory is that the material exhibits a reasonable degree of ductility, which is not apparent in materials such as brickwork or concrete. The limited ductility of these materials is allowed for by use of an empirical factor, ν, called the effectiveness factor, which is determined experimentally and is applied to the compressive strength of the material.

It is assumed that:

(i) the beam is in a state of plane stress;

(ii) the reinforcement behaves in a rigid-perflectly plastic manner;

(iii) the brickwork is rigid-perfectly plastic and obeys a modified Coulomb's failure surface in which the compressive strength is equal to $\nu \cdot f_m$ and the tensile strength is zero.

The modified Coulomb failure criterion is shown in Figure 7.2.1. This criterion has been developed for concrete. However, recent experimental work by Page[76] in which a large number of brickwork panels were tested under biaxial compression at varying ratios of principal stresses and orientations to the bedjoint, infers that the failure surface is rectangular, Figure 7.2.2, and not significantly affected by the angle of the bedjoint. It is reasonable, then to apply the same yield locus used by Nielsen and Braestrup[26] to brickwork, especially since the compressive strength of the brickwork in the beam at failure is obtained by correlation with the experimental results to determine ν, the effectiveness factor.

The ultimate load may be determined by finding the lowest upper bound or the highest lower bound. An upper bound is found by assuming a failure mechanism and equating the internal and external work. A lower bound is found by assuming a statically admissible stress distribution and calculating the corresponding loads. When both the upper and lower bound yield the same results, the exact plastic solution has been found.

7.2.1 Upper Bound Solution

The failure mechanism assumed by Nielsen et al[26,75] is shown in Figure 7.2.3. This consists of a yield line running from support

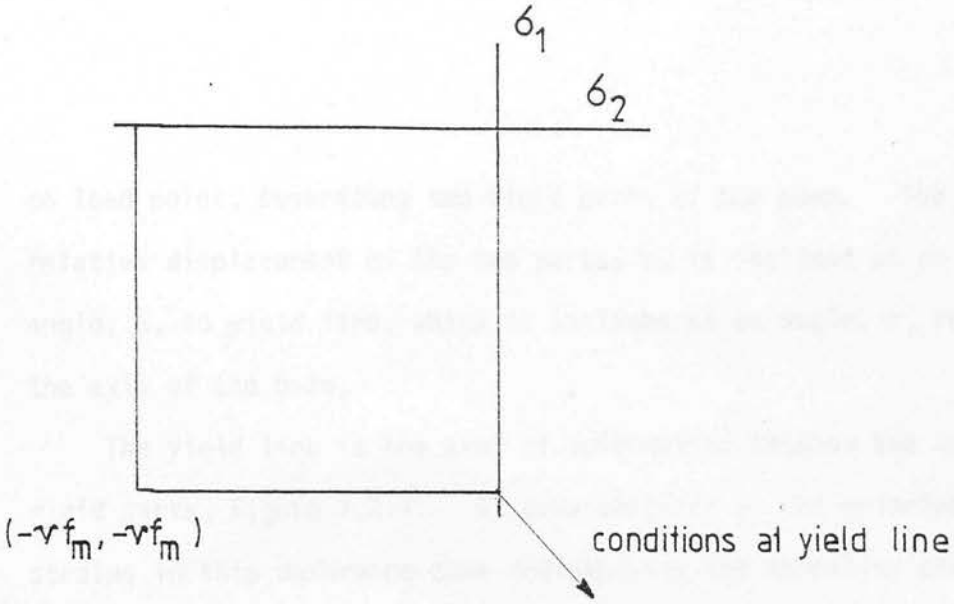

fig.7.2.1 Modified Coulomb failure criterion

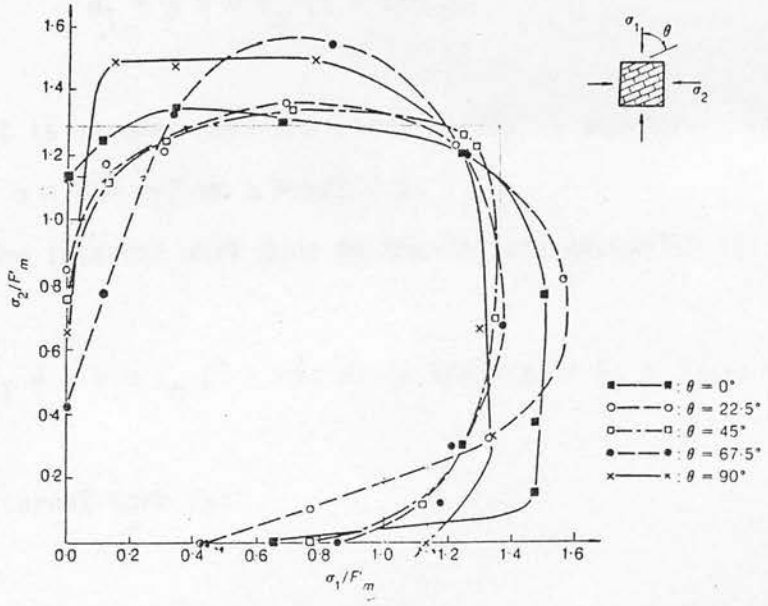

fig.7.2.2 Failure surface for brickwork in bi-axial compression (after Page).

to load point, separating two rigid parts of the beam. The relative displacement of the two parts, v, is inclined at an angle, α, to yield line, which is inclined at an angle, β, to the axis of the beam.

The yield line is the area of deformation between the two rigid parts, Figure 7.2.4. By consideration of the principal strains in this deforming zone and applying the normality condition[77], which states that the principal rates of strain are normal to the yield surface, Jensen[78] showed that the only stress state which satisfies this condition corresponds to the corner of the yield surface shown in Figure 7.2.1. From this he derived the following expression for the internal work per unit area of the yield line:

$$W_I = \tfrac{1}{2} v \nu f_m (1 - \sin \alpha) \qquad (7.2.1)$$

It is assumed that the steel yields in tension. For this to happen $\alpha + \beta \geqslant \pi/2$ or $\alpha \geqslant \pi/2 - \beta$.

The internal work done by the failure mechanism is:

$$W_I = \tfrac{1}{2} v \nu f_m (1 - \sin \alpha) (b\ h/\sin \beta) - F_Y v \cos(\alpha + \beta) \qquad (7.2.2)$$

The external work is:

$$W_E = V v \sin (\alpha + \beta) \qquad (7.2.3)$$

The average shear stress can be defined as:

$$\tau = \frac{V}{b\ h} \qquad (7.2.4)$$

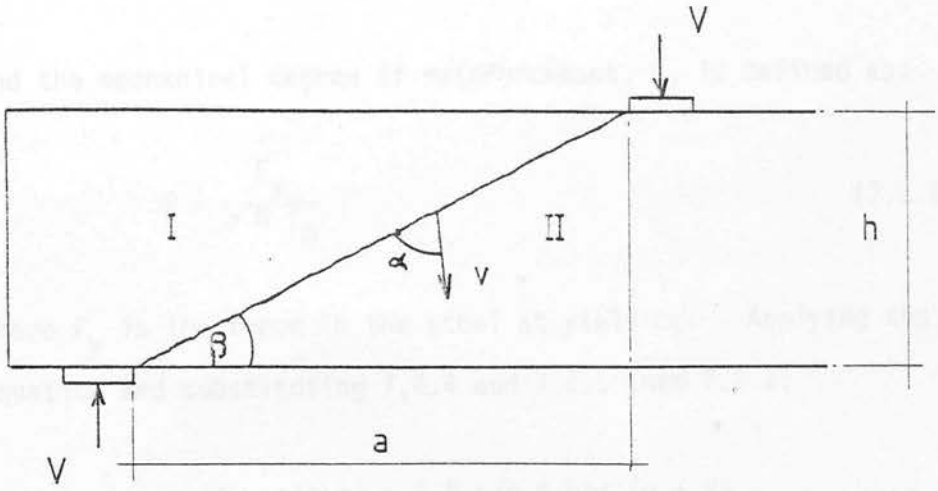

fig.7.2.3 Failure mechanism for beam.

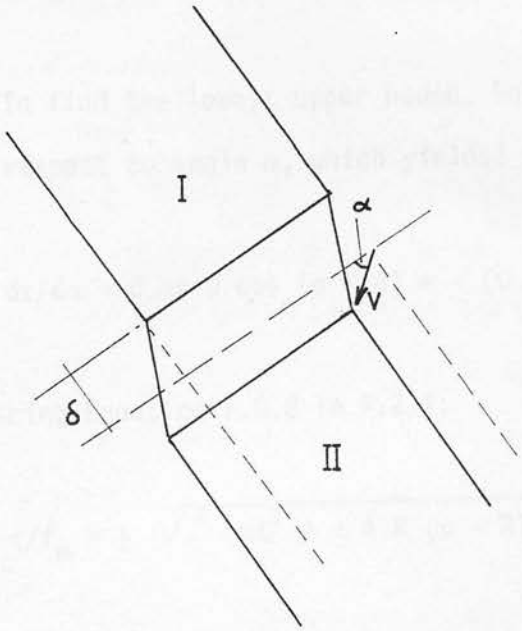

fig.7.2.4 Deformation zone between two rigid parts.

and the mechanical degree of reinforcement, R, is defined as:

$$R = \frac{F_y}{b\ h\ f_m} \qquad (7.2.5)$$

where F_y is the force in the steel at yielding. Applying the work equation and substituting 7.2.4 and 7.2.5 into 7.2.2:

$$\tau/f_m = \frac{\nu\ (1 - \sin\alpha) - 2\ R \sin\beta \cos(\alpha + \beta)}{2 \sin\beta \sin(\alpha + \beta)} \qquad (7.2.6)$$

which becomes:

$$\tau/f_m = \frac{\nu - \nu \cos\beta \sin(\alpha + \beta) + (\nu - 2\ R) \sin\beta \cos(\alpha + \beta)}{2 \sin\beta \sin(\alpha + \beta)} \qquad (7.2.7)$$

To find the lowest upper bound, Equation 7.2.7 is minimised with respect to angle α, which yields:

$$d\tau/d\alpha = 0 \text{ at } \nu \cos(\alpha + \beta) = -(\nu - 2\ R) \sin\beta \qquad (7.2.8)$$

replacing Equation 7.2.8 in 7.2.7:

$$\tau/f_m = \tfrac{1}{2} \left(\sqrt{\nu^2 \cot^2\beta + 4\ R\ (\nu - R)} - \nu \cot\beta\right) \qquad (7.2.9)$$

$$\cot\beta = a/h,$$

$$\tau/f_m = \nu/2 \left(\sqrt{(a/h)^2 + \frac{4\ R\ (\nu - R)}{\nu^2}} - a/h\right) \qquad (7.2.10)$$

If the reinforcement is sufficiently strong, such that $R > \nu/2$

then from Equation 7.2.8, Equation 7.2.10 does not apply. As R increases, the angle $(\alpha + \beta)$ decreases (Equation 7.2.8). When $R > \nu/2$, $\alpha + \beta < \pi/2$; the steel does not yield. Nielsen et al[26] showed that when $\alpha + \beta \leqslant \pi/2$ the lowest upper bound is obtained when $\alpha + \beta = \pi/2$. Referring back to Equation 7.2.7, when $(\alpha + \beta) = \pi/2$ is inserted the term with R disappears, Equation 7.2.10 then becomes:

$$\tau/f_m = \nu/2 \left(\sqrt{(a/h)^2 + 1} - a/h\right) \qquad (7.2.11)$$

7.2.2 Lower Bound Solution

The stress distribution in Figure 7.2.5 is assumed. The compressive force is transmitted via a brickwork strut running from the load point to support. This stress distribution is similar to a 'tied arch' and it assumed that the reinforcement is bonded only at the support. The regions immediately above and below the support and load points are assumed to be in a state of biaxial, hydrostatic, compression of depth y. At the support this implies a small moment which is ignored in the analysis. From Figure 7.2.5 it can be seen that:

$$h - y = (a + y \tan\theta) \tan\theta \qquad (7.2.12)$$

therefore:

$$\tan\theta = \tfrac{1}{2}\, y \left(\sqrt{a^2 + 4\, y\, (h - y)} - a\right) \qquad (7.2.13)$$

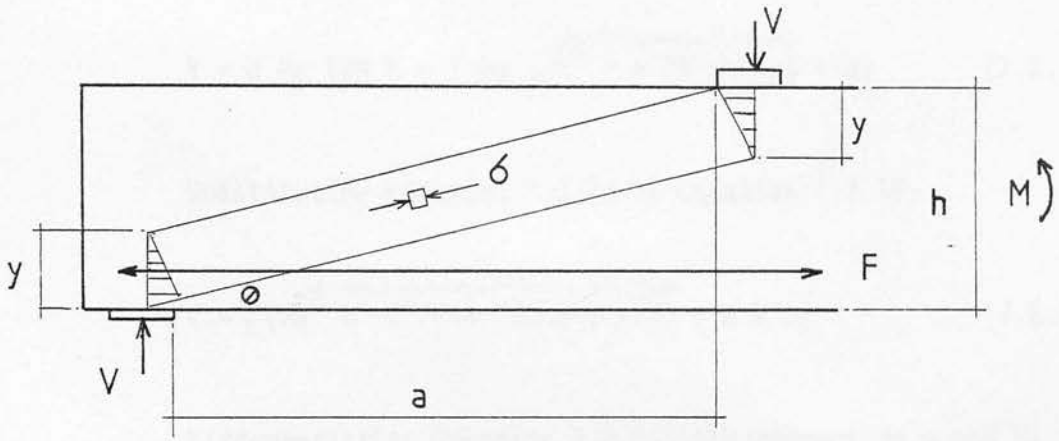

fig.7.2.5 Stress distribution in lower bound solution.

By considering equilibrium of the horizontal forces, the depth y may be obtained, F is the force in the reinforcement:

$$b\ y\ \sigma = F \therefore y = \frac{F}{b\sigma} \qquad (7.2.14)$$

Considering equilibrium of the vertical forces, V is found:

$$V = \sigma\ by \tan\theta = \tfrac{1}{2}\ b\sigma\ (\sqrt{a^2 + 4\ (h\ y - y)} - a) \qquad (7.2.15)$$

Substituting Equation 7.2.14 in Equation 7.2.15:

$$V = \tfrac{1}{2}\ (\sqrt{a^2\ b^2\ \sigma^2 + 4\ F(h\ b\ \sigma - F)} - a\ b\ \sigma) \qquad (7.2.16)$$

Differentiating Equation 7.2.16 with respect to σ and F, it is found that $dv/d\sigma$ is always greater than zero and that:

$$dv/dF \gtrless 0 \text{ when } F \gtrless \tfrac{1}{2}\ h\ b\ \sigma \qquad (7.2.17)$$

The highest lower bound will be obtained when σ is a maximum, i.e. $\sigma = \nu\ f_m$.

When F is less than $\frac{1}{2}\ h\ b\ \nu\ f_m$ the steel is yielding and F is determined from the maximum force in the reinforcement:

$$F = R\ b\ h\ f_m \qquad (7.2.18)$$

If F is greater than $\frac{1}{2}\ b\ h\ \nu\ f_m$, the maximum force in the steel is governed by the brickwork and the highest lower bound is found with:

$$F = \tfrac{1}{2}\, b\, h\, \nu\, f_m \qquad (7.2.19)$$

Substituting Equations 7.2.18 and 7.2.19 into 7.2.16, two expressions for τ/f_m are obtained:

$$\tau/f_m = \nu/2 \left(\sqrt{(a/h)^2 + \frac{4R(\nu - R)}{\nu^2}} - a/h\right) \qquad (7.2.20)$$

when $R \leqslant \nu/2$ and

$$\tau/f_m = \nu/2 \left(\sqrt{(a/h)^2 + 1} - a/h\right) \qquad (7.2.21)$$

when $R \geqslant \nu/2$.

These two expressions, 7.2.20 and 7.2.21, are identical to the two expressions obtained from the upper bound solution, Equations 7.2.10 and 7.2.11, therefore an exact plastic solution has been found.

Nielsen and Braestrup[26] agreed that their interpretation of the stress distribution might be over-simplified and that the failure mechanism assumed in the upper bound solution does not always occur. They concluded however, that because it was possible to obtain a failure mechanism and a stress state corresponding to the same ultimate load, their method provided a valid solution.

7.2.3 The Effectiveness Factor, ν

As shown in Equations 7.2.9, 7.2.10, 7.2.20 and 7.2.21, the practical utility of the method lies with the effectiveness factor, ν. The effectiveness factor is obtained experimentally, rearranging

Equation 7.2.20:

$$\nu = \frac{(\tau/f_m)^2 + R^2}{R - a/h\ \tau/f_m} \qquad (7.2.22)$$

The function of ν is to reduce the compressive strength, f_m, to allow for the brittle nature of the material, which does not conform completely to the assumptions of rigid-plastic behaviour. The effectiveness factor also acts to soak up any deficiencies in the theory.

7.3 Plastic Theory Applied to Reinforced Brickwork

Prior to adopting the plastic theory for the beams tested in this work, Nielsen and Braestrup's method was applied to previously reported[45,73] tests on reinforced brickwork beams without shear reinforcement. Figure 7.3.1 shows the results of Sinha[45] on reinforced brickwork slab specimens and Figure 7.3.2 the results of Suter and Hendry[73]. The value of ν was obtained using Equation 7.2.22 with the shear strengths of each of the experimental results. The average value of ν was then used to predict the shear strengths with Equations 7.2.20 or 7.2.21.

Although there was some dispersion in the experimental results, the predicted shear strengths appear to give very good agreement. The average values of ν for both groups were very similar, this may be purely coincidental. Nielsen and Braestrup[26], when applying their method to various sets of experiments on concrete beams, found that, although very good correlation between experimental and theoretical results were obtained for individual sets of results

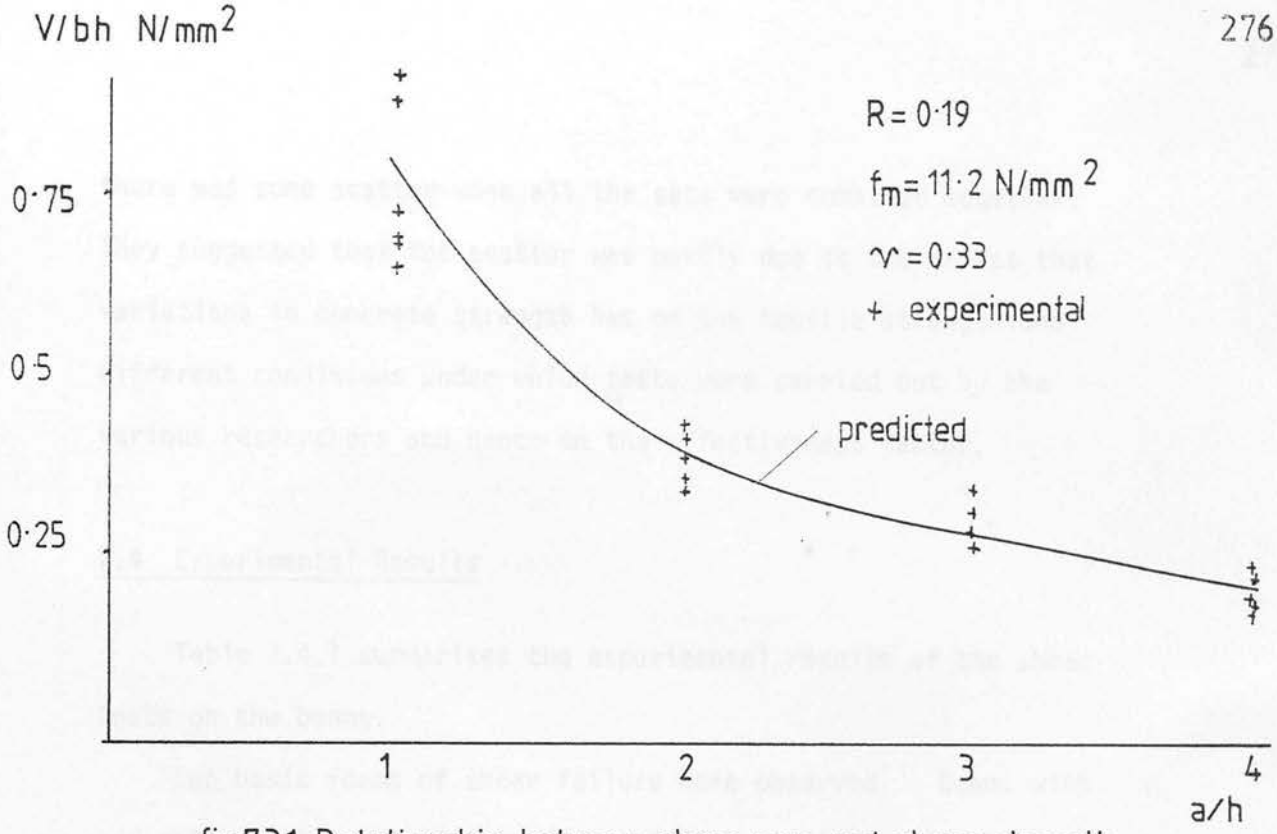

fig.7.3.1 Relationship between shear span and shear strength (after Sinha), for reinforced brickwork beams.

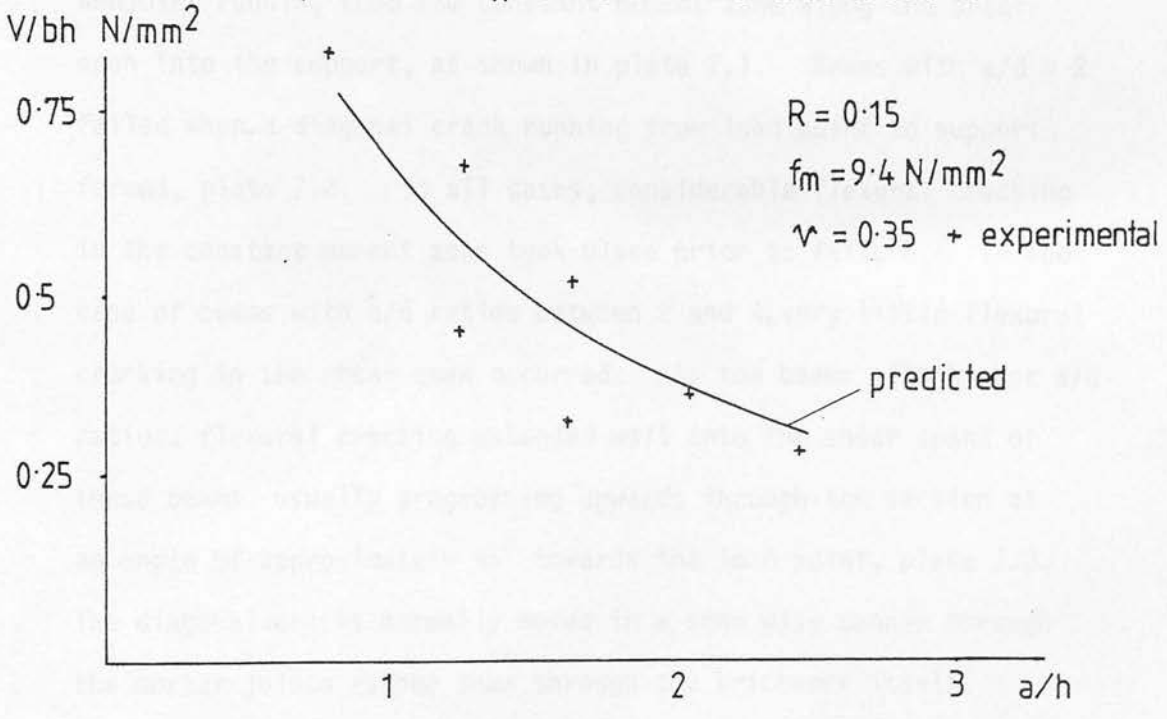

fig.7.3.2 Relationship between shear span and shear strength for reinforced brickwork beams (after Suter & Hendry).

there was some scatter when all the sets were combined together. They suggested that the scatter was partly due to the effect that variations in concrete strength has on the tensile strength and different conditions under which tests were carried out by the various researchers and hence on the effectiveness factor.

7.4 Experimental Results

Table 7.4.1 summarises the experimental results of the shear tests on the beams.

Two basic forms of shear failure were observed. Beams with a/d ratios between 4-11.2 tended to fail by splitting of the top bedjoint running from the constant moment zone along the shear span into the support, as shown in plate 7.1. Beams with a/d = 2 failed when a diagonal crack running from load point to support formed, plate 7.2. In all cases, considerable flexural cracking in the constant moment zone took place prior to failure. In the case of beams with a/d ratios between 2 and 4, very little flexural cracking in the shear span occurred. In the beams with higher a/d ratios, flexural cracking extended well into the shear spans of these beams, usually progressing upwards through the section at an angle of approximately 45^{o} towards the load point, plate 7.3. The diagonal cracks normally moved in a step wise manner through the mortar joints rather than through the brickwork itself.

7.4.1 Influence of Shear Span/Effective Depth Ratio on Shear Strength

Beams BB2-BB10 had the same area of steel and were prestressed to the same degree. From Table 7.4.1 and Figure 7.4.1 it can be

Table 7.4.1 Experimental Results

Beam	$\frac{\text{Shear Span}}{\text{Eff. Depth}}$	V/bd (exp) N/mm^2	$\frac{M_{exp}}{M_{single}}$
BB1	11.21	0.66	0.93
BB2	11.21	0.55	0.78
BB3	11.21	0.55	0.77
BB4	11.21	0.57	0.81
BB5	4.0	1.33	0.75
BB6	4.0	1.27	0.71
BB7	2.0	2.15	0.64
BB8	2.0	2.71	0.78
BB9	7.0	0.75	0.80
BB10	7.0	0.70	0.75
BS3	11.21	0.76	1.09
BS4	11.21	0.70	1.00
BA1	11.21	0.55	0.96
BA2	11.21	0.60	1.06
BA4	11.21	0.53	0.94

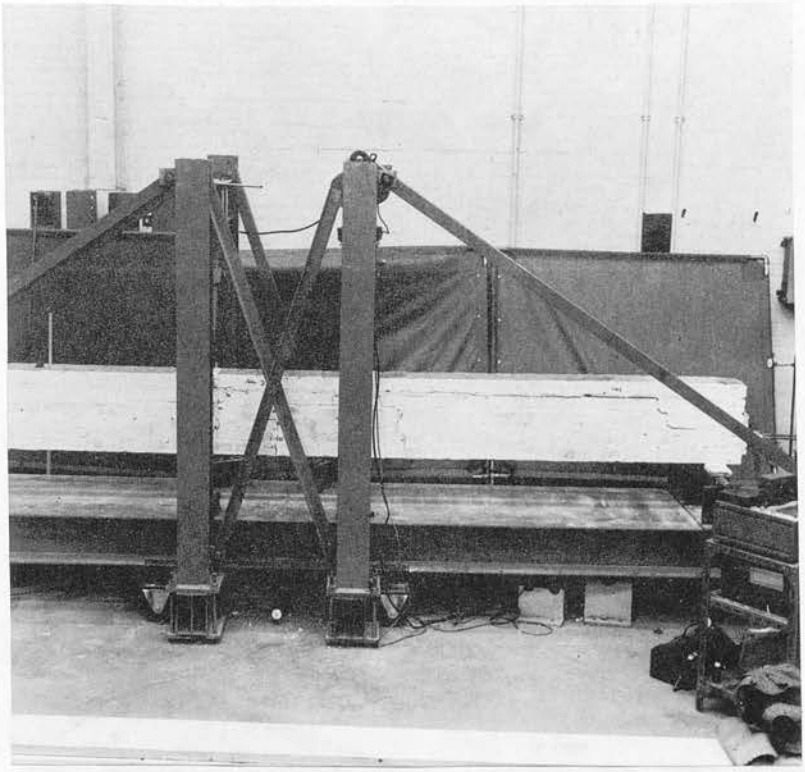

Plate 7.1 Typical splitting shear failure.

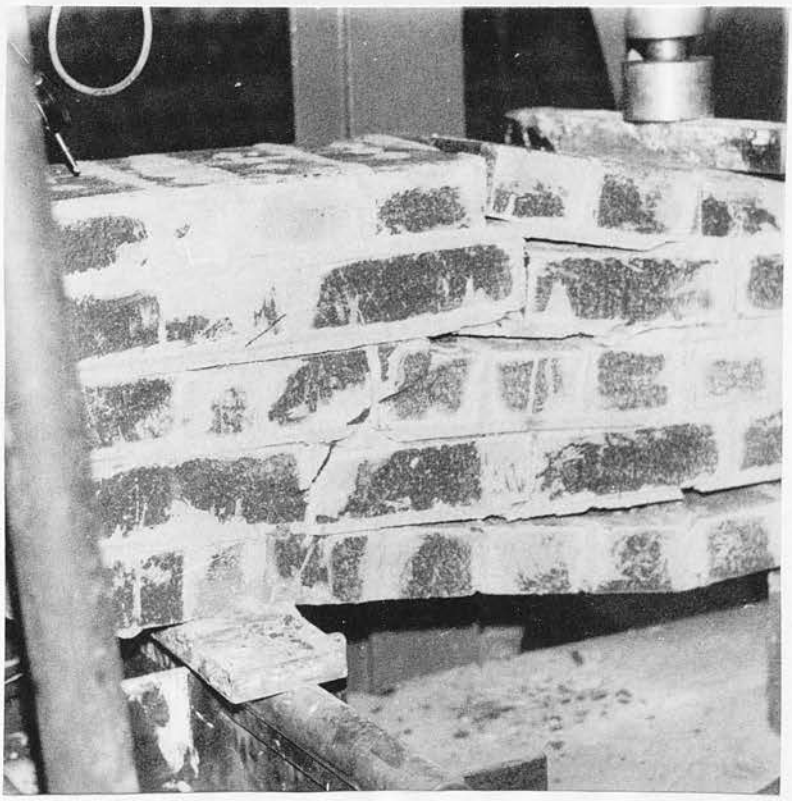

Plate 7.2 Typical diagonal shear failure.

Plate 7.3 Diagonal cracking.

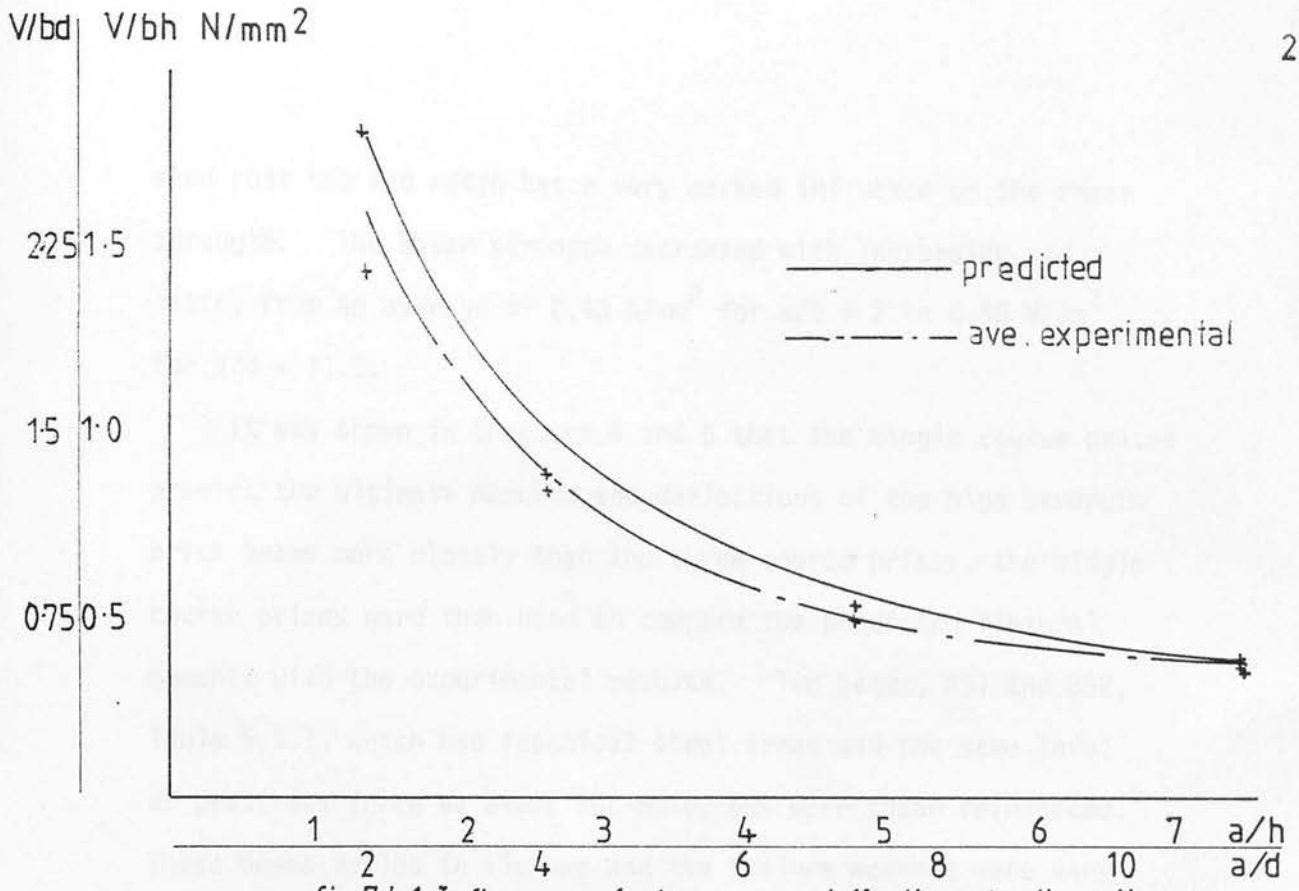

fig.7.4.1 Influence of shear span/effective depth ratio on the shear strength of prestressed brickwork beams.

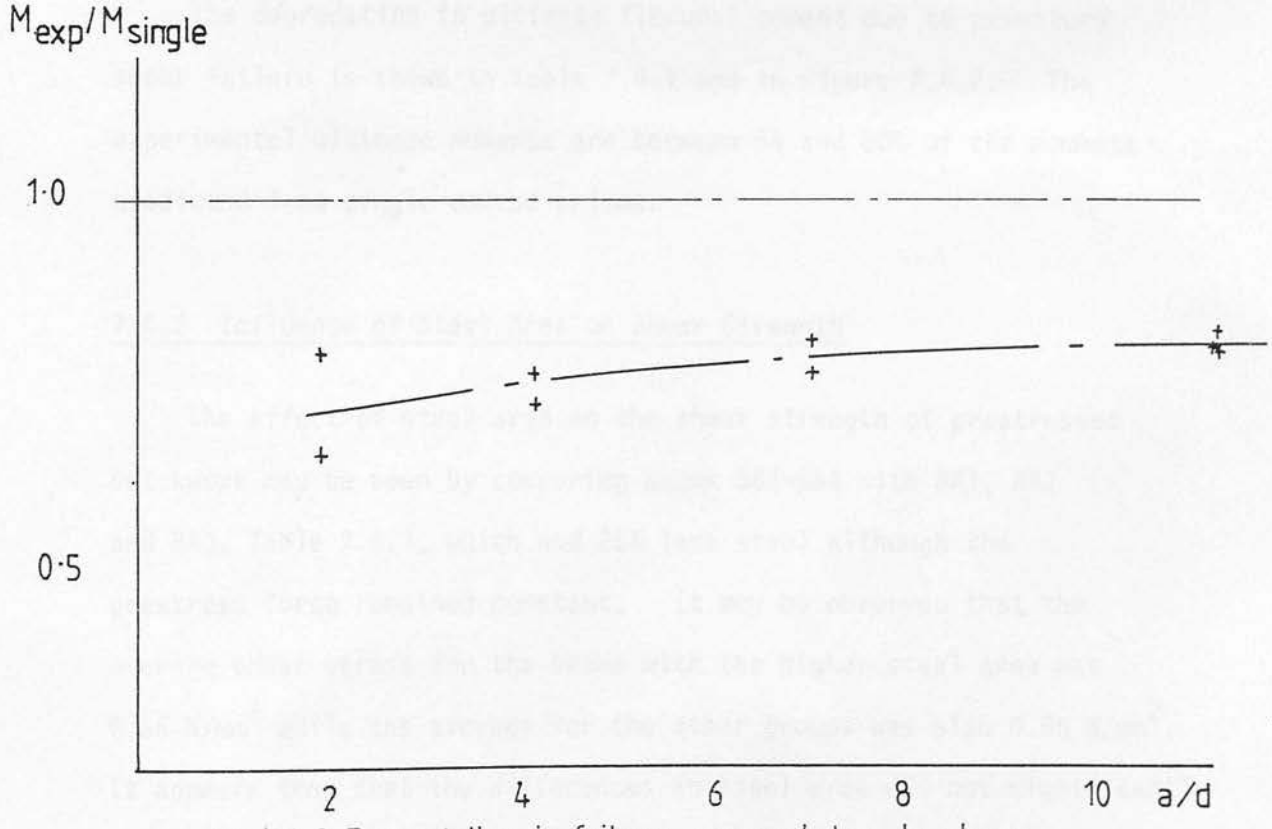

fig.7.4.2 Degredation in failure moment due to shear.

seen that the a/d ratio has a very marked influence on the shear strength. The shear strength decreased with increasing a/d ratio, from an average of 2.43 N/mm^2 for a/d = 2 to 0.56 N/mm^2 for a/d = 11.2.

It was shown in Chapters 5 and 6 that the single course prisms predict the ultimate moments and deflections of the high strength brick beams more closely than the three course prisms, the single course prisms were then used to compare the predicted flexural moments with the experimental results. Two beams, BS1 and BS2, Table 5.3.1, which had identical steel areas and the same level of prestress force as beams BB2-BB10, but were shear reinforced. These beams failed in flexure and the failure moments were very closely predicted with the single course prisms as shown in Table 5.4.1.

The degredation in ultimate flexural moment due to premature shear failure is shown in Table 7.4.1 and in Figure 7.4.2. The experimental ultimate moments are between 64 and 80% of the moments predicted from single course prisms.

7.4.2 Influence of Steel Area on Shear Strength

The effect of steel area on the shear strength of prestressed brickwork may be seen by comparing beams BB2-BB4 with BA1, BA2 and BA3, Table 7.4.1, which had 25% less steel although the prestress force remained constant. It may be observed that the average shear stress for the beams with the higher steel area was 0.56 N/mm^2 while the average for the other groups was also 0.56 N/mm^2. It appears then that the differences in steel area did not significantly

affect the shear strength. However, it can be seen from Table 7.4.1 that the beams with lower steel areas did not exhibit the same degree of degredation in moment and, in fact, the shear failure moments were very close to the predicted flexural moments, using the single course prisms.

The remaining beam in this group, BA3, underwent a flexural failure at a moment very similar to the other three beams as shown in Table 5.3.1. This particular area of steel, 0.411% steel then represents the transition point between a flexural failure and steel failure, such that any slight increase in steel area will most certainly result in a shear failure, whilst a decrease will probably cause a flexural failure.

It has previously been shown[45,74] that the area of steel has an effect on the shear strength of reinforced brickwork beams, but this trend is not apparent from the limited tests in this work. In the case of reinforced brickwork beams, an increase in the steel area may increase the contribution of dowel action to the shear strength. The strand used in prestressed brickwork beams was very much more flexible than ordinary reinforcement and thus may not be very effective in transmitting shear due to dowel action. The effect of dowel action in prestressed concrete is generally considered less effective than in reinforced concrete[6].

7.4.3 Effect of Shear Reinforcement on Shear Strength

Four beams, BS1-BS4, were constructed with four strands and shear reinforcement. The first two beams, BS1 and BS2, were prestressed to the same level as BB2-BB4. Both beams failed in

flexure, Table 5.3.1. As discussed in section 7.4.1, beams BB2-BB4 showed a degredation in failure moment of around 20% of the flexural moment, therefore the shear reinforcement in BS1 and BS2 was effective in increasing the shear strength.

The remaining two beams, BS3 and BS4 were prestressed to the same level as BB1. Both these beams failed in shear, however, from Table 7.4.1, the shear strength was slightly greater than BB1. It was very difficult to determine from the experiments whether or not the shear reinforcement had yielded. It is more likely that bond slip between the steel and the mortar occurred. It was difficult to provide proper shear reinforcement, as in concrete members, and straight rods were used in the prestressed brickwork beams.

7.4.4 Comparison Between Predicted and Experimental Results

Table 7.4.2 presents the predicted shear strengths of the prestressed brickwork beams using the plastic theory[26,75]. The effectivness factor for each beam was calculated using Equation 7.2.22. The average value of effectiveness factor was then used to predict the shear strengths using either Equations 7.2.20 or 7.2.21. The determination of both the effectiveness factor and the reinforcement index, R, depend on the compressive strength of the brickwork. As the single course prism proved most accurate in the determination of the flexural moment and deflections, it was also used to determine these two factors. The average value of ν was then 0.341.

Figure 7.4.1 compares the predicted shear strengths with the

Table 7.4.2 Comparison Between Experimental and Theoretical Shear Strengths

Beam	a/h	τ_{exp} N/mm^2	Eff. Factor ν	Degree of Reinforcement R	τ_{theo} N/mm^2	$\frac{\tau_{theo}}{\tau_{exp}}$
BB1	7.33	0.437	0.407	0.186	0.372	0.85
BB2	"	0.365	0.339	"	0.372	1.02
BB3	"	0.361	0.336	"	0.372	1.03
BB4	"	0.383	0.353	"	0.372	0.97
BB5	2.66	0.891	0.316	"	0.99	1.11
BB6	"	0.846	0.305	"	0.99	1.17
BB7	1.33	1.457	0.292	"	1.826	1.25
BB8	"	1.826	0.343	"	1.826	1.00
BB9	4.77	0.519	0.321	"	0.565	1.09
BB10	"	0.485	0.306	"	0.565	1.17
BA1	7.33	0.365	0.353	0.137	0.355	0.98
BA2	"	0.399	0.414	"	0.355	0.89
BA4	"	0.359	0.345	"	0.355	0.99

experimental shear strengths for beams BB2-BB10. Very good agreement between the predicted and the experimental results were obtained although the predicted results are slightly greater.

The trend of decreasing shear strength with increasing a/d ratio can be explained very simply by considering the stress distribution assumed in the lower bound solution. The behaviour of the beam has been idealised as that of a tied arch with a compression strut running from load point to support. The strength of this strut is νf_m. With increasing a/d ratio the angle of the strut to the axis of the beam decreases. Therefore the vertical force which may be transmitted through strut that is necessary to cause the stress in the strut to reach νf_m is reduced.

Very close agreement is obtained for the beams with lower steel areas (BA1, BA2, BA4). The shear strength of BB1 which had the greatest prestress force was underestimated somewhat. It is likely that the effectiveness factor will increase with the prestress force. The greater the prestress force the greater the load at which cracking and hence arching of the brickwork takes place. Therefore, although the prestress force may not actually affect the final failure mechanism, it is likely to influence the degree to which the stresses redistribute prior to failure.

7.5 Conclusions

1. The shear strength of prestressed brickwork beams decreases with increasing shear span/effective depth ratio.

2. From the limited test results it appears that the shear

strength of prestressed brickwork beams is not affected by the % of steel.

3. Shear reinforcement increases the shear strength of prestressed brickwork beams from the small number of tests.

4. The shear strength of prestressed brickwork beams without shear reinforcement may be accurately determined using the plastic theory as developed for reinforced concrete.

CHAPTER 8 : SUMMARY AND CONCLUSIONS

8.1 General

This thesis presents the results of a study into the behaviour of post-tensioned brickwork beams, in which a total of 51 full-scale beams were tested. Coincident with this work a series of small specimen tests were undertaken to evaluate the material properties of the brickwork used in a theoretical analysis. The influence of a number of variables on the strength and flexure of prestressed brickwork beams was considered.

8.2 Conclusions

Based on this study the following general conclusions can be drawn:

(1) Increases in brick and mortar strength increase the ultimate flexural moment of prestressed brickwork beams. The increase in strength was minimal for under-reinforced sections.

(2) Increasing the % of steel increases the ultimate flexural moment of prestressed brickwork beams. However, the shear strength of prestressed brickwork beams does not appear to be influenced by the % of steel.

(3) In beams in which the steel is not fully stressed up to

70% of its ultimate stress, further increases in prestress increased the flexural moment.

(4) The shear span/effective depth ratio affects the shear strength of prestressed brickwork beams.

(5) Shear reinforcement increases the shear strength of prestressed brickwork beams.

(6) The moment-curvature relationship of prestressed brickwork beams exhibits either two or three phase behaviour. These phases correspond to the initial uncracked section, the cracked section with steel still in the elastic range and the cracked section with steel yielding.

(7) In beams with higher steel areas the third phase of the moment-curvature relationship diminishes and may disappear entirely if the section is over-reinforced.

(8) The cracking moment of prestressed brickwork beams, which determines the transition from the uncracked to cracked state, increases with increasing prestress force, and decreases when the mortar changes from grade I to grade II.

(9) Flexural cracks in prestressed brickwork beams initiate at the brick/mortar interface. The spacing of these cracks is influenced by the initial height of crack and cover to the reinforcement.

(10) Flexural crack widths in prestressed brickwork beams are

directly proportional to the average strain in the beam at the level of the crack.

(11) The method proposed for the prediction of the flexural behaviour of prestressed brickwork beams, based on the non-linear stress/strain relationship of brickwork and taking tension stiffening into account, correlates very well with the experimental results.

(12) The stress/strain relationship and the compressive strength obtained from uni-axial compressive tests on single course prisms more closely predicts the flexural behaviour and ultimate strength of prestressed brickwork beams, than the three course prisms.

(13) The crack widths of prestressed brickwork beams can be predicted by the formula suggested in this work.

(14) The plastic method of determining the shear strength of prestressed concrete beams can be successfully applied to prestressed brickwork beams.

8.3 Suggestions for Future Research

The work carried out in this study explains the flexural behaviour of post-tensioned brickwork beams and provides a method of analysis based on the non-linear material stress/strain relationship of brickwork. A method of calculating the crack width and the plastic method for predicting the shear strength are also outlined. Before these methods are universally applied, it would

be worthwhile to carry out further research in the following areas:

(1) In the case of the present work the stress/strain relationship and strength obtained from the single course prisms predicted the deflection and ultimate moment of the beams. The draft code of practice[14] suggests a number of prism types that may be used to predict the compressive strength of brickwork. Further work needs to be carried out in this area to determine which prism types are most suited to the prediction of the flexural strength.

(2) Cracking in brickwork flexural members has received little or no attention. The influence of bonding patterns of brickwork, type of reinforcement and depth of cover may influence the formation of cracks and crack widths. The influence of these factors need to be explored further.

(3) The plastic theory for predicting the shear strength of concrete beams seems to apply equally well to brickwork. This method should be extended to encompass the whole range of brickwork flexural members that are likely to fail in shear.

(4) Some of the adverse effects of prestressing such as excessive camber and anchorage forces may be minimised by partial prestressing. The methods of analysis presented in this study apply equally well to partially

prestressed beams. Future work should extend into this field to determine the influence that the ratio of tensioned to non-tensioned and type of reinforcement has on the flexural behaviour of prestressed brickwork beams.

REFERENCES

1. British Standards Institution, 'The Structural Use of Masonry', Part 1, Unreinforced Masonry, B.S.5628, Part 1, London, 1978.

2. Schneider, R. and Dickey, W.L. 'Reinforced Masonry Design', Prentice-Hall, New Jersey, 1980.

3. Haseltine, B.A. and Tutt, J.W. 'Brickwork Retaining Walls', Brick Development Association publication, Westerham Press, 1977.

4. Thomas, K. 'Current Post-Tensioned and Prestressed Brickwork and Ceramics in Great Britain', Designing, Engineering and Constructing with Masonry Products, ed. F.B. Johnson, Gulf, Houston, Texas, 1969, pp.94-100.

5. Gadebuku, C.B.K. 'A Study of the Magnitude and Distribution of the Stresses in the End Block of Post-Tensioned Concrete Beams', Ph.D. Thesis, Rutgers University, New Jersey, 1980.

6. Bruce, R.N. 'The Action of Vertical, Inclined and Prestressed Stirrups in Prestressed Concrete Beams', Journal of the Prestressed Concrete Institute, Vol.9, Pt.1, 1969, pp.14-25.

7. Mehta, K.C. and Fincer, D. 'Structural Behaviour of Pretensioned Prestressed Masonry Beams', Proc. 2nd International Brick Masonry Conference, ed. H.W.H. West and K. Speed, Stoke-on-Trent, 1970, pp.215-219.

8. Williams, E.O.L. and Phipps, M. 'Bending Behaviour of Prestessed Masonry Box Beams', Proc. 6th International Brick Masonry Conference, ed. Laterconsult, Rome, 1982, pp.981-994.

9. Curtin, W.G. and Phipps, M. 'Prestressed Masonry Diaphragm Walls', Proc. 6th International Brick Masonry Conference, ed. Laterconsult, Rome, 1982, pp.971-980.

10. Baxter, W. 'The Strength of Unbonded Prestressed Brickwork Beams', 4th Year Honours Project, Department of Civil Engineering, University of Edinburgh, 1979.

11. McDonald, G.C.A. 'The Ultimate Strength of Prestressed Brickwork Beams', 4th Year Honours Project, Department of Civil Engineering, University of Edinburgh, 1980.

12. Robson, I.J., Hulse, R., Ambrose, R. and Morton, J. 'Performance of Post-Tensioned Brickwork Beams Under Service and Ultimate Load Conditions', Proc. 3rd Canadian Masonry Conference, ed. J. Longworth and J. Warwaruk, Edmonton, Canada, June 1983, paper no.14.

13. Pedreschi, R.F. and Sinha, B.P. 'Development and Investigation of the Ultimate Load Behaviour of Post-Tensioned Brickwork Beams', The Structural Engineer, Vol.60B, No.3, September 1982, pp.63-67.

14. British Standards Institution, 'The Structural Use of Masonry, Part 2, Reinforced and Prestressed Masonry', B.S.5628, Part 2, Draft issued for comment.

15. Neil, J.S. 'Post-Tensioned Brickwork', Clay Products Technical Bureau, Technical Note, Vol.1, No.9, 1966.

16. Curtin, W.G., Beck, J.K., Shaw, G. and Pope, 'Post-Tensioned Free Cantilever Diaphragm Wall Project', Proc. 6th International Brick Masonry Conference, ed. Laterconsult, Rome, 1982, pp.1645-1656.

17. Bradshaw, R.E., Drinkwater, J. and Bell, S.E. 'A Multi-Purpose Farm Builing Incorporating Prestressed Brickwork Diaphragm Walling', Proc. of British Ceramic Society, Load Bearing Brickwork (7), ed. H.W.H. West, Stoke-on-Trent, September 1982, pp.308-315.

18. Foster, D. 'Design and Construction of a Prestressed Brickwork Water Tank', Proc. 2nd International Brick Masonry Conference, ed. H.W.H. West and K.H. Speed, British Ceramic Research Association, Stoke-on-Trent, 1971.

19. Wass, R.J. and Turner, D.J. 'A Prestressed Clay Masonry Floor', Designing Engineering and Constructing with Masonry Products, ed. F.B. Johnson, Gulf, Houston, Texas, 1969, pp.200-209.

20. Plowman, J.M., Sutherland, R.J.M. and Couzens, M.L. 'The Testing of Reinforced Brickwork and Concrete Slabs Forming Box Beams', The Structural Engineer, Vol.45, No.11, November 1967, pp.379-394.

21. Baker, A.L.L. 'The Flexural Action of Masonry Structures Under Lateral Load', Ph.D. Thesis, Deakin University, Australia, July 1981.

22. Plummer, H.C. and Blume, J.A. 'Reinforced Brick Masonry and Lateral Force Design', Structural Clay Products Ltd., Washington D.C., 1953.

23. 'Reinforced and Prestressed Masonry', July 1981, London, The Institution of Structural Engineers.

24. Leonhardt, F. 'Prestressed Concrete', Wilhelm Ernst and Sohn, Berlin, 1964.

25. Abeles, P.W. 'An Introduction to Prestressed Concrete Vol.1', Concrete Publications Ltd., London, 1964.

26. Nielsen, M.P. and Braestrup, M.W. 'Shear Strength of Prestressed Concrete Beams Without Shear Reinforcement', Mag. of Concrete Research, Vol.30, No.103, September 1978, pp.119-128.

27. Hodgkinson, H.R. and Davies, S. 'The Stress/Strain Relationship of Brickwork When Stressed in the Direction Other Than Normal to the Bedjoint', Proc. 6th International Brick Masonry Conference, ed. Laterconsult, Rome, 1982, pp.290-299.

28. Lenczner, D. and Foster, D. 'Strength and Deformation of Brickwork Properties in Three Directions', 5th International Brick Masonry Conference, ed. J.A. Wintz, Washington, 1979, pp.49-55.

29. British Standards Institution, 'Clay Bricks and Blocks', B.S.3921, 1974, London.

30. British Standards Institution, 'Specification for Building Sands from Natural Sources', B.S.1200, 1976, London.

31. Special Publication 91, Design Guide for Reinforced and Prestressed Masonry, Structural Ceramics Advisory Group.

32. Hendry, A.W. 'Structural Brickwork', The Macmillan Press, London, 1981.

33. Powell, B. and Hodgkinson, H.R. 'The Determination of the Stress/Strain Relationship of Brickwork, 4th International Brick Masonry Conference, Brugges, 1976, Paper 2.a.5.

34. Turnsek, V. and Cacovic, F. 'Some Experimental Results on the Strength of Brick Masonry Walls', 2nd International Brick Masonry Conference, British Ceramic Research Association, Stoke-on-Trent, pp.149-156.

35. Sinha, B.P. and Pedreschi, R.F. 'Compressive Strength and Some Elastic Properties of Brickwork', International Journal of Masonry Construction, Vol.3, No.1, 1983, pp.19-25.

36. Sinha, B.P. 'An Ultimate Load Analysis of Brickwork Flexural Members', International Journal of Masonry Construction, Vol.1, No.4, 1981, pp.151-155.

37. Popovics, S. 'A Review of the Stress/Strain Relationships for Concrete', Journal of American Concrete Inst., Vol.67, 1970, pp.243-247.

38. Pedreschi, R.F. and Sinha, B.P. 'The Stress/Strain Relationship of Brickwork', 6th International Brick Masonry Converence, ed. Laterconsult, Rome, 1982, pp.321-334.

39. British Standards Institution, 'Code of Practice for the Structural Use of Concrete', C.P.110, London, 1972.

40. The British Standards Institution, 'The Structural Use of Concrete in Buildings', C.P.114, London, 1969.

41. The British Standards Institution, 'Structural Recommendations for Load Bearing Walls', C.P.111, London, 1970.

42. Hendry, A.W. 'Safety Factors in the Limit State Design of Masonry', International Journal of Masonry Construction, Vol.2, No.4, 1982, pp.178-180.

43. Kong, F.K. and Evans, R.H. 'Reinforced and Prestressed Concrete', Nelson, London, 1975.

44. Evans, R.H. 'The Plastic Theories for the Ultimate Strength of Reinforced Concrete Beams', Journal of the Inst. of Civil Engineers, Vol.21, No.2, 1943, pp.98-120.

45. Sinha, B.P. 'Grouted Cavity Shear Tests', S.C.P.16, Structural Clay Products Ltd., Herts.

46. Whitney, C.S. 'Plastic Theory of Reinforced Concrete Design', Trans. A.S.C.E., Vol.107, 1942, pp.251-326.

47. Sinha, B.P. 'Ultimate Load Analysis of Reinforced Brick Beams', B.C.R.A. Seminar on Theory of Masonry Structures, July 1980.

48. Beard, R. 'A Theoretical Analysis of Reinforced Brickwork in Bending', Proc. British Ceramic Society, No.30, September 1982, pp.272-282.

49. Cavanagh, C.J. and Edgell, G.J. 'Stress/Strain Relationships for Brickwork', Bearing Walls, C.I.B. Proceedings, Publication 63, Stoke-on-Trent, England, 1981.

50. Scott, R.H. and Gill, P.A.T. 'Developments in the Measurement of Reinforcement Strain Distribution in Concrete Members', Strain, Vol.18, No.2, May 1982, pp.61-63.

51. Timoshenko, S. 'Strength of Materials, Part 1', Van Nostrand, New York, 1955.

52. Branson, D.E. 'Deformation of Concrete Structure', McGraw-Hill, New York.

53. Beeby, A.W. and Taylor, H.P.J. 'Short-Term Deformations of Concrete Structures', C. and C.A. Technical Report TRA 408, March 1968.

54. Beeby, A.W., Keyder, E. and Taylor, H.P.J. 'Cracking and Deformations of Partially Prestressed Concrete Beams', Cement and Concrete Association, London, January 1972, Technical Report, 42, 465.

55. Shaikh, A.F. and Branson, D.E. 'Non-Tensioned Steel in Prestressed Concrete Beams', Journal of Prestressed Concrete Inst., February 1970, pp.15-36.

56. Mohamedbhai, G.T.G. 'Short-Term Deflections of Beams: A New Approach to Calculation', Concrete, pp.33-34, March 1976.

57. Burns, N.H. 'Moment-Curvature Relations for Partially Prestressed Concrete Beams', Journal of the Prestressed Concrete Inst., Vol.9, 1964, pp.52-63.

58. Warwuk, J., Sozen, M.A. and Seiss, C.P. 'Investigation of Prestressed Concrete for Highway Bridge, Part III, Strength and Behaviour in Flexure of Prestressed Concrete Beams', University of Illinois, Bulletin No.464, 1962.

59. Priestley, M.J.N., Park, R. and Lu, F.P.S. 'Moment-Curvature Relationships for Prestressed Beams in Constant Moment Zone', Mag. of Concrete Research, Vol.23, No.75-76, June 1971, pp.69-78.

60. Tadjogueu, E.W. 'Nonlinear Analysis of Reinforced Concrete Beams by Finite Element Method', Ph.D. Thesis, State University of New York at Buffalo, September 1980.

61. Duncan, W. and Johnarry, T. 'Further Studies of the Constant Stiffness Method of Non-Linear Analysis of Concrete Structures', Proc. Inst. of Civil Engineers, Part 2, Vol.67, December 1979, pp.951-968.

62. Page, A.W. 'The In-Plane Deformation and Failure of Brickwork', Ph.D. Thesis, University of Newcastle, Australia, 1977.

63. Samarsinghe, W., Page, A.W. and Hendry, A.W. 'Behaviour of Brick Masonry Shear Walls', The Structural Engineer, Vol.59B, No.3, September 1981, pp.42-48.

64. Rao, P.S. and Subrahmanyam, B.V. 'Trisegmental Moment-Curvature Relations for Reinforced Concrete Members', Proc. A.C.J., Vol.70, No.5, May 1973, pp.346-351.

65. Ghali, A. and Neville, A.M. 'Structural Analysis: A Unified Approach', Chapman and Hall, London, 1971.

66. British Standards Institution, 'The Structural Use of Concrete for Retaining Aqueous Liquids', B.S.5337, 1976, London.

67. Bennett, E.W. and Chandrasekhar, C.S. 'Calculation of the Width of Cracks in Class 3 Prestressed Concrete Beams', Proc. Inst. of Civil Engineers, Vol.49, 1971, pp.333-346.

68. Meier, S.W. and Gergely, P. 'Flexural Crack Widths in Prestressed Concrete Beams', Proc. A.S.C.E., Jnl. of the Struct. Div., Vol.107, February 1981, pp.429-433.

69. Desayi, P. 'A Method for Determining the Spacing and Width Cracks in Partially Prestressed Concrete Beams', Proc. Inst. of Civil Engineers, Part 2, Vol.59, September 1975, pp.441-428.

70. Base, G.D., Read, J.B., Beeby, A.W. and Taylor, H.P.J. 'Crack Control in Concrete Beams', C.E.R.A., Research Report, No.6, C. and C.A., 1966.

71. Beeby, A.W. 'The Prediction of Crack Widths in Hardened Concrete', The Structural Engineer, Vol.57A, No.1, January 1979, pp.9-17.

72. Sinha, B.P. 'Reinforced Grouted Cavity Brickwork', Building Research and Practise, Vol.10, No.4, July 1982, pp.226-243.

73. Suter, G.T. and Hendry, A.W. 'Shear Strength of Reinforced Brickwork Beams', The Structural Engineer, Vol.53, No.6, 1975, pp.249-253.

74. Osman, Y. and Hendry, A.W. 'Shear Transmission in Reinforced Grouted Cavity Brickwork Beams', Sixth Int. Brick Masonry Conf. Rome, 1982, ed. Laterconsult, pp.817-830.

75. Nielsen, M.P., Braestrup, M.W., Jensen, B.R. and Bach, F. 'Concrete Plasticity Beam Shear - Shear in Joints, Punching Shear', Danish Society for Structural Science and Engineering, Special Publication, Technical University of Denmark, Copenhagen, October 1978.

76. Page, A.W. 'The Biaxial Compressive Strength of Brickwork', Proc. Inst. of Civil Engineers, Part 2, Vol.71, September 1981, pp.893-906.

77. Prager, W. 'An Introduction to Plasticity', Addison-Wesley, Massachusetts, 1959.

78. Jensen, B.C. 'Lines of Discontinuity for Displacements in the Theory of Plasticity of Plain and Reinforced Concrete', Mag. of Concrete Research, Vol.27, No.92, September 1975, pp.143-150.

APPENDIX 1 : COMPUTER PROGRAMME

A.1.2 Data Input Instructions

Line		Format
1	BREADTH, STRSSMX, PRESTR1, PRESTR2	4F10.5
2	STRMX, DEPTH, RMODULUS	3F10.6
3	EFFD1, EFFD2, ASTL1, ASTL2	4F10.5
4	NLD, NDV, NMOM, KLM, LTS	5I3
5	SPAN, BAP, ANDV, ANLD	4F10.5
6	COFF(1), COFF(2), COFF(3), COFF(4)	4F10.5
7	STRN1(1), STRN2(1), EMOD(1), EMODA(1), EMODB(1)	5F11.5
8	STRN1(2), STRN2(2), EMOD(2), EMODA(2), EMODB(2)	5F11.5
9	ULT1, ULT2	2F10.5

A.1.2 Definition of Variables

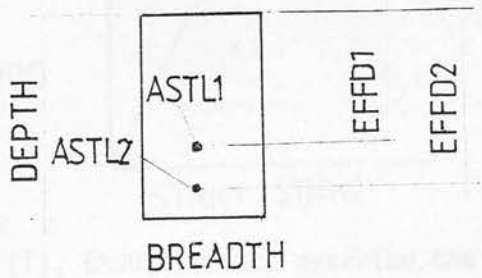

STRSSMX - compressive strength of masonry, N/mm^2

STRMX - ultimate compressive strain of masonry x 10^5

RMODULUS - modulus of rupture, N/mm^2

PRESTR1, PRESTR2 - prestressing forces in kN applied to ASTL1 and ASTL2 respectively

NLD - number of increments of load applied to beam

NDV - number of nodes along span of beam

NMOM - number of increments for M - ϕ relationship (always 25)

KLM - 0

LTS - if LTS $\neq$ 1 then effects of tension-stiffening ignored

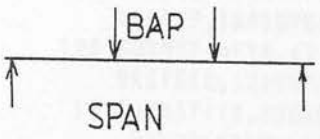

ANLD - number of load increments

ANDV - NLD + 1

COFF(1) - COFF(4) - coefficients of stress/strain relationship of brickwork

i.e. $f/f_m = COFF(1)\ \varepsilon/\varepsilon_m + COFF(2)\ (\varepsilon/\varepsilon_m)^2 + COFF(3)\ (\varepsilon/\varepsilon_m)^3 \ldots$

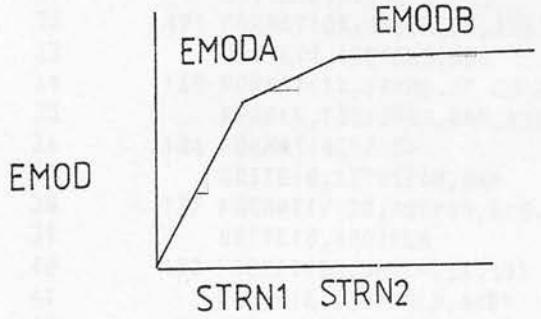

STRN1(1), EMOD(1), etc. describe the stress/strain relationship of ASTL1

STRN1(2), EMOD(2), etc. describe the stress/strain relationship of ASTL2

ULT1 - ultimate strength of steel, ASTL1, N/mm^2

ULT2 - ultimate strength of steel, ASTL2, N/mm^2

```
EDINBURGH FORTRAN(G) COMPILER VERSION 70.3

 1            PROGRAM MAIN
 2            DIMENSION DNARRY(20),MOMENT(25),COFF(4),CURVE(25)
 3            DIMENSION STRST(20),SPND2(30),PLOAD(40),DEFLEX(40)
 4            DIMENSION STRN1(2),STRN2(2),EMOD(2),EMODA(2),EMODB(2)
 5            DIMENSION ESTEELS(20),STRAINS(20),SMOM(5),CURVEP(5)
 6            COMMON/DASC/NAIL,MOMENT,DNA,CURVE
 7            COMMON/ALB/ELAST,PRESTR1,PRESTR2,STRSSMX,STRMX,SMOM,CURVEP
 8            COMMON/BAT/E1,CRKMOM,FRSTRN1,PRSTRN2,STEEL1,STRAIN
 9            DOUBLE PRECISION DIFF(19,19),BMAT(19),DEFL(19),DIFFT(19,19)
10           .,WKS1(30),WKS2(30)
11            DOUBLE PRECISION MOM(25),CURV(25),ASD(12),REF
12            READ(9,100)BREADTH,STRSSMX,PRESTR1,PRESTR2
13         100 FORMAT(4F10.4)
14            WRITE(8,12)BREADTH,STRSSMX,PRESTR1,PRESTR2
15          12 FORMAT(1X,8HBREADTH=,F10.5,1X,8HSTRSSMX=,F10.5,1X,8HPRESTR1=,F10.5
16           .,P8HPRESTR2=,F10.5)
17            READ(9,110)STRMX,DEPTH,RMODULUS
18         110 FORMAT(3F10.5)
19            WRITE(8,115)STRMX,DEPTH,RMODULUS
20         115 FORMAT(19HSTRMX DEPTH MODULUS,1X,F10.5,1X,F10.5,1X,F10.5)
21            STRMX=STRMX/100000.0
22            READ(9,120)EFFD1,EFFD2,ASTL1,ASTL2
23         120 FORMAT(4F10.5)
24            WRITE(8,125)EFFD1,ASTL1
25         125 FORMAT(1X,9HEEFECTIVE,1X,6HDEPTH=,F10.5,1X,5HAREA=,F10.5,3HMM2)
26            WRITE(8,125)EFFD2,ASTL2
27            READ(9,133)NLD,NDV,NMOM,KLM,LTS
28         133 FORMAT(5I3)
29            WRITE(8,19)NMOM
30          19 FORMAT(2X,17HNO.OF MOMENT INCS,2X,I3)
31            WRITE(8,491)LTS
32         491 FORMAT(2X,3HLTS,2X,I3)
33            WRITE(8,135)NLD,NDV
34         135 FORMAT(1X,11HNO.OF LOADS,1X,I3,1X,15HNO.OF DIVISIONS,1X,I3)
35            READ(9,136)SPAN,BAP,ANDV,ANLD
36         136 FORMAT(4E10.5)
37            WRITE(8,137)SPAN,BAP
38         137 FORMAT(/,2X,4HSPAN,E10.5,2X,10HJACK SPACE,1X,E10.5)
39            WRITE(8,400)KLM
40         400 FORMAT(2X,3HKLM,2X,I3)
41            WRITE(8,138)ANLD,ANDV
42         138 FORMAT(2X,9HANLD ANDV,2X,E10.5,2X,E10.5)
43            READ(9,6)COFF(1),COFF(2),COFF(3),COFF(4)
44           6 FORMAT(4E10.5)
45            WRITE(8,7)
46           7 FORMAT(2X,28HCOEFFICENTS OF STRESS/STRAIN)
47            DO 9 I=1,4
48            WRITE(8,3)COFF(I)
49           3 FORMAT(2X,E14.5)
50           9 CONTINUE
51            READ(9,78)STRN1(1),STRN2(1),EMOD(1),EMODA(1),EMODB(1)
52          78 FORMAT(5E11.5)
53            WRITE(8,700)STRN1(1),STRN2(1),EMOD(1),EMODA(1),EMODB(1)
54         700 FORMAT(1X,5HSTRN1,1X,E10.5,2X,5HSTRN2,1X,E14.5,2X,4HEMOD
55           .,1X,E10.5,2X,5HEMODA,1XE10.5,2X,5HEMODB,1X,E10.5)
56            READ(9,79)STRN1(2),STRN2(2),EMOD(2),EMODA(2),EMODB(2)
57          79 FORMAT(5E11.5)
58            WRITE(8,701)STRN1(2),STRN2(2),EMOD(2),EMODA(2),EMODB(2)
59         701 FORMAT(1X,5HSTRN1,1X,E10.5,2X,5HSTRN2,1X,E14.5,2X,4HEMOD
60           .,1X,E10.5,2X,5HEMODA,1X,E10.5,2X,5HEMODB,1X,E10.5)
61            READ(9,1)ULT1,ULT2
```

```
      1 FORMAT(2E10.5)
        WRITE(8,34)ULT1,ULT2
     34 FORMAT(2X,15HULTIMAT STRESS,2X,E10.5,2X,E10.5)
        DO 2 II=1,25
        MOM(II)=0.0
        CURV(II)=0.0
      2 CONTINUE
        CALL PRESTRESS(RMODULUS,EFFD1,EFFD2,ASTL1,ASTL2,BREADTH,DEPTH,
     .MOM,CURV,COFF,EMOD)
C       WRITE(8,410)STEEL1
C  410 FORMAT(2X,6HSTEEL1,2X,E12.5)
        CALL MOMCUR(STRMX,EFFD1,EFFD2,ASTL1,ASTL2,STRSSMX,COFF1,COFF2,
     .STRAIN,BREADTH,PRSTRN1,PRSTRN2,DEPTH,MOM,CURV,RMODULUS,
     .STEEL1,KLM,COFF,STRN1,STRN2,EMOD,EMODA,E1,CRKMOM,EMODB,
     .ULT1,ULT2,LTS)
        BENMOM=MOMENT(20)/1000000.0
        WRITE(8,5)BENMOM
      5 FORMAT(3X,24HULTIMATE BENDING MOMENT=,F12.5,1X,3HKNM)
C       WRITE(8,7)DNA
C     7 FORMAT(3X,10HN.A.DEPTH=,1X,F12.5,1X,2HMM)
        IJ=25-NAIL
        DO 140 I=1,IJ
        MOM(I)=MOM(I)/1000000.0
    140 CONTINUE
        IM=24-NAIL
        DO 10 I=1,IM
        K=I+1
        IF(MOM(I).LT.MOM(K)) GO TO 10
        MOM(I)=MOM(K)-0.01
     10 CONTINUE
        WRITE(8,149)
    149 FORMAT(//,1X,38HCOMPLETE MOMENT CURVATURE RELATIONSHIP,)
        WRITE(8,193)
    193 FORMAT(3X,23HWITH TENSION STIFFENING,//)
        DO 155 IK=1,IJ
        WRITE(8,151)MOM(IK),CURV(IK)
    151 FORMAT(2X,E14.5,2X,E14.5)
    155 CONTINUE
C       CALL E02ACF(MOM,CURV,25,ASD,KPOLY,REF)
C       WRITE(8,152)
C  152 FORMAT(2X,6HCOEFFS)
C       DO 154 K=1,KPOLY
C       WRITE(8,153)ASD(K)
C  153 FORMAT(2X,F20.18)
C  154 CONTINUE
C       WRITE(8,156)REF
C  156 FORMAT(2X,5HREF =,E20.15)
        SPN=SPAN/ANDV
        NDV2=(NDV+1)/2
        SPND1=0.0
        DO 850 J=1,NDV2
        SPND1=SPND1+SPN
        SPND2(J)=SPND1
    850 CONTINUE
        SPN2=SPN*SPN
C  ASSEMBLE MATRIX OF DEFLECTION COEFFICENTS
C  SET ALL TERMS TO ZERO
        DO 500 I=1,NDV
        DO 500 J=1,NDV
        DIFF(I,J)=0.0
    500 CONTINUE
```

```
C  FORM NON ZERO TERMS IN MATRIX
      DO 502 K=1,NDV
      DIFF(K,K)=2.0
      KK=K-1
      KKK=K+1
      IF(K.EQ.1)GO TO 503
      DIFF(K,KK)=-1.0
      IF(K.EQ.NDV)GO TO 502
  503 DIFF(K,KKK)=-1.0
  502 CONTINUE
C      DO 508 I=1,NDV
C      WRITE(8,507)(DIFF(I,J),J=1,NDV)
C  507 FORMAT(1X,D10.2)
C  508 CONTINUE
      SSPN=(SPAN-BAP)/2.0
      ULOAD=(BENMOM/SSPN)*2000.0
      WRITE(8,302)ULOAD
  302 FORMAT(/,3X,13HULTIMATE LOAD,1X,E14.5)
      WRITE(8,880)
  880 FORMAT(2X,4HLOAD,6X,10HDEFLECTION)
      WRITE(8,881)
  881 FORMAT(12X,20HPROFILE FROM SUPPORT)
      WRITE(8,851)(SPND2(I),I=1,NDV2)
  851 FORMAT(17X,30E10.5,//)
      NCUR=(NMOM-1)-NAIL
      SPN=SPAN/ANDV
      NDIV=NDV+1
      SPNTWO=SPN/2.0
C  1ST LOAD INCREMENT
      PLOD=ULOAD/(2.0*ANLD)
      PLODA=PLOD
      KL=0
   80 CONTINUE
      SPND=SPN
      DEFLT=0.0
      K=1
C  LOOP FOR BEAM SECTIONS
      SST=SSPN+BAP
   96 CONTINUE
C  CALCULATE BM AT EACH NODE POINT
      IF(SPND.GT.SSPN.AND.SPND.LT.SST) GO TO 385
      IF(SPND.GT.SST) GO TO 387
      BM=(SPND*PLOD)/1000.0
      GO TO 386
  385 BM=(PLOD*SSPN)/1000.0
      GO TO 386
  387 BM=(PLOD/1000.0)*(SPAN-SPND)
  386 CONTINUE
C      WRITE(8,600)BM
C  600 FORMAT(2X,2HBM,2X,E10.5)
      SPND2(K)=SPND
         SPND=SPND+SPN
C  CALCULATE CURVATURE FROM POLYNOMIAL
      DO 101 I=1,NCUR
      IL=I+1
      IF(BM.LT.MOM(1)) GO TO 170
      IF(BM.GT.MOM(I).AND.BM.LT.MOM(IL)) GO TO 160
      GO TO 101
  170 FACT=BM/MOM(1)
      CURT=FACT*CURV(1)
      GO TO 161
```

```
      160 FACT=(BM-MOM(I))/(MOM(IL)-MOM(I))
          CURT=CURV(I)+(FACT*(CURV(IL)-CURV(I)))
          GO TO 161
      101 CONTINUE
      161 CONTINUE
          BMAT(K)=CURT*SPN2
CC        WRITE(8,900)BMAT(K)
      900 FORMAT(2X,4HBMAT,2X,D10.3)
          K=K+1
          IF(K.EQ.NDIV) GO TO 98
          GO TO 96
       98 CONTINUE
          KL=KL+1
               DO 867 II=1,NDV
          DO 867 KK=1,NDV
          DIFFT(II,KK)=DIFF(II,KK)
      867 CONTINUE
          CALL F04ARF(DIFFT,NDV,BMAT,NDV,DEFL,WKS1,0)
          WRITE(8,200)(PLOD,(DEFL(I),I=1,NDV2))
      200 FORMAT(/,2X,E10.5,4X,30D10.3)
          PLOD=PLODA+PLOD
          IF(KL.EQ.NLD) GO TO 102
          GO TO 80
      102 CONTINUE
          STOP
          END


          SUBROUTINE MOMCUR(STRMX,EFFD1,EFFD2,ASTL1,ASTL2,STRSSMX,COFF1,
         .COFF2,STRAIN,BREADTH,PRSTRN1,PRSTRN2,DEPTH,MOM,CURV,RMODULUS,
         .STEEL1,KLM,COFF,STRN1,STRN2,EMOD,EMODA,E1,CRKMOM,EMODB,
         .ULT1,ULT2,LTS)
          DIMENSION STRST2(20),STRST(20),STRAINS(20),ESTEELS(20)
          DIMENSION STRN1(2),STRN2(2),EMOD(2),EMODA(2),EMODB(2)
          DIMENSION DNARRY(20),MOMENT(20),COFF(4),CURVE(20)
          COMMON/DASC/NAIL,MOMENT,DNA,CURVE
          DOUBLE PRECISION MOM(25),CURV(25)
          STRAIN=STRAIN*2.0
          STRAINT=STRAIN
          DNA=EFFD1*0.7
C     THIS ROUTINE CALCILATES THE MOMENT CURVATURE
          J=0
          I=0
          DF=2.0
          IF(ASTL1.EQ.0.0.OR.ASTL2.EQ.0.0)DF=1.0
          PSTL=((ASTL1+ASTL2)*DF)/((EFFD1+EFFD2)*BREADTH)
          IF(J.EQ.0)GO TO 12
       10 STRAIN=STRAIN+STRINC
       12 CONTINUE
          IF(J.EQ.0)STRAIN=STRAINT
          IF(J.EQ.20) GO TO 54
C    CALCULATE STREIN IN STEEL
       20 CONTINUE
          XDEPTH1=EFFD1-DNA
          ESTEELT=STRAIN*(XDEPTH1/DNA)
          ESTEEL1=ABS(ESTEELT)
          XDEPTH2=EFFD2-DNA
          IF(ASTL2.EQ.0.0)XDEPTH2=0.0
          ESTEELA=STRAIN*(XDEPTH2/DNA)
          ESTEEL2=ABS(ESTEELA)
C          WRITE(8,45)ESTEEL1,ESTEEL2
C    45 FORMAT(7HSTRAINS,2X,E14.5,2X,E14.5)
          STRN3=STRN2(1)-STRN1(1)
```

```
245           STRN31=STRN2(2)-STRN1(2)
246           ESTEEL1=ESTEEL1+PRSTRN1
247           ESTEEL2=ESTEEL2+PRSTRN2
248           ESTL1=ESTEEL1-STRN1(1)
249           ESTL2=ESTEEL2-STRN1(2)
250           ESTEELY1=ESTEEL1-STRN2(1)
251           ESTEELY2=ESTEEL2-STRN2(2)
252           IF(ESTEELY1.LT.0.0)ESTEELY1=0.0
253           IF(ESTEELY2.LT.0.0)ESTEELY2=0.0
254           IF(ESTEEL1.LT.STRN1(1))EMOD1=0.0
255           IF(ESTEEL2.LT.STRN1(2))EMOD2=0.0
256           IF(ESTEEL1.LT.STRN1(1))ESTL1=0.0
257           IF(ESTEEL2.LT.STRN1(2))ESTL2=0.0
258           IF(ESTEEL1.GT.STRN1(1).AND.ESTEEL1.LT.STRN2(1))EMOD1=EMODA(1)
259           IF(ESTEEL2.GT.STRN1(2).AND.ESTEEL2.LT.STRN2(2))EMOD2=EMODA(2)
260           IF(ESTEEL1.GT.STRN2(1))ESTL1=STRN3
261           IF(ESTEEL2.GT.STRN2(2))ESTL2=STRN3
262           IF(ESTEEL1.GT.STRN1(1))ESTEEL1=STRN1(1)
263           IF(ESTEEL2.GT.STRN1(2))ESTEEL2=STRN1(2)
264     C   CALCULATE TENSION FORCE
265           STRSS1=(EMOD(1)*ESTEEL1)+(EMODA(1)*ESTL1)+(ESTEELY1*EMODB(1))
266           STRSS2=(EMOD(2)*ESTEEL2)+(EMODA(2)*ESTL2)+(ESTEELY2*EMODB(2))
267           TF1=ASTL1*STRSS1
268           TF2=ASTL2*STRSS2
269           TFORCE=TF1+TF2
270     C       WRITE(8,3)TFORCE
271     C     3 FORMAT(2X,6HTFORCE,2X,E1(2)(1)0.5)
272           ULTFORCE=(ASTL1*ULT1)+(ASTL2*ULT2)
273           IF(TFORCE.GT.ULTFORCE)TFORCE=ULTFORCE
274     C  CALCULATE COMP. FORCE
275           STRAINM=STRAIN/STRMX
276           ALAYER=DNA/50.0
277           EGRAD=STRAINM/50.0
278           EDIVS=EGRAD
279           EDIV=EGRAD/2.0
280           ALEV=ALAYER/2.0
281           TMOMT=0.0
282           COMPT=0.0
283           K=1
284     C  LAYER STRAINS
285        25 CONTINUE
286           K=K+1
287           IF(K.EQ.51) GO TO 50
288           ELAY=STRAINM-EDIV
289           STRS=(COFF(1)*ELAY)+(COFF(2)*(ELAY*ELAY))+(COFF(3)*ELAY*
290          .(ELAY*ELAY))
292           COMP=(STRS*ALAYER)*(STRSSMX*BREADTH)
293           COMPT=COMPT+COMP
294           ALEVR=DNA-ALEV
295           ALEV=ALEV+ALAYER
296           EDIV=EDIV+EGRAD
297           TMOM=COMP*ALEVR
298           TMOMT=TMOMT+TMOM
299           GO TO 25
300     C  COMPARE TENSION AND COMPRESSION FORCES
301        50 DIVIS=COMPT/TFORCE
302     C       WRITE(8,4)COMPT,DIVIS
303     C     4 FORMAT(2X,5HCOMPT,1X,E10.5,2X,5HDIVIS,1X,E10.5)
304           IF(DIVIS.GT.0.99.AND.DIVIS.LT.1.01) GO TO 30
305           DELTA1=((COMPT+TFORCE)/(2.0*COMPT))*DNA
```

```
306          WRITE(8,46)DELTA1
307       46 FORMAT(2X,6HDELTA1,1X,E14.5)
308          DNA=DELTA1
309          GO TO 20
310       30 CONTINUE
311     C  CALCULATE CENTROID OF COMP FORCE
312          CENTROID=TMOMT/COMPT
313          ALEVER1=EFFD1-(DNA-CENTROID)
314          ALEVER2=EFFD2-(DNA-CENTROID)
315     C  CALCULATE MOMENT
316          IF(J.GT.0)GO TO 600
317     C  COMPARE APPLIED MOMENT WITH CRACKING MOMENT
318          CMOM=(ALEVER1*TF1)+(ALEVER2*TF2)
319          COMPMOM=CMOM/CRKMOM
320          IF(COMPMOM.LT.1.03.AND.COMPMOM.GT.0.97)GO TO 600
321          STRAIN=STRAIN/COMPMOM
322          WRITE(8,675)STRAIN
323       675 FORMAT(2X,6HSTRAIN,2X,E10.5)
324          GO TO 20
325       600 J=J+1
326          IF(J.GT.1) GO TO 610
327          STRINC=(STRMX-STRAIN)/19.0
328          WRITE(8,612)STRAIN
329       612 FORMAT(2X,13HBRICK STRAIN,2X,E10.5)
330       610 MOMENT(J)=(ALEVER1*TF1)+(ALEVER2*TF2)
331          STRST(J)=STRSS1
332          STRST2(J)=STRSS2
333          STRAINS(J)=STRAIN
334          ESTEELS(J)=ESTEEL1+ESTEELY1+ESTL1
335          CURVE(J)=(STRAINS(J)+ESTEELS(J)-PRSTRN1)/EFFD1
336          DNARRY(J)=DNA
337     C       WRITE(8,57)MOMENT(J),CURVE(J),DNARRY(J)
339     C   57 FORMAT(2X,19HMOMENT CURVE DNARRY,2X,E14.5,2X,E14.5,2X,E14.5)
340          IF(STRAIN.LT.STRMX)GO TO 10
341       54 CONTINUE
342          WRITE(8,501)
343       501 FORMAT(///,3X,44HMOMENT-CURVATURE ACROSS CRACK AFTER CRACKING)
344       55 WRITE(8,60)
345       60 FORMAT(///,6X,10HMOMENT NMM,8X,9HCURVATURE,5X,12HN.A.DEPTH MM,5X,
346         .12HSTEEL STRAIN,14X,14HSTEEL STRESSES,10X,16HMAX.BRICK STRAIN,//)
347          DO 80 II=1,20
348          WRITE(8,70)((MOMENT(II)),(CURVE(II)),(DNARRY(II)),(ESTEELS(II))
349         .,(STRST(II)),(STRST2(II)),(STRAINS(II)))
350       70 FORMAT(3X,E14.5,3X,E14.5,3X,E14.5,3X,E14.5,3X,
351         .E14.5,3X,E14.5,3X,E14.5)
352       80 CONTINUE
353          NAIL=0
354          DO 90 K=1,20
355          IF(MOMENT(K).GT.CRKMOM) GO TO 92
356          NAIL=NAIL+1
357       90 CONTINUE
358       92 CONTINUE
359     C  TENSION STIFFENING,STRAIN IN STEEL AFRTER CRACKING
360          ESTEEL=ESTEELS(1)
361          FSCR=STRST(1)
362          WRITE(8,98)FSCR,ESTEEL
363       98 FORMAT(2X,37HSTEEL STRESS @ STRAIN AFTER CRACKING,2X,
364         .E14.5,2X,E14.5)
365     C  ADJUST CURVATURES TO ALLOW FOR TENSION STIFFENING
366          WRITE(8,400)PSTL
```

```
  400 FORMAT(/,4X,4HPSTL,2X,E14.5,/)
      WRITE(8,790)
  790 FORMAT(/,2X,34HAVERAGE ADDITIONAL STRAIN IN STEEL,/)
      DO 100 M=1,20
      FS=STRST(J)-(PRSTRN1*EMOD(1))
      ESTLS=ESTEELS(M)-PRSTRN1
C  CALCULATE TENSION STIFFENING COEFFICENT K
      TK=1.00-(0.97*(FSCR/STRST(M)))
      ESM=ESTLS-(TK*(RMODULUS/(200000.0*PSTL)))
      IF(ESM.LT.0.0)ESM=ESTLS
      IF(LTS.EQ.1) GO TO 789
      ESM=ESTLS
  789 CONTINUE
C      ESM=ESTLS-((4.0/PSTL)*0.000001)
      WRITE(8,200)ESM
  200 FORMAT(2X,E14.5)
      CURVE(M)=(STRAINS(M)+ESM)/EFFD1
  100 CONTINUE
      DO 102 L=1,20
      IF(L.LT.NAIL.OR.L.EQ.NAIL) GO TO 102
      LL=L-NAIL
      MOMENT(LL)=MOMENT(L)
      CURVE(LL)=CURVE(L)
  102 CONTINUE
      IK=20-NAIL
      DO 104 II=1,IK
      KK=5+II
      MOM(KK)=MOM(KK)+MOMENT(II)
      CURV(KK)=CURV(KK)+CURVE(II)
  104 CONTINUE
      RETURN
      END


      SUBROUTINE PRESTRESS(RMODULUS,EFFD1,EFFD2,ASTL1,ASTL2,BREADTH,
     .DEPTH,MOM,CURV,COFF,EMOD)
      DIMENSION SMOM(5),COFF(4),CURVEP(5)
      COMMON/DASC/NAIL,MOMENT,DNA,CURVE
      COMMON/ALB/ELAST,PRESTR1,PRESTR2,STRSSMX,STRMX,SMOM,CURVEP
      COMMON/BAT/E1,CRKMOM,PRSTRN1,PRSTRN2,STEEL1,STRAIN
      REAL MOMI,MI
      DOUBLE PRECISION MOM(25),CURV(25)
C   CALCULATE SECTION PROPERTIES
      DEPTHSQ=DEPTH*DEPTH
      AREA=DEPTH*BREADTH
      ZZM=(BREADTH*DEPTHSQ)/6.0
      MOMI=(BREADTH*DEPTHSQ*DEPTH)/12.0
      ECCEN1=EFFD1-(DEPTH/2.0)
      ECCEN2=EFFD2-(DEPTH/2.0)
C  PROPERTIES OF TRANSFORMED UNCRACKED SECTION
C  MODULAR RATIO
      RM=(EMOD*STRMX)*(1.9/STRSSMX)
C  CENTORID OF SECTION
      CENTR=((AREA*(DEPTH/2.0))+(RM*ASTL1*EFFD1)+(RM*ASTL2*EFFD2)
     .)/(AREA+(RM*(ASTL1+ASTL2)))
CC  CALCULATE PRESTRESS EFFECTS
      AXIAL1=(PRESTR1/AREA)*1000.0
      AXIAL2=(PRESTR2/AREA)*1000.0
      BEND1=(1000.0*PRESTR1*ECCEN1)/ZZM
      BEND2=(1000.0*PRESTR2*ECCEN2)/ZZM
C    STRESS AT TOP
      SIGMAC=(AXIAL1+AXIAL2)-(BEND1+BEND2)
      SIGMAT=(AXIAL1+AXIAL2)+(BEND1+BEND2)
```

```
428           PRSTRN1=(PRESTR1*1000.0)/(ASTL1*EMOD)
429           IF(ASTL2.EQ.0.0)GO TO 77
430           PRSTRN2=(PRESTR2*1000.0)/(ASTL2*EMOD)
431           GO TO 81
432        77 PRSTRN2=0.0
433           WRITE(8,700)PRSTRN1,PRSTRN2
434       700 FORMAT(2X,17HPRESTRESS STRAINS,2X,E10.5,2X,E10.5)
435        81 CONTINUE
436           ERUP=RMODULUS/(STRSSMX*1.9)
437     C  CALCULATE DISRTIBUTION OF PRESTRESS
438     C  RESULTANT OF PRESTRESS
439           IF(PRESTR1.EQ.0.0)GO TO 505
440           RESULT=((EFFD1*PRESTR1)+(EFFD2*PRESTR2))/(PRESTR1+PRESTR2)
441       505 CONTINUE
442           ELAST=1.9
443        75 CONTINUE
444           END1=SIGMAC/(ELAST*STRSSMX)
445           END2=SIGMAT/(ELAST*STRSSMX)
446           IF(SIGMAC.LT.0.0) GO TO 78
447     C  STRAINS WITHIN KERN OF PRESTRESS
448           EGRAD=(END2-END1)/20.0
449           ALAYER=DEPTH/20.0
450           GO TO 79
451     C  PRESTRESS OUTSIDE KERN
452        78 CONTINUE
453           RATIO=SIGMAC/SIGMAT
454           DCOM=DEPTH/(1+(-1.0*RATIO))
455           EGRAD=END2/20.0
456           EN=END1
457           END1=0.0
458           ALAYER=DCOM/20.0
459        79 CONTINUE
460           EDIV=EGRAD
461           EDIVS=EDIV/2.0
462     C  1ST LAYER STRAINS
463           COMPT=0.0
464           K=1
465        80 CONTINUE
466           IF(K.EQ.21) GO TO 90
467           ELAY=END1+EDIVS
468           STRS=(COFF(1)*ELAY)+(COFF(2)*(ELAY*ELAY))+(COFF(3)*ELAY*
469          .(ELAY*ELAY))
471           COMP=(STRS*ALAYER)*(STRSSMX*BREADTH)
472           COMPT=COMPT+COMP
473           EDIVS=EDIVS+EDIV
474           K=K+1
475           GO TO 80
476        90 CONTINUE
477     C  COMPARE C AND T
478           IF(PRESTR1.EQ.0.0)GOTO 621
479           RAT=COMPT/((PRESTR1+PRESTR2)*1000.0)
480           IF(RAT.LT.1.02.AND.RAT.GT.0.98)GO TO 95
481           ELAST=RAT*ELAST
482           GO TO 75
483        95 CONTINUE
484           WRITE(8,99)
485        99 FORMAT(2X,17HPRESTRESS STRAINS)
486           ENDT=END1
487           IF(END1.EQ.0.0)ENDT=EN
488           WRITE(8,100)ENDT,END2
```

```
      100 FORMAT(2X,E14.5,2X,E14.5)
          PRECURV=(STRMX*(END2+ENDT))/DEPTH
          WRITE(8,201)PRECURV
      201 FORMAT(2X,27HCURVATURE DUE TO PRESTRESS,2X,E14.5)
C     STRAIN TO CAUSE CRACKING
          E1=END2
          IF(PRESTR1.EQ.0.0)GOTO 621
          ECRAC=END2+ERUP
          GO TO 622
      621 ECRAC=ERUP
          GO TO 602
      622 CONTINUE
          EINT=0.0
          EINC=ECRAC/5.0
          ENT=END1
          EINCT=0.0
          END22=END2
          LL=0
          WRITE(8,135)ECRAC
      135 FORMAT(1X,16HCRACKING STRAINS,1X,E14.5)
          EINCST=EINC*STRMX
          DT=CENTR
          ESTINC=0.0
      105 CONTINUE
          LL=LL+1
          EINT=EINC+EINT
          EINCT=EINCT+EINC
          IF(LL.EQ.6) GO TO 120
          END2=END22-EINCT
C     CALCULAT STRAINS AND FORCES IN STEEL
      199 CONTINUE
          STEEL1=(EINCT*STRMX)*((EFFD1-DT)/(DEPTH-DT))
          STEEL2=(EINCT*STRMX)*((EFFD2-DT)/(DEPTH-DT))
          TF1=ASTL1*(EMOD*(STEEL1+PRSTRN1))
          TF2=ASTL2*(EMOD*(STEEL2+PRSTRN2))
          TFORCE=TF1+TF2
C          WRITE(8,240)TFORCE
C     240 FORMAT(2X,6HTFORCE,2X,E10.5)
          EINTT=EINT
C     STRAINS IN BRICWORK
          END1=ENT+EINTT
          WRITE(8,140)END1,END2
      140 FORMAT(2X,13HBRICK STRAINS,1X,E14.5,2X,E14.5)
          IF(END1.LT.0.0) GO TO 102
          IF(END2.LT.0.0) GO TO 110
          EGRAD=(END2-END1)/20.0
          ENR=END1
          ALAYER=DEPTH/20.0
          DCOM=DEPTH
          GAP=0.0
          GO TO 104
      102 CONTINUE
          RATIO=END1/END2
          DCOM=DEPTH/(1+(-1.0*RATIO))
          EGRAD=END2/20.0
          GAP=0.0
          ALAYER=DCOM/20.0
          ENR=0.0
          GO TO 104
      110 CONTINUE
          RATIO=END2/END1
```

```
550           DCOM=DEPTH/(1+(-1.0*RATIO))
551           ENR=END1
552           EGRAD=(-1.0*END1)/20.0
553           ALAYER=DCOM/20.0
554           GAP=DEPTH-DCOM
555         104 CONTINUE
556           ALEV=ALAYER/2.0
557           ALEVS=ALAYER
558           EDIV=EGRAD
559           EDIVS=EDIV/2.0
560       C  1ST LAYER STRAINS
561           TMOMT=0.0
562           COMPT=0.0
563           K=1
564         106 CONTINUE
565           IF(K.EQ.21) GO TO 108
566           ELAY=ENR+EDIVS
567           STRS=(COFF(1)*ELAY)+(COFF(2)*(ELAY*ELAY))+(COFF(3)*ELAY*
568          .(ELAY*ELAY))
569           COMP=(STRS*ALAYER)*(STRSSMX*BREADTH)
570           COMPT=COMPT+COMP
571       C      WRITE(8,129)COMPT
572       C  129 FORMAT(2X,5HCOMPT,2X,E14.5)
573           ALEVR=(DCOM-ALEV)+GAP
574           K=K+1
575           TMOM=COMP*ALEVR
576           TMOMT=TMOMT+TMOM
577       C      WRITE(8,130)TMOMT
578       C  130 FORMAT(2X,5HTMOMT,2X,E14.5)
579           EDIVS=EDIVS+EDIV
580           ALEV=ALEV+ALEVS
581           GO TO 106
582           WRITE(8,145)GAP
583         145 FORMAT(2X,3HGAP,1X,F10.5)
584         108 CONTINUE
585       C  COMPARE TENSION AND COMPRESSION FORCES
586       C      WRITE(8,250)COMPT
587       C  250 FORMAT(2X,5HCOMPT,1X,E10.5)
588           TFORCE=TFORCE+((GAP*BREADTH)*(RMODULUS/2))
589           CT=COMPT/TFORCE
590           IF (CT.LT.1.05.AND.CT.GT.0.95)GO TO 200
591           WRITE(8,204)CT
592         204 FORMAT(2X,2HCT,2X,E10.5)
593           CT=(COMPT*2.0)/(TFORCE+COMPT)
594           DT=DT/CT
595           EINT=(EINCT*DT)/(DEPTH-DT)
596           WRITE(8,260)DT
597         260 FORMAT(2X,2HDT,2X,E10.5)
598           GO TO 199
599       C  LEVER ARM
600         200 ALEVARM=TMOMT/COMPT
601           SMOM(LL)=(ALEVARM*COMPT)-((TF1*(DEPTH-EFFD1))+(TF2*(DEPTH-EFFD2)
602          .+(GAP*BREADTH*(RMODULUS/6.0)))
603           CURVEP(LL)=((END1-END2)*STRMX)/DEPTH
604       C      WRITE(8,119)ALEVARM,COMPT
605       C  119 FORMAT(1X,15HALEVERARM COMPT,1X,E14.5,2X,E14.5)
606           GO TO 105
607         120 CONTINUE
608           WRITE(8,790)
609         790 FORMAT(//,2X,44HMOMENT-CURVATURE RELATIONSHIP UP TO CRACKING,//)
610           WRITE(8,791)
611         791 FORMAT(2X,6HMOMENT,8X,9HCURVATURE,/)
```

```
612             IF(PRESTR1.NE.0.0)GO TO 291
613          602 CONTINUE
614             MI=BREADTH*(DEPTH*DEPTH)*(DEPTH/12.0)
615             CRKMOM=RMODULUS*(MI/CENTR)
616             ECRAC5=(STRMX*ECRAC)/5.0
617             CRKMOM5=CRKMOM/5.0
618             CRK=0.0
619             ERC=0.0
620             DO 290 L=1,5
621             CRK=CRK+CRKMOM5
622             ERC=ERC+ECRAC5
623             CURVEP(L)=ERC/(DEPTH-CENTR)
624             SMOM(L)=CRK
625          290 CONTINUE
626          291 CONTINUE
627             DO 125 L=1,5
628             MOM(L)=MOM(L)+SMOM(L)
629             CURV(L)=CURVEP(L)
630             WRITE(8,123)SMOM(L),CURVEP(L)
631          123 FORMAT(2X,E14.5,2X,E14.5)
632          125 CONTINUE
633             WRITE(8,126)SMOM(L)
634          126 FORMAT(1X,15HCRACKING MOMENT,2X,E14.5)
635             CRKMOM=SMOM(L)
636             STRAIN=ECRAC*STRMX
637             WRITE(8,878)STRAIN
638          878 FORMAT(2X,6HSTRAIN,E10.5)
639             RETURN
640             END


CODE   19552 BYTES      PLT + DATA   12472 BYTES
STACK   1888 BYTES      DIAG TABLES   3244 BYTES      TOTAL  37156 BYTES
COMPILATION SUCCESSFUL

 640 Statements compiled

Command:
```